National Library of Canada
Bibliothèque nationale du Canada

Canadian Theses Service
Service des thèses canadiennes

Ottawa, Canada
K1A 0N4

NOTICE

The quality of this microform is heavily dependent upon the quality of the original thesis submitted for microfilming. Every effort has been made to ensure the highest quality of reproduction possible.

If pages are missing, contact the university which granted the degree.

Some pages may have indistinct print especially if the original pages were typed with a poor typewriter ribbon or if the university sent us an inferior photocopy.

Reproduction in full or in part of this microform is governed by the Canadian Copyright Act, R.S.C. 1970, c. C-30, and subsequent amendments.

AVIS

La qualité de cette microforme dépend grandement de la qualité de la thèse soumise au microfilmage. Nous avons tout fait pour assurer une qualité supérieure de reproduction.

S'il manque des pages, veuillez communiquer avec l'université qui a conféré le grade.

La qualité d'impression de certaines pages peut laisser à désirer, surtout si les pages originales ont été dactylographiées à l'aide d'un ruban usé ou si l'université nous a fait parvenir une photocopie de qualité inférieure.

La reproduction, même partielle, de cette microforme est soumise à la Loi canadienne sur le droit d'auteur, SRC 1970, c. C-30, et ses amendements subséquents.

NL-339 (r. 88/04) c

Canada

UNIVERSITY OF ALBERTA

AN AUTOMATED DIRECT SAMPLE INSERTION SYSTEM FOR THE INDUCTIVELY COUPLED PLASMA

by

WILLIAM E. PETTIT ©

A THESIS
SUBMITTED TO THE FACULTY OF GRADUATE STUDIES AND RESEARCH IN
PARTIAL FULFILMENT OF THE REQUIREMENTS FOR THE DEGREE OF
DOCTOR OF PHILOSOPHY

DEPARTMENT OF CHEMISTRY

EDMONTON, ALBERTA

SPRING 1991

National Library
of Canada

Bibliothèque nationale
du Canada

Canadian Theses Service

Service des thèses canadiennes

Ottawa, Canada
K1A 0N4

The author has granted an irrevocable non-exclusive licence allowing the National Library of Canada to reproduce, loan, distribute or sell copies of his/her thesis by any means and in any form or format, making this thesis available to interested persons.

The author retains ownership of the copyright in his/her thesis. Neither the thesis nor substantial extracts from it may be printed or otherwise reproduced without his/her permission.

L'auteur a accordé une licence irrévocable et non exclusive permettant à la Bibliothèque nationale du Canada de reproduire, prêter, distribuer ou vendre des copies de sa thèse de quelque manière et sous quelque forme que ce soit pour mettre des exemplaires de cette thèse à la disposition des personnes intéressées.

L'auteur conserve la propriété du droit d'auteur qui protège sa thèse. Ni la thèse ni des extraits substantiels de celle-ci ne doivent être imprimés ou autrement reproduits sans son autorisation.

ISBN 0-315-66730-3

Canada

UNIVERSITY OF ALBERTA

RELEASE FORM

NAME OF AUTHOR: William E. Pettit

TITLE OF THESIS: An Automated Direct Sample Insertion System for the Inductively Coupled Plasma.

DEGREE FOR WHICH THIS THESIS WAS PRESENTED: Ph.D.

YEAR THIS DEGREE GRANTED: 1991

Permission is hereby granted to THE UNIVERSITY OF ALBERTA LIBRARY to reproduce single copies of this thesis and to lend or sell such copies for private, scholarly or scientific research purposes only.

The author reserves other publication rights, and neither the thesis nor extensive extracts from it may be printed or otherwise reproduced without the author's written permission.

(Signed) William E. Pettit

PERMANENT ADDRESS:

Department of Chemistry, MS-74
Eastern Washington University
Cheney, Washington U.S.A. 99004-2499

Date: April 10, 1991

THE UNIVERSITY OF ALBERTA

FACULTY OF GRADUATE STUDIES AND RESEARCH

The undersigned certify that they have read, and recommend to the Faculty of Graduate Studies and Research for acceptance, a thesis entitled An Automated Direct Sample Insertion System for the Inductively Coupled Plasma submitted by William E. Pettit in partial fulfilment of the requirements for the degree of Doctor of Philosophy in Analytical Chemistry.

B. Kratochvil

Dr. B. Kratochvil, Committee Chairman

Gary Horlick

Dr. G. Horlick, Supervisor

Dr. N. Dovichi, Committee Member

Dr. K. Kopecky, Committee Member

Dr. S.E. Hrudey, Committee Member

Dr. R.K. Marcus, External Examiner

Date: Mar 5, 1990

DEDICATION

To

my parents,

my wife Rachel,

and my children James and Sarah.

ABSTRACT

A major limitation of inductively coupled plasma optical emission spectrometry (ICP-OES) systems has been the almost exclusive use of pneumatic nebulization to introduce samples into the plasma. This sample introduction method requires that samples either be liquid or be converted to a solution form and that normally several milliliters of sample be available. A flexible new sample introduction system for the direct analysis of a wide range of samples including small liquid volumes, botanical powders, coal, coal ash, oil, and a variety of other solids has been developed.

With this system, sample-carrying cups can be sequentially and automatically inserted into an ICP discharge using a pneumatically controlled transport device. An unlimited number of samples can be handled, since sample cup carousels are readily exchanged without disturbing ICP operation. This pneumatic delivery system also lends itself to modification for remote sampling applications (eg. in toxic environments).

The sample is pneumatically delivered to a simple mechanical positioner located just under a modified ICP torch. This device allows for sample cup location relative to the plasma discharge to be programmed through "dry," "ash," and "vaporize" cycles. Results obtained with a new CW CO_2 laser asher are compared with ashing directly under the ICP discharge.

This system also incorporates a novel water-cooled torch and argon/oxygen or argon/hydrogen mixed gas coolant flow. With the argon/oxygen mixture, it is possible to totally consume graphite cups containing biological samples in a controlled fashion. Temporal data reveals enhanced volatilization of specific analytes from the graphite cups in an argon/oxygen discharge relative to a pure argon plasma.

In an effort to increase the precision of analysis for elements such as manganese and nickel, volatilization of analyte from molybdenum, tantalum, and tungsten sample cups in an argon/hydrogen plasma was studied. Tungsten cups gave the best precision for multielement standard solutions. This data is superior to that obtained for the same solutions analyzed by insertion of graphite cups into an argon/oxygen plasma. These results suggest that in certain cases where total sample consumption is not necessary, the metal cup/reducing plasma technique may be more appropriate.

ACKNOWLEDGEMENTS

Special thanks to Professor Gary Horlick for his patient guidance.

Thanks to my fellow chemistry students, the chemistry faculty, and the staff of the glass, machine, and electronic shops for all their support.

TABLE OF CONTENTS

CHAPTER PAGE

I INTRODUCTION 1
  A. Why Automate? 1
  B. Automation of Sample Introduction and Preparation in the Analytical Laboratory 5
  C. Automated Continuous Flow Systems for Sample Introduction and Preparation 11
    1. Sample Introduction for Flame and Plasma Sources 12
      a. Nebulization 13
      b. Auto Samplers 14
    2. Sample Preparation for Flame and Plasma Sources 15
      a. Auto Diluters 17
      b. Flow Injection 18
      c. Liquid Chromatography 22
    3. Introduction and Preparation of "Difficult" Samples 24
  D. Automated Discrete Systems for Sample Introduction and Preparation 26
    1. "Modular" Systems 28

2. Robot Arm-Based or "Robotic" Systems 33

E. Summary of Trends in Automatic Sample Introduction and Preparation and a Proposal for a New Direct Sample Insertion Device for the ICP 42

II DIRECT SAMPLE INSERTION FOR THE ICP: A REVIEW 51

A. Introduction and Historical Perspective 51

1. Wire-in-Flame 51

2. Boat-in-Flame 57

3. "Delves Sampling Cup" Techniques 57

4. Other Methods of Direct Solids Introduction 65

B. Direct Sample Insertion into the ICP 67

1. Cup-in-Plasma 68

2. Wire-in-Plasma 126

3. Rod-in-Plasma 135

III AUTOMATED DIRECT SAMPLE INSERTION DEVICE (DSID) DEVELOPMENT 139

A. Introduction 139

B. ICP Source 144

1. DSID Installation 144
2. Gas Supply 144
3. Torch and Transport Assembly Development .. 149
4. Sample Cup Composition 156

C. Carousel for Sequential Sample Presentation ... 160
1. Mounting 166
2. Torch Coupling 171

D. Pneumatic Sample Insertion and Retraction 174
1. Sample Insertion 174
2. Sample Retraction 177

IV DATA ACQUISITION AND DSID CONTROL 181

A. Introduction 181

B. Photodiode Array-Photomultiplier Tube (PDA-PMT) Combination Spectrometer 184
1. Optics 184
2. Detector Support Electronics and Array Cooling 190

C. Minicomputer Systems and Interfacing 195
1. Introduction 195

CHAPTER PAGE

2. Laboratory Peripheral System (LPS) and Analog-to-Digital Conversion of the PDA Output 198
3. DSID Control 201

V AUTOMATED SAMPLE PREPARATION WITH THE DSID 203
A. Introduction 203
B. A Survey of Methods of Sample Drying and Decomposition for Use With the DSID 205
1. Sample Drying 212
2. Sample Decomposition 216
a. Thermal Decomposition 217
b. Chemical Reagent-Based Decomposition .. 219
i. Open Flask Digestion 220
ii. Reflux Digestion 224
iii. Bomb Digestion 226
iv. Fusion 227
C. The Role of the DSID 229
D. CO_2 Laser Sample Preparation 231
1. Introduction 231
2. Laser Development 234
E. Positioner for Sub-Plasma Sample Preparation .. 242

1. Introduction 242

2. Positioner Development 247

    a. Cooling 250

    b. Mechanical Detail 252

    c. Computer Control 257

VI DIRECT LIQUID INTRODUCTION WITH THE DSID 263

A. Introduction 263

1. Discrete Nebulization 264

2. Alternatives to Nebulization 269

    a. Hydride Generation 270

    b. Volatile Chelates 271

    c. Mercury Cold Vapor Techniques 272

    d. Volatile Compounds and Gases 273

B. Liquid Analysis with the DSID 274

1. Graphite Sample Cups in an Argon Plasma ... 275

2. Graphite Sample Cups in an Argon-Oxygen Mixed Gas Plasma 281

3. The Effect of Internal Standards and Sample Cup Age on Precision 296

4. Alternate Sample Cup and Plasma Coolant Gas Compositions 298

CHAPTER PAGE

    5. Metal Sample Cups in an Argon-Hydrogen Mixed Gas Plasma 301

VII DIRECT SOLIDS INTRODUCTION WITH THE DSID 321
  A. Introduction 321
    1. Nebulization of "Difficult" Samples 322
      a. Traditional Nebulizers 322
      b. Babington Nebulizers 325
      c. Disadvantages of Nebulization 327
    2. Direct Solids Nebulization 328
      a. Conducting Samples 328
        i. Arc and Spark Discharges 328
        ii. Toward Separate Optimization of Sampling and Excitation 331
      b. Non-Conducting Samples 334
        i. Spark Discharges 334
        ii. Direct Powder and Slurry Introduction 335
  B. Oil and Solid Analysis with the DSID 340
    1. Preparation and Insertion of Oil Standards 340
      a. Laser Ashing 341

        b. Oil Analysis by Direct Insertion into the ICP 342
    2. Preparation and Insertion of Plant Standards 344
        a. Laser Ashing 344
        b. Sub-Plasma Ashing 344
        c. Analysis by Direct Insertion into the ICP 345
    3. Preparation and Insertion of Geological Standards 348

VIII SUMMARY 352

BIBLIOGRAPHY 373

LIST OF TABLES

Table	Description	Page
II.1	Advances in Direct Sample Insertion for Flames.	52
II.2	Advances in Direct Sample Insertion for Plasmas.	69
II.3	Optimized Conditions for ICP Direct Sample Insertion.	76
III.1	ICP Source and Typical Running Conditions.	145
III.2	ICP Gas Supply Components.	148
III.3	Transport Assembly Specifications.	154
III.4	Sample Cup Specifications.	159
III.5	Carousel Tray Specifications.	163
III.6	Sample Carousel Mount Specifications.	169
III.7	Output Coupler Specifications.	173
III.8	Valve Specifications.	180
IV.1	PDA-PMT Spectrometer Specifications.	186
IV.2	Minicomputer System Specifications.	196
IV.3	PDA Analog Signal Processing Electronics	199
V.1	Laser Specifications.	236
V.2	Laser Gas Supply Circuit Specifications.	241
V.3	Sample Positioner Specifications.	254

Table	Description	Page
VI.1	Advances in Continuous Flow Liquid Introduction for Flames and Plasmas.	265
VI.2	Sample Size vs. Precision.	280
VI.3	Percent Oxygen vs. Precision.	295
VI.4	Alien Gas and Cup Material vs. Precision.	315
VI.5	Detection Limits with Metal Cups.	316
VII.1	Advances in Continuous Flow Solid Introduction for Flames and Plasmas.	323

LIST OF FIGURES

Figure	Description	Page
1	Original manual insertion device.	48
2	Automatic pneumatic insertion system concept.	50
3	Automatic direct insertion system.	143
4	Modified ICP gas circuit. (See Table III.2 for component identification).	147
5	(a) Standard ICP torch, (b) initial pneumatic injection torch and sample transport assembly.	150
6	(a) Pneumatic injection ICP torch with integrated guide tube and reflective collar, (b) simplified design.	153
7	Sample cups. (a) Graphite, (b) graphite base with tungsten cup, (c) graphite base with molybdenum, tantalum, or boron nitride cup (or molybdenum cup with teflon cup insert).	158
8	Sample carousel.	162
9	Sample carousel mount.	168
10	Torch-to-carousel coupling.	172
11	Sample insertion.	175
12	Sample retraction.	178
13	Computerized data acquisition system.	183

Figure	Description	Page
14	PDA-PMT spectrometer.	185
15	PDA signal processing electronics; $R_1=R_3=100k\Omega$, $R_2=30k\Omega$, $R4=R5=1M\Omega$; $C_1=C_2=C_3=15\mu F$, 25V, $C_4=C_5=0.001\mu F$.	200
16	(a) CO_2 laser asher, (b) anode modification.	235
17	CO_2 laser power supply circuit diagram; $R_1=R_2=0$-115V reostat; $R_3=R_4=100k\Omega$, 200W ballast resistor; $T_1=T_2=15$kVAC, 60mA neon sign transformer; $C_1=C_2=1.6\mu F$, 25kV; $V_{in}=115$VAC, 60Hz; $V_{out}=10.5$ kVDC @ 50 mbar. laser discharge tube gas pressure.	238
18	Laser gas supply and vacuum system. (See Table V.2 for component identification).	240
19	Sub-plasma sample positioner and water-cooled torch.	249
20	Positioner mechanical detail.	253
21	(a) Positioner clamp, (b) demountable aerosol tube.	258
22	Sample positioner control signal generation circuit and drive mechanism.	259
23	Spectrum from 10 µl 1000 ppm zinc solution (10 µg Zn) in graphite cup.	277

Figure	Description	Page
24	Multielement spectra from graphite sample cup in plasma with 6% O_2 (a), and without O_2 (b).	284
25	Background emission from graphite sample cup in an Ar-6% O_2 plasma (a), and residual after spectral and fixed-pattern background subtraction (b).	285
26	Multielement spectrum from graphite cup in an Ar-1% O_2 plasma.	286
27	Temporal behavior for Mn, Cd, Zn, Ni, and In in a graphite cup in an Ar-0.5% O_2 plasma.	287
28	Temporal profiles for In II 230.6 nm, Cd I 228.8 nm, and Zn I 213.8 nm emission with graphite sample cup in Ar and Ar/O_2 mixed gas plasma (% indicates level of O_2 added to Ar coolant).	289
29	Temporal profiles for Mn II 257.6 nm emission with graphite sample cup in Ar and Ar/O_2 mixed gas plasma (% indicates level of O_2 added to Ar coolant).	290

Figure	Description	Page
30	Temporal profiles for Ni II 221.6 nm emission with graphite sample cup in Ar and Ar/O_2 mixed gas plasma (% indicates level of O_2 added to Ar coolant).	291
31	Boron emission from a boron-treated graphite sample cup.	300
32	Cadmium and zinc spectrum obtained with a 1200 lines/mm grating. Graphite sample cup in an Ar-1% O_2 plasma.	305
33	Cadmium and zinc spectrum obtained with a 2400 lines/mm grating. Graphite sample cup in an Ar-1% O_2 plasma.	306
34	Temporal profiles for Mn II 257 nm emission intensity with graphite (C), Mo, Ta, and W sample cups.	307
35	Temporal profiles for Zn I 213.8 nm emission intensity with graphite (C), Mo, Ta, and W sample cups.	308
36	Temporal profiles for Cd II 214 nm emission intensity with graphite (C), Mo, Ta, and W sample cups.	309

Figure	Description	Page
37	Temporal profiles for In II 230.6 nm emission intensity with graphite (C), Mo, Ta, and W sample cups.	310
38	Temporal profiles for Ni II 221.6 nm emission intensity with graphite (C), Mo, Ta, and W sample cups.	311
39	Relative temporal emission profiles of Zn, Cd, In, and Ni with W sample cups.	313
40	Working curve for nickel with tungsten sample cups.	317
41	Temporal emission profile for 1 ng of Zn with tungsten sample cup in Ar-1% H_2 plasma.	319
42	Temporal behavior of elemental emission from unashed (a), and laser-ashed (b) NBS SRM 1571 orchard leaves.	347
43	Calibration plot for zinc in biological SRMs.	349
44	Calibration plot for zinc in geological SRMs.	350
45	Calibration plot for zinc in biological and geological SRMs.	351

CHAPTER I

INTRODUCTION

A. Why Automate?

Fundamental chemical knowledge from basic research laboratories is being transferred at an ever increasing rate to applications-oriented fields such as chemical and biological engineering and materials science and finally to chemical, pharmaceutical, and electronics industries and health services. These are only a few of the many areas impacted by the application of chemical knowledge.

This increased application of chemistry in diverse fields means that the analytical chemist is being challenged to provide data for samples with increasingly varied compositions. In addition to the problem of such diversity, the analytical chemist is further burdened by the sheer numbers of samples generated from, for example, exploratory geochemical (1), baseline environmental (2) and health surveys (3) and from quality control of manufactured products (4).

As the director of the Center for Analytical Chemistry at the National Bureau of Standards, H.S. Hertz, pointed out in a recent interview (4), as a better understanding develops "...of the relationship between chemical and physical properties of manufactured products, as well as functional properties of the materials...more and more chemical measurements will be made to check products before they leave manufacturing facilities [and] 'that will place a greater burden on analytical chemists'."

In order to meet these challenges in an efficient manner, the analyst will rely on automation to an ever greater extent. According to Hertz, the "major driving force" for the development and application of laboratory automation "...is to improve quality assurance and to improve the efficiency with which chemical measurements are made." But the underlying reason for the current interest in automation is necessarily economic. The approximately 250 million chemical measurements conducted daily in the U.S. have an annual price tag of about $50 billion (4). Laboratory managers realize that the only effective way to counter high costs and meet rising demand is to increase productivity, but they are generally financially unable to support increases in staff. This sentiment is expressed in a Canadian Research article (5) entitled "Automation: the key to improving laboratory productivity."

In this article the head of Vancouver General Hospital's Division of Clinical Chemistry, Dr. D.J. Campbell, states that his hospital runs 4,000 analyses per day and plans to increase the load to 6,000 to 9,000 tests per day. But at the same time his division has been asked to cut its budget by 17%. "The solution to this type of dilemma being implemented by progressive labs everywhere," he says, "is automation."

Automation is therefore actually viewed as an efficient means to increase productivity without a corresponding increase in staff (6). The relationship between productivity and automation is explored in an editorial in the same issue of Canadian Research (7) mentioned above. Douglas Dingeldein, editor and publisher of this magazine, points out in his editorial that Japan's vital economic statistics serve as excellent examples of the benefits of intelligently planned and implemented automation. With no labor unrest and a tenth of the "man-days lost to industrial action" as compared to Canada, Japan boasts an average annual growth in GNP of 5%, a 4.9% increase in consumer prices, an unemployment level of 2.2%, single digit interest rates and a merchandizing trade balance in the black by "tens of billions of dollars." Dingeldein feels that Japan's economic strength depends in part on "...an almost fanatic devotion to productivity..." and states that this productivity "...has been technology driven with increasing implementation of automated processes."

North American industry has been slow to take heed of Japan's lesson and as a result Japan's 1982 trade surplus to America was about 12 billion dollars which was equivalent to 480,000 jobs lost to the Japanese. And as Deputy Commerce Secretary Clarence Brown said recently (8), "Time and again we have seen foreign competitors, most notably but not exclusively the Japanese, turn our technological developments into their commercial product successes." This situation is not likely to improve unless innovative automation is vigorously pursued (9). In fact, a newly-released report by the National Bureau of Standards and the Department of Commerce entitled "The Status of Emerging Technologies: An Economic/Technological Assessment to the Year 2000" warns that the "...nation's economic future will depend in large measure on how effectively these new areas [including automation] can be developed and used" (8).

B. Automation of Sample Introduction and Preparation in the Analytical Laboratory

Having identified automation as the means to improving laboratory productivity, the important question remains: what is the current critical target area in the analytical laboratory for the implementation of automation? Attempting to define laboratory automation helps focus on the answer to this question.

According to the International Union of Pure and Applied Chemistry (IUPAC) (10), automation is defined as "the use of combinations of mechanical and instrumental devices to replace, refine, extend, or supplement human effort and facilities in the performance of a given process, in which at least one major operation is controlled without human intervention, by a feedback mechanism." If a feedback mechanism is not present, IUPAC considers a process to be only mechanized.

Certainly, human effort has been at least extended by the widespread application of microprocessor technology in analytical instrumentation (11). But few of these instruments are in fact automated in terms of the IUPAC definition as they generally lack a true feedback mechanism. Instruments that can take data and then act on inferences made from the data, all in unattended fashion, are only in the early stages of development. But interest in this development is keen and involves scientists from many disciplines.

For example, C.H. Lochmuller of Duke University predicted at the 1985 Eastern Analytical Symposium in New York City (12) that a laboratory robot guided by a microcomputer might someday be used by clinical chemists "...to run a profile of tests on a patient overnight" with the computer "...confirm(ing) the prospective diagnosis or suggest(ing) alternative diagnoses and the tests that would be needed to confirm them."

The appearance of new expert system* software like G. Horlick's "Human Processor Interface" (13,14) and new hardware including microelectronic transducers (15), signal - processors with embedded software (16), microprocessors (11), parallel processors (17,18), computer networks (19), neural networks (20), and optical disks (21, 22) augurs well for a near future more spectacular even than Lochmuller's: one in which chemists will "...carry out completely computer-controlled cybernetic experiments" (24) and will "...simply [place] a chart or list of data under the computer's eye and [ask] it 'what it thinks about the results'" (25).

---

* "The knowledge base (database) and approach to thinking (logic system or inference engine) that an expert in the field might use" available to anyone on a computer (23).

Obviously, most of the exciting developments mentioned here deal with the data acquisition and manipulation end of chemical analysis. Much less attention has been given in the literature to optimization of the process of preparing samples and introducing them into instruments for analysis. But for an analytical method to be considered truly automated, sample preparation and introduction and data acquisition and manipulation all need to be mechanized and linked by feedback. Such a unified system represents a definition of ideal laboratory automation.

If competitive laboratory productivity depends on the realization of this ideal laboratory automation, and the mechanization of data acquisition and manipulation is receiving sufficient attention, then the critical target area for work is the mechanization of sample preparation and introduction.

It should be noted at this point that the term automation is used extensively in the literature in reference to processes that would technically be considered only mechanized. For the purpose of consistency with the analytical literature, the generic description of automation favored by Stockwell and Foreman (10) will be used in the remainder of this work, that is: "...all those developments that minimize human intervention in chemical analysis."

Because sample character can vary widely and preparation schemes can therefore be numerous and complex, automation of sample preparation and introduction has been slow in coming. For this reason, these steps remain the most time consuming of most analytical procedures (26). Laboratory managers are aware of this inefficiency and their feelings about it are probably fairly represented in a letter written to Analytical Chemistry (27). An excerpt follows:

> The 30 to 240 minutes per sample [for preparation] still displeases the administration and the public who has to pay for it. If, for some reason, preparation time could be automated and substantially shortened, the savings could lead to a much larger output of data and true innovation in the field of analytical chemistry.

Equally unflattering comments have been expressed concerning sample introduction. For example, R.F. Browner (28), a specialist in sample introduction processes for atomic spectroscopy, suggests in the title of a recent review that sample introduction is "the Achilles' heel of atomic spectroscopy." In this review, Browner laments that even though liquid sample introduction is simple and reliable;

> Nevertheless, an ICP [inductively coupled plasma] spectroscopist observing 99% of a hard won analyte solution passing to waste, or having to wait 60s between the introduction of successive samples to the spectrometer, is aware of the need for improvement. In atomic absorption spectroscopy, no higher than 10% efficiency can be expected. In ICP spectroscopy, a typical value is 1%.

If the goal of sample introduction is, as Browner (28) states, "...the reproducible transfer of a representative portion of sample material to the atomizer cell, with high efficiency and no adverse interference effects," then it is obvious that a breakthrough in sample introduction is needed.

Therefore, significant advances in both sample introduction and preparation are required if the final goal of ideal laboratory automation is to be reached. But the mechanization of existing techniques will not be adequate. Since, as Browner (29) points out, "... in any real analysis sample introduction is an extension of sample preparation," any advance in overall efficiency will necessarily accrue only from an experimental design which addresses both areas in concert.

Before proposing an experimental design for a new ICP sample introduction and preparation system which will make a significant contribution toward the goal of attaining ideal laboratory automation, the subject of automatic sample introduction and preparation will be briefly reviewed.

The progress which has been made in the area of automatic sample preparation and introduction has historically been confined largely to the clinical laboratory. The main reasons for this are; there is little sample diversity (mostly serum and plasma), a small number of assays are generally run on large numbers of samples in series, and sample preparation is the most labor-intensive step of the analysis. In contrast, industrial samples are generally run in small lots on samples of great compositional variety (6).

Such automated methods can be classified into two main categories: continuous flow and discrete (10). In continuous flow systems, liquid samples are transported through tubes by the action of a peristaltic pump. Individual samples are generally isolated from one another by air bubbles. In discrete (or "batch") methods, the individual samples are kept isolated from one another, for example, in small beakers. The sample containers are transported to various preparation stages by mechanical means such as conveyor belts or carousels.

C. Automated Continuous Flow Systems for Sample Introduction and Preparation

The original work of L.T. Skeggs, Jr. (30) on continuous flow systems for clinical analysis eventually led to a commercial product called the AutoAnalyzer (Technicon Instruments Corp., Terrytown, N.Y.). The main advantages of the continuous flow approach are simplicity of design, operation, and maintenance. Also, since the various reagents are added simply by the merging of tubes, one multichannel pump is required for the entire system. Mixing can be accomplished by simply pumping the reactants through a coiled section of tubing. Disadvantages are the possible cross contamination and confusion of identities of individual samples.

Obviously, the form in which the sample is to be introduced to the measurement instrument or analysis cell governs the choice of preparation procedure. Since an automatic clinical analysis is generally performed with a colorimetric finish, the sample is simply pumped into the analysis cell in its original liquid state. Sample preparation is therefore greatly simplified. Consequently, automatic clinical continuous flow systems have reached a high degree of sophistication.

For instance, multichannel capabilities (more than one test per sample) are available on Technicon's latest version of the AutoAnalyzer; the SMAC II (simultaneous multiple analyzer plus computer). The SMAC II splits each sample into 24 subsamples for individual testing and the system can test 150 samples per hour. The SMAC II therefore generates 3600 diagnostic test results in that time (31).

1. Sample Introduction for Flame and Plasma Sources

In automatic clinical analysis systems like the SMAC, the final analytical determination is conducted by pumping the entire liquid sample into a flow cell colorimeter. Therefore, the prepared sample is introduced into the analytical "source" with 100% efficiency and sample viscosity and salt content are of no great concern. The situation is more complex, however, for analytical methods incorporating flame or plasma spectrometric finishes.

Aside from the special cases where the analyte can be directly volatilized or where it can be converted to a volatile form by chelation or hydrogenation (28), nebulization is the general method of choice for sample introduction into flame or plasma sources. This means that sample viscosity and salt content parameters become critical (32) and as much as 95% of the sample volume can be lost during the nebulization process (33).

a. Nebulization

In an effort to improve the efficiency of nebulization, several variations in nebulizer construction have been explored. Ultrasonic (34) and glass frit nebulizers (35) can deliver more aerosol per unit time than standard pneumatic nebulizers. Removal of excess solvent by heated desolvation ("aerosol desolvation") can further increase sample delivery rate (32). For instance, an approximately 10-fold increase in sample delivery rate was noted for an inductively coupled plasma (ICP) system employing aerosol desolvation in conjunction with ultrasonic nebulization (36). A recent application of a high performance liquid chromatography-mass spectrometry (HPLC-MS) thermospray interface to flow injection analysis-inductively coupled plasma (FIA-ICP) spectroscopy also appears promising (37). Recent improvements in nebulizer spray chamber design have also led to greater nebulization efficiency (38).

Although these alternative designs can provide greater nebulization efficiencies, they are no more amenable to automation than standard pneumatic nebulizer designs. Problems such as prolonged wash cycles between samples (39), memory effects associated with aerosol desolvation (32), contamination (39), and the effects of sample viscosity, surface tension, and depth (40), make automation unattractive. This situation is not likely to change until fundamental studies of aerosol transport mechanisms by workers such as Browner (41) lead to a better understanding and more efficient utilization of nebulizers with flame and plasma sources (42).

b. Auto Samplers

Because the theory of nebulization hasn't yet reached a sufficient level of maturity, automation of the sample introduction process has, for the most part, developed only to the extent of computer-controlled sample turntables or so-called "auto samplers." Auto samplers aspirate liquid samples from racks or carousels into flame or plasma nebulizers in a sequential fashion. The same type of sampler can be applied in atomic absorption analysis by electrothermal atomization. In this case the liquid sample isn't nebulized but is delivered as a small aliquot directly into the atomizer.

In either case, any number of blanks and standards can recur in the analysis sequence. It would be more efficient if one blank and one set of standards could be reused when necessary. Sunderland et al. (43) accomplished this by constructing a random access sampler. In their design, an aspirating tube affixed to a rotating arm is dipped into any one of a number of sample cups arranged about the arm in a circle. The sampling process is computer-controlled.

2. Sample Preparation for Flame and Plasma Sources

Since automation of sample introduction into flame and plasma sources has been hampered by the inefficiency of the nebulization process, automation of sample preparation has progressed only to the level of computer-controlled "auto diluters." More sophisticated automated sample preparation schemes are just in their infancy.

Since nebulization is generally the sample introduction method of choice for these analytical sources, flowing systems such as those used in flow injection analysis (FIA) or high performance liquid chromatography (HPLC) would appear attractive for "front-end" sample preparation. In addition to offering more versatility than the older segmented continuous flow systems, a directly interfaced FIA or HPLC sample preparation system would eliminate the aspiration of air bubbles. This is especially important for inductively coupled plasma sources where aspiration of air between samples can cause destabilization (44). But the interfacing of FIA and HPLC systems to these sources isn't a straightforward matter.

One of the biggest obstacles to the development of these hybrid instruments has been the inability to deliver small liquid volumes to analytical sources which have traditionally used continuous nebulization. As pointed out earlier, 95% of the solution entering a typical nebulizer ends up going down the drain. Obviously then, the effort spent on a complex sample preparation may be wasted if a standard nebulizer is used. Therefore, automation of sample preparation will not advance significantly beyond the level of auto diluters until a highly efficient method of sample introduction is found.

Since the ICP direct sample insertion device (DSID) elaborated on in the body of this work affords the requisite efficiency, the potential of FIA and HPLC "front-end" sample preparation methods for flame and plasma sources will be considered after a brief examination of auto diluters.

a. Auto Diluters

An alternative to Sunderland's (43) random access sampler for improving the efficiency of blank and standard utilization is to automatically prepare the solutions on demand. Malmstadt's (45) "Rapid Sequential Analyzer" incorporates a computer-controlled delivery system which can automatically dilute samples and prepare series of standards from stock solution (46). The system employs a computer-controlled multiport valve in line with reagent reservoirs and an electronic weight sensor for precise liquid delivery.

Various experimental in-line dilution and standardization systems have been interfaced to atomic absorption (47,48) and ICP (49,50) spectrometers and a commercial system called the PS-75 PrepStation is available from Thermo Jarrell Ash Corp. (Franklin, MA).

One of the drawbacks of automatic diluters has been their limited dynamic range. Crouch et al. (51) have devised a microcomputer-controlled reagent preparation system based on stepper motor driven syringes (1 or 5 ml) and dilution vessels (0.1 or 1 l) which can provide a dilution range up to five orders of magnitude with a precision of 0.05% RSD. Although originally intended for wet chemistry kinetic studies, this system has the potential for interfacing to atomic sources. It would be particularly beneficial in the case of atomic absorption spectroscopy (AAS) as the dynamic range of the method is typically one order of magnitude and much time can be lost diluting samples. In fact, it has been pointed out that automation of multielement analysis by AAS may be seriously hindered by the different dilutions required by various elements (26)

b. Flow Injection

An interesting variation of the older continuous flow systems called flow injection analysis (FIA) is receiving increasing attention as a method of rapid sample preparation (52,53,54). Whereas the continuous flow systems described above use air bubble segmentation of aspirated samples, the FIA technique relies on precise injection of samples into an unsegmented flowing stream. Before Beecher et al. (55) and Ruzicka and Hansen (56) reported on FIA 1975, it was thought that air bubble segmentation was necessary in continuous flow systems to prevent excess dilution, generate turbulent flow for mixing, and to scrub the tube walls to prevent contamination. It has since been found, however, that FIA can not only account for these factors, but can in addition offer the advantages of high sample throughput (about 120 per hour), rapid response (less than one minute), variable flow rates and sample dispersion, baseline resolution between samples, no stabilization time, and fast instrument start up and shut down (less than five minutes each) (52,57).

Fitted with an automatic sampler and injector, an FIA setup has the potential of performing all the operations normally handled by segmented continuous flow systems (dialysis, ion exchange, redox reactions, solvent extraction, etc.), not only with the advantages noted above, but also with greater simplicity of operation.

Potential advantages of the union between FIA and ICP are explored in a paper by Greenfield (58). Attractive features include the ability to nebulize samples of relatively high solute content, freedom from viscosity effects, potential for automatic system optimization based on "instant" signal-to-background ratios, and the precise injection of small samples. In addition, it should be possible to carry out automatic dilutions and calibrations with reference standards. Greenfield suggests that calibration plots might be quickly constructed by injecting different volumes of the same multielement standard. Finally, by allowing some mixing of sample and carrier, in-line chemical reactions could be executed for sample preparation.

Some of the advantages of FIA-ICP foreseen by Greenfield are now being realized. For instance, copper can be determined in concentrated matrices (59) and automatic dilution and standardization is possible with a "computer intelligent flow injection ICP emission spectrometry system" (60). The latter development relies on the combination of a 36-channel direct-reading ICP spectrometer and a flow injection system outfitted with a 76-position autosampler. This system can automatically execute the following functions: analysis of undiluted samples, fixed dilution and analysis, sequential dilutions to bring all analytes into an optimum calibration curve range, up to about 200-fold dilution by stream merging, and the addition of standards for standard addition studies.

Greenfield (58) has also discussed some preparation schemes possible with FIA-ICP. In addition to solvent extraction and ion-exchange, he suggests that even hydride generation might be successfully carried out in an FIA system. In fact, reports on the atomic absorption determination of bismuth (61) and arsenic, antimony, and selenium (62) by FIA-hydride generation have appeared recently.

It is interesting to note in this regard that Browner et al. (63) have modified their volatile ß-diketonate preconcentration procedure so that xylene solutions of metal complexes are nebulized directly into an ICP. As their scheme involves a peristaltic pump, they and other "...workers in the field of ICP-AES who already have reliable peristaltic pumps, are more than halfway toward a flow injection system" (58).

There are, of course, other approaches to solution transport in FIA-ICP systems. An inexpensive alternative proposed by Ripson and De Galan (64) relies on argon gas pressure instead of mechanical pumps. The main advantages besides economy are rapid solution transport and pulse-free operation.

HPLC pumps can also provide pulse-free operation but are more expensive than peristaltic pumps. Browner et al. (65) have presented preliminary results for an FIA-ICP system constructed from an HPLC pump and injection valve interfaced to a conventional pneumatic nebulizer. Precisions of about 2% RSD were obtained for 1-50 µl injections of metal ion solutions. This compares well with a precision of 0.5% for continuous nebulization. Pyen and Browner (62) have recently developed another FIA-ICP system providing pulse-free operation for hydride generation. Using pressurized reagent vessels, these authors achieved about 2% RSDs for 750 µl injections of 50 µg/l As, Se and Sb solutions. These results represented a 150% improvement in precision, but the continuous hydride generation method still gave superior detection limits. Perhaps the undesirable tradeoff between precision and detection limits could be overcome with an ICP-MS combination detection scheme (66).

In any case, it is a short step from systems of this type to a more general HPLC/FIA preparation-ICP detection scheme.

c. Liquid Chromatography

Sample preparation by separation on an HPLC column followed by element-specific detection with ICP spectroscopy was separately suggested by Fraley (67,68) and Gast (69) in 1979. Since that time, interesting HPLC-ICP applications including determination of metal chelates (70), nucleotides (71), and the biologically-important arsenic species arsenate, arsenite, methylarsonic acid, and dimethyl arsinic acid (72) have been reported. The III and VI oxidation states of chromium have been speciated (73) and the metals Cu, Cd, Pb, and Zn have been preconcentrated from high salt solutions including seawater (74). The coupling of HPLC to an ICP-mass spectrometer for elemental speciation has recently been described by Thompson and Houk (75).

An automatic sample injector would increase the efficiency of an HPLC-ICP system. Berndt and Slavin (76) reviewed automatic sample injection for discrete nebulization into flames in 1978 and the interfacing of liquid chromatography to flame atomic absorption was referenced. However, since this form of nebulization entails the aspiration of air between small ("discrete") volumes of sample, automatic injection into a continuously-flowing stream would be better suited for plasma sources.

Wolf and Stewart's (77) Automated Multiple Flow Injection Analysis (AMFIA) system incorporated injection of this type. Although their AMFIA was developed for flame AAS, the authors recognized the potential for its interfacing to the ICP.

As pointed out by Ranger (57) in a review of the FIA technique, HPLC is similar to FIA in many respects except that FIA is not restricted to sample separation by column. The two techniques are complimentary and readily combined. Therefore, FIA could be used for in-line pre- or post-column treatments. Interfacing of the FIA/HPLC combination to an atomic source offers the potential of a nearly complete automatic analysis for liquid samples. However, two main problems limit its general applicability at present. These limitations are the inability to handle samples other than relatively "clean" and non-viscous liquids and the poor efficiency of sample transport into the source by nebulization. An additional problem which relates to transport efficiency is sample dispersion during nebulization (33). Discrete sample zones maintained in an FIA line are dispersed when injected into a nebulizer and sensitivity is therefore degraded. This, together with poor transport efficiency, may pose serious problems for trace analysis even if preconcentration is used.

3. Introduction and Preparation of "Difficult" Samples

Generally, a time-consuming digestion is required before solids, viscous fluids, or liquids containing particulates ("difficult samples") can be injected into flowing systems for further preparation and analysis. This is particularly true for flow injection and liquid chromatography instruments where even a low level of suspended solids can foul the precision valves and pumps (78).

The older air-segmented continuous flow systems are relatively immune to fouling and untreated biological fluids are routinely aspirated, digested and analyzed with these instruments. Lubricating oils have been successfully handled with a modified Technicon Automatic Digester (79). Barabas

(80) developed an interesting automated method for rapidly dissolving certain metals and introducing the resulting solutions into a Technicon AutoAnalyzer. Using a small rod of copper or steel as the cathode against a graphite anode in an electrolysis cell, any desired amount of the metal could be dissolved and then routed to the AutoAnalyzer. Phosphorous was determined in copper in three minutes by this method. Steel determinations were degraded by interferences, however, and it can be concluded that the method is useful only for a very limited number of metal types.

In contrast, some liquid samples may need to be preconcentrated if the analytical technique employed lacks sufficient sensitivity. The major techniques used for this purpose are liquid-liquid extraction, ion-exchange (batch, column, and membranes), surface adsorption, precipitation, immobilized reagent extraction, electrodeposition, and solvent evaporation (81). Liquid-liquid extraction, ion-exchange and, in addition, dialysis have all been successfully utilized in the automated clinical continuous flow analyzers described earlier (6).

D. Automated Discrete Systems for Sample Introduction and Preparation

Discrete systems are more flexible than continuous flow systems in that a wider variety of sample preparations can be utilized. However, discrete systems are also more complex since mechanisms such as autopipettes, slider valves or rotating valve pipettes are generally used for reagent delivery (82). In addition, some mechanism for mixing reagents and sample must be provided. The mechanical complexity of discrete systems increases the chances of their breakdown (83).

A system called the automated clinical analyzer (aca, DuPont Company, Wilmington, Delaware) overcomes the main disadvantages of discrete systems in a clever fashion. An individual disposable plastic pack functions as sample compartment, prepackaged reagent container, mixing chamber, and optical analysis cell. As seals in the pack are broken at appropriate times during the analysis by hydrostatic pressure, reagents mix with sample. Mixing is completed by agitation of the pack. For optical measurements, the pack is squeezed into a die so the plastic package itself becomes the analysis cell (84).

Systems such as the aca are sequential since the individual steps of the analysis are carried out on one sample at a time. Efficiency could obviously be improved if analyses were executed in parallel. This was accomplished with the development of centrifugal fast ("continuous rotation" (83)) analyzers by N.G. Anderson at Oak Ridge National Laboratory (ORNL) (85,86). These analyzers rely on centrifugal force for mixing of reagents in many sample compartments simultaneously. In addition to providing micro-volume liquid transfer unaffected by air bubbles, viscosity, or surface tension (87), centrifugal fast analyzers can perform filtration and ion-exchange "on-the-fly" (88). Allied Instrumentation Laboratory (Lexington, Mass.) produces a commercial version of the ORNL centrifugal fast analyzer called the Multistat.

Another interesting discrete parallel single channel system called the FP-901 analyzer has recently been developed by Labsystems Oy (89). The central feature of this system is a Finnpipette with nine tips incorporated into a single disposable block. Nine samples or reagents can be transported simultaneously to a plastic block containing nine test tubes. This block in turn fits into a centrifuge or incubator depending on the procedure. The final unit of the system is a block with nine cuvettes, each with an optical quality window on the bottom. These cuvette blocks are fed into a photometer which measures absorbances of the samples simultaneously. A more elaborate version of this system is both parallel and multichannel (Titertek Multiskan MC, Eflab Oy) in that the absorbances of eight samples can be measured simultaneously and absorbances at different wavelengths can be measured sequentially.

Another method of rapid discrete multichannel analysis has been developed by Malmstadt, et al. (45). The heart of this "Rapid Sequential Analyzer" is a computerized stopped flow module which can rapidly draw and mix reagents and sample and then deliver the reaction mixture to an observation cell. Various wavelengths can also be selected with a programmable monochromator. The system is particularly suited for kinetic studies.

1. "Modular" Systems

The automation of discrete analysis methods for a wider variety of sample types has been promoted in particular by R.W. Arndt (Mettler Instruments AG, Greifensee, Switzerland). Arndt and Werder (6) proposed that assay methods be considered in a modular format. By examining the assays conducted on a routine basis in industrial organic production laboratories, the authors found that two thirds of all the assays utilized only eight basic operations. They therefore suggested "...that basic operations should be automated in order to automate individual analyses. This is in contrast to the development in clinical chemistry where with the automation of serial analysis entire assay methods have been automated."

The success of such an approach would depend on reliable sample transport and flexible control of individual operations. As Arndt and Werder (6) state: "If it is possible to automate a limited number of basic operations and combine them with an infrastructure of transport mechanisms and electronic controls which still allows them to be tailored to the particular situation in the laboratory, then a large part of the analytical workload in a typical laboratory becomes amenable to automation."

The authors caution however, that in addition to reliable hardware, the following criteria must be met if an automated discrete system is to be accepted by its potential users:

(a) the accuracy and reproducibility are as good as or better than with manual work,
(b) the adaptation of assay methods to a machine procedure is achieved simply,

(c) intermediate manual steps remain a possibility,
(d) a system can be built up in a modular manner,
(e) the final design will appear transparent to the operator.

In cooperation with Ciba-Geigy AG (Basle, Switzerland), Mettler commercialized one of the first automated discrete analysis systems which met the criteria outlined above (6). Separate analytical modules capable of performing the basic operations of weighing, dispensing, dissolution, dilution, solid-liquid extraction, and titration could be controlled with a desk top calculator or minicomputer, depending on a particular analytical scheme's complexity. Samples were transported in individual cups between modules on a continuous track. In one particular implementation of this modular system, the operator first identified and weighed the sample with the aid of a sample entry station. This station consisted of an automatic balance and console interfaced to a minicomputer. The sample was then automatically transported through the various stages of a complete titrimetric analysis. Execution of the analytical procedures, data collection and calculation or results were all under computer control. The analysis result and sample ID could be transmitted to other computers for statistical or administrative purposes.

Arndt and Werder (6) state that it was possible to adapt a wet chemical procedure to this system in one to two hours and precisions better than 0.1% could be obtained.

In addition, the system could operate unattended at night and "...200 samples could be analyzed in a 24-hour period, corresponding approximately to the output of 5 to 10 laboratory technicians with currently available equipment."

Arndt and Werder's criteria for acceptable laboratory automation have been refined and expanded in the years since their initial work. A more detailed picture of an acceptable automated system is provided by the former clinical products manager for Hamilton Company, T.H. Crouch (90). He advises that any laboratory supervisor contemplating the introduction of automation into their facility should answer the following questions. Will lab efficiency actually increase? Will the lab personnel be able to perform other duties? Do the errors of manual sample preparation really warrant more accurate automated methods? Will the automated system use smaller amounts of costly reagents? Will the automated system be adaptable to the available plumbing and electrical supplies? What are the real costs of supplies and maintenance and does anticipated growth and change justify a large initial capital outlay?

Crouch's concerns are echoed by B. Howard and coauthors in their review of the 1987 Pittsburgh Conference: "Improving the efficiency of sample handling is still a major challenge to the instrumentation industry. Such systems are expensive and require laboratory managers to undertake a careful evaluation of needs and procedures" (91).

Attention to the real issue underlying all these questions - the economic impact - has promoted a trend in laboratory automation away from the original continuous track-based systems to newer robot arm-based or "robotic" systems (92). As B. J. McGrattan and D. J. Macero point out in a review entitled "Laboratory robotics-Past performances, present considerations, and future trends;" "This interest in robotics exists because there is a gaping hole in the automated laboratory: the automation of physical manipulations" (93). And as J. G. Liscouski, a vocal proponent of laboratory robotics, stated recently, of the three key trends in laboratory automation (communications, expert systems, and robotics), it is robotics that is addressing "...the remaining human intensive portion...sample preparation" (94).

2. Robot Arm-Based or "Robotic" Systems

The Institute of Scientific Information (ISI) defines robotics as the "...technology concerned with the design, construction, and operation of robots in automation" (95). The growing interest in robotics in general is reflected in a 516% increase from 1981 to 1984 in the appearance of the term robotics (from 63 to 388 occurrences) in the titles of source items indexed by the ISI (95). The term robotic is used in the current analytical chemistry literature in reference to both the simple extensions of the random access sample changers discussed earlier and the more flexible systems based on light-duty robot arms. In the former case, the term "microrobotic" is often applied. For instance, Varian's 9090 autosampler is referred to by its designers (96) as an application of microrobotics. This liquid chromatography sample preparation device uses a 105-position random access carousel in conjunction with a syringing system to mix, extract and dilute samples in their vials before injection into a liquid chromatograph.

If a robot is defined simply as "A machine or device that works automatically or by remote control" (97), then perhaps units like the Varian 9090 could be correctly referred to as microrobotic devices. But the term robot actually has a quite different original meaning. In his 1920 play "R.U.R." (Rossum's Universal Robots), the Czech author K. Capek (98) invented the term robot as a label for "A mechanical apparatus that resembles a human being and is capable of performing human tasks or behaving in a human manner" (97).

It is these more humanoid robots that are really attracting the attention of various production industries. And as R. Dessy points out in a two part review (99,100) entitled "Robots in the laboratory;" "...there is an obvious analogy to be made between the industrial and analytical laboratory use of robots;

> In production-line applications the quality of product is increased and the cost is decreased by installing robots capable of identification of objects, parts insertion, grinding, welding, painting, and palletizing. The analytical laboratory is a production environment in which it is necessary to identify samples, and then aliquot, dilute, concentrate, extract, crush or grind, filter, or move them prior to analysis.

Dessy goes on to say that "The industrial use of robots is driven by the simple fact that where human labor costs about $20/h, robots cost about $5/h." Interestingly, an important conclusion of an almost two decade old review of clinical laboratory automation (83) is as pertinent today as it was then; i.e., that "As wage rates continue to rise and skilled help becomes scarcer, the robot's utility will become more attractive." Again we see that it is really cost control that is driving the development of automation.

Large robots are beginning to bridge the gap between industrial and laboratory applications. For example, Sandia National Laboratories of Albuquerque, N.M. will be the first integrated circuit (IC) research and prototype facility to use a robot with access to all stations of a fabrication line (101). Since robots are ideally suited for situations where contamination needs to be kept to a minimum, a good application of robots is in clean room operations. The Sandia facility will realize this benefit, and in addition will maximize process repeatability, as the robot moves from station to station along a reflective tape track in a large clean room.

Like the "automated" instruments mentioned in the early part of this discussion, few industrial or laboratory robots are truly automated. According to G. Chacko (102), professor of systems science at the University of Southern California, the U.S. needs to develop "heuristic" robots in order to increase productivity and compete with the Japanese. A heuristic robot should be capable of constructively interacting with its environment based on what it has previously learned, in other words, a feedback loop needs to be established (perhaps with machine vision) between the robot and its environment. Chacko points out that much work remains to be done with software in order to close this feedback loop since current expert systems don't deal with interacting variables and participants. The closing of this feedback loop is critical for chemical applications since, as McGrattan and Macero (93) state; "The chemistry laboratory is too dangerous a place for a robot that does not actively interact with its environment."

The realization of a heuristic robot will no doubt require not only advances in software, but hardware developments like those mentioned in the initial discussion of analytical laboratory automation.

These introductory considerations of heuristic robotics versus microrobotics brings attention to a current controversy about the proper way to implement the automation of sample manipulation in the analytical laboratory. Whether one takes an economic perspective like Dessy's, or the perhaps more esoteric view which considers the advantages of robotics only in terms of reduced contamination, increased precision, and manipulations in hazardous environments, there is no doubt that there is an important role for robotics to play in the analytical laboratory. But exactly what form analytical laboratory robotics should take has not been settled.

Some chemists feel that since human motor and cognitive abilities are so advanced, robots can't function in the lab as a human would. Comments by workers at Dow Chemical Company (Midland, MI.) (103) illustrate this position. They state that since it would be too costly to mimic completely human performance, the robot's "task performance" must be modified. In other words, "It is not essential to exactly emulate humans for successful implementation of robotics. Rather, the tasks must be optimized for the robot's capabilities" (103).

This "task optimization" really equates in most instances to "instrument optimization;" the modification of existing instruments to fit the limitations of a particular commercial robotics system. But optimization of individual instruments is a time-consuming and expensive proposition. For instance, the experiences of workers at Procter and Gamble Co. (Cincinnati, Ohio) (100) in applying robotics to laboratory automation has shown them that a large fraction of development time is spent building specialized mechanical devices for individual instruments. Therefore, these and other workers are "...look[ing] forward to the development of more intelligent and low cost robots equipped with complete position feedback and error recovery capability."

This enhanced robot flexibility is not likely to result from the simple addition of more detailed program steps. What is needed is a breakthrough in, for example, machine vision so there is better sensor interaction with the environment. Although as R. Dessy has observed: "The magnitude of the information flow and the difficulties in emulating the pattern recognition capabilities of the human eye-mind combination make robot vision a formidable task" (99). Once the necessary breakthroughs have been achieved, instrument modification will no longer be necessary and "...general laboratory equipment [could] be used as much as possible so that robot operations conform closely to the way a human would work" (93).

It might seem that the realization of this scenario is far into the future, but robots are rapidly becoming more humanoid. For example, Universal Machine Intelligence Inc. (Ann Arbor, Michigan) is offering a robot arm called the RT-X with abilities placing it somewhere between industrial robots and small robot arms (104). This 6-axis, 8 lb payload, 27 inch reach arm can work between floor and tabletop height with 1.1 m/s velocity and ± 0.018 inch repeatability. A force control safety feature makes this robot "coworker friendly." The company plans to offer a mobile version with two RT-X arms, vision, speech recognition, tactile sensing and interchangeable grippers. And robotic vision systems are evolving ("coevolving?") along the lines of human vision. For example, the Naval Research Laboratory in Washington, D.C. has developed a robotic crystallization chamber which incorporates the optical recognition of crystals (105).

Most of today's commercial laboratory robotics systems incorporate Zymark or Mitsubishi robot arm hardware (106). The first robot arm application in chemistry referenced in the literature (107) used a Minimover-5 robot (Microbot, Menlo Park, CA). The Minimover and Mitsubishi robot arms are very similar in construction and mimic the human arm whereas the Zymark arm has fewer axes of motion.

Relative to the older fixed-track mechanisms, light-duty robot arms give greater flexibility in sample transport between analysis stations. In fact, two new laboratory automation systems combine robot arms with movable tracks for an additional level of flexibility. Fisher offers an overhead track system and Perkin-Elmer's (Norwalk, CT) MasterLab II system has a five-axis articulated arm and an optional linear transport device provides a sixth axis of motion (105).

In accordance with the modular approach suggested by Arndt and Werder (6), the new robot arm-based systems emphasize the automation of basic or "unit" lab operations. For instance, the Zymate II (Zymark Corp.) incorporates FASTPak (Fast Applications and Startup Techniques Package) software for common lab unit operations including pipetting, capping, dispensing, centrifuging, weighing and powder pouring (4). As in the earlier Ciba-Geigy system, analysis results from these robotic systems can be forwarded to a minicomputer system such as the Digital Equipment Corp. VAX LIMS (laboratory information management system) (108).

Robot-based laboratory automation systems have recently been applied to drug dissolution measurements (109,110), quality assurance procedures in an oil industry lab (111), the determination of caffeine (112), GC derivitization analysis (113), electrochemical measurements and the electroplating of semiconductors (93), complexometric analysis (114), gaseous sample collection and injection (115), and the analysis of antipyrine in human serum (116). A robot arm has even been used to prepare a GC-flame ionization detector (FID) interface too delicate to prepare by hand (117).

Robots have also been used in organic synthesis. G.W. Kramer and coworkers at Purdue University have developed the

Purdue Automated Synthesis System (PASS) in response to the labor-intensive problem of optimizing reaction conditions by repetition (118). A vial transport system is used to pass samples between synthesis and analysis robotic workstations.

This recent progress is certainly impressive, however, it must be kept in mind that although these discrete systems are more flexible than continuous flow systems, much remains to be done when a broad range of sample types and desired analyses is considered.

For instance, although the titrating module in the Ciba-Geigy system described by Arndt and Werder (6) can automatically dissolve solid samples and a solid-liquid extraction unit can grind them, the "solids" consist of pharmaceutical tablets. The grinding and dissolution of, for example, rock samples is a different story. In addition, like the clinically-oriented discrete and continuous flow systems described earlier, the final determination is carried out electrochemically or spectrophotometrically. Presentation to an atomic source would involve the various difficulties already discussed. It is probably more difficult procedures such as these that Arndt and Werder had in mind when commenting on future developments: "Some basic operations may be automated in a straightforward way; others will necessitate more refined, or even new, technology and will take longer to become available" (6).

E. Summary of Trends in Automatic Sample Introduction and Preparation and a Proposal for a New Direct Sample Insertion Device for the ICP

The examples cited in this introduction reveal an accelerating trend toward the complete automation of sample introduction and preparation in the analytical laboratory. Although the major gains in this area have historically been confined to the clinical analysis of relatively "clean" fluids, there is a growing interest in the automation of methods for the analysis of more "difficult" samples. Based on this trend, one can now consider what further development in sample introduction and preparation would make a significant contribution to analytical chemistry.

The automatic clinical methods generally employed colorimetric "finishes," but a newer and more flexible finish should be considered if automatic methods for diverse samples are to be developed. Automatic methods employing final analysis by atomic emission would cover the broadest range of sample analysis problems and as far as an atomic emission source is concerned, the inductively coupled plasma (ICP) would be the logical choice. The ICP offers high temperature, wide analytical dynamic range, low background and relative freedom from chemical interference effects. Once this source is chosen, the goal is to find a way of introducing a wide variety of sample types while at the same time retaining the ICP's attractive capabilities.

It is proposed that a device that directly inserts solid or liquid samples into an ICP-the Direct Sample Insertion Device or DSID-can not only attain this goal, but at the same time can ameliorate some of the ICP's important limitations.

As the authors R.F. Browner and A.W. Boorn (28) note in their review "Sample Introduction: The Achilles' Heel of Atomic Spectroscopy?," good sample transport between the vaporizer and plasma is critical for optimal ICP performance. The DSID is expected to meet this important criteria perfectly since the sample will vaporize **from a point inside the plasma**. Preparation (drying and ashing) of the sample at selectable positions just below the plasma will insure that the main benefits of the ICP source mentioned above will be preserved and enhanced.

As Browner and Boorn (28) point out, the solvent normally nebulized with a sample can reduce an ICP's temperature. The DSID's ability to temporally separate solvent evaporation from sample volatilization by preparation below the plasma will eliminate this problem. In regard to sample introduction by nebulization, Browner and Boorn (28) also note that discrepancies in interference and detection limit data may actually be due to variations in drop size distributions, not poor technique. These discrepancies will of course also be eliminated by preparation and direct insertion of the sample with the DSID. The ability to automatically prepare samples below the plasma before insertion is expected to significantly enhance the ICP's capabilities.

The trends in automatic ICP sample preparation are nicely summarized by R. M. Barnes in his review for Spectroscopy (119) entitled "Sample Preparation and Presentation in Inductively Coupled Plasma Spectrometry."

He observes that even though "Most samples appear in the laboratory in a form that may not, and probably does not, correspond to the optimum one for both the information sought and the spectrochemical measurement to be made," progress

> ...appears to to have concentrated upon dispensing and diluting samples, and the full potential of automated digestions and enrichment techniques has yet to be explored with ICP spectrometry. To summarize the message-to enhance the effectiveness

of an ICP measurement, automatic premeasurement chemistry procedures are essential.

Not only is the DSID expected to offer convenient premeasurement preparation of liquids, it should also be able to directly handle more "difficult" solid samples. This ability will significantly enhance ICP measurements since, as Barnes (119) observes: "The means to deal with sample forms other than liquids also remains an unresolved complication [of ICP spectrometry]."

The trend in mechanical implementation of sample introduction and preparation is toward robotics and the DSID will be designed in accordance with this trend. The DSID-ICP will then be capable of the type of efficiency that, for example, Procter and Gamble Co. (100) achieved with their robotic NMR system. Using a robot with a four foot long translation base for automatic fat sample delivery to an NMR, they realized a 600 person-hours per year savings.

In terms of the computer's role in an automatic system of this type, we agree with the Procter and Gamble Co. investigators' (100) conclusion "...that the full power of the microcomputer in the laboratory environment would not be felt without a flexible, articulate mechanical interface."

We understand that a significant gain in efficiency won't be realized without proper planning. As Frank Zenie, president of Zymark Corp., has warned (105): "Nearly every robotic application has a degree of uniqueness to the system. This may be a roadblock to robot use unless creative problem solving and careful planning are used to overcome obstacles." The investigators at Procter and Gamble Co. (100) further caution: "Each application has different requirements for these devices and the success of the entire system rests on their reliability."

Considering these qualifications, a compromise will be found somewhere between a "micro" and "heuristic" robotic implementation of the DSID. The idea that interfacing to a future robot arm-based system should be straightforward will be kept in mind as some specialized equipment is developed for interfacing to the ICP. Therefore, the DSID will be designed to appear as a module or "station" to a more advanced laboratory automation system.

The expense of specialized interfacing to the ICP will be offset by significant gains in ICP performance and flexibility. To quote Barnes (119) again:

> Automated sample preparation based upon robotics, flow injection, and intelligent instrumentation (such as computer-controlled sample digestor) have the potential for resolving many of the remaining problems in ICP-AES and for minimizing new problems

being uncovered with ICP-MS. The cost of added front-end equipment to achieve these premeasurement treatment steps is justified by the improved capabilities of the ICP spectroscopy that would result.

In order to put our DSID design in perspective, a review of the progress in automatic direct sample insertion for atomic emission spectrometry with flames and plasmas is presented in the next chapter. It should be noted at this point that although initial reports by Sommer and Ohls (120) and Kirkbright et al. (121, 122, 123) were included in this review for completeness, they appeared in the literature after this thesis research was well underway. The present thesis research was undertaken in an effort to both expand the capabilities of and to automate the direct sample insertion technique originally reported by Salin and Horlick (124) for the ICP.

Chapter III details the design and construction of an automated DSID capable of significantly reducing the imprecision inherent in Salin and Horlick's (124) original manual apparatus (Figure 1). Reproducible sequential delivery of samples into a stable and continuously running discharge was desired. Major modifications of existing plasma sources or addition of complex and cumbersome devices

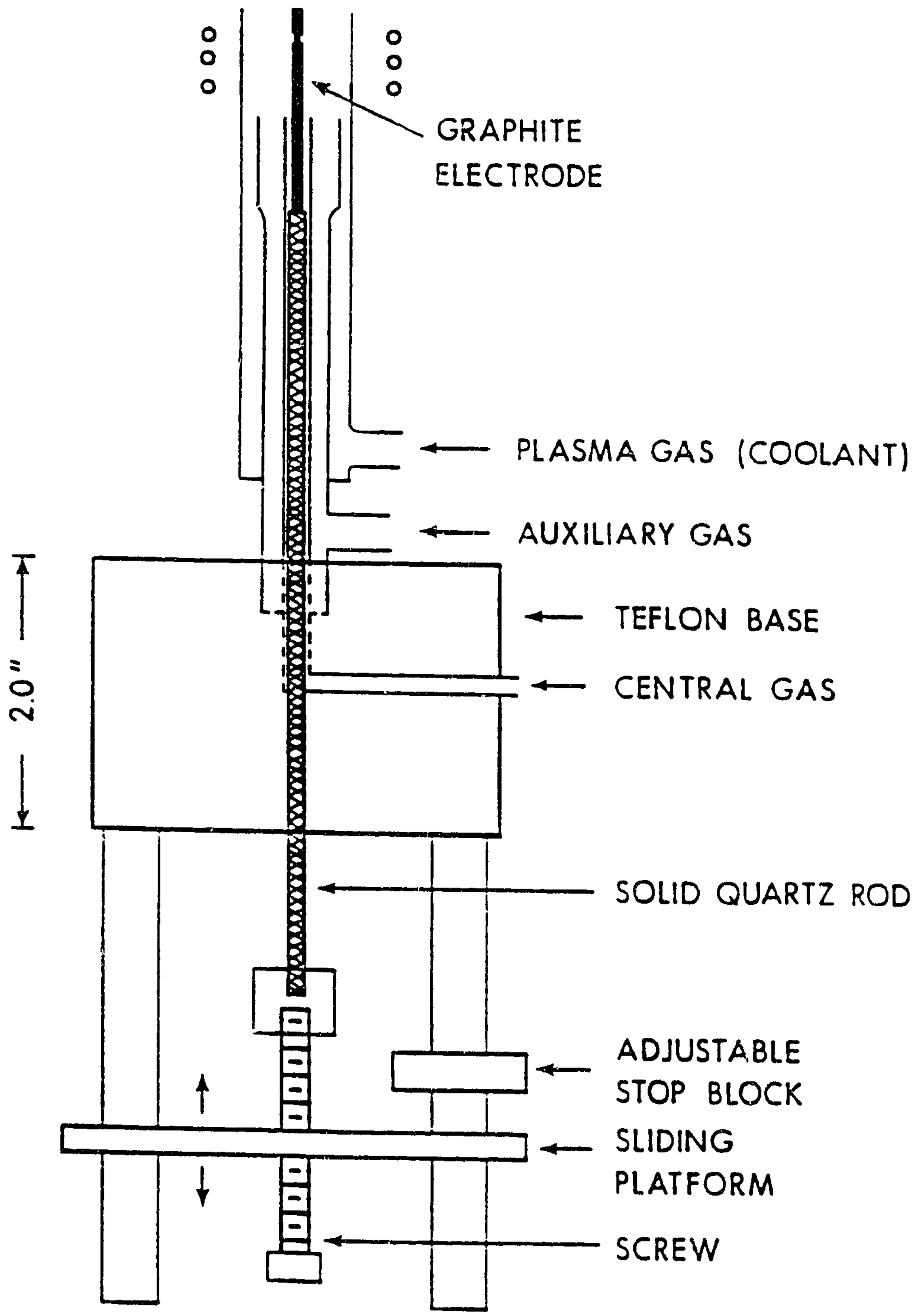
GRAPHITE ELECTRODE
PLASMA GAS (COOLANT)
AUXILIARY GAS
TEFLON BASE
CENTRAL GAS
2.0"
SOLID QUARTZ ROD
ADJUSTABLE STOP BLOCK
SLIDING PLATFORM
SCREW

Figure 1. Original manual insertion device.

to these sources was to be avoided. A pneumatic approach to sample delivery fulfilled these requirements in a straightforward fashion (Figure 2). Samples were transported upward with argon gas and gravity returned them downward. The drilling of a small hole to allow passage of a pneumatic delivery tube was the only plasma source housing modification required. Samples could be sequentially exchanged at the lower end of this tube without disturbing plasma operation.

Chapter IV describes the development of the data acquisition system required for the investigation of both time resolved and integrated optical emission behavior of various samples after direct insertion into the plasma discharge. An understanding of emission behavior would hopefully result in extended analytical working ranges and low detection limits for analytes in a variety of sample types by intelligent manipulation of experimental parameters.

The design of a DSID-based automatic sample preparation system is described in Chapter V and the DSID's performance in the analysis of liquid and solid samples is detailed in Chapter VI and VII, respectively.

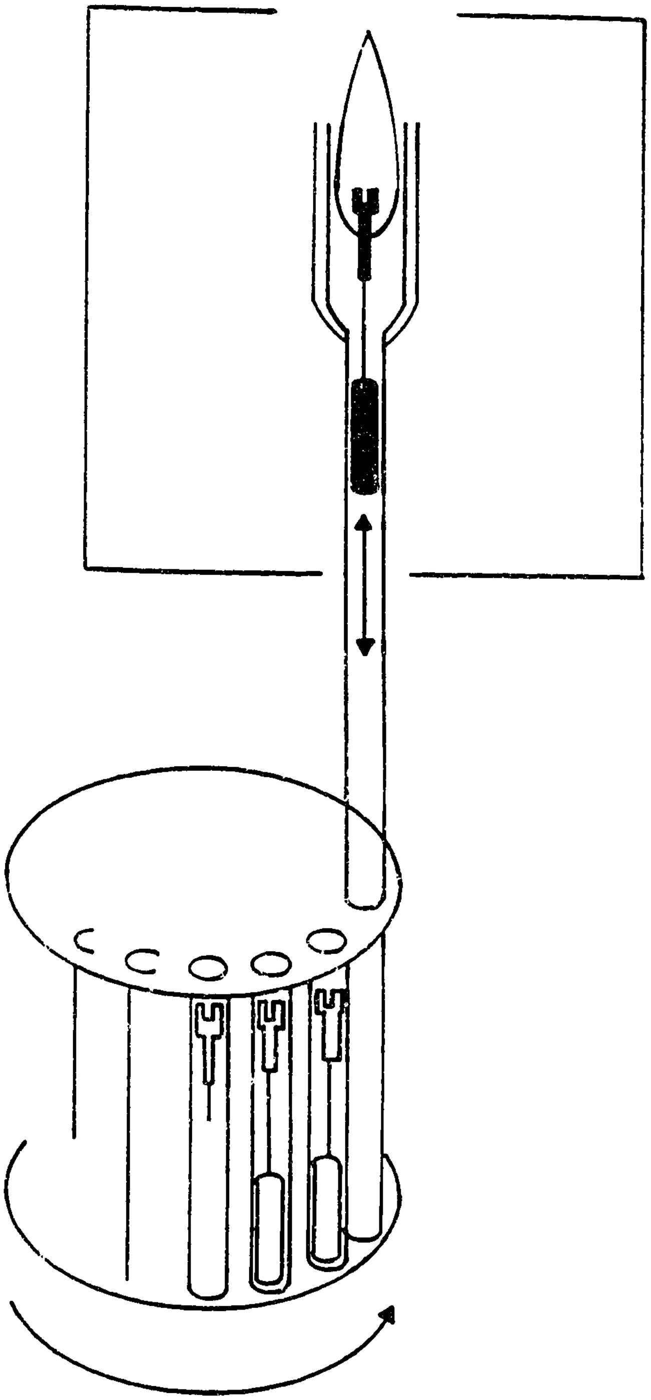

Figure 2. Automatic pneumatic insertion system concept.

CHAPTER II

DIRECT SAMPLE INSERTION FOR THE ICP: A REVIEW

A. Introduction and Historical Perspective

This chapter will deal with the progress made in direct sample insertion into flames and plasmas for atomic emission spectrometry. Particular attention will be given to µl-volume solution, powder, and solid samples. It is the analyses of samples of these types which are currently receiving much attention and which would benefit from automation. Table II.1 provides a quick outline and some figures of merit for the more important historical advances in direct insertion.

1. Wire-in-Flame

Kirchhoff and Bunsen's wire-in-flame method is an historical landmark in spectrochemical analysis (125). Although Marggraf had observed the difference in colors imparted to a flame by sodium and potassium nitrate in 1762, and Talbot had made similar observations in 1862 by burning a wick treated with various sodium and potassium salt solutions

TABLE II.1

ADVANCES IN DIRECT SAMPLE INSERTION FOR FLAMES

Technique	Flame Type	Matrix/ sample size (sample/hr)	Element	%RSD/ Level (D.L.)	Yr./ Ref.
Wire-in flame	air/coal gas	aqueous/nl (10)	Na	3/ng	'50/ 127
Wire-in-flame (air piston)	air/coal gas	aqueous	K Na	28/60pg 17.5/40 pg	'53/ 128
Wire-in-flame (motor drive)	air/ propane	serum, urine/0.2µl	K, Na	pg	'60/ 129
Wire-in-flame	air/ hydrogen	urine/0.1-1nl	K, Na	pg	'67/ 130
Wire-in-flame	air/ acetylene	0.5-2µl	Ag, Cu, Mg, Mn, Pb	(ng)	'69/ 132
Boat-in-flame	air/ acetylene	methanol/ 1ml urine, 15% aq Bi/1ml	As Pb	(0.1ng Ag (aq))	'68/ 133
Delves cup	air/ acetylene	blood/10µl (>15)	Pb	4/3ng	'70/ 134
Delves cup	air/ acetylene	blood/10µl (30-50)	Pb	10-15/0.3 mg/ml	'71/ 136
Wire-in-flame	nitrogen/ hydrogen	aqueous/5µl	Hg	(170pg)	'72/ 138

Continued...

TABLE II.1 (Continued)

Technique	Flame Type	Matrix/ sample size (sample/hr)	Element	%RSD/ Level (D.L.)	Yr./ Ref.
Cup-in-flame	air/ acetylene	rock/mg	Cd	20/10 ppm	'72/ 140
		KCl/mg	Li	20/1ppm	
Delves cup	air/ hydrogen	aqueous/ 10µl	Tl	3.4/5ng	'74/ 145
Cup-in-flame (Pt/Ir cups)	nitrous oxide/ acetylene	aqueous	Co, Cr, Cu, Fe, Ni	(ng)	'75/ 146
Delves cup	air/ acetylene	urban air particulate on cellulose filters (21)	Pb	10	'80/ 149
Delves cup	air/ acetylene	grasses, orchard & tomato leaves/20µl	Pb	5/0.072 -240 µg Pb/g dry veg.	'81/ 150
Paper rolls	air/coal gas	mushroom parts	Ag, Ca, Cu, Fe, K, Li	semi-quant photo-plate	'30/ 151
Screw threads	air/ acetylene	rock samples/ 70mg	Rb	4/390 ppm	'71/ 154

(126), it is the original papers by Kirchhoff and Bunsen elaborating results for alkali and alkaline earth elements that "...mark a clear departure from previous works, as well as the beginning of spectrochemical analysis. In combination, the colorless Bunsen flame, one of the first spectroscopes, and Bunsen's chemical knowledge and skill, which insured that all salts were highly purified, provided unprecedented experimental reliability" (125).

Although in 1874 Truchot reported on the insertion of a platinum spiral into a Bunsen burner flame for the analysis of solutions (126), it was not until 1950 that any significant advance was made in wire-in-flame determinations. In this year Ramsay (127) at the University of Cambridge reported on a mechanical device for the insertion of small volume solutions into an air-coal gas flame. The aim was to determine sodium in solution volumes which could not be handled by nebulizer-flame photometry. Solutions of 1 nl volume were pipetted onto a platinum wire, dried, and inserted into the flame. Using a simple spectrometer, PMT detection, and integrating readout, Ramsey could detect about 0.5 ng NaCl with about 3% RSD. The cycle time was about 10 samples per hour.

A more elegant sample delivery system was constructed by Ramsey, Brown and Fallon (128) in 1953 based on a compressed air piston and spring retraction unit mounted on a swinging carriage. A two channel optical system permitted simultaneous determination of Na and K down to 0.04 ng (17.5% RSD) and 0.06 ng (28% RSD), respectively. The authors also noted variations in peak shapes in signal oscillograms and recognized that the time constant of their detection system wasn't fast enough for signals of less than one second duration.

Ramsey's method was taken up by Bott (129) in the USA. She upgraded Ramsey's insertion device with a motor drive and extended analysis to 0.2 µl serum and urine samples. Sodium and potassium could be determined in these samples at the pg level. Similar work was undertaken in Sweden by Oberg, Ulfendahl, and Wallin (130). They quickly and reproducibly aliquoted 0.1 to 1 nl urine volumes (<10% error) by dipping a Pt-Ir wire loop into an oil bath containing sample droplets. Volumes were calculated by measuring particle diameters with the aid of a microscope. A two-channel instrument (Na and K) was devised incorporating photocells and operational amplifier integrators. The smallest sample analyzed by direct insertion of the Pt-Ir wire into an air-hydrogen flame contained about 0.004 ng of K.

Ramsey's original work was further extended in the USA by Katz (131) in 1968. He noted that signal peak shape was related to the mass of the platinum loops, pans, and buckets inserted into his air-propane flame. Pretreatment of the platinum with $BaCl_2$ eliminated prolonged temporal behavior for KCl and NaCl. He could deduce the anion (Cl^-, OH^-, SO_4^{2-}, HPO_4^{2-}) in sodium salts by observing differential temporal behavior. Katz also proposed independent heating of the Pt wire by electric current and suggested that "...the resulting emission signal would be a spectrum based on evaporation temperatures much like that which a spectrophotometer generates based on wavelength."

The integral flame method pioneered by Ramsey was also investigated in the USSR. In 1969, L'vov and Plyushch (132) extended the method to Mg, Mn, Cu, Ag, and Pb by first drying 0.5 to 2 µl aliquots on tungsten wire loops and then inserting the loops into an air-acetylene flame. Absolute sensitivities in the ng range were achieved and a 100-fold excess of $Al(NO_3)_3$ caused no interference with the determination of Mg at this level. The authors suggested that low volatility elements might be successfully determined by employing a carbon arc-in-flame.

L'vov and Plyushch's wire-in-flame method differed from the earlier work in that atomic absorption and not emission was employed. In the previous year (1968) Kahn, Peterson, and Schallis (133) had suggested atomic absorption measurement for pulsed vaporization an air-acetylene flame and L'vov and Plyushch made reference to this work.

2. Boat-in-Flame

Kahn et al. (133), at Perkin-Elmer in Connecticut, were interested in improving the sensitivity of AAS. They felt that a boat-in-flame approach would offer a simple alternative to the L'vov and Massman electrothermal devices. Solutions of 1 ml volume were loaded into a tantalum boat and dried at the periphery of an air-acetylene flame. Insertion of the boat into the flame then gave a pulse of analyte vapor. Peak height absorption measurements resulted in improvements in detection limits for 10 elements from 5-fold (As) to 65-fold (Zn) relative to nebulizer-flame AAS. Lead was successfully determined in urine and in the presence of 15% bismuth and arsenic was determined in methanol, all without standard additions.

3. "Delves Sampling Cup" Techniques

In 1970 Delves (134), at the Hospital for Sick Children at London University, modified the Perkin-Elmer group's boat-in-flame method to accommodate the determination of lead in small blood samples. Whole blood samples of 10 µl volume were pipetted into nickel-foil microcrucibles, dried, and partially oxidized with hydrogen peroxide. After placing a nickel crucible in a platinum wire holder, it was manually introduced into an air-acetylene flame with the aid of a mechanical guide. Reproducibility was improved by suspending a nickel absorption tube in the flame just above the sample crucible. Sample vapor then entered the tube through an orifice in its bottom surface and then diffused out the tube ends. The light from a lead hollow cathode lamp was directed through the absorption tube. Problems with sensitivity variations due to inconsistency of beam profile in the flame above different crucibles was therefore eliminated. In his 1970 paper (134), Delves credits a 1969 conference paper by R.A. White for the absorption tube idea.

Using this technique, Delves could determine lead in blood at the 3 ng level with ±4% standard deviation with less than four minutes spent per sample. His approach generated much interest so it and similar methods came to be known collectively as "Delves Sampling Cup" techniques.

In the same year Kahn and Sebestyen (135) at Perkin-Elmer extended their boat-in-flame work to the determination of lead in blood but it was not until Fernandez and Kahn (136) adopted the Delves cup method that an efficient commercial system was devised. The latter workers achieved a cycle rate of 30-50 blood lead determinations per hour using off-line batch sample preparation. The authors noted, however, that if better than 10-15% RSD at the 0.3 mg/ml level was desired, careful matching of crucibles (in terms of sensitivity) was necessary. No sign of crucible deterioration was evident after 40 runs but gradual destruction of the nickel absorption tube necessitated "periodic" replacement. Just as in the original Delves method, standard additions were necessary for calibration.

Kerber and Fernandez (137) went on to determine nine relatively volatile elements in addition to lead with the Delves Sampling Cup method. Reported absolute detection limits for most of the elements were as good or better than those achieved with the earlier boat-in-flame method. Selenium and tellurium had poorer detection limits, however.

In the UK, West and coworkers (138) extended the Delves method to mercury by inserting tungsten wire loops below a nickel absorption tube in a nitrogen-hydrogen diffusion flame. A detection limit of 0.17 ng Hg (5 µl sample volume) was reported but double absorption peaks were noted at this level.

The need for standard additions in the Delves method for Pb in blood and urine was overcome by Olsen and Jatlow (139).

They pretreated their nickel cups with dilute albumin solution prior to the addition of aqueous standards. These standards contained NaCl to compensate for molecular absorption effects. Their Perkin-Elmer instrument was an improved version incorporating a more resilient silica absorption tube. An "Inconel" cup holder also replaced the earlier Pt-Ir supports.

Solid sample analysis utilizing the microcrucible-in-flame method (no absorption tube) was reported by the Russian worker Prudnikov (140) in the same year (1972). Using platinum crucibles, mg-size samples, and an air-acetylene flame, lithium was determined in KCl by emission and cadmium in rock by absorption at the 1 * 10-6% and 1 * 10-5% level, respectively, with RSDs on the order of 20%. The author attributed the poor precision to the measurement technique. As with all the cup-in-flame methods described so far, signal peak height measurements were used. Aqueous calibration standards were closely matched in composition to specimens.

Several further refinements of the Delves technique were reported during the 1970s. Screening of blood samples for both lead and cadmium using an APDC/MIBK (ammonium pyrrolidine dithiocarbamate/methyl isobutyl ketone) extraction system was reported by Joselow and Bogden (141). Ediger and Coleman (142) avoided the preoxidation step in blood cadmium determination by charring the sample outside the flame. However, standard additions were required and the authors admitted their procedure was "...difficult to use in that it (required) meticulous attention to detail." Peak area absorption measurements were advocated by Aldous et al. (143) to reduce the dependence of analyte vaporization rate on sample matrix and differences between sample cups. Fernandez (144) made detailed study of the influence of absorption tube and cup alignment, burner stabilization, sample collection and contamination, pipetting procedure, and standardization on the accuracy and precision of blood lead determinations.

An atomic emission and fluorescence version of the Delves method was developed by Grime and Vickers (145). Since the absorption tube was eliminated, meticulous alignment wasn't required and rapid switching between continuous nebulization and the discrete system was then possible. A pivoting device aided manual transport of nickel cups between a hot plate for drying and a nitrogen-sheathed air-hydrogen flame. Thallium could be detected by fluorescence at the 0.5 ng level in a 10 µl aqueous sample. At ten times this level an RSD of 3.4% was obtained. As the same cup was used for all determinations, a 60 s cooling cycle was required.

A hotter flame was advocated by Mitchell et al. (146) in order to extend the Delves method to less volatile elements. These authors employed a ceramic absorption tube suspended in a nitrous oxide-acetylene flame and tungsten, ceramic, and platinum-iridium sample supports. The best sensitivities were obtained with tungsten strips but platinum-iridium cups gave superior precisions. Detection limits in the ng range were reported for Cr, Co, Cu, Fe, and Ni.

This first hot flame system apparently suffered from the disadvantages of explosive flashback and sample cup, cup holder, and absorption tube degradation. Kahl et al. (147) designed a new system to overcome these initial problems. A silicon carbide absorption tube was suspended in the laminar flame of a special pre-mix burner. Molybdenum cups and support loops were injected with a stable mechanical device and cooled in a nitrogen sheath on retraction. The cups were usable for about 50 runs.

A renewed effort to automate the Delves method was undertaken more recently by Pachuta and Cline-Love (148). They developed a hard-wired logic controlled injector which could pick up a cup from a 36-position tray, deliver it into an air-acetylene flame, and then return it to the tray. The authors also designed an analog transient signal integrator into the system for precise peak area measurements. Peak profiles reflected the physical condition of the nickel cups and analyte vaporization rates. Signal peak areas could be used to monitor atomization collection efficiency and residence times and to compensate for vaporization interferences.

The authors found that between-cup variability in lead determinations by peak height accounted for 40-60% of the overall RSD. This error was eliminated using peak area measurements. It was also noted that sensitivity was degraded for older cups if peak heights were used. Pachuta and Cline-Love's system had a 43 s cycle time and was well-suited for off-line batch sample pretreatment. In contrast to earlier manual systems, the operator was free to prepare the next batch of samples and evaluate data as a tray of samples was automatically analyzed. The authors also pointed out that their system avoided the lengthy dry-ash-atomize-workhead cooldown cycles encountered in electrothermal furnace instruments since their source (flame) was always "on." The same advantage would also apply in principle to all the Delves-type methods described earlier.

Pachuta and Cline-Love (149) employed their auto-Delves system in the determination of lead in urban air particulates. Disks of 0.50 cm2 area were punched out of the cellulose filters used in a high-volume air sampler, placed in nickel cups, and directly inserted into the flame. They found that "instant ashing" gave better results than various pretreatments although the ash would occasionally be ejected from a cup before completion of signal recording. The use of synthetic standards prepared from lead-spiked cellulose disks provided results in accord with XRF and nebulizer-flame AAS data. Precision averaged about 10% RSD compared to 4% for aqueous standards. The authors attributed the differences in precision to differences in sample combustion patterns. Average daily urban lead particulate levels range from about 0.1 to 10 μgm-3 and their technique provided between-day consistency of ±0.1 μgm-3 or less at these levels. A sampling rate of 21 runs per hour was achieved.

Another example of solid sample analysis by the Delves cup technique was recently reported by Jackson et al. (150). They obtained fairly representative sampling of grasses, orchard and tomato leaves, and clover by suspending 0.5 g of dried and ground vegetation in 10 ml of deionized water and then pipetting 20 μl aliquots of this suspension into nickel Delves cups. The sample was then dried at 110°C and inserted into an air-acetylene flame for atomic absorption determination of lead. Standard additions provided linear calibration over the range 0.072 to 240 μg lead per gram dry vegetation with a precision of about 5% RSD. This method was well-suited for environmental impact assessment of roadways and land-fill sites using indigenous plants as indicators.

4. Other Methods of Direct Solids Introduction

There have been a few reports of discrete solids analysis using thermal vaporization and excitation which are sufficiently different from the wire-in-flame or Delves method to be mentioned separately. In 1930, Ramage (151) determined K, Li, Ca, Cu, Ag, and Fe in mushroom parts by wrapping dried portions in filter paper, inserting the rolls into a flame and recording emission with a spectrograph. Semiquantitative results were obtained by spectral comparison with standards (presumably aqueous) photographed on the same plate used for samples.

Ramage's method was adapted for routine use by Roach (152) in 1939. He found that the "Reproducibility of results depended on the uniformity of feeding the roll into the flame. This was made difficult by the roll bursting into flame just outside the oxy-coal-gas flame." This problem was overcome by carbonizing the sample packet before insertion. Conversion of minerals to their chlorides by immersion of the carbonized packet in ammonium chloride vapor further increased reproducibility. Sample rolls impregnated with known mixtures of salts were used as standards and semiquantitative results were obtained by spectrographic comparison. Roach attributed increased variation of leaf sample results relative to replicate solution analyses to sample inhomogeneity. Variation in results of solution-impregnated paper analyses was thought to arise from inconsistent burning. The method was adequate for a mineral-status survey of trees, however.

An interesting alternative to this type of direct flame analysis was presented by Venghiattis (153) in 1967. He combined a powdered sample with a solid state oxidant-fuel mixture and ignited a pellet of the mix under the primary source beam of an AA spectrophotometer. Although no data was presented, the author claimed that sensitivities for Ni, Ag, and Bi determinations in gold were comparable with those obtained by conventional nebulizer-flame AAS.

Powdered silicate rock samples were deposited in the threads of an iron screw and directly inserted into an air-acetylene flame by Govindaraju et al. (154) in 1971. A fairly homogeneous sample was prepared by a 2-fold dilution of powdered rock with NaCl followed by grinding the mixture to give particles of less than 50 µm diameter. About 70 mg of sample was then impregnated in the screw threads. One point calibration with a geochemical standard of relatively high rubidium content (granite, 390 ppm) was sufficient for the determination of this element in 12 rock samples ranging from granites to basalts. Cutting and weighing chart recordings gave results with RSDs of about 6%. Later implementation of electronic signal integration improved this precision to about 4%.

B. Direct Sample Insertion into the ICP

A modification of a simple device like the Delves cup represents an attractive alternative for sample introduction into the ICP. A wide variety of sample types could be introduced into the plasma with relatively simple instrumentation. The introduction of an entire discrete sample into the plasma would afford high analytical sensitivity without the complexities of separate vaporization/atomization schemes. In addition, such a system would be amenable to automation and rapid sample cycling could be achieved.

A review of the recent progress in the development of systems of this type follows. Table II.2, Advances in Direct Sample Insertion for Plasmas, puts this progress in perspective in terms of sample types and analytical figures of merit. The optimum plasma discharge and sample preparation and analysis parameters for the various systems are condensed into Table II.3. Reference citations link the tables to one another and to the text that follows.

1. Cup-in-Plasma

The direct introduction of discrete samples into an ICP was described by Salin and Horlick (124) in 1979. These authors demonstrated the feasibility of directly inserting samples held in graphite cups into an ICP for analysis by optical emission spectroscopy. Their "Direct Sample Insertion Device" (DSID) consisted of a standard dc arc undercut graphite electrode mounted on the end of a quartz rod (Figure 1). Manual vertical displacement of the quartz rod allowed fairly smooth insertion of the graphite cup into an ICP discharge.

The authors found it necessary to desolvate liquid samples prior to insertion. This was accomplished by positioning a graphite cup in the center of the ICP's RF coils and then applying a low level of forward power. The cup was then lowered below the coils and the plasma ignited in the normal fashion. Emission analysis commenced after a one second period required for reinsertion of the graphite

TABLE II.2

ADVANCES IN DIRECT SAMPLE INSERTION FOR PLASMAS

Technique	Matrix/ Sample Size (sample/hr)	Element (Working Range or Level, *%RSD*, **Detection Limit**)	Yr./ Ref.
Cup-in-plasma	aqueous/5µl	Zn(1-100ppm,*15*)	'79/ 124
	graphite/ 15mg (10)	Zn(1.8ng-[illegible].3µg,**0.1ng**)	
Cup-in-plasma	aqueous/ 50µl	Al(**3.75µg**);Co(**650ng**); Cu(**1.5µg**);Mn(**37.5ng**); Ni(**1.45µg**);Si(**2.25µg**): *RSDs ranged from 5-10%*	'80/ 120
	oil/5µl	B(1-25µg)	
	steel/5mg	Ni(0.25-12%); Cu(0.005-0.0725% & 0.5-0.45%)	
	steel/30mg	Al(**57ng**);Co(**75ng**);Cu(**16.2ng**); Mn(**1.02ng**);Ni(**75ng**);Si(**33ng**): *RSDs ranged from 5-10%*	
Rod-in-plasma	aqueous/5µl	Cd(**19.5pg**);Co(**20.5pg**);Cu(**20pg**); Fe(**39pg**);Mn(**6pg**);Ni(**63.5pg**); Pb(**35pg**)	'82/ 121
Rod-in-plasma (Ar-0.1% Freon injector gas)	aqueous/5µl	Ag(**1.8pg**);B(**1.3pg**);Cr(**20pg**); Cu(**7.3pg**);Mo(**1.0ng**); Ti(7,**0.89ng**);U(**1.9ng**); Zr(**1.1ng**);Zn(**4pg**); Ag,Cr,Cu,Zn(0.1-100ng); B,Mo,Ti,U,Zr(10-1000ng)	'82/ 122

Continued...

TABLE II.2 (Continued)

Technique	Matrix/ Sample Size (sample/hr)	Element(Working Range or Level, *%RSD*, **Detection Limit**)	Yr., Ref.
Cup-in-plasma	aqueous/5µl 5% glucose/ 5µl (21)	Mn(*2*,**0.25ng**) Mn(50ppb)	'83/ 123
Cup-in-plasma	aqueous	Cr(5mg/L,*2*,**110pg**); Mn(5mg/L,*1*,**33pg**); Ni(5mg/L,*6*,**270pg**); Pb(5mg/L,*5*,**140pg**)	'84/ 156
Cup-in-plasma	U_3O_8 with 5% AgCl carrier/ 100mg	B(0.1-20ppm,*10*,**8pg**); Be(0.1-5ppm,*8*,**1pg**); Cd(0.1-10ppm,*15*,**2pg**); Co(1.0-200ppm,*13*,**14pg**); Cr(5.0-100ppm,*12*,**290pg**); Cu(1.0-100ppm,*16*,**10pg**); Fe(5-1000ppm,*17*,**150pg**); K(5-1000ppm,*6*,**350pg**); Li(1-200ppm,*6*,**1pg**); Mn(1-200ppm,*15*,**12pg**); Na(1-200ppm,*15*,**94pg**); Ni(1-100ppm,*17*,**110pg**); Pb(1-200ppm,*18*,**130pg**)	'84/ 160
Cup-in-plasma	aqueous/ 10µl	Cr(5.7 OM,*6.4*,**97.0pg**); Mn(5.0 OM,*4.1*,**4.0pg**); Ni(5.7 OM,*12.0*,**148pg**); Pb(4.7 OM,*6.0*,**58.0pg**); Zn(4.0 OM,*13.0*,**18.0pg**)	'84/ 157

Continued...

TABLE II.2 (Continued)

Technique	Matrix/ Sample Size (sample/hr)	Element(Working Range or Level, *%RSD*, **Detection Limit**)	Yr./ Ref.
Cup-in-plasma	aqueous/ 5µl	Al(5.7 OM,*1.9*,**1.03ng**); Ca(5.7 OM,*4.3*,**5.96ng**); Cd(4.7 OM,*3.5*,**13pg**); Co(4.7 OM,*2.2*,**98pg**); Cr(4.7 OM,*2.7*,**71pg**); Cu(5.3 OM,*5.6*,**0.14ng**); Fe(4.7 OM,*4.0*,**0.81ng**); K(5.7 OM,*5.5*,**1.81ng**); Mg(5.3 OM,*3.0*,**0.15ng**); Mn(5.7 OM,*3.0*,**43pg**); Na(5.0 OM,*12*,**5.67ng**); Ni(4.7 OM,*2.2*,**0.18ng**); P(5.0 OM,*3.6*,**0.64ng**); Pb(4.4 OM,*3.8*,**63pg**); Zn(4.4 OM,*5.0*,**0.12ng**)	'84/ 158

Continued...

TABLE II.2 (Continued)

Technique	Matrix/ Sample Size (sample/hr)	Element(Working Range or Level, *%RSD*, **Detection Limit**)	Yr./ Ref.
Cup-in-plasma	cellulose/ 2mg	Al(*4.7*,**26.0ng**);As(*2.6*,**10.0ng**); B(*10*,**46.4ng**);Ba(*19*,**40.0ng**); Be(*12*,**8.60ng**);Ca(*17*,**139ng**); Cd(*10*,**3.28ng**);Co(*5.7*,**1.30ng**); Cr(*7.0*,**1.58ng**);Cu(*1.4*,**1.06ng**); Fe(*4.8*,**19.1ng**);K(*1.6*,**167ng**); La(*4.6*,**135ng**);Mg(*2.7*,**9.82ng**); Mn(*2.5*,**2.16ng**);Na(*5.2*,**76.0ng**); Ni(*5.6*,**2.10ng**);P(*2.7*,**29.6ng**); Pb(*2.7*,**2.80ng**);Sn(*4.4*,**2.50ng**); Sr(*26*,**10.9ng**); Ti(*11*,**104ng**); Zn(*13*,**3.54ng**)	'85/ 15[illegible]
Cup-in-plasma	electrol. preconc. from aq. soln.	Cu(3.15-0.00315 µg/ml,*11.5 max*,**1.9ng**)	'84/ 167
Wire-in-plasma	aqueous/ 10µl	Cu(4 OM,*5*,**2pg**);Zn(**0.8pg**)	'84/ 168
Cup-in-plasma	electrol. preconc. from artificial seawater	Cd(**175ppb**);Co(**259ppb**); Cu(63ppb,*4*,**2.4ppb**); Ni(**25ppb**);Pb(**680ppb**); Zn(**2.0ppb**)	'85/ 169
Cup-in-plasma	hair/1mg	Zn(280ppm,*17*,**50ppb**); Cu(33.2ppm,*30.1*,**30ppb**)	'86/ 165

Continued...

TABLE II.2 (Continued)

Technique	Matrix/ Sample Size (sample/hr)	Element (Working Range or Level, *%RSD*, **Detection Limit**)	Yr./ Ref.
Wire-in-plasma/ MS	aqueous/ 10μl	Ag(100ppb,*5*,**0.2pg**); As(100ppb,*13*,**5pg**); Cd(100ppb,*5*,**0.5pg**);Cd(4 OM); Cu(100ppb,*9*,**0.27pg**); Li(100ppb,*13*,**0.75pg**); Mn(100ppb,*6*,**0.9pg**); Pb(100ppb,*7*,**0.3pg**)	'86/ 170
Wire-in-plasma	aqueous/ 10μl	Ag(1ppm,**0.4pg**); As(1000ppm,**700pg**); Cd(10ppm,**3pg**);Cu(10ppm,*2*,**2pg**); Mg(1ppm,**0.07pg**);Pb(10ppm,**30pg**); Se(100ppm,**200pg**); V(100ppm,**80pg**);Zn(1ppm,**0.7pg**)	'89/ 171
Horizontal cup-in-plasma	U_3O_8 with 5% AgCl-NaF carrier/ 50 mg (64)	Al(*8*,**3ppm**);B(*7*,**0.06ppm**); Ba(*8*,**0.15ppm**);Bi(*5*,**0.4ppm**); Cd(*12*,**0.015ppm**);Co(*19*,**4ppm**); Cr(*7*,**0.6ppm**);Cu(*30*,**0.3ppm**); Fe(*5*,**2ppm**);Mg(*20*,**4ppm**); Mn(*10*,**0.3ppm**);Mo(*4*,**3ppm**); Nb(*10*,**2.5ppm**);Ni(*8*,**2ppm**); Pb(*12*,**0.25ppm**);Sb(*25*,**0.3ppm**); Si(*12*,**3ppm**);Sn(*5*,**0.5ppm**); Sr(*5*,**1.5ppm**);Ti(*11*,**0.4ppm**); V(*5*,**1.5ppm**);Zn(*4*,**0.15ppm**)	'85/ 161

Continued...

TABLE II.2 (Continued)

Technique	Matrix/ Sample Size (sample/hr)	Element(Working Range or Level, *%RSD*, **Detection Limit**)	Yr., Ref.
Cup-in-plasma	aqueous/ 10µl	Ag(0.1-100ppm,*3.6*,**0.11ng**); As(*4.0*,**0.37ng**);Cd(*2.9*,**0.03ng**); Cr(1-100ppm,*3.6*,**0.25ng**);Cu(*7.2*); Ge(*2.2*,**0.47ng**);In(*3.8*,**1.1ng**); K(*1.8*,**0.3ng**);Li(*1.8*,**0.06ng**); Mg(*2.7*,**0.85**);Mn(*1.9*,**0.1ng**); Na(*4.6*,**2.7ng**);Pb(*3.0*,**0.4ng**); Sb(*2.9*,**1.2ng**);Sn(*3.7*,**3.5ng**); Zn(*3.1*,**0.2ng**);	'86/ 155
	graphite, silicon dioxide, aluminum oxide base dc arc powdered standards /10mg	Ag(1-100ppm,*5.3*,**0.021ppm**); As(1-1000ppm,*2.8*,**0.044ppm**); Ge(1-1000ppm,*16.6*,**0.12ppm**); In(1-1000ppm,*4.4*,**0.32ppm**); Li(1-1000ppm,*6.5*,**0.07ppm**); Pb(1-1000ppm,*6.1*,**0.33ppm**); Sb(1-1000ppm,*9.4*,**0.074ppm**); Sn(1-1000ppm,*6.7*,**0.06ppm**) Zn(1-100ppm,*5.6*,**0.09ppm**)	

Continued...

TABLE II.2 (Continued)

Technique	Matrix/ Sample Size (sample/hr)	Element (Working Range or Level, *%RSD*, **Detection Limit**)	Yr., Ref.
Horizontal cup-in-plasma	nickel alloy chips/5mg	Cd(0.5-5ng,**0.004µg/g**); Mg(20-100ng,**0.01µg/g**); Pb(5-100ng,**0.08µg/g**); Zn(1-50ng,**0.04µg/g**): *RSDs of 6-14 at µg/g level*	'86/ 162
Cup-in-plasma	silicate rock/50mg	Cu(10-100 ppm,*±10-15*)	'87/ 166
Cup-in-plasma	graphite & ceramic powders	Doping with Fe-59 to study vaporization	'89/ 163

TABLE II.3

OPTIMIZED CONDITIONS FOR ICP DIRECT SAMPLE INSERTION

Yr./	Sample			Plasma		
Ref.	Dry position/ Time	Ash position/ Time	Analyze position/ Time	Obs. hgt. mm ATOC	Pwr kW	Coolant/ Aux./ Inj.gas (l/min)
'79/ 124	center of coil, plasma extinguished(~50W on coil)/60s		slightly ATOC/ ∫12.5s (liquid) ∫0.64s (solid)		2	Ar(17)/ none/ none
'80/ 120				10	3	N_2(28)/ Ar(15)/ none
'82/ 121	heat gun outside plasma		4mm ATOC	19	1	Ar(16)/ Ar(0.9)/ Ar(0.2)
'82/ 122	heat gun outside plasma		-3.0-6.0mm ATOC (depending on analyte)	15-24	.71-.97	Ar(13.5-15.5)/ Ar(0.35-1.00)/ Ar-0.1% Freon(0-1.25)

Continued...

TABLE II.3 CONTINUED

Yr./ Ref.	Sample			Plasma		
	Dry position/ Time	Ash position/ Time	Analyze position/ Time	Obs. hgt. mm ATOC	Pwr kW	Coolant/ Aux./ Inj.gas (l/min)
'83/ 123	34-56mm BTOC (aqueous) 48.5mm BTOC/30s (glucose)	26mm BTOC/ 120s (gluc.)	2mm BTOC (aqueous) 1.5mm BTOC/20s (glucose)	20	1	Ar(16)/ Ar(9)/ Ar(0.1)
'84/ 160	heated, tapped & vented outside plasma		TOC/∫45s	15	1.4	Ar(22)/ Ar(1)
'84/ 157	with IR lamp before insertion		4mm ATOC/ 30s chart record	16	0.9	Ar(17)/ Ar(1.4)
'84/ 158	32-38mm BTOC/ 120s	32-25mm BTOC/15s	2mm ATOC/ ∫15s	16	0.95	Ar(17)/ Ar(0.6)/ Ar(0.1)
'84/ 167	2cm ATOC plasma extinguished (30W on coil, 16l/min Ar)/60s to remove mercury		TOC/chart recorder	15	2	Ar(16)-O_2(1.7)/ Ar(0.41)

Continued...

TABLE II.3 CONTINUED

Yr./ Ref.	Sample			Plasma		
	Dry position/ Time	Ash position/ Time	Analyze position/ Time	Obs. hgt. mm ATOC	Pwr kW	Coolant/ Aux./ Inj.gas (l/min)
'84/ 168	20mm below plasma/60s		loop 2mm BTOC	16	1.75	Ar(16) Ar(0.8)
'85/ 169	2cm ATOC, plasma extinguished /60s(16 l/min Ar)		5mm ATOC	15	2	Ar(18)-O_2(1.4)/ Ar(0.2)
'85/ 159		11mm below plasma/ 5min	2.2mm ATOC/∫30s	14	1.2	Ar(17)/ Ar(0.6)/ Ar(0.1)
'86/ 165	RT, overnight outside plasma		5mm ATOC	18	2.0	Ar(18)/ Ar(1.4)
'86/ 170	10mm outside horizontal plasma		9mm BTOC		0.95	Ar(14)/ Ar(2.0)/ Ar(0.75)
'86/ 155	in Al holder on hot plate at 80-90°C for 5-10 min		2mm BTOC/ chart recorder or ∫40s	15	1.2 or 1.5	Ar(10.5) Ar(0.65) He(0.40)

Continued...

TABLE II.3 CONTINUED

Yr./ Ref.	Sample			Plasma		
	Dry position/ Time	Ash position/ Time	Analyze position/ Time	Obs. hgt. mm ATOC	Pwr kW	Coolant/ Aux./ Inj.gas (l/min)
'85/ 161			8mm ATOC/ $\int$7s	17	1.4	Ar(16)/ Ar(0)/ Ar(1)
'86/ 162	warm in a flame ~10s		$\int$10s	15	1.0	Ar(16)/ Ar(1.6)
'89/ 171	22mm BTOC/ 20-30s		2mm BTOC	17	1.75	Ar(16)/ Ar(1)
'87/ 166			8mm ATOC/ $\int$7s	17	1.25 & 2.0	Ar(16)/ Ar(0)/ Ar(1)
'89/ 163					3,4, &5	N_2-Ar

cup. It was necessary to extinguish the plasma between each analysis in order to replace the graphite cup or reload it with a new sample.

Linear calibration curves were obtained for zinc in solution and in graphite powder matrix. No internal standardization was necessary in the direct powder analysis. The authors attributed large relative standard deviations for solutions of the same concentration to errors in pipetting and to the manual control of sample desolvation and insertion steps.

Comparative spectrographic analysis of 49 element Spex G-standards (graphite powder matrix) led the authors to conclude that their direct insertion system had quantitative, semiquantitative, and qualitative capabilities for powders equal to or better than the dc arc.

Preliminary results for NBS SRM 1632 coal and SRM 1571 orchard leaves also indicated that at least qualitative analysis could be obtained for organic matrix samples by direct insertion with no pretreatment.

This data suggested to Salin and Horlick that direct insertion had potential as an adjunct capable of greatly expanding the analytical utility of ICP-OES just as electrothermal atomization had broadened the horizons of atomic absorption spectroscopy.

In 1986 Shao and Horlick (155) reported a new mechanized DSID design. In addition to allowing precise sample cup movement, the device could be readily attached to standard commercial ICP spectrometers. For example, no modifications of their ARL 34000 were necessary. The new design was based on the original Salin and Horlick (124) DSID and consisted of a graphite sample cup (based on classic dc arc design) mounted on a quartz rod which was in turn precisely driven by a leadscrew on a reversible motor. The total sample travel time was less than five seconds. The sample injection position was adjusted manually with a gear knob; the final motor position being set by a microswitch. In an effort to give more flexible control over insertion position, the authors planned to replace the reversible motor with a stepper motor.

The ICP torch had a central tube of 7 mm i.d. and was fitted with a solenoid-actuated glass shutter to prevent the escape of plasma gas. A flow of helium injector gas minimized the formation of a filament discharge between the sample cup and plasma. Before insertion, sample solutions were dried in an aluminum holder on a hot plate at 80-90°C for 5-10 minutes. Sample cup changing was done manually with the aid of a holder assembly that could be swung out from under the plasma.

Temporal emission profiles revealed that vaporization from dried solution samples occurred in about 2-10 seconds for volatile elements and in about one minute for less volatile elements (for example chromium). The observed volatilization sequence: As, Pb, Cd, Zn, In, Ge, Ag, Li, Na, Sb, Mn, Cu, Mg, Cr, Fe was similar to that found in dc arc emission work. The authors found more rapid volatilization behavior with smaller cups and suggested that this was probably due to more rapid heating. Forward power had little effect on vaporization behavior.

In exploring the figures of merit for their system, the authors chose a compromise signal integration time of 40 s as integration times for specific elements couldn't be individually set with the ARL 34000. Using 10 µl solution samples, the authors got linear working curves for the volatile elements As, Cu, In, Li, Mg, Na, Pb, Sb, Cd, Mn, Sn, and Zn. For example, silver gave a linear working range of 0.1-100 ppm. For these elements, working curves were superimposable for forward powers of 1.2 and 1.5 kW. In contrast, the elements chromium and potassium gave power dependent linear working curves. The elements Al, B, Ba, Ca, Fe, Mo, Ni, Si, Sr, Ti, and V had non-linear working curves; not an unexpected behavior according to the authors, since these elements can be difficult to volatilize and may form carbides.

The authors also found that sample cup size affected precision. The best average (16 elements) RSD (3.3% (10 µl, 10 ppm)) was obtained with a 4.5 mm diameter cup. Smaller cups gave poorer precision possibly because of a greater percentage of noise being integrated in the time profiles. Larger cups were also unsuitable because they disrupted the plasma.

Since sample insertion position affected plasma geometry and spatial structure, it also affected precision. With signal observation height fixed at 15 mm above the top of the load coil (ATOC), the authors found that a one millimeter difference in position gave a 10% signal change with powdered samples.

The inflexibility of the author's commercial ICP instrument became apparent again in the pursuit of detection limits. As a result, detection limits were calculated from data obtained with an external amplifier and a chart recorder. Background standard deviation was determined with eleven repeat blank water runs. Sample cup impurities were significantly reduced by "pre-burning" cups in the plasma.

"Real sample" capability was tested with digested NBS SRM 1575 pine needles and Spex dc arc powdered standards including G-standards, TS-6 silicon dioxide-base standards, and TS-6 aluminum oxide-base standards. An average accuracy [illegible] was obtained using 10 µl digest aliquots. Linear working curves were calculated for the volatile elements Ag, As, Ge, Li, In, Pb, Sb, Sn, and Zn. Neither forward power or sample matrix (graphite, SiO_2, Al_2O_3) had significant effect on the working curves. Precision averaged about 7% RSD for 10 mg samples of the powders.

The authors also tried NaF as a "volatilization enhancement reagent" for powdered samples. Whereas most of the elements Zr, V, Sn, Ba, Al, Si, and K normally gave no significant emission signal at the 33 ppm level, "considerable enhancement" above background was noted with an NaF:sample ratio of 1:2. They concluded that it would be beneficial to consult the dc arc and electrothermal atomization atomic absorption spectroscopy (ETAAS) literature as a guide to further extending the DSID method to less volatile elements.

Based on their experiences with commercial instruments, the authors also concluded that a more flexible simultaneous readout spectrometer system with customized data processing on each channel was desirable. The authors responded to this need by building their own "high-speed multiplexed multichannel computer based measurement system." The authors also suggested that developments in basic DSID design like metal cups, wire loops, and automation would help achieve the full potential the DSID had to offer.

A year after Salin and Horlick's original report (124), a paper in German by Sommer and Ohls (120) appeared describing results of their preliminary experiments with a direct insertion device for ICP spectroscopy. Apparently, the latter authors had been igniting their ICP for years with the aid of a graphite rod and had recently come on the idea of doping the rod with samples for analysis.

In contrast to Salin and Horlick's original DSID, the German's apparatus could be run continuously without extinguishing the plasma between samples. Sample cups were transported to and from the plasma pneumatically with the aid of a piston and valve system mounted below the ICP torch box. A 4 mm diameter graphite sample cup was mounted on a 5 cm long glassy carbon rod which in turn fit into a quartz rod. This quartz rod apparently fit into a Teflon piston in the pneumatic system. Although no further mechanical details were given, the authors stated that the "pneumatic apparatus" could be lowered sufficiently to permit exchange of graphite sample cups just below the lower end of the ICP torch's central [illegible]e.

These workers stated that their "Sample Elevator Technique" (SET) was practical only with a relatively high power plasma. They noted a decrease of more than 50% in Ar I 404.4 nm line intensity when a graphite cup (with lid) was inserted into the plasma. The authors had previously noted a linear relationship between this argon line intensity and coil power, however, no study of analyte signal-to-noise ratio versus coil power was undertaken.

Samples were weighed directly into the graphite cups to prevent contamination and loss and the cups could be reused many times as their masses remained constant. Open cups could not be used with the SET because "...sometimes the plume of the plasma (was) altered (altering the observation height) by the explosive vaporization of the sample substance and, at other times, visible particles (flew) through the plasma" (120). This problem and the attendant degradation of precision were avoided by covering sample cups with perforated lids.

Steel turnings and metal oxides inserted into the plasma in graphite cups gave analyte emission signals with a range of temporal behaviors. The elements Te, As, Hg, Cd, and Tl all had narrow profiles with emission intensities returning to baseline about 2 s after insertion. These elements were relatively volatile and the emission intensity profiles would be expected to reflect their rapid vaporization from the sample cup. The element nickel, however, exhibited a less intense and broader time profile. In addition, although peak intensity was registered after 4.7 s and had fallen to 73% of this value after 14 s, it remained at the 73% level for the next 32 s without returning to the original baseline. No explanation for this anomalous behavior was given. An intermediate time behavior was registered for lead whose signal intensity returned to baseline after 6.5 s. The emission intensity time behavior for pure metals and their oxides were practically identical and the authors presumed this was due to reduction of the oxides in the graphite cups. Cup temperature was estimated from the melting and sintering of tungsten wire to be about 3000°C.

Calibration plots were constructed for nickel and copper in shavings of reference steel and analysis of liquid samples was demonstrated by the determination of boron in a sample prepared from Conostan Standard lubricating oil.

Based on its good performance, the ICP-SET was chosen as a reference method for GFAAS in the authors' laboratory. This was in contrast to the reverse situation in the past.

On the heels of Salin and Horlick's (124) and Sommer and Ohls's (120) reports came publications by Kirkbright and coworkers at the University of Manchester detailing the enhancement of direct insertion device performance by automation (123) and improved sample cup design (156).

Their 1983 publication (123) described a stepper motor-driven graphite cup insertion device which significantly improved analytical precision. The lower end of the sample cup assembly was push-fitted into the top of a glass tube which in turn fit into a sliding mechanism. A stepper motor-controlled lead screw attached to the slide governed its vertical displacement. Precise control of sample position was therefore possible.

The ICP torch injector tube was extended downward to a bulb pipet-shaped glass manifold. This manifold was equipped with a port through which samples could be pipetted. In contrast to an earlier version (in which samples were evaporated on a graphite rod (121,122)), graphite cups were employed to accept samples.

A microcomputer interfaced to the stepper motor permitted software control of sample insertion height and timing. The heights and times for drying, ashing, and atomization stages of sample analysis were therefore readily programmed. The authors found that a central flow af argon was necessary in order to remove condensate formed in the injector tube during sample drying. A hot sample cup descending from the plasma would rapidly vaporize any condensate and the resulting piston effect would extinguish the discharge. The sample drying process could be monitored by observing plasma reflected power level. Reflected power would initially increase to about 100 W and then would return to less than 3 W on completion of desolvation. Samples held too far below the plasma wouldn't dry and subsequent sample insertion would extinguish the plasma. The same result would occur for samples dried too rapidly above the specified range. The optimum sample drying position was little affected by plasma coolant and auxiliary gas flows, but forward power and injector gas flows were important. Using experimental conditions optimized for the determination of manganese at 257.6 nm, the authors achieved a 3% improvement in RSD relative to results from their earlier manual insertion device.

A preliminary ashing experiment was conducted with a glucose solution containing manganese. With drying, ashing, and atomization positions and times optimized, essentially identical manganese emission temporal profiles were obtained for glucose and aqueous solutions. As in past experiments (121,122), the sample support was reused which necessitated a preburn sequence to eliminate contamination or memory effects. This sequence, together with a requisite cooldown period before sample addition, would result in a sample cycle period greater than the quoted analysis time of 170 seconds.

In their conclusion, Kirkbright et al. (123) stated that the application of their insertion device to the analysis of solid samples such as semiconductors, soils, and other biological materials was under investigation. In addition, the authors envisioned extension of microcomputer control to data processing. In contrast to the previous manual reading of peak heights from chart recordings, peak areas could then be automatically acquired from an integrator.

After achieving an improvement in their insertion device's analytical precision by partial automation, Kirkbright and his colleagues (156) went on to investigate four different graphite cup designs in an effort to further improve the device's performance.

Reasoning that an improvement in sensitivity would depend on rapid heating to give a high concentration of analyte in the plasma's observation zone, the authors investigated the heating and cooling characteristics of four different "graphite cup furnace" designs. The first design (A) looked very similar to a standard dc arc graphite electrode mounted on an graphite rod. All cup assemblies were supported by alumina rods. The remaining designs (B, C, and D) differed from the first in that the undercut portions extended much further and no graphite rods intervened between the cups and alumina rods. Design C differed from B and D in that it had a glassy carbon undercut portion. Design D had a very narrow undercut portion and therefore the smallest mass of graphite.

Heating curves were obtained for the different designs by monitoring temperature as a function of time with a radiation thermometer focused on cups positioned 6-8 mm ATOC. Cooling curves were also acquired by turning off RF power and gas flows five to eight seconds after a cup reached its equilibrium temperature. It was found that a cup's rate of cooling was proportional to the ratio of the cup's surface area to it's volume and it was inversely proportional to any of the cup's linear dimensions. Newton's law of cooling was therefore obeyed. Heating rates increased from design A to D and cooling rates followed the reverse order.

Once heating and cooling curves were known, the authors tried to correlate them to the analytical sensitivities of the elements Ni, Cr, Mn, and Pb. A positive correlation between sensitivity and heating rate was found for the relatively less volatile elements nickel and chromium, but a big difference in nickel and chromium behavior with the last two cup configurations suggested a complex vaporization mechanism. Lead sensitivity seemed to be inversely related to heating rate and the sensitivity of manganese showed no correlation with cup configuration.

The authors felt that all differences in vaporization behavior couldn't be accounted for by simple differences in boiling points or compound forms in solution. They suggested that other parameters such as the condition of the cup's internal surface, the nature of any residue left after sample drying, and the surface diffusion of analyte might be important.

Compromise settings of plasma gas flow rate, viewing height, and forward power were used in making detection limit and reproducibility measurements. The best detection limits (defined as two times blank standard deviation) were obtained with cup design D (the one having the smallest mass and fastest heating rate). Relative standard deviations were calculated from peak height measurements of signals. The RSDs showed no significant correlation with cup design.

It was concluded that analyte vaporization behavior depended on more than heating rates and equilibrium temperatures. In an effort to help elucidate the exact vaporization mechanisms, the authors planned to employ modifications including a better optical setup to give the outside temperatures of cups, better cup fabrication techniques to give reproducible cup dimensions and surface character, cup lids, and pyrolytic coating to improve reproducibility, and gases such as oxygen, hydrogen and methane to improve sensitivity.

Efforts to further optimize a manual graphite cup direct insertion device were detailed beginning in 1984 in a series of three papers by Haraguchi and coworkers (157,158,159) at the University of Tokyo. In their first two papers (157,158), these authors focused on the optimization of a system used to analyze solutions in a continuous fashion with a low power argon plasma. The authors discussed the addition of computer control and the extension of the direct insertion method to solid samples in their third paper (159).

Using the signal-to-background ratio for the 257.6 nm manganese emission line (5 µl of 50 ng/ml), Haraguchi et al. (157) optimized sample cup size, rod height, and plasma operating parameters with a univariate search procedure. The authors settled on a cup size of 2.5 mm i.d. by 3.3 mm o.d. by 2 mm deep. These home-built graphite cups were pre-burned 5 times to minimize contaminants and could be used more than 20 times. Liquid samples were then transferred to the cups with a pipet and dried with an IR lamp before insertion into the ICP. An adjustable teflon stop controlled the final insertion height.

A spark to the sample cup was observed as it approached the ICP load coil. Upon insertion, a decrease in plasma brightness accompanied by a significant baseline drift on the chart recorder was also observed. The authors suggested the latter phenomenon may have been due to a shift in RF power matching as the transmitter coupled to the graphite cup.

Temporal profiles revealed two general groups of analyte emission behavior. The temporal emission signals of Mn, Zn, and Pb were all narrow (Zn and Pb were completely vaporized within four seconds), but Cr and Ni signals were broad and accompanied by significant baseline drift.

In the same year (1984), the Tokyo group (158) extended their "platform elevated direct graphite cup insertion" technique to simultaneous multielemental analysis. The authors again employed a univariate search method to find compromise conditions for the simultaneous determination of 15 elements in μl-size solutions. However, the best signal integration time was found by manual study of intensity vs. time curves. Only after this procedure were the best distance between the bottom of the sample cup and the top of the ICP load coil, forward power, and observation height optimized according to the signal-to-background ratio.

Once again, the insertion method was manual with the final insertion position determined by an adjustable stop.

The detection equipment was improved, however, by replacing the chart recorder on single channel with a polychrometer.

Detection limits for Al, Ca, Fe, K, and Na were not as good as other elements studied and the authors suggested that this might be due to residual impurities in the graphite.

Temporal profiles again fell into two main groups. For example, Pb and Zn were completely vaporized in five seconds, whereas other elements like Al and Mn needed about fifteen seconds to reach the same point. Therefore, a fifteen second integration time was chosen for further work.

Signal-to-background ratios (SBRs) for Mn, Cu, Co, Mg, and Pb increased with insertion height, but SBRs for Cr, Na, and Ni decreased with insertion height so a compromise insertion height of two millimeters above the top of the ICP load coil (ATOC) was chosen.

As far as forward ICP power was concerned, SBRs for Co, Mg, and Pb were better at about 0.7 kW, but Ni was better at greater than 1.1 kW. The best SBRs for the remaining elements were found at 0.95 kW of forward power.

The best observation height for Ni and Fe was 10 mm ATOC and for the remaining metals it was 16 mm ATOC.

The analyte SBRs were not significantly influenced by gas flows, but an injector gas flow was needed to prevent plasma instability during drying and ashing operations. The progress of drying could be tracked by watching reflected power levels. Reflected power increased to about 50 W and then fell back to 15 W when drying was complete. If the sample contained any traces of water on insertion, plasma extinction occurred. No sample loss was recorded in up to six minutes of drying time.

A discharge between the plasma and sample cup was observed during the sample ashing stage. If the sample cup became too hot during this stage, the plasma was extinguished. "Prolonged ashing" caused losses of the elements Cd, Pb, and Zn. An ash was found at the top of the injector tube after repetitive sample insertions. This residue apparently accelerated drying and ashing rates and shifted the optimum cup height to lower positions.

The authors investigated optimum cup positions and drying and ashing times for various acid solutions. Solutions made 1 molar in HCl, $HClO_4$, HNO_3, and H_2SO_4 completely vaporized only during the ashing stage. The plasma was extinguished on insertion of the sample if this vaporization wasn't complete. The higher boiling acids $HClO_4$ and H_2SO_4 altered the emission intensities of some of the elements at the 2 μg/ml level. For example, $HClO_4$ reduced Cu 324.7 nm emission intensity by 76%, but it increased Al 308.2 nm emission intensity by almost 300%. Mn 257.6 nm emission intensity was decreased 37% in the presence of H_2SO_4, but Zn 213.8 nm intensity was increased by 50%. The authors offered no explanations for the acid effects and suggested that matrix matching be employed in the analysis of samples containing these acids.

Interelement interference effects were also examined. The effects of 500 μg/ml of Al, Ca, Fe, K, Mg, Na, and P on 5μg/ml each of Cd, Co, Cr, Cu, Mn, Ni, Pb, and Zn were studied and it was discovered that Al and Fe gave interferences with all elements.

Since it was difficult to measure interferences accurately, the authors used matrix matching in the analysis of plant digests. Their procedure consisted of digesting a one gram quantity of spinach or orchard leaves with a nitric-perchloric acid mixture and then evaporating the digest to dryness. In the case of spinach, an additional treatment with a hydrofluoric-perchloric acid mixture was necessary to remove silica. The residues were then dissolved in nitric acid and diluted to 50 ml with water. Blanks were prepared in a similar fashion.

The authors noted some additional problems in the analysis of these "real samples." For one, it appeared that the porosity of the graphite cup increased with use which resulted in a small memory effect for most analytes. Whereas a cup could be used thirty times if analyte concentrations were less than 10 µg/ml, it could only be used ten times in the case of plant digests. The authors found it necessary to do a preburn with each sample in order to saturate the graphite pores with analyte. In addition, two or three burns of the cup with reagent blank between runs were required to eliminate contamination. It was also necessary to wait seven minutes between consecutive sample insertions in order to let the plasma stabilize.

Recoveries of fifteen elements from National Bureau of Standards standard reference materials (NBS SRMs) 1570 spinach and 1571 orchard leaves were, with a few exceptions, in good agreement with certified values. High values resulted for Pb in spinach and for Ni, Co, and Cd in orchard leaves. The authors felt the discrepancy might be due to interferences from major elements and thus an inaccuracy in matrix matching.

Another problem concerning possible carbide formation was noted. Large errors were associated with calcium results and the elements B, La, Sr, Ti, Zr, and Y could not even be determined.

In their conclusion, the authors noted that further improvements in the performance of their method would depend on the implementation of two modifications. First, automation would eliminate the imprecision associated with the mechanical insertion sequence and second, use of pyrolytic or zirconium-coated graphite cups would help reduce the imprecision due to analyte loss and memory effects.

Partial implementation of the first modification was detailed by Haraguchi's group in their 1985 report (159). They built a slider mechanism based on a stepper motor, standard timing belt, and three standard pulleys. This mechanism could provide vertical displacement of a graphite cup-rod-handle assembly to within ±0.14 mm. The cup-rod-handle assembly was manually installed into the slider with each sample. Also, control of injector argon was not automatic. A valve below the ICP torch was manually opened and closed between each sample to prevent downward escape of injection gas.

In this study, the authors were interested in the analysis of solid samples, particularly powdered plant material. The authors apparently inserted powdered soils, rocks, metals, metal alloys or oxides without trouble, but direct injection of plant material extinguished the plasma. Ashing these samples helped, but they still spattered. A graphite lid with a 1 mm diameter hole was therefore devised to prevent "spitting" and to direct sample vapors into the ICP's central channel. These lids were good for one hundred four minute insertions. A graphite cup 3 mm deep by 3 mm i.d. held 1-5 mg of powdered plant sample.

Software for the automation of the ashing and atomization of these samples was written in BASIC together with machine code subroutines. The software essentially controlled a stepper motor to position the slider mechanism for an analysis cycle consisting of ashing, atomization, precooling, cooling, cup return to starting position, and blank burn. A constant vertical displacement of 6.9 cm/s or accelerations of 6.9-13.8 cm/s could be programmed. At top acceleration, it took about 0.4 s to insert a sample cup into the plasma from the ashing step. Signal integration was initiated by pressing the return key on a NEC microcomputer seven seconds after hitting the same key on a JA-Atomcomp MKII ICP.

In order to study the effects of ashing time and interelement interferences, synthetic solid standards were prepared from 100-200 mesh cellulose powder. Standard solutions were then added to one gram of cellulose powder in a platinum crucible, mixed with about five milliliters of acetone, and then dried with an IR lamp followed by drying in an electric oven at 100°C for three or more hours. Two milligrams of the dried powder was then placed in a graphite sample cup.

Before ashing times and other parameters were optimized, the best signal integration times were deduced from temporal emission profiles. For manganese in a four milligram sample of NBS SRM 1571 orchard leaves and lead and cadmium in the same quantity of NBS SRM 1573 tomato leaves, it took about twenty seconds for complete volatilization from a point of insertion 5.5 mm ATOC. But with the same quantity of spiked cellulose powder, Pb and Cd took less than five seconds and Mn took less than ten seconds to volatilize. An integration time of thirty seconds was therefore chosen. The authors felt that the more prolonged vaporization from plant samples might be due to vaporization effects caused by major elements.

Once the best signal integration times had been found, a Simplex procedure based on the SBRs for analyte emission lines was used to optimize ashing position. For example, the SBR for Mn 257.6 nm emission was used to optimize ashing of 2 mg of SRM 1571 orchard leaves. Background measurements were taken at a 0.03 nm higher wavelength with the same sample. During ashing, the authors noted an initial increase in reflected power level from 15 W to 100 W followed by a return to 15 W. This reflected power fluctuation could be used to monitor the progress of sample ashing.

After ashing, plant samples were inserted to an optimum position above the top of the ICP load coil (ATOC) and after a "few seconds" in this position, vaporization of analyte began.

In order to help select the best ashing times, the authors attempted to determine the temperature inside a capped graphite sample cup inserted into the ICP. They monitored the emission intensities of one to three milligrams of 100-300 mesh metal powders. Copper (b.p. 2868 K), cobalt (b.p. 3173 K) and iron (b.p. 3273 K) all vaporized within thirty seconds, but titanium (b.p. 3533 K) wasn't vaporized even after six minutes. Based on these results, a cup temperature of about 3200 K was suggested.

The effect of ashing time on loss of analyte was also investigated. The elements P, Zn, As, Pb, and Cd were monitored during ashing of National Institute for Environmental Studies (NIES) No. 1 pepperbush and it was discovered that zinc and phosphorus were lost with increasing ash time. It was also noted that ashing rates increased for less dense samples and decreased for more dense samples. Optimized conditions gave complete ashing of samples of any density within five minutes.

Interelement interference effects were also studied by adding 2% Na, K, Ca, and Mg as their chlorides to 50 µg/g Cd, Pb, Zn, K, and P and 100 µg/g of 18 additional elements in a cellulose matrix. Background correction was accomplished by measuring cellulose with and without the interfering element. As an aid to studying the interference effects, the authors defined intensity factors as the "...ratios of net emission intensity of the analyte in the presence of 2% major element to that of the analyte in the absence of the major element."

Addition of interfering elements generally resulted in intensity factors greater than unity, although the elements Mg, Mn, P, Pb, and Sn in the presence of NaCl and the elements Mg, Mn, Na, and P in the presence of KCl gave intensity factors less than unity. Significant enhancement was observed for the carbide forming elements Ba, La, Sr, and Ti in the presence of NaCl and KCl, but Ba, La, and Sr were totally suppressed with $CaCl_2$ and $MgCl_2$.

Although the authors concluded that most of the interference effects were attributable to the influence of major elements on analyte volatilization, they felt that further investigation of the enhancement effect of NaCl and KCl on carbide forming elements was required. Results of the interference studies suggested that for plant material containing Na, K, Ca, and Mg, reference standards with similar compositions or synthetic standards prepared by matrix matching would be required.

With optimized conditions, absolute detection limits and RSDs (10 measurements) for eighteen elements in 2 mg samples of cellulose matrix were at the nanogram level and 1.4-13%, respectively. Results were poorer for the elements Al, B, Ba, Ca, K, La, and Ti. Detection limits for these latter elements could be lowered to the nanogram level if 2% sodium was added as the chloride.

Calibration curves were also constructed for Pb, As, and Mn in NIES No. 1 pepperbush, NBS SRMs 1570 spinach, 1571 orchard leaves, 1573 tomato leaves, 1573 tomato leaves, and 1575 pine needles. These elements were chosen based on their wide range of concentrations in these standards and their relative freedom from interference from major components. The authors cautioned, however, that careful background correction was necessary for elements at low concentrations in samples with widely different major component compositions.

An analysis of orchard leaves was successfully calibrated with SRMs or cellulose standard. Slight deviations of element concentrations from certified values was ascribed to errors in standard preparation and to the weighing of milligram-size samples. Any memory effects for these elements could be minimized by two or three blank insertions. The elements Al, Ca, B, and Sr couldn't be determined, however, because of refractory carbide formation. Deposits of these elements in the graphite cups were noted to cause memory effects. Only washing with HCl followed by several insertions into the plasma could alleviate this problem.

The authors concluded that it might be possible to determine these elements and La and Ti by using matrix modification with NaCl, or the argon-0.1% Freon-23 injector gas mixture developed by Kirkbright (122) (see below).

A good example of the analytical utility of matrix modification for direct insertion work was presented in 1984 by A.G. Page (160) and colleagues in the Radiochemistry Division of the Bhabha Atomic Research Center in Bombay, India. They had been using a dc arc carrier distillation procedure to determine trace elements in uranium oxide and they wanted to somehow combine the high sensitivity of dc arc with the precision of the ICP for analysis of these refractory solids.

Figuring that the solutions to problems in classic dc arc analysis might also apply to solid sample analysis by ICP, they ground high purity U_3O_8 with 5% AgCl carrier together until a particle size smaller than 200 mesh was achieved. Standard dc arc electrodes were charged with this mixture and heated, tapped, and vented before being capped with modified graphite lids. The authors noted that this procedure gave reliable injection of vapors into the analytical zone of the ICP discharge after sample insertion to a fixed height. Although the entire procedure was manual, the electrode could be removed once the plasma was running and the graphite lids could be reused after a clean-out burn.

The authors optimized integration time, observation height, and forward power with a modified Simplex procedure by monitoring the signal-to-blank ratio (SBR) of boron. Representative temporal profiles of Fe, Li, and B emission are displayed in the paper. When the crucibles were capped, the signal-to-blank ratio improved for most elements, but no trends were seen in RSDs. The SBRs for K, Na, and Pb didn't improve with capped crucibles, possibly because of diffusion through openings caused by pressure build-up.

Precision for most elements was better than by dc arc carrier distillation even though electrode temperature was estimated at about 1800°C which is somewhat lower than dc arc. The authors assumed that little uranium vapor was present in the plasma as 3859.6 Å uranium radiation was absent. Detection limits were based on the concentration in micrograms corresponding to blank U_3O_8 plus three times the standard deviation in its determination.

The authors concluded that their "...method will be capable of further improvement with development in solid sample insertion systems in the near future."

Taking the cue from Page's group, A. Lorber and Z. Goldbart at the Negev Center for Nuclear Research in Beer-Sheva, Israel made the ICP carrier distillation technique even more convenient with a horizontal direct insertion system (161).

These authors were interested in a new approach to the carrier distillation analysis of impurities in uranium oxide. The traditional dc arc carrier distillation method gets around the degradation of detection limits due to high background signal by selectively volatilizing analyte from the refractory uranium matrix. If the traditional method could somehow be combined with the newer ICP emission source, even better detection limits might be realized.

The authors considered ICP direct solid introduction by electrothermal evaporation, fluidization, and rod or cup insertion, but were dissatisfied with these techniques because of analyte loss and memory effects and the necessity of turning off the plasma between samples or of building special sample manifolds. The authors therefore suggested inserting samples horizontally into the tail region of the ICP discharge. This technique offered the advantages of simple sample replacement and sequential reuse of sample containers.

An individual sample cup was made by drilling a 3 mm diameter by 6 mm deep hole in one end of a 3/16 inch National SPK graphite rod. The other end of the graphite rod was held by an alumina rod which in turn could slide back and forth in a horizontal notch. Reproducible sample positioning in the plasma was achieved with a magnetic stop on the horizontal notch. Solid sample mixtures consisting of uranium oxide plus 2% AgCl-NaF (5+3, m/m) carrier were pressed into the sample cups. Liquid samples were pipetted into the cups.

The authors noted that insertion of sample cups distorted the normal conical shape of the plasma discharge. In order to ascertain whether this distortion affected the plasma's ionic line emission zone, they nebulized a yttrium solution and monitored emission before and after cup insertion with a direct reader (focused 17 mm ATOC and 9 mm above the sample cup) and with color photographs. The photos of the plasma before sample insertion clearly revealed a blue color from yttrium ionic transitions and a red color from molecular yttrium oxide bands. Additional photos taken after sample insertion showed that the blue emission zone above the cup could still be seen but was distorted by the intrusion of red molecular emission. This visual evidence indicated a cooling of the plasma above the cup (perpendicular to the optical axis). This conclusion was supported by the inverse relationship between sample cup insertion depth and background signal revealed by direct reader measurements. Apparently, this cooling didn't affect other regions of the plasma tail or its core inside the induction coil. In contrast to what was observed for the ionic zone perpendicular to the optical axis, the ionic zone along the optical axis was relatively insensitive to rod position.

Using an optical pyrometer, the authors also found that the temperature of the sample rod along its axis was power dependant and that at incident powers of 1200 to 2200 W, the center of the sample cup was between 1600 and 2050°C.

The temporal emission profile of uranium was acquired by monitoring its 385.958 nm ionic line. The profile peaked eight seconds after insertion and had a five second width. Analyte lines were monitored simultaneously with the direct reader. Most analytes vaporized along with the matrix with volatile elements peaking one second before, and less volatile elements peaking one second after the matrix maximum, respectively. However, the temporal profiles for the elements boron and copper were significantly different. Boron's emission signal maximized four seconds after insertion and copper's signal began with uranium's and continued for fourteen seconds after insertion. The authors therefore chose signal integration periods of two-to-five and five-to-fourteen seconds after insertion for further analysis of boron and copper, respectively. A compromise integration period of seven seconds beginning anywhere from five to eleven seconds after sample insertion was picked for all remaining elements.

Table II.3 gives the author's SBRs and RSDs for 22 elements. The net analyte signal was found by subtracting the blank signal from a 10 µg/g sample's signal. The RSD values were based on three measurement sets of eight blanks and eight samples each. Blank RSDs were in the range of 5-10% for most elements. The authors explained that the higher blank RSDs (20%) for Si and Mg were due to contamination. Signal RSDs were in the range of 4-12% except for the elements Sb, Co, Mg, and Cu which were unexplainably high (19-30%). No memory effect was found and most of the analyte signal RSDs compared favorably with the 5-15% RSDs typically found for other ICP solid sample introduction techniques.

The authors also used the detection limits for 22 trace elements in uranium to provide a comparison of the analytical performance of their horizontal direct insertion method and the performance of Page's vertical direct insertion method, ETV-ICP, and liquid nebulization of 0.5% m/V uranium. Based on this comparison, the authors concluded that solid sampling of uranium was better than nebulization and that horizontal-solid sampling-carrier distillation was better than ETV. Their horizontal direct insertion method performed about as well as Page's more complex vertical insertion method.

The authors also pointed out that their method could provide the detection limits recently reported for boron and cadmium (0.02 μg Cd/g) (elements important in analysis of nuclear materials) by impurity extraction methods without all the procedural complexity.

In the following year (1986), a report appeared by C.W. McLeod, P.A. Clarke and D.J. Mowthorpe (162) describing the extension of the direct solid insertion-ICP technique to the quality control of trace elements in nickel-base alloys. The authors point out that even though trace levels of elements like Cd, Mg, Pb, and Zn are important in high-temperature (eg. aerospace) applications of nickel-base alloys, few analytical techniques exist for the direct trace determination of elements like these in solids. They go on to say that the weakness of recently reported electrothermal atomization-atomic absorption (ETA-AA) and low pressure hot hollow cathode discharge (HHCD) methods for this type of analysis is that matrix-matched standards or certified reference materials are needed. In contrast, the authors found that only simple non-matrix matched (aqueous) standards were required for calibration if mg-quantities of nickel-base alloy chips were directly inserted into an ICP.

Their direct insertion apparatus was of the vertical type. The injector tube tip of a standard ICP torch was ground off to allow passage of the sample cup into the plasma. The sample insertion probe was a three-piece unit consisting of a 7 mm length, 3 mm o.d., 2 mm i.d., 1.5 mm deep cup, a 37 mm length by 2 mm o.d. neck piece, and a 300 mm long by 3 mm o.d. shaft; all fashioned from high purity graphite rod. This probe was in turn mounted via a teflon adaptor on an electrically-operated car aerial. This unit was in turn supported on a lab jack. A variable dc power supply controlled the sample elevation rate and a mechanical stop controlled the final sample insertion position.

All sample cups were precleaned by insertion into the plasma. The cups could be used repeatedly for solution standards, but matrix element residues prevented reuse in the case of solid samples. After dispensing an aqueous standard by micro-pipette into a cup, the 5 µl aliquot was brought to dryness by gently warming the cup with a flame for about ten seconds.

Initial experiments with aqueous solutions showed that both the volatile elements As, Cd, Mg, Pb, Se, and Zn and the less volatile elements Al, Co, Cr, and Ni gave strong emission signals. However, titanium and molybdenum gave no emission signals. The authors felt that this was due to refractory carbide formation. Increased plasma power levels didn't improve the situation so these elements were not included in further studies.

Analyte emission time profiles were then employed in the study of selective volatilization of the elements As, Cd, Mg, Pb, Se, and Zn from five milligrams of alloy. The authors were surprised to find that the elements arsenic and selenium didn't give emission signals even though their concentrations in the samples were relatively high. It was suggested that these two elements may have formed stable compounds in the sample melt. An analogous situation exists in ETA-AA where furnace temperature of 3200°C are needed for the analysis of these two elements. The elements Mg, Pb, Cd, and Zn all gave similar-looking temporal profiles, but the profile shapes for analyte volatilized from solid and liquid residue were different. The volatilization of solid samples generally gave relatively broad profiles with double peaks. The onset of analyte emission was also delayed relative to liquid residue samples.

No correlation between temporal emission maxima and analyte volatility was found for solid samples, but it was seen for some solution residues. At a forward power of 1.0 kW, emission maxima occurred at four seconds after insertion for Cd, Mg, Pb, and Zn from solid, but for liquid residues, the maxima occurred at 1.5 seconds for Cd and Zn, 2 seconds for Pb, and 3.5 seconds for Mg. The authors suggested that solid samples needed additional time to melt and release volatile elements. The positions of analyte emission maxima also depended on power applied to the ICP.

The authors wanted to know if emission signals for the matrix elements Al, Co, Cr, and Ni had a similar power dependence which might then be used to control their vaporization. They found a general increase in emission intensity from these elements with increasing plasma power and therefore concluded that relatively low power levels should be used in the analysis of nickel-based alloys.

Using a compromise signal integration period of ten seconds for all elements, the authors next examined several parameters affecting signal-to-background ratios. It was observed that SBRs varied with plasma power in the same way for solids and liquid residues. The maximum SBRs occurred at the relatively low plasma power levels of 0.8-1.0 kW and the best signal observation region was 13-17 mm above the top of the plasma load coil (ATOC).

After examining temporal profiles and SBRs, the authors used certified reference nickel-base alloys (Bureau of Analyzed Samples BAS 345, 346 and NBS SRM 898) to check the accura [illegible] ision, and detection limits of their new method. [illegible] ment standard solutions gave good working curve lin [illegible] over several concentration ranges of Cd, Mg, and Zn. Since the fit between results for the solid reference materials and liquid residues was generally good, the aqueous solutions could be used as standards in most cases. A notable exception was the element lead. The authors suggested that lead's misbehavior might be due to some unknown matrix effect. The reference material BAS 346 was therefore used as a standard for the determination of lead in NBS SRM 898.

Detection limits for solids were based on five milligram samples and seven insertions of a blank cup. The results were good in comparison to ETA-AA and HHCD-AES methods for the determination of elements present below the μg/g level.

The mechanism of selective volatilization from solid materials directly inserted into the ICP was further examined in the Julich Nuclear Research Company's Institute for Nuclear Materials by H. Nickel and coworkers (163). These authors used radioactive iron-59 to quantitatively measure the evaporation rate of elements from graphitic and ceramic matrices. Iron-59 diffusion was successfully utilized by Gorsuch (164) in his studies of analyte loss associated with various sample preparation methods. The application of this technique to direct insertion-ICP permitted Nickel and his colleagues to separate the sample's evaporation process from its excitation process.

Their direct insertion mechanism looked much like that of Sommer and Ohls (120); even the plasma gas mixture was the same: N_2-cooled argon. However, the graphite crucible's insertion speed could be continuously varied.

The authors observed a significant enhancement of Fe(II) 259.9 nm emission when a mixture of 2% NaF-2% $(C_2F_4)_n$ was added to a graphite matrix. "Similar results" were noted for the elements silicon, manganese, and tungsten. Iron-59 activity measurements were then taken before and after exposure of samples to the plasma. With the additive, over 90% of the iron-59 activity was lost within ten seconds of sample insertion. Without the additive, 35% of the iron activity remained within the same time period and even after 300 seconds, "significant" activity was still detected. The authors suggested that at least some of this residual activity was due to the diffusion of iron into the graphite crucible.

They checked this assumption by comparing the iron-59 activity in the residual graphite sample powder with whatever diffused into the crucible and found that a larger proportion of the radioactive iron diffused into the graphite crucible in samples without additives. For example, at 3 kW of plasma power, samples without additive gave about 8% residual activity in the cup and about 8% in the sample residue. With the additive, about 0.2% activity remained in the cup and about 0.5% in the residue. Increasing the power from 3 to 4 kW reduced the residual activity from 17 to 9% without additive, but a further increase to 5 kW had no significant effect even thirty seconds after insertion. Increasing power for samples with additives only led to increased residual activity in the sample cups.

For a ceramic (86% Al_2O_3/14% SiO_2) matrix, the additive had no enhancing effect. The authors therefore proposed to investigate in the future different additives such as ammonium chloride.

In the same year (1986), C.V. Monasterios, A.M. Jones, and E.D. Salin (165) tried the graphite cup direct insertion method on another "real matrix"; human hair.

Hair samples one centimeter in length were cleaned with acetone, rinsed with distilled-deionized water, rewashed with acetone, and then dried overnight at room temperature. The hair samples were then placed in graphite electrodes which had been precleaned by insertion for thirty seconds in a running plasma. A sample electrode was constructed from 3/16 inch o.d. graphite rod by drilling a 20 mm deep hole to achieve a sample cup volume of 106 cubic millimeters. The authors didn't want to use larger electrodes because of their lower heating rate and consequently poorer detection limits. Boiler caps were not used on the electrodes.

Although complete vaporization of zinc was achieved, a small shoulder appeared on its temporal emission (213.8 nm) profile. This extra peak was thought to be due to the volatilization of zinc oxide.

Calibration with aqueous standards gave high copper and zinc values compared to those obtained by flame atomic absorption and liquid nebulization ICP. The authors therefore concluded that their direct insertion method could not be used for high accuracy work.

The direct graphite cup insertion method was recently applied in the analysis of a particularly difficult "real sample" by Lorber and Goldbart from Israel's Negev Center for Nuclear Research and I.B. Brenner from that country's Geological Survey in Jerusalem (166).

These authors used Lorber and Goldbart's DSI procedure (horizontal cup insertion, (161)) to look at trace elements in silicate rocks. They were particularly interested in interference effects due to thermochemical reactions occurring in the graphite cup and in the thermal disruption of the plasma due to the perturbation of plasma gas flow. Volatilization behavior was studied as a function of time, plasma power, and the addition of graphite. They tried to compensate for interference effects with internal standardization.

The spatial variation of spectral line intensity was studied by nebulizing a scandium solution (10 mg/l) with and without a cup inserted into the plasma. Without a graphite cup present in a 1.25 kW plasma, the ScII/ScI ratio varied approximately from 0.65 at 0 mm ATOC to 0.2 at 25 mm ATOC, with the maximum intensity occurring at about 5 mm ATOC. For a 2.0 kW plasma, the ratio varied about from 0.8 to 0.5 over the same displacements from the top of the load coil. The maximum ratio value was again at about 5 mm ATOC. With a cup inserted into the plasma, the ion-to-neutral line behavior was quite different at both plasma power settings. The ScII/ScI ratio continuously decreased with increasing observation height above the load coil. The authors therefore concluded that plasma temperature also decreased above the graphite cup.

The authors next examined the temporal behavior of cadmium, copper, and zinc in silicate samples at different plasma powers and with and without the addition of graphite. Without graphite added to the sample, analyte volatilization was delayed (about 10 s from insertion in the case of zinc), double peaks were observed in the temporal profiles, and these profiles "tailed off," especially at plasma powers of 1.5 kW. At 2 kW of forward power, more intense analyte emission was obtained and the cadmium and zinc profiles were very similar in appearance. The authors therefore concluded that since cadmium and zinc had similar volatilization behaviors, cadmium could be used as an internal standard for other volatile elements like zinc.

With the addition of graphite (one part silicate to five parts graphite), analyte emission intensities increased significantly and the double peaks, seen for example in zinc's profile, were eliminated at both 1.25 and 2 kW of forward power. Copper's emission intensity also increased, but the "tailing" of its temporal profile was still observed, even at the higher power setting.

Finally, natural silicate standard reference materials were used to calibrate a trace multielement determination. Using "fast measurement electronics and peak height or area" measurements, the authors achieved an analytical accuracy of

±10-15%. Only copper's calibration curve was presented (with a range of about 10-100 ppm copper).

A different approach to overcoming the sample matrix problems encountered with the direct insertion method has been pursued by Salin and his colleagues at McGill University in Quebec (165,167,168,169,170,171). These investigators have been particularly interested in applying electrochemical preconcentration techniques to direct insertion-ICP analysis.

In their first report (167), M.M. Habib and Salin describe a cathodic deposition preconcentration technique for use with a direct insertion device. Noting that controlled potential electrolytic deposition into mercury had been successfully employed in electrothermal atomic absorption, direct current arc and helium-microwave-induced plasma spectrometries, the authors hoped to use this method to improve detection limits and accomplish the selective separation of elements from difficult matrices for ICP spectrometry.

It was found that a separate thirty second precoating of a graphite electrode with mercury worked better than adding Hg(II) ions directly to the sample solution. This precoating was followed by a one minute oxidation period to remove trace impurities, several rinses with distilled-deionized water, a one minute deaeration, and then a five minute electrolysis with copper nitrate solution. The electrode was then rinsed again and placed in a direct insertion device.

The direct insertion device was modeled after Salin and Horlick's (124) original DSID. Standard dc arc graphite electrodes were still used as sample containers, but the original one-piece DSID torch was replaced with a demountable version. Once the prepared electrode was mounted on the DSID's quartz rod elevator, it was inductively heated in the plasma load coils to remove the mercury. Violent vaporization before insertion would occur if this step wasn't included in the procedure. The electrode was then lowered to one cm below the auxiliary gas tube so the plasma could be ignited. After a thirty second period for plasma stabilization, the electrode was rapidly inserted to the top edge of the load coil. The authors found that the addition of a 1.7 l/min flow of oxygen to the plasma gas aided in heating and insured that the outer electrode layer was removed. With optimized operating conditions, the copper 324.754 nm line was most intense approximately five seconds after electrode insertion.

A maximum error of 11.5% was recorded over a four order of magnitude copper concentration range. The authors suggested that the residual nonlinearity might have been due to changes in sample solution pH.

Background-corrected peak heights for five determinations of copper solutions were used to study precision. Manual extraction of data from a strip chart gave a slightly better RSD than when a computerized approach (AIM-65/BASIC) was used.

Detection limits depended on deposition time, electrode design, and stirring rate. A detection limit (defined as a signal-to-noise ratio of 3:1) of 1.2 ng/ml copper was achieved with a five minute deposition time. When deposition time was increased to two hours, a detection limit of 0.07 ng/ml resulted. If deposition times were extended above two hours, nonlinearity in copper signal vs. time plots became pronounced. A conventional nebulizer with the same demountable torch system gave a copper detection limit of 23 ng/ml. If it was assumed that about 3% of the available copper was deposited in five minutes, then an absolute detection limit of 1.9 ng copper was achieved. This result was checked by the direct addition of 20 µl copper solutions to graphite electrodes. This check gave a detection limit of 0.16 ng copper. The authors proposed that the latter result was better because of the higher atom population generated in the observation region. In contrast to a pretreated electrodes (which expelled analyte from its entire surface), analyte was volatilized only from the electrode's crater.

In contrast to the detection limit results, the RSD of electrochemical method (3%) was better than for direct liquid additions (12% for 9 determinations of three standard solutions (1260, 126, and 12.6 ng)). The authors suggested that this may have been due to the more regular deposition of analyte on the electrodes surface by electrolysis.

The authors concluded that their method should be applicable to the trace and ultratrace analysis of mercury-soluble elements, but sample pretreatment might be required when direct electrodeposition isn't feasible. Although µl-size samples couldn't be used with the current method, this limitation might be overcome by somehow using the electrode crater as both a sample container and working electrode. For instance, a cylindrical graphite flow-through cell might be used with injector plasma gas flowing through it to give a standard annular-shaped plasma. This approach might also decrease detection limits by confining analyte to the plasma's central viewing zone.

In 1985, M.M. Habib and Salin (169) described an extension of their electrochemical preconcentration work to the simultaneous determination of several heavy metals in a "difficult sample matrix;" artificial seawater.

Their electrolysis cell was essentially a 40 ml Teflon cell with a graphite cathode, an SCE reference electrode, and a platinum auxiliary electrode. The graphite electrode was a standard 1/4 inch graphite necked crater dc arc electrode. After electrolysis, the graphite electrodes were again inductively dried within the coils of an extinguished plasma.

An alternative electrolysis procedure utilizing a hanging mercury drop electrode (HMDE) was also tried. After the electrolysis, a mercury drop was transferred to the crater of an electrode. Heating the electrode in an oven at 120°C for 20 minutes completely vaporized the mercury. The authors concluded that deposition on mercury-coated graphite gave better results.

After insertion of the treated electrodes into the plasma, two adjacent emission peaks were observed in the cadmium and zinc temporal profiles. A small peak was also seen prior to the main peak in cobalt's temporal emission profile. The authors felt that the double peaks in the zinc and cadmium profiles were due to volatilization of zinc and cadmium oxides formed with the oxygen they had added to the plasma gas. No explanation was given for the double peaks in colbalt's profile. Single emission peaks were observed for all three elements when the oxygen was eliminated from the argon plasma gas.

Detection limits for zinc and cadmium were therefore calculated from argon plasma gas data. Since an argon-oxygen mixed gas plasma gave better results for the elements copper, lead, nickel, and cobalt, their detection limits were determined with this system. The addition of oxygen apparently increased the graphite electrode's heating rate and resulted in faster analyte vaporization. Electrolytic deposition times of five minutes and compromise plasma conditions were employed in the detection limit (S/N=3) experiments.

Standard additions were used for the determination of copper in artificial seawater (3.5% salinity, 30.2 g/l NaCl and 3.8 g/l Na_2SO_4). An additional wash step was required since sodium chloride residue caused stray light spectral interferences.

2. Wire-in-Plasma

In 1984 Salin and R.L.A. Sing (168) described a pneumatically-powered wire loop direct insertion system. The pneumatic system permitted sample drying under a running plasma and subsequent fast sample insertion.

Liquid samples were placed on two 2 mm diameter loops at the end of a 4 cm by 0.46 mm tungsten wire. The wire loops were then pneumatically raised to a position beneath the plasma for drying. The authors noted an increase in plasma intensity of about 30% during sample drying. The plasma's intensity then returned to normal upon completion of drying. Data acquisition began automatically as a mechanical stop was released to allow the sample to continue upward into the plasma. It took about fifty milliseconds for the wire to travel to its final insertion stop. Degradation of precision due to embrittlement and surface pitting of the wire loops contraindicated their use for more than about one hundred insertions. Exposure of the wire loops to air on return from the hot plasma accelerated their degradation.

Copper and zinc emission signals peaked 310 ms and 270 ms after insertion, respectively, and the copper samples were completely vaporized within about 0.1 s. It was found that spectral overlap of the analyte zinc 213.856 nm line with the sample support tungsten 213.815 nm line could be resolved temporally. However, the authors pointed out that selective atomization of the sort possible with furnace and tantalum wire separate atomization methods was not possible.

The authors also investigated the effect of 0.1% calcium on the temporal behavior of copper. Changes were noted in the copper signal's peak height and shape and the slope of copper's calibration curve was decreased by 65% if peak height data were used to construct the curve. No change in the calibration curve was found if peak area data were used.

The authors felt that many more sample matrices needed to be examined in order to fully explore matrix effects.

No advantages were found to operation of the plasma above 1.75 kW of forward power. A Simplex optimization was carried out on the values of observation height and final sample position (see Table II.3 for results).

In 1986 D.W. Boomer, M. Powel, Sing, and Salin (170) reported on the extension of their previous wire loop DSID work to ICP-mass spectrometry (ICP-MS). The Ontario Ministry of the environment needed improved detection limits for metals in water samples and the authors reasoned that since ICP-MS with electrothermal atomization (ETA) had shown improved detection limits relative to conventional nebulization ICP-MS, a wire loop DSID-ICP-MS might give even better results.

Samples were inserted horizontally into a Sciex ELAN model 250 ICP-MS by pneumatic action. Sample retraction was performed either manually or by vacuum. Sample drying was accomplished about 10 mm away from the running plasma.

A univariate optimization was performed for manganese which resulted in a factor of forty improvement in detection limits (based on a signal three times the standard deviation of a blank) over conventional nebulization. The authors claimed that the detection limits obtained with their DSID-

ICP-MS system rivalled those of ETV(electrothermal vaporization)-ICP-MS.

The authors concluded that the main advantage of both ETV-ICP-MS and their DSID-ICP-MS was a decrease in oxide formation due to sample desolvation prior to atomization.

Sing and Salin (171) have recently modified their wire loop direct insertion system to provide better control over sample drying. Replacing the pneumatic insertion device with a computer-controlled stepping motor provided precise motion control. With a vertical sample velocity of 20 cm/s, rapid final insertion was still possible. In addition, a special purged chamber was no longer necessary to cool the wire to prevent oxidation; the sample was simply cooled in the lower portion of the ICP torch. A solenoid-driven door closed the base of the plasma torch when a sample was retracted.

The sample holder consisted of two side-by-side 2 mm diameter loops formed from 0.5 mm diameter wire. The lower end of the holder was fused into 3 mm diameter glass rod. Liquid samples were applied either manually with an Eppendorf micropipet or with a home-built automatic device. The automatic device consisted of a swinging arm with a PVC tube attached to peristaltic pump. This device could deliver about 14 µl sample aliquots and was useful for repeated insertions of the same solution.

For 30 automatic insertions (taking 25 minutes) of 100 µg/l copper solutions, RSDs ranged from 0.9-3.5% for peak height measurements and from 0.5-2.0% for peak area measurements. Over a period of 3.3 hours, 250 automatic insertions gave RSDs of 5.4% by peak height and 1.4% by peak area. In contrast, RSDs of 3-15% were obtained for 10 consecutive manual insertions of 10 µl solutions.

Once a liquid sample was applied to the wire loop, drying was accomplished by convective, radiative, and inductive heating from the plasma. The main factors affecting drying time were the sample's distance from the plasma discharge and the plasma's forward power and auxiliary gas flow rate. If the liquid sample was brought closer to the plasma than 20 mm BTOC, a rise in reflected power was noted as the plasma became destabilized and restricted in size. Sample sputtering was also observed at this distance. Attempting to dry a sample closer than 15 BTOC often resulted in extinction of the plasma. Drying time was noted to vary inversely with plasma power and directly with auxiliary gas flow rate. Based on these observations, the authors chose to dry further samples for 20-30 seconds at 22 mm BTOC.

Temporal profiles revealed different vaporization times for seven analytes (10 µl aliquots deposited on tungsten wire loops). Upon ranking, these vaporization times looked to the authors like the corresponding oxide volatility series for dc arc emission. The analyte temporal profiles also indicated oxidation of the sample wire loop in the moist environment formed during the sample drying stage as all profiles except copper's exhibited a peak in the analyte and blank scans which was not seen in the corresponding bare wire scans. The authors therefore attributed the additional peaks to spectral overlap from tungsten oxide.

Even though the tungsten spectrum was very rich in emission lines, the spectral overlap of most analyte and tungsten emission could be avoided by careful temporal separation. However, this technique didn't work for lead. This problem stimulated the authors to try tantalum wire as an alternative sample support.

Temporal profiles for cadmium, zinc, and lead emission from a tantalum wire support indicated that tantalum emission didn't begin until all the analyte was volatilized. This result was expected since tantalum oxide is the last member of dc arc emission series (tungsten oxide lies near the middle of this series). But tantalum wires turned out to be inconvenient since they disintegrated after thirty to fifty insertions. No explanation for this behavior was offered. In contrast, the tungsten loops lasted for over 250 insertions. It was therefore decided to use tungsten loops for all analytes but those which gave temporally unresolvable spectral overlap.

Using analysis conditions optimized for copper, detection limits on the order of 100 µg/l were obtained for most analytes. Arsenic's detection limit of 1000 µg/l was an exception. Detection limits were defined as the signal corresponding to three times the standard deviation of five or more blank insertions. If a significant blank peak was observed, the authors used the standard deviation of measurements from bare wire insertions in the calculation of the detection limit. Measurements based on peak heights gave slightly better results than those based on peak areas.

With the exception of arsenic and vanadium, these results were one or two orders of magnitude better than results obtained by traditional liquid nebulization sample introduction. They were also better than ETV and graphite cup DSID introduction techniques. The authors proposed that the superior detection limits were due to rapid analyte vaporization from the sample support wire and the resulting high transient analyte concentration in the plasma.

A further improvement in detection limits was realized with multidrop sample insertions. A multidrop sample was prepared by automatically applying an aliquot of liquid sample to a wire support and drying it and then repeating the process. This preconcentration procedure was tested with one to ten drops of 1 μg/l copper and cadmium solutions on tungsten wire and one to ten drops of 1 μg/l cadmium solutions on tantalum wire.

For multidrop samples up to five drops in size, a linear increase in analyte signal with the number of sample drops was observed and improvements of at least an order of magnitude in detection limits resulted. However, severe matrix effects were encountered with multidrop samples larger than five drops. For example, the tungsten signal become enormous after five applications of cadmium solution because of oxidation of the sample support wire. As a result, working curves became nonlinear when more than five drops of each standard were applied to the wire.

The authors also investigated the spatial intensity distribution of copper emission and interference effects other than those caused by oxidation of the sample support wire. They were particularly interested in the changes in analyte temporal signal shape caused by the presence of calcium. Spatial profiles of the emission given by 100 μg/l copper solutions showed that analyte was channeled into the plasma's center. The profiles were broader than those obtained with solution nebulization, although, unlike nebulization, no drop in emission intensity low in the plasma due to cooling was observed. It was therefore assumed that the sample support wasn't significantly cooling the plasma.

Copper signal was unaffected over the entire calcium range of 0-10,000 mg/l, but the area of cadmium signal peaks decreased when calcium concentration exceeded 1,000 mg/l. Peak height measurements gave worse results than peak area measurements and this reduced the benefits of temporal separation. Both analyte peak height and area varied when tantalum wire sample loops were used, but the authors didn't suggest an explanation for this behavior. It was concluded that the effect of interfering calcium was to somehow change the sample volatilization process, but not analyte residence time in the plasma or plasma excitation conditions.

The authors were also interested in the effect of wire replacement on the reproducibility of results. Four tungsten loops were made as similar as possible and each of these was used for four sets of ten insertions of 100 µg/l copper solution. Wire replacement and even repositioning of the same wire affected results significantly. An overall RSD of 4.8% was calculated and the authors felt that if this value could somehow be reduced, carousels of sample wires might be used to both increase sample throughput and to interface the system to FIA and LC.

3. Rod-in-Plasma

In a series of papers beginning in 1982 (121,122,123,156), Kirkbright and coworkers described the development of their own version of an ICP direct insertion technique. They were interested in combining the two main attractive features of Salin and Horlick's (124) DSID and Sommer and Ohls' (120) SET; namely low power and continuous operation, respectively.

In 1982, Kirkbright and Walton (121) achieved this combination. They used a graphite rod 30.5 cm long and 3.05 mm in diameter and equipped with an insulated handle. Liquid samples were applied to the end of the rod, desolvated with a heat gun, and then the rod was inserted into the plasma from below via an injector tube. An adjustable stop controlled the insertion height. The authors found that prior desolvation of the sample was necessary in order to prevent disturbance or extinction of the plasma.

Like Sommer and Ohls (120), these authors noted "...an immediate diminution of plasma intensity as power was coupled to the rod..." and a significant drop in baseline emission intensity. Temporal profiles revealed that this baseline shift was resolved from analyte signal in all cases examined except cadmium. These profiles were similar to those obtained by Salin and Horlick (124) and Sommer and Ohls (120). As observed by the latter authors, the nickel signal did not return to the original baseline level. Iron and cobalt behaved similarly and Kirkbright and Walton stated that "...prolonged heating does not change this and the effect may be attributable to change in rod position or physical condition after heating."

The authors initially chose not to use a sample well at the end of their graphite rod as manganese emission intensity was observed to decrease as well depth increased. Therefore, sample volume was restricted to 5 µl.

The authors determined detection limits for seven elements using experimental conditions optimized according to Mn II 257.6 nm signal-to-background ratio. Precisions were noted to degrade with increased rod use even if peak area measurement was employed. Direct insertion of a tungsten wire loop was tried but greater blank imprecision degraded detection limits and embrittlement shortened the wire's lifetime. Although it was felt that it might be possible to determine refractory elements by using pyrolytic carbon as a sample support, an attractive alternative was described later in 1982 by Kirkbright and Li-Xing (122).

An in-situ method of preventing refractory carbide formation was developed by Kirkbright and Snook (172) for use with an electrothermal ICP sample introduction device. The method relied on the preferential formation of volatile fluorides and was adapted for use with direct graphite rod insertion by Kirkbright and Li-Xing (122). An argon-0.1% Freon-23 mixture was routed into the graphite rod injector tube via a sidearm located below the ICP torch. Experimental parameters including argon/Freon injector gas flow rates were optimized for each of nine elements. No improvement in the detection limits of the relatively volatile elements Ag, Zn, and Cu was noted with the addition of the argon/Freon mixture. Similarly, little improvement for Mo, B, and Cr was noted, but detection limits for U, Zr, and Ti decreased by more than two orders of magnitude.

Kirkbright and Li-Xing (122) argued that the lower heating rate and higher final temperature of the directly inserted graphite rod relative to an electrothermally heated graphite furnace might encourage carbide formation. The authors estimated that a surface temperature of about 4000°C was attained within a few seconds of insertion. The carbides of boron and chromium have boiling points below this temperature and therefore probably vaporize from the rod and decompose in the hotter plasma tailflame. The authors proposed this as an explanation for the lack of improvement in analytical sensitivity for these two elements when Freon was injected. Carbides of the elements U, Zr, Ti, and Mo all have boiling points above 4000°C and would therefore be inefficiently volatilized without the addition of Freon. The authors felt that the lack of improvement in sensitivity for molybdenum when Freon was employed may have been due to the preferential formation of Mo VI oxide which sublimes at 1155°C. They suggested that greater sensitivities might be obtained by increasing the percentage of Freon in the injector gas mixture.

CHAPTER III

AUTOMATED DIRECT SAMPLE INSERTION DEVICE (DSID) DEVELOPMENT

A. Introduction

The rationale for development of an automatic direct sample insertion system for an inductively coupled plasma was presented in Chapter I. Using a manual device (Figure 1), Salin and Horlick (124) demonstrated the feasibility of direct insertion and concluded that the technique had "... the potential of significantly expanding the overall analytical capability of the inductively coupled plasma."

Before further research was initiated, a rethinking of the original insertion mechanism in terms of automation was undertaken. The time spent in consideration of automation during the development of direct insertion would certainly promote fulfillment of the technique's potential recognized by Salin and Horlick (124).

In this regard it is useful to recall Arndt and Werder's (6) guidelines for the successful automation of discrete analysis methods mentioned in Chapter I. A reliable sample transport mechanism and flexible control of individual operations are important in terms of hardware. In addition, accuracy and precision of analysis, adaptation of existing methods, the possibility of intermediate manual steps, modularity, and transparency of operation must also be considered in the automated design.

As outlined at the end of Chapter I, a pneumatic mechanism (Figure 2) was chosen for sample transport in the new direct insertion system. Pneumatic transport was mechanically simple and proved reliable after sufficient development. The remaining functional units were incorporated into the overall system in order to retain flexible control of individual operations.

Once developed to a sufficient degree, this system met the remaining criteria important for successful automation. First of all, continuous plasma operation and automatic sample insertions resulted in a significant improvement in analytical precision relative to the original discontinuous manual method.

The relatively low power argon plasma and convenient graphite sample cups for liquids and powders were attractive features of Salin and Horlick's (124) original design. These features were retained and enhanced in the automated version. Alternate plasma gas and sample cup compositions gave further improvements in analytical precision and sensitivity.

Secondly, existing methods of discrete sample analysis like the "Delves Sampling Cup" technique discussed in Chapter II could readily be adapted to the new ICP insertion system. In particular, sample drying and ashing pretreatment steps were implemented in a controlled fashion.

Thirdly, because samples were held in individual open cups in a removable carousel, intermediate manual steps were possible. Thus, the modification of an analytical procedure could be tried either on-line or off-line without disturbing plasma operation. The presentation of individual sample cups from a carousel provided additional benefits. Sequential one-shot use of cups avoided contamination and memory effects. Rapid sample cycling was possible because pre-burn and cooldown stages were not required.

A direct insertion system based on the pneumatic transport of samples from a carousel also fulfilled the fourth criterion, modularity. The system could be retrofitted to most commercial ICP sources with minimum effort. In addition, the ICP direct insertion instrument could be envisioned as a modular subunit of a larger analytical system. Samples would be pneumatically transported to various other modules for pretreatment and/or alternative analysis.

The final criteria, transparency of operation, was met in the late stages of system development. Once the mechanical problems had been overcome, the system could be reliably operated under computer control. It was necessary only to load a carousel and input operating parameters at the computer terminal; the system would run automatically from that point.

A generalized diagram of the successfully implemented automatic direct insertion system is given in Figure 3. The system's functional sub-units will be described in this and the following two chapters.

The torch and sample carousel sub-units constitute the basic direct sample insertion device (DSID) and its development will be described in this chapter after a brief look at the ICP source.

The remaining photodiode array spectrometer, computer data acquisition, and pneumatic injection control sub-units will be covered in chapter IV.

The incorporation of an in-situ sample pretreatment device in the DSID will be described in chapter V along with an alternative laser pretreatment device.

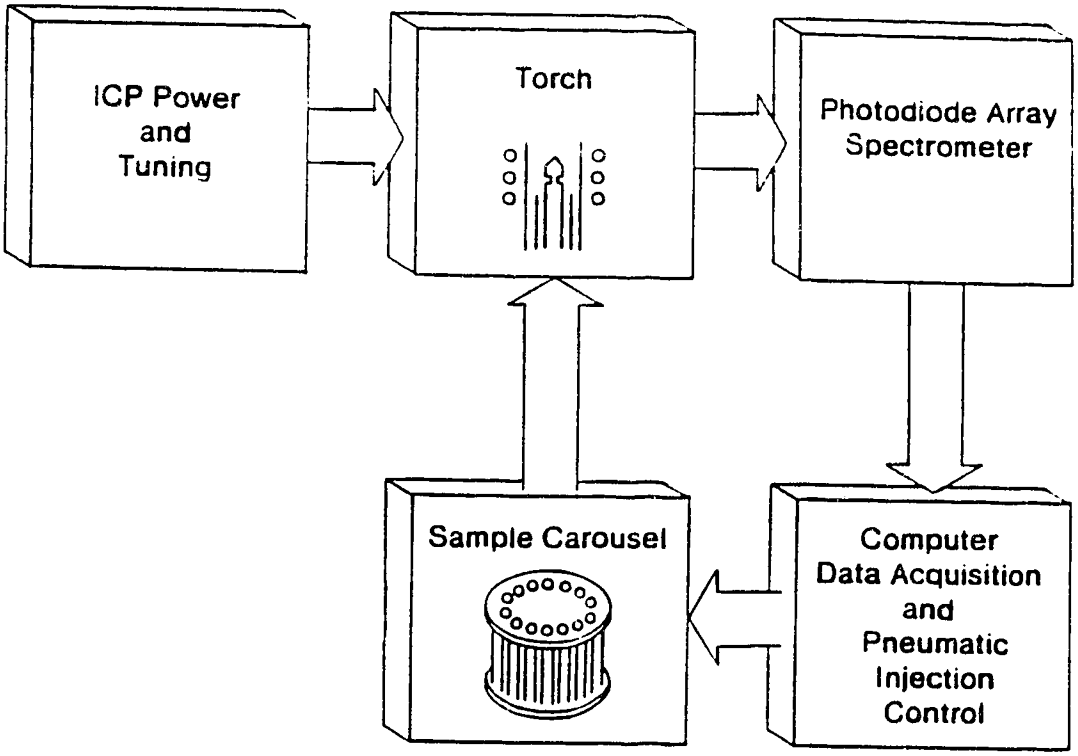
ICP Power
and
Tuning
Torch
Photodiode Array
Spectrometer
Sample Carousel
Computer
Data Acquisition
and
Pneumatic
Injection
Control

Figure 3. Automatic direct insertion system.

B. ICP Source

1. DSID Installation

The DSID was installed in a Plasma-Therm (Route 73, Kressan, N.J.) Model 5000 ICP. Further source details including typical running conditions are given in Table III.1. As mentioned at the end of Chapter 1, the DSID was designed so that little modification of the Plasma-Therm ICP would be required for installation. It was only necessary to drill three small holes in the base of the torch box and to upgrade its plumbing. One hole permitted passage of a sample delivery tube (Section 3) and the other two were used to install a new torch mount (Chapter V). The plumbing improvements are described below.

2. Gas Supply

It was of interest to study the effects of mixed-gas plasmas on the behavior of directly inserted samples. In order to provide mixed-gas capability, the gas circuit in the 5 kW source used for DSID development was rerouted and upgraded (Figure 4).

The original polyethylene tubing used inside the ICP

TABLE III.1

ICP SOURCE AND TYPICAL RUNNING CONDITIONS

Plasma-Therm Inc. ICP-5000 Source

Component	Model
Torch box	PT-1
Matching network	AMN-5000E
RF generator	HFS-5000D

Typical Running Conditions

Parameter	Specification
Forward power	2.0 kW
Reflected power	0.05 kW
Frequency	27.12 MHz
Coolant gas	Ar/1% O_2 or H_2, 20 l/min
Auxiliary gas	Ar, 1 l/min
Snuffer gas	Ar, 1 l/min
Observation height	18 mm above load coil

source's torch box could not withstand the additional heat generated by a mixed argon-oxygen plasma sustained with more than 1.5 kW RF power. It was therefore replaced by copper tubing with Swagelok fittings. Coolant and auxiliary gas lines were rerouted to Swagelok bulkhead connectors in the torch box's rear panel as outlined in Figure 4. The addition of alien gases to coolant and/or auxiliary argon via external mixers (Table III.2) was then a simple matter. A bypass could be readily installed between input and output connectors if no mixing was desired.

Each needle valve on the external gas mixer (Figure 4) was moved from the normal position at its metering tube's inlet to its outlet in order to provide flow readings independent of backpressure.

The original flowmeters mounted on the ICP torch box now measured total coolant and auxiliary gas flows to the torch after external mixing. The nebulizer gas line was also rerouted to a bulkhead connector in the torch box's rear panel (Figure 4). An external three-way solenoid valve was used to switch gas from this line either to an external purge line or back into the torch box via another bulkhead connector to a snuffer line. Purge and snuffer line functions will be described in following sections.

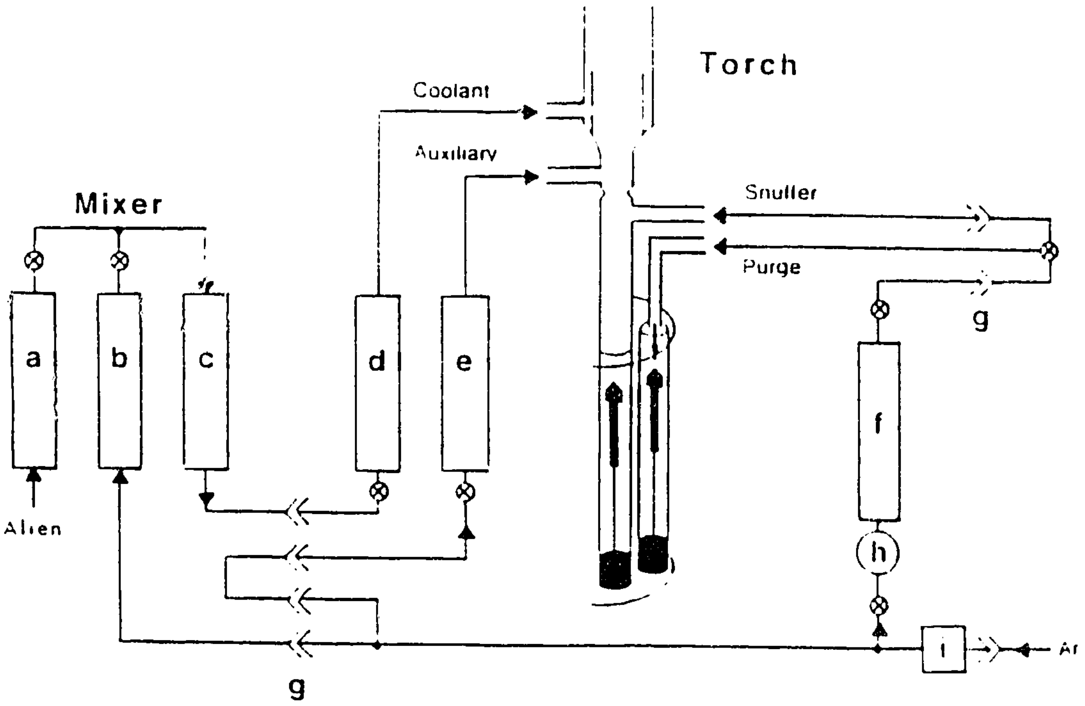
Torch
Coolant
Auxiliary
Mixer
Snuffer
Purge
a
b
c
d
e
f
g
h
i
g
Alien
Ar

Figure 4. Modified ICP gas circuit. (See Table III.2 for component identification).

TABLE III.2

ICP GAS SUPPLY COMPONENTS

Mixing Rotameters (Outside Torchbox)

(Supplied by Matheson Gas Products, E. Rutherford, N.J.)

Component	Figure Label
Ar/O_2 or N_2 Plasma	
#603 tube for O_2 or N_2	(a)
#605 tube for Ar	(b)
#7351 T Gas Proportioner	(c)
Ar/H_2 or CH_2F_2 Plasma	
#601 tube for H_2 or CH_2F_2	(a)
#605 tube for Ar	(b)
#7352 T Gas Proportioner	(c)

Delivery Rotameters and Other Components (Inside Torchbox)

(Bulkheads supplied by Crawford Fitting, Niagara Falls, Ont. and remaining items by Plasma-Therm, Kresson, N.J.)

Component	Figure Label
Coolant rotameter, 0-25 l/min	(d)
Aux. rotameter, 0-1 l/min	(e)
Nebulizer rotameter	(f)
Swagelok bulkheads, 1/4 in	(g)
Nebulizer pressure gauge	(h)
Argon flow interlock	(i)

3. Torch and Transport Assembly Development

In order to permit pneumatic transport of samples into a plasma discharge, the central aerosol tube found in standard ICP torches (Figure 5a) was removed and replaced with a tube of larger diameter (Figure 5b). This tube functioned as a guide for samples moving along its interior. With the experimental torch mounted in the 5 kW plasma unit's RF coil, this guide tube extended about 30 cm below the coil housing through a hole cut in the housing's base. In the pilot version used for initial testing, the guide tube was held in the torch with a teflon bushing.

A standard 3/16 inch diameter dc arc undercut graphite electrode mounted in a cylindrical teflon plug served as the sample transport assembly (Figure 5b) in initial trials of the pneumatic delivery concept. A small lip at the upper end of the guide tube functioned as a stop for the teflon plug. The maximum height to which the sample cup could be inserted into the plasma was therefore governed by the graphite electrode's length and the position of the guide tube within the torch.

Preliminary experiments showed that the graphite electrode could be pneumatically transported into an argon plasma sustained with 1.5 kW RF power, but two main problems

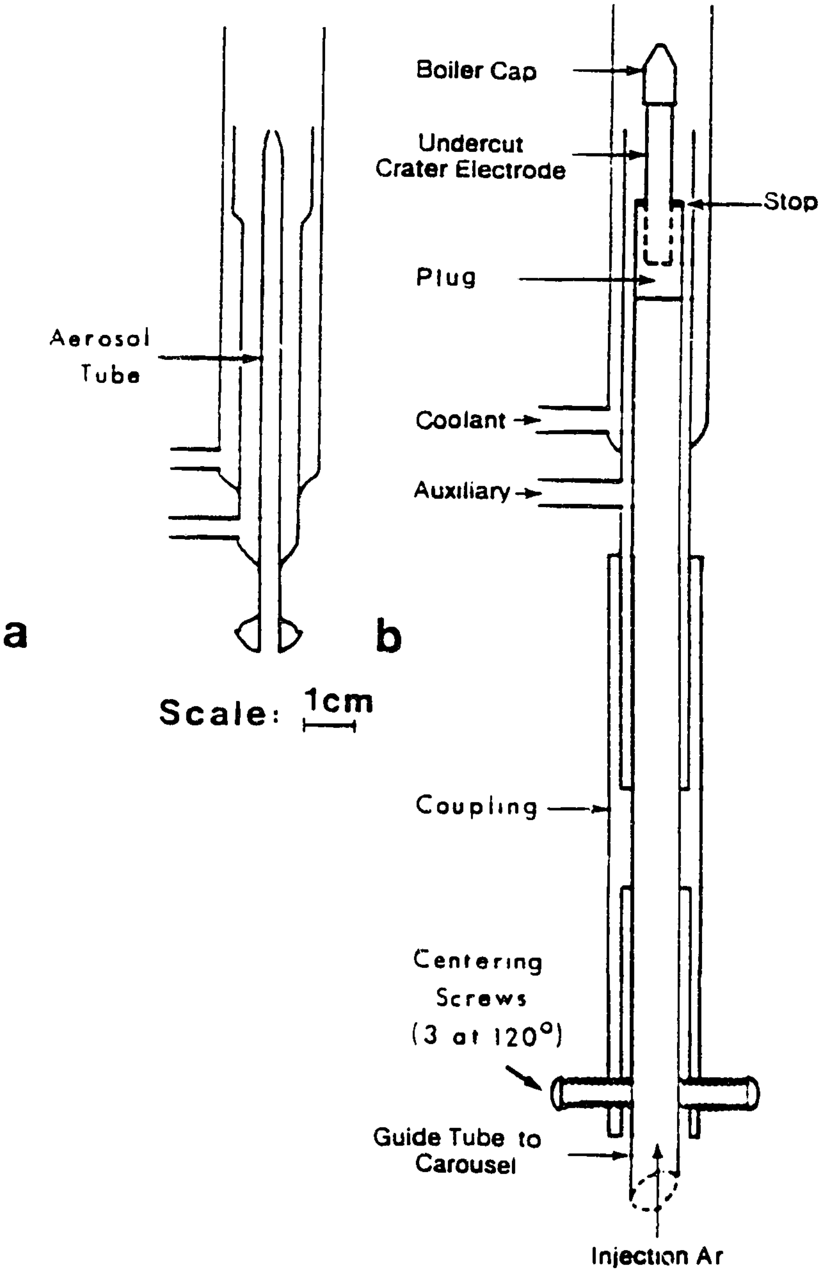
Boiler Cap
Undercut
Crater Electrode
Stop
Plug
Aerosol
Tube
Coolant
Auxiliary
a
b
Scale: 1cm
Coupling
Centering
Screws
(3 at 120°)
Guide Tube to
Carousel
Injection Ar

Figure 5. (a) Standard ICP torch, (b) initial pneumatic injection ICP torch and sample transport assembly.

were encountered.

First, it was found that air could not be used as the injection gas because it destabilized the plasma and often extinguished it as the sample rose toward the plasma. This problem was overcome by using argon as the injector gas.

Secondly, gravity return of the sample assembly was unreliable because heat transferred to the teflon plug often caused it to expand and jam. High temperature Vespel plastic worked somewhat better, but the problem wasn't eliminated until the plug was fashioned from machinable glass.

It was then possible to pneumatically insert a graphite cup into the discharge, retract it, remove the cup assembly entirely from the guide tube, and then to repeat the entire process. The automatic retuning feature of the ICP power supply limited the reflected RF power to only a momentary rise of about 25 W during sample insertion and retraction. However, a new problem often occurred during sample retraction.

A bright filamentous discharge would often make contact with the top of the graphite sample cup during its withdrawal from the plasma. It would then extend down the torch guide tube as the sample assembly was further retracted. In several instances this filament melted through the guide tube wall to make contact with an adjacent metal object. This caused an immediate extinction of the plasma.

This filamentous discharge could be snuffed out if the guide tube was purged with argon immediately after the sample was retracted from the plasma. Provision was made for this purging in the torch shown in Figure 6a. The additional filament snuffer gas line was constructed such that its flow was blocked by the sample-carrying plug when it was fully inserted into the torch. This automatic valve action thus prevented any disturbance of the plasma due to the "snuffer gas" during the final stage of sample insertion.

Pneumatic sample delivery looked very promising at this point. The next step was to increase speed and reliability of delivery by upgrading the transport assembly.

Thermal isolation was provided by a quartz stem separating the sample cup from its pneumatic plug (Figure 6a and Table III.3). The plug was formed from Vespel as this plastic was much easier to work than machinable glass.

The pedestal guide tube was now integrated directly into the torch's lower end. Maximum insertion height was therefore governed by the length of the quartz stem in the transport assembly.

Although the above changes gave better performance, the sample plug would still occasionally jam at its stop. A

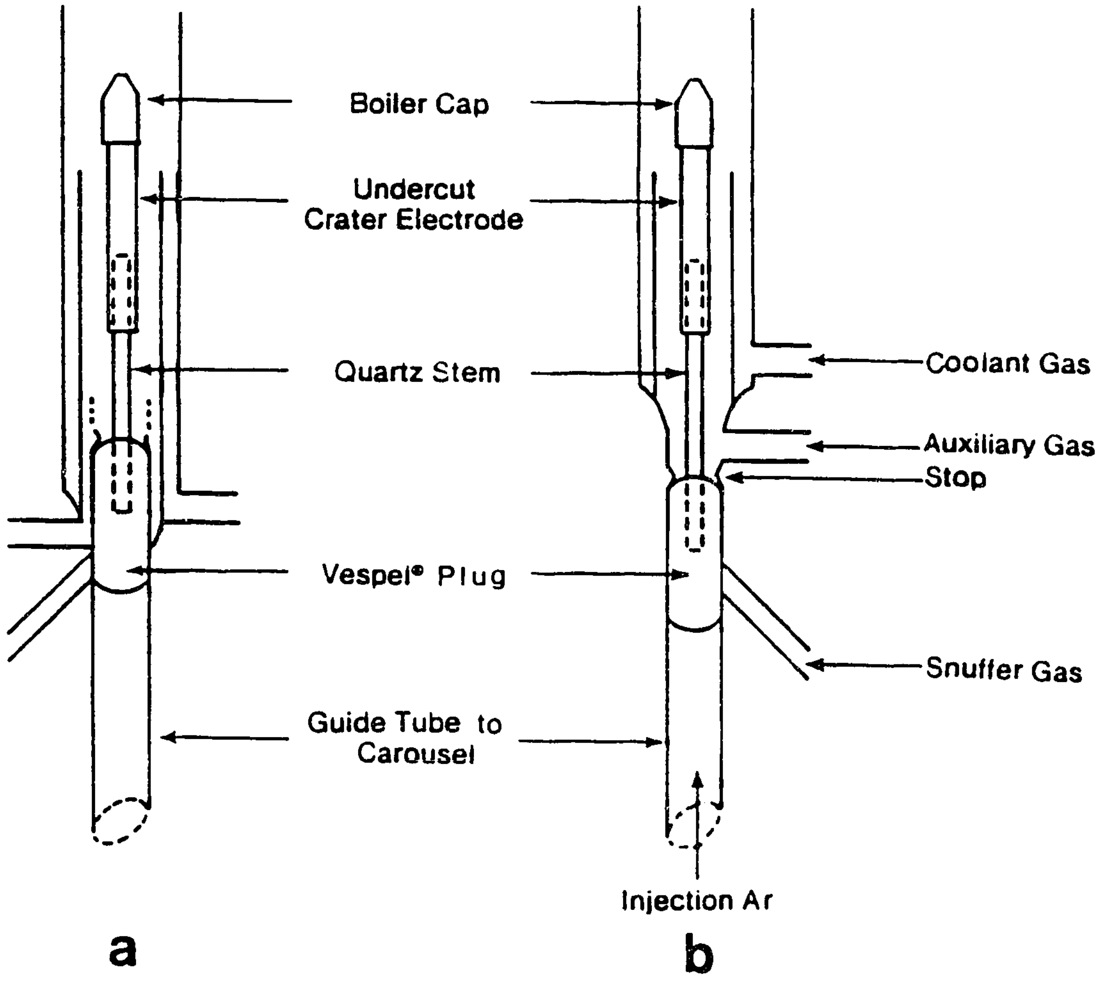
Boiler Cap
Undercut Crater Electrode
Quartz Stem
Vespel® Plug
Guide Tube to Carousel
Coolant Gas
Auxiliary Gas
Stop
Snuffer Gas
Injection Ar
a
b

Figure 6. (a) Pneumatic injection ICP torch with integrated guide tube and reflective collar, (b) simplified design.

TABLE III.3

TRANSPORT ASSEMBLY SPECIFICATIONS

Stems

Parameter	Specification
Material	quartz rod
O.D.	4.2 mm
Length	85.9 mm

Plugs

Parameter	Specification
Material	Vespel (Dupont) or Delrin (Dupont) machinable plastic
O.D.	10.4 mm
Length	44.3 mm with both ends rounded to help prevent jamming
Quartz stem receptacle	16.8 mm x 4.2 mm hole in one end

collar installed above the stop (Figure 6a, dashed lines) helped reflect heat away from the plug, but reliable performance wasn't achieved until the design given in Figure 6b was used. More efficient cooling of the transport assembly was realized by lengthening its quartz stem and by routing auxiliary gas directly over the top surface of its plug.

The torch design was now greatly simplified; the plug stop consisted merely of three small indentations in the upper end of the guide tube. Centering of the guide tube was now an easy exercise for the glass blower.

The standard 3/16 inch diameter graphite electrodes used as sample cups had 3/32 inch deep undercut craters. These dimensions permitted a maximum sample weight of about 15 mg for powdered biological tissue, but as described in Chapter IV, preliminary studies indicated that an increased sample capacity would significantly improve analytical capability.

As the 3/16 inch electrodes were the largest that could be successfully inserted into the existing plasma, a discharge of greater volume was required for the insertion of larger electrodes. This in turn meant that a larger RF coil was needed. Experiments indicated that the largest coil the RF generator's matching network could tune was four turns and 35 mm in diameter. An ICP torch similar to the one shown in

Figure 6b with an outer concentric diameter of 25 mm was constructed to fit this RF coil. The largest commercially available (1/4 inch o.d.) dc arc undercut crater electrodes were successfully inserted into a plasma sustained in this large torch. These electrodes provided a maximum sample size of about 30 mg.

The use of larger electrodes as sample cups resulted in advantages in addition to increased sample size. New sample carousels and transport assemblies of increased dimensions were constructed for use with the larger sample cups and torch. A larger carousel-to-torch coupling was also built. Machining of these larger units proved to be less tedious as tolerances were less critical relative to the smaller versions. Most importantly, the larger DSID proved to be significantly more reliable in operation.

For these reasons, all further experiments were performed with the larger DSID. The specifications for all DSID subunits, with the exception of the original torches, are therefore reported for the larger version.

4. Sample Cup Composition

Undercut graphite electrodes were very attractive candidates for use as sample cups in view of their ready availability and the ease of fitting them to quartz rod by a simple drilling operation. The availability of boiler caps to fit these electrodes was also an important factor during the early phase of research. Samples were initially inserted directly into the plasma without pretreatment (i.e. drying and/or ashing) and these caps served to help control volatilization.

As mentioned in the preceding section, the largest commercial electrodes could hold a maximum of about 30 mg of powdered biological tissue. Any further increase in capacity would have required custom machining of sample cups - a factor which could have hindered initial acceptance of DSID by potential users.

During the later stages of research, the effect of sample cup composition on analyte optical emission behavior was examined. Sample cups were machined from the metals molybdenum, tantalum, and tungsten and from the nonmetallic materials boron nitride and Teflon. The various cups are depicted in Figure 7 and their specifications are given in Table III.4.

Machining of Teflon and molybdenum was straightforward and could be done with standard tools. Boron nitride was very brittle and required extra care during fabrication. Tantalum was both brittle and very hard and required cooling

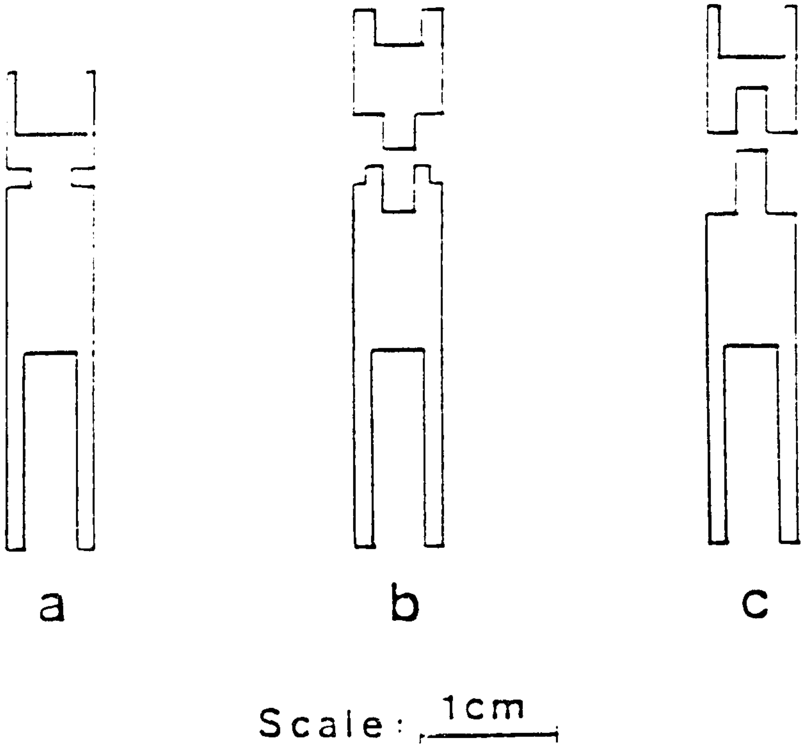

Figure 7. Sample cups. (a) Graphite, (b) graphite base with tungsten cup, (c) graphite base with molybdenum, tantalum, or boron nitride cup.

TABLE III.4

SAMPLE CUP SPECIFICATIONS

(See Figure 7 for additional dimensions)

Graphite Cups

Parameter	Specification
Material	spectroscopically pure graphite
Necked crater electrodes	Spex # 4000 HPND 1/4 in diameter, 5/32" deep
Boiler caps	Spex # 4022 1/4 in
Quartz stem receptacle	15 mm deep x 4.2 mm wide holes

Metal Cups

Parameter	Specification
Material	1/4 in diameter high purity rod stock
Base	machined from 1/4 in diameter spectroscopically pure graphite rod stock

Boron Nitride and Teflon Cups

Parameter	Specification
Material	3/16 in diameter virgin Teflon rod stock and boron nitride block stock

during turning. Drilling in this material was very difficult by standard methods.

Tungsten was the most difficult material to fabricate. Although the outer surface of tungsten rod could be ground, it was impossible to drill using the bits available. An ultrasonic impact drill (Sonorode, Kerry's Ultrasonics Ltd., Hunting Gate, Wilbury 13 Way, Hitchin, U.K.) was required to fashion cups. An aqueous suspension of silicon carbide particles (220 mesh) was continually recirculated between bit and work to provide abrasion. Monitoring and adjustment of this recirculation, the impact frequency, and bit dimensions were necessary during drill operation. An average progress of about 0.01 inch of depth per hour made this process extremely time-consuming.

C. Carousel for Sequential Sample Presentation

Once the various problems discussed in the preceding section were solved, a dependable direct insertion torch-sample transport assembly design was realized. Then, in order to retain the flexibility of the pneumatic sample insertion approach, a carousel was constructed to sequentially present sample assemblies to the torch guide tube. A carousel tray held 24 samples, but there was no inherent limit to sample capacity as trays could be exchanged without disturbing plasma operation. A linear sample cartridge design was also considered, but it was discarded in favor of the more compact carousel design.

Details of the sample carousel tray and its drive are given in Figure 8 and Table III.5. The tray was constructed by sandwiching 24 pyrex tubes between an aluminum upper plate and a plexiglass lower plate. Holes extended through the upper plate and the pyrex tubes were nearly flush with its top surface. The tubes were glued into recesses in the lower plate. Smaller diameter holes passed through to the bottom surface in order to leave support for the sample plugs. Three steel standoffs and a central plexiglass standoff provided rigidity.

This tray design proved to be very functional as the pyrex tubes withstood repeated exposures to hot sample cups without degradation and the tray was easy to handle during laboratory operations such as sample loading and removal.

Sample plugs were machined to close tolerances to insure reproducible injection velocities between samples. A minimal clearance between plug and guide tube wall also permitted the use of low injection gas pressure. These close tolerances in turn dictated a precise indexing between the carousel tray and torch guide tube. A precise drive and stable mount were

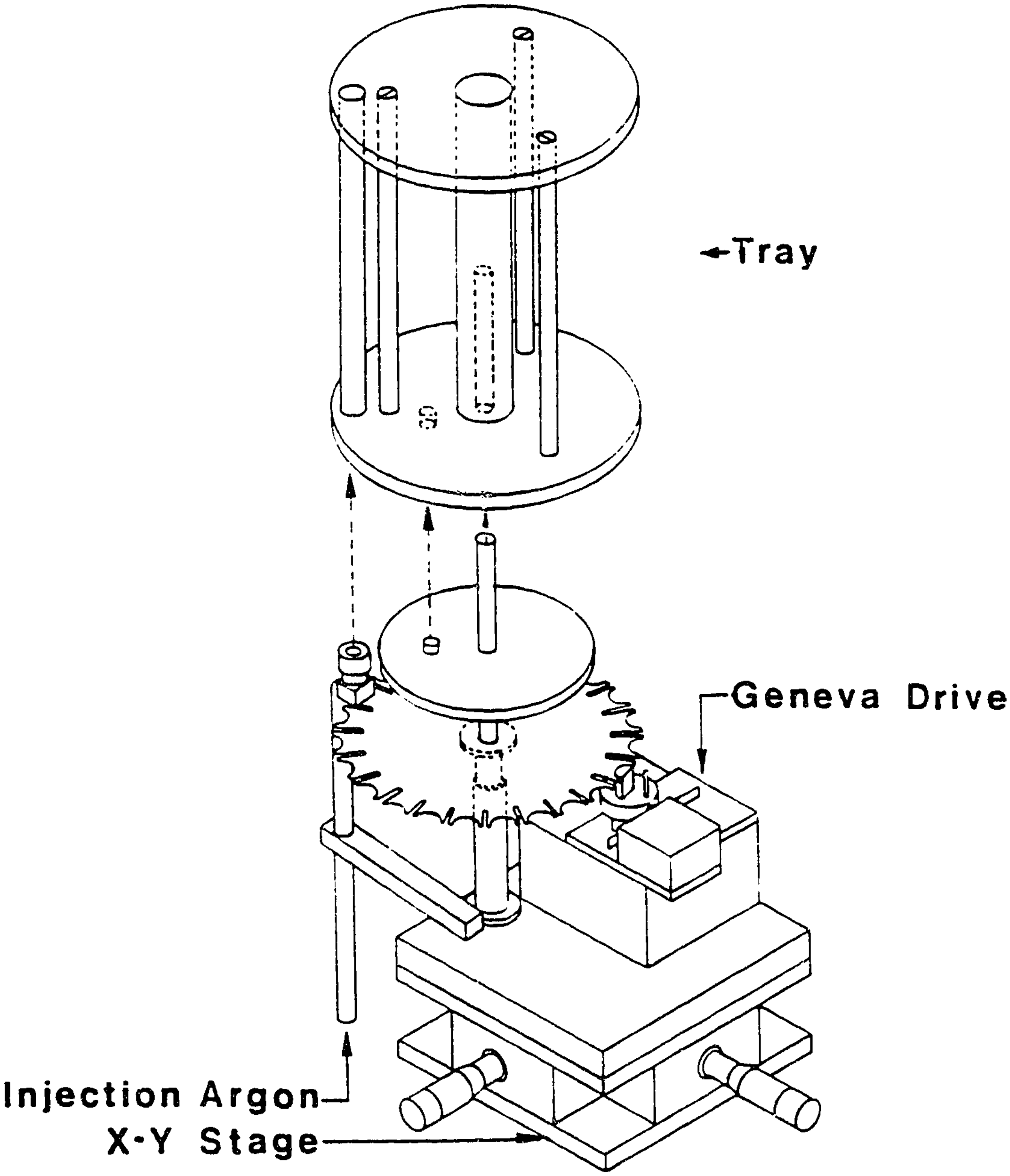
Tray
Geneva Drive
Injection Argon
X-Y Stage

Figure 8. Sample carousel.

TABLE III.5

CAROUSEL TRAY SPECIFICATIONS

Top Plate

Parameter	Specification
Material	aluminum
Diameter	176 mm
Thickness	9.7 mm
Sample tube holes	Twenty four 13 mm holes centered 11 mm from plate edge and 19.6 mm from one another.
Outer standoff holes	Three 6.4 mm holes centered 36 mm from plate edge and 88 mm from one another.
Center standoff recess	9.5 mm diameter center hole 6.6 mm deep then 25.6 mm wide remaining distance to bottom of plate.

Sample Tubes

Parameter	Specification
Material	pyrex glass
O.D.	12.95 mm
I.D.	10.6 mm
Length	150 mm

Continued...

TABLE III.5 (Continued)

Outer Standoffs

Parameter	Specification
Material	steel
Outer Diameter	8 mm
Length	146 mm with 4 mm of each end cut to 6.4 mm diameter and center tapped to accept 4 mm diameter screws

Center Standoff

Parameter	Specification
Material	plexiglass
Center Diameter	25.6 mm
Length	147.2 mm
Carousel drive shaft receptacle	9.5 mm x 68 mm hole in bottom of standoff

Continued...

TABLE III.5 (Continued)

Bottom Plate

Parameter	Specification
Material	plexiglass
Diameter	176 mm
Thickness	6 mm
Sample tube holes	Twentyfour 13 mm wide x 3.4 mm deep recesses with 4.7 mm wide holes centered in each recess and extending remaining distance through plate for injection gas.
Outer standoff holes	Holes same as for the top plate.
Center standoff recess	25.6 mm wide x 3.5 mm deep recess for the center standoff with a 9.5 mm hole continuing through the plate for the drive shaft.
Driveshaft locating key	7.3 mm hole centered 58.5 mm from the plate edge.

therefore required for the carousel.

A refurbished liquid chromatography sample changer motor provided the requisite precision in the carousel drive. This motor's output was governed by a mechanism ("Geneva mechanism") which accommodated imprecision in primary shaft position to give precise rotary displacement of the driven shaft.

The original driven shaft was replaced with an extended version fit with a circular plate on which the carousel tray could rest. The length of shaft above this plate then fit into a hole drilled into the lower end of the tray's central standoff. A small key on this plate also fit an indentation in the bottom surface of the tray to insure reproducible positioning.

1. Mounting

Stability of the carousel was guaranteed by suspending it below the ICP source in a sturdy mount. The mount was essentially a miniature rail system incorporating a sliding carriage (Figure 9 and Table III.5). This rail system provided a rapid and reproducible horizontal displacement of the sample carousel so that sample trays could be interchanged conveniently.

At first, mounting of the sample changing mechanism inside the ICP source appeared attractive, but the issues of access and electrical isolation favored suspension of the mechanism in an undercarriage.

The rails were mounted between two heavy rectangular aluminum plates which were in turn bolted to the ICP source support above them. The rail carriage consisted of two riders with two sleeve bearings each for smooth, stable horizontal displacement. Rough positioning in relation to the torch was accomplished by turning a nut along a threaded shaft extending from one of the riders (see Figure 9). The carriage could be locked in place by sliding this shaft through a small plate fixed between the rails and then threading on a nut onto the shaft.

Fine horizontal adjustment of the carousel was provided by a micrometer x-y stage (Newport Research Corp., Fountain Valley, Calif., model #400) fastened between the carousel riders and drive (Figures 8 and 9). Adjustments were only necessary after initial set-up of the carousel mount and after experimental torch modifications.

The carousel mount was designed to give a vertical separation of about 40 cm between the ICP source RF coils and the sample tray. This value was chosen only as a matter of convenience. In fact, this displacement need not have

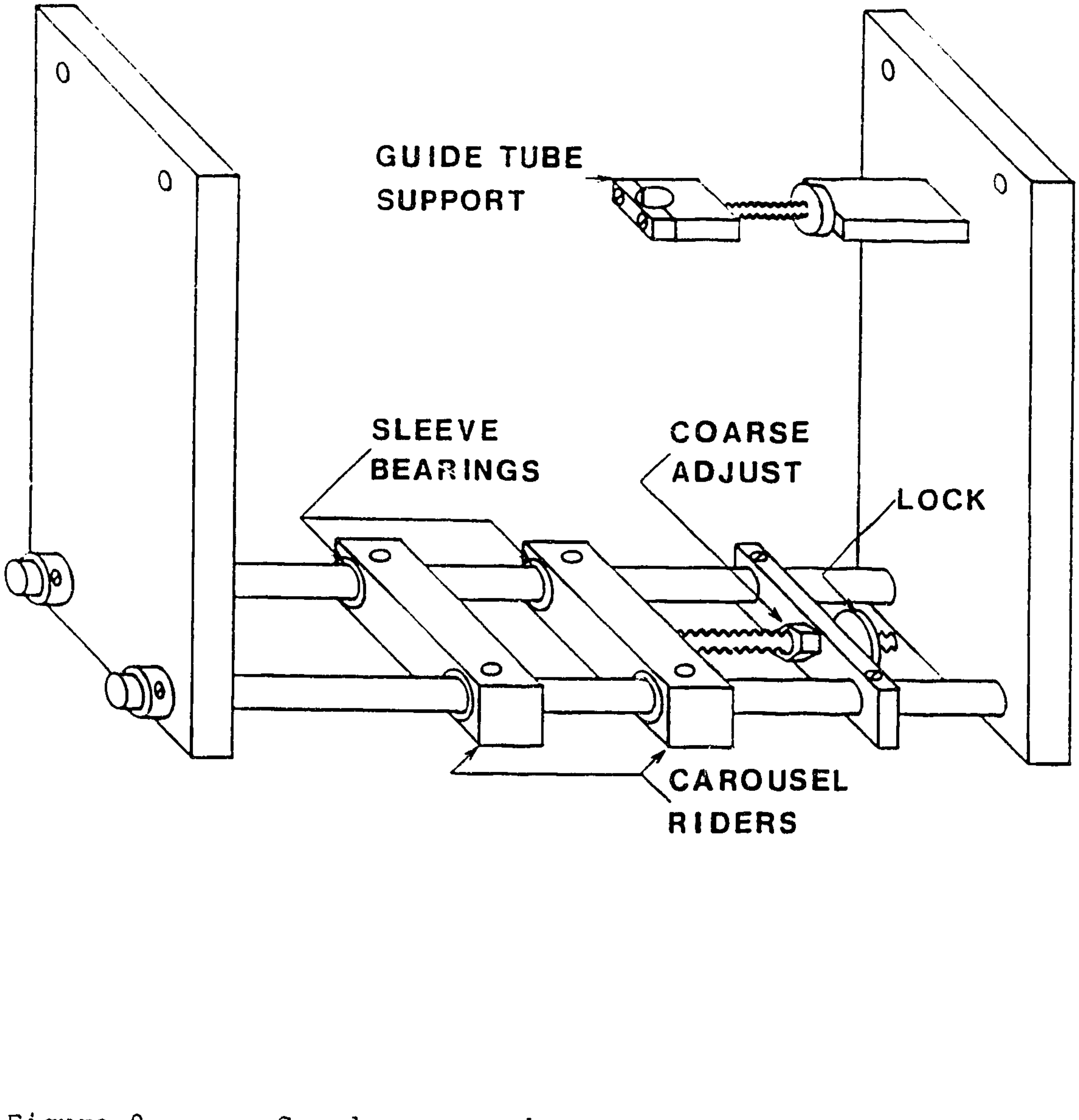
GUIDE TUBE SUPPORT
SLEEVE BEARINGS
COARSE ADJUST
LOCK
CAROUSEL RIDERS

Figure 9. Sample carousel mount.

TABLE III.6

SAMPLE CAROUSEL MOUNT SPECIFICATIONS

Hangers

Parameter	Specification
Material	aluminum
Height	484 mm
Width	138 mm
Thickness	19 mm

Rails

Parameter	Specification
Material	steel
Length	631 mm
Diameter	12 mm
Hanger attachment	Spaced 105 mm center-to-center and 25.5 mm in from the lower corners of hangers. Plastic sleeves with set screws retained rails in hangers.

Continued...

TABLE III.6 (CONTINUED)

Riders

Parameter	Specification
Material	aluminum
Height	35 mm
Width	31.5 mm
Length	140 mm
Sleeve bearings	Two installed in each rider.
X-Y stage	Tapped holes provided in the upper faces of riders for mounting. Separation between riders of 77 mm with x-y stage installed.
Carousel position coarse adjustment	140 mm bolt mounted in center right face of right rider (see Figure 9).

been vertical and could have been made as great as desired. Sample assemblies might therefore be transported between, for example, a robot sampler in some toxic environment and an ICP spectrometer located at a safe distance.

2. Torch Coupling

The sequential pneumatic approach to sample injection demanded that flexible gas-tight seals be maintained between the ICP torch, sample tray, and the injection gas line during tray rotation. Spring-loaded plastic couplers were therefore designed to permit free rotation of the sample tray while at the same time maintaining gas-tight seals (Figure 10 and Table III.7). Precise location of the couplers relative to the tray was provided by a rigid support (Figures 9 and 10).

In order to prevent jamming of the sample plugs, the tray-to-torch (output) coupler had a two-piece construction. The lower end of the torch guide tube fit tightly into a Vespel plastic conical receiver whose lower end cleared the top surface of the sample tray by about 1 mm. The conical receiver together with the rounded edges of the sample plugs provided a smooth transfer of sample plugs between the tray and guide tube. A spring-loaded Teflon sleeve then fit around the receiver to provide a gas-tight seal with the

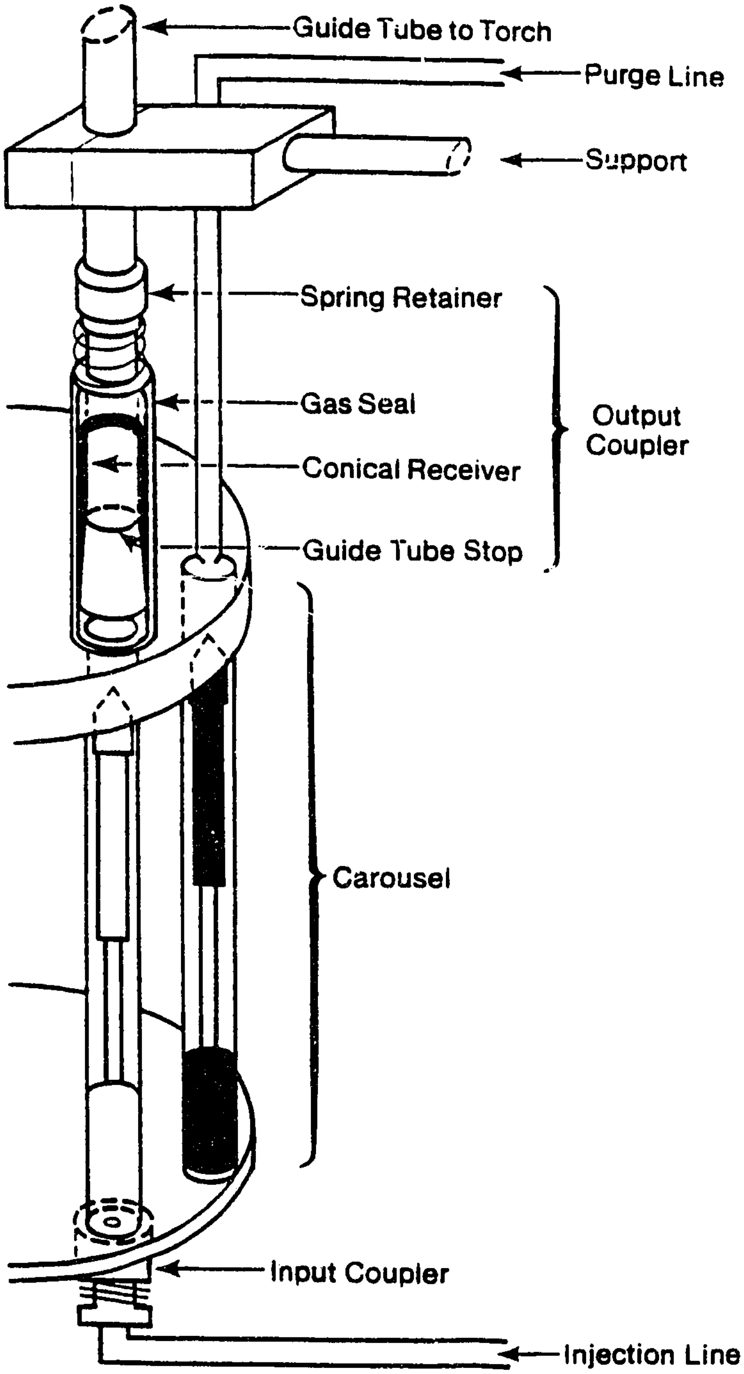
Guide Tube to Torch
Purge Line
Support
Spring Retainer
Gas Seal
Conical Receiver
Guide Tube Stop
Output Coupler
Carousel
Input Coupler
Injection Line

Figure 10. Torch-to-carousel coupling.

TABLE III.7

OUTPUT COUPLER SPECIFICATIONS

Conical Receiver

Parameter	Specification
Material	Vespel (Dupont) plastic
O.D.	15 mm
I.D.	12.4 mm at lower end sloping up along 15.8 mm to a diameter of 10.8 mm then a 12.8 mm diameter from this point to top end.

Gas Seal

Parameter	Specification
Material	Teflon (Dupont) plastic
O.D.	17.8 mm
I.D.	15.2 mm from lower end along 30 mm to 13.3 mm for 5 mm and then 15.2 mm again to top end. (Smaller diameter inner ring provides gas seal and retains spring at sleeve's top end).

tray. In order to locate a new sample tray under the guide tube, it was only necessary to momentarily lift this sleeve.

As mentioned in a previous section, injection of air destablized the plasma discharge. In order to prevent the transport of air along with a sample assembly, an argon line was installed on the guide tube support (Figure 10). An awaiting sample assembly could then be purged with argon before tray rotation and injection.

D. Pneumatic Sample Insertion and Retraction

1. Sample Insertion

As discussed in section C.2 above, before a sample assembly was positioned under the torch guide tube by carousel tray rotation, it was purged with argon. This insured that the plasma would not be destabilized by air injected along with the sample. When activated, a three-way solenoid valve (installed outside the ICP source) switched argon from the rerouted nebulizer gas line (Figure 4) into a purge line (Figure 11).

After purging, sample assemblies were pneumatically transported up the torch guide tube. Smooth delivery required the careful adjustment of injector gas pressure and

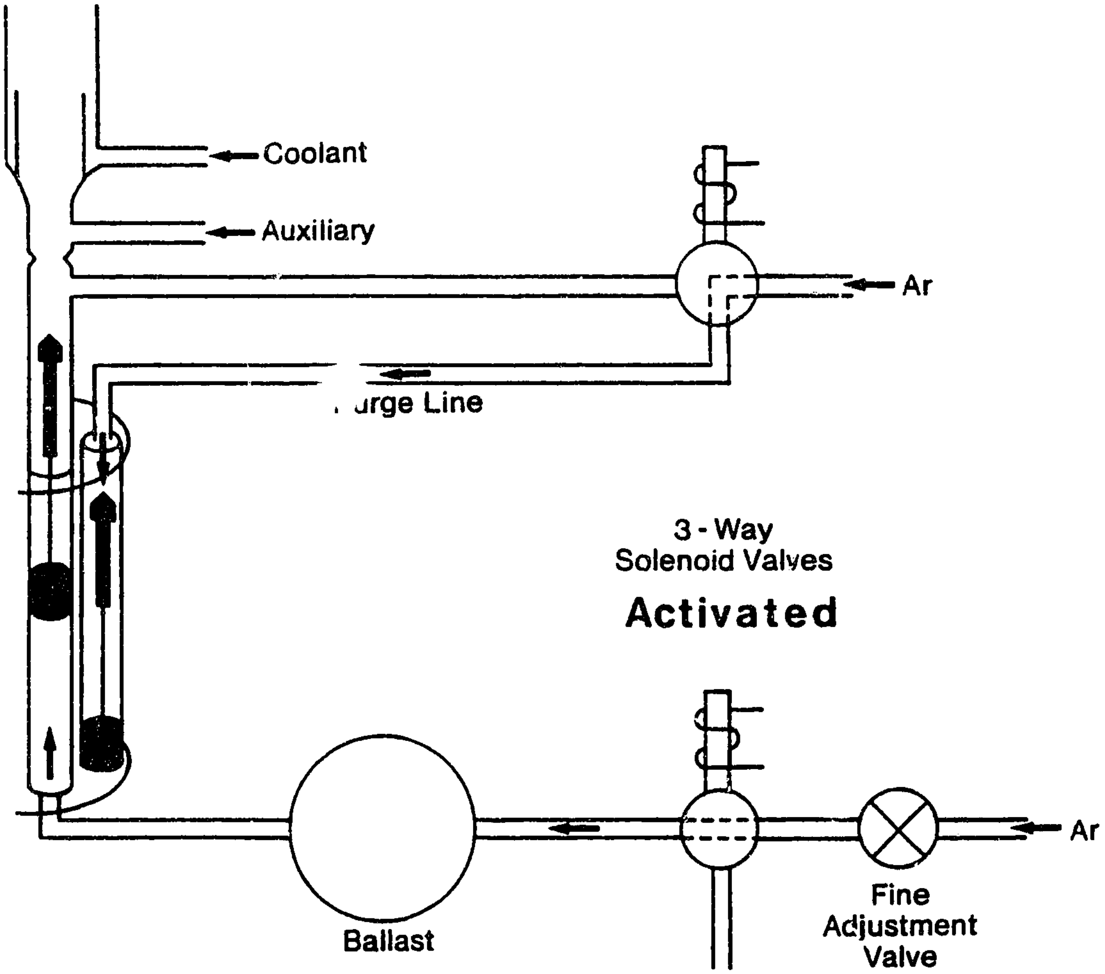
Coolant
Auxiliary
Ar
urge Line
3 - Way
Solenoid Valves
Activated
Ar
Ballast
Fine
Adjustment
Valve

Figure 11. Sample insertion.

velocity. An additional gas connection could not be integrated with the supply circuits discussed above without disrupting their functions. A separate supply external to the ICP source was therefore devised.

Argon at lower pressure (6 psi) than that supplied to the ICP source (35 psi) was used for sample insertion. It was routed to a three-way solenoid valve wired in parallel with the one used for purge control. Activation of the valves thus simultaneously inserted the current sample and purged the adjacent sample (Figure 11). However, further refinements were needed for the reliable sequential insertion of samples. Although rapid insertion could be tolerated by the plasma, a sudden increase in sample velocity as the sample rose from the carousel tray would occasionally extinguish the discharge.

In addition, particularly in the case of Ar/O_2 mixed-gas plasmas, a slow final stage insertion often caused the plasma to deform and ride on top of the sample cup instead of surrounding it.

The problem was then to provide an initially smooth low acceleration vertical displacement followed by a rapid final insertion. This problem was answered nicely by the placement of a four liter Erlenmeyer flask between the solenoid valve and the sample tray as a ballast tank (Figure

11). An additional valve in the gas supply line was used for fine adjustment of sample upward velocity.

2. Sample Retraction

As discussed in section B.3 above, a snuffer gas input was needed to prevent the formation of a filamentous discharge between the plasma and the sample during sample retraction. Since the snuffer and purge functions were temporally separated during torch operation, a single three-way solenoid valve could be used to switch gas from purge to snuffer lines as required (Figures 11 and 12). The rotometer originally intended for nebulizer operation (Figure 4) was used to monitor and adjust snuffer and purge gas flows. A bypass was attached between the snuffer/purge bulkhead connectors on the ICP source for experiments requiring a nebulizer.

Deactivation of the two parallel-wired solenoid valves caused the switching from purge to snuffer lines and the exhaust of gas from beneath a sample pedestal to occur simultaneously (Figure 12). The ballast tank insured an initially rapid sample descent followed by a slower return into the sample tray. This sequence had two advantages. It guaranteed that any filamentous discharge to the sample cup

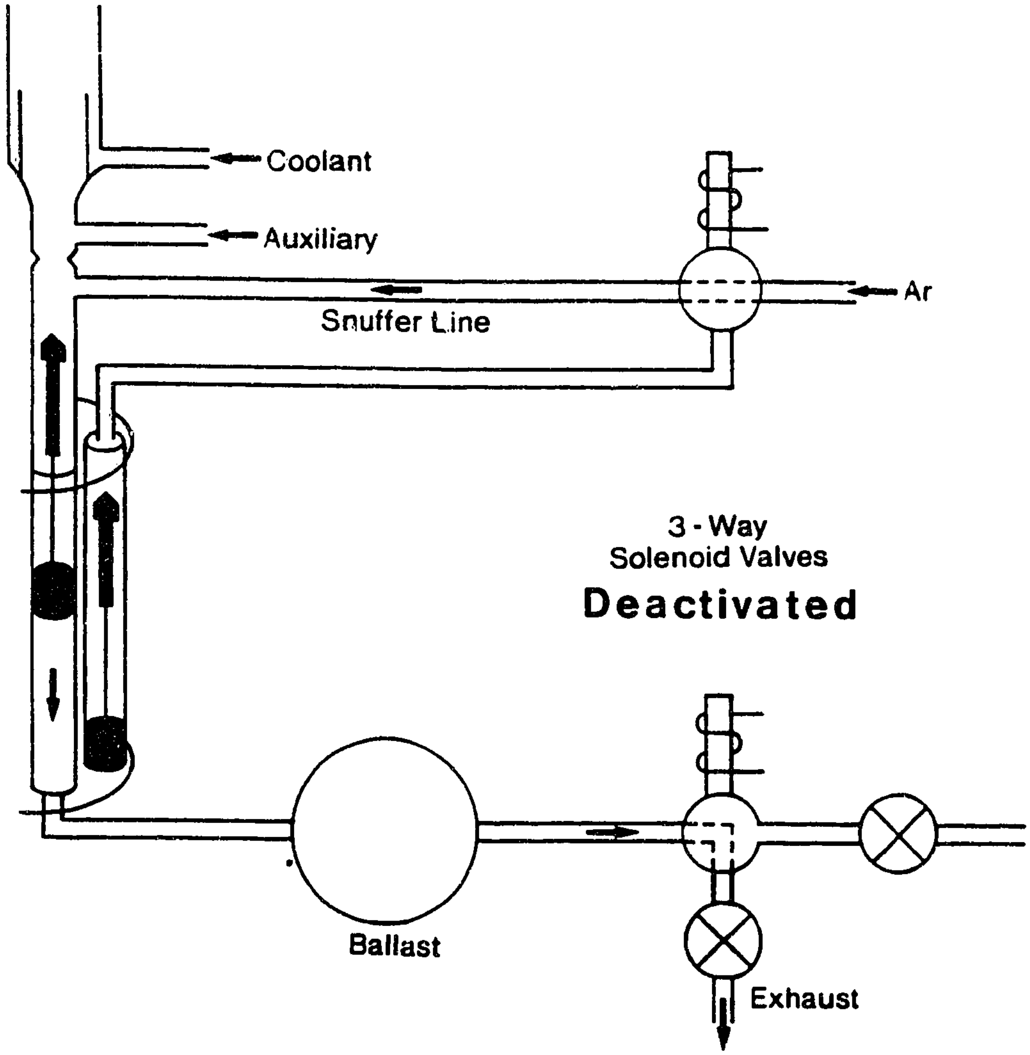
Coolant
Auxiliary
Ar
Snuffer Line
3 - Way
Solenoid Valves
Deactivated
Ballast
Exhaust

Figure 12. Sample retraction.

during this initial descent was quickly extinguished. It also prevented contamination of the carousel tray with loose sample residue dislodged from a sample assembly during its impact with the bottom of the tray. The final descent of sample assemblies into the tray could be adjusted to a reasonable rate with a valve located at the exhaust port (Figure 12). Details of this valve and the others mentioned previously are given in Table III.8.

TABLE III.8

VALVE SPECIFICATIONS

Snuffer/Purge

Parameter	Specification
Supplier	Ascolectric Limited, Brantford, Ontario
Type	115 VAC, 1/4 in pipe, 1/8 in orifice, 25 psi solenoid
Model	# 83148

Injector

Parameter	Specification
Supplier	Ascolectric Limited, Brantford, Ontario
Type	115 VAC, 1/4 in pipe, 1/8 in orifice, 25 psi solenoid
Model	# 8320A89

Injector Fine Adjust and Exhaust Valves

Parameter	Specification
Supplier	Nupro Company, Willoughby, Ohio
Type	"J" Series miniature forged body, straight pattern, 1/4 in male NPT
Model	# B4J2

CHAPTER IV

DATA ACQUISITION AND DSID CONTROL

A. Introduction

Detailed characterization of the optical emission behavior of liquid and solid samples directly inserted into an inductively coupled plasma discharge required a data acquisition system with the following properties: fast response time, discrete sampling or integrating capability in the temporal domain, high sensitivity and wide dynamic range of response, simultaneous sampling over a readily selected wavelength range, and the ability to rapidly process and store large amounts of acquired information.

These instrumental requirements were dictated by the compositions of the samples investigated and by the nature of their interactions with the plasma discharge.

Rapid volatilization and atomization of elements such as cadmium gave transient signals with typical peak intensity lifetimes of less than a second. Both intensity and temporal structure were important characteristics of the transient signal. A detection system with discrete sampling capability and a response time sufficiently rapid to prevent signal distortion was therefore required.

Once an element's temporal behavior was characterized and perhaps improved by changes in experimental parameters such as plasma gas or sample cup composition, the next step was to investigate analytical sensitivity and precision for that particular element. Signal integrating capability was preferred for precision comparisons and high sensitivity and wide dynamic range were necessary for the calculation of detection limits and the construction of working curves.

The type of preliminary studies mentioned above could be carried out with single element aqueous solutions and a single channel detection system. However, rapid simultaneous multichannel detection was desired for the analysis of more complex solutions, powders, or solids. It would then be possible to efficiently compare intensities and temporal behaviors of different elements, to explore internal standardization as a method of improving precision, and to observe spectral overlaps and background changes. An appropriate computer system would in turn be required to rapidly acquire, process, and store the large amount of data generated by the multichannel system.

A computerized data acquisition system based on a photodiode array-photomultiplier tube (PDA-PMT) combination spectrometer (Figure 13) had all the desirable properties mentioned above. In addition, the computer was used to

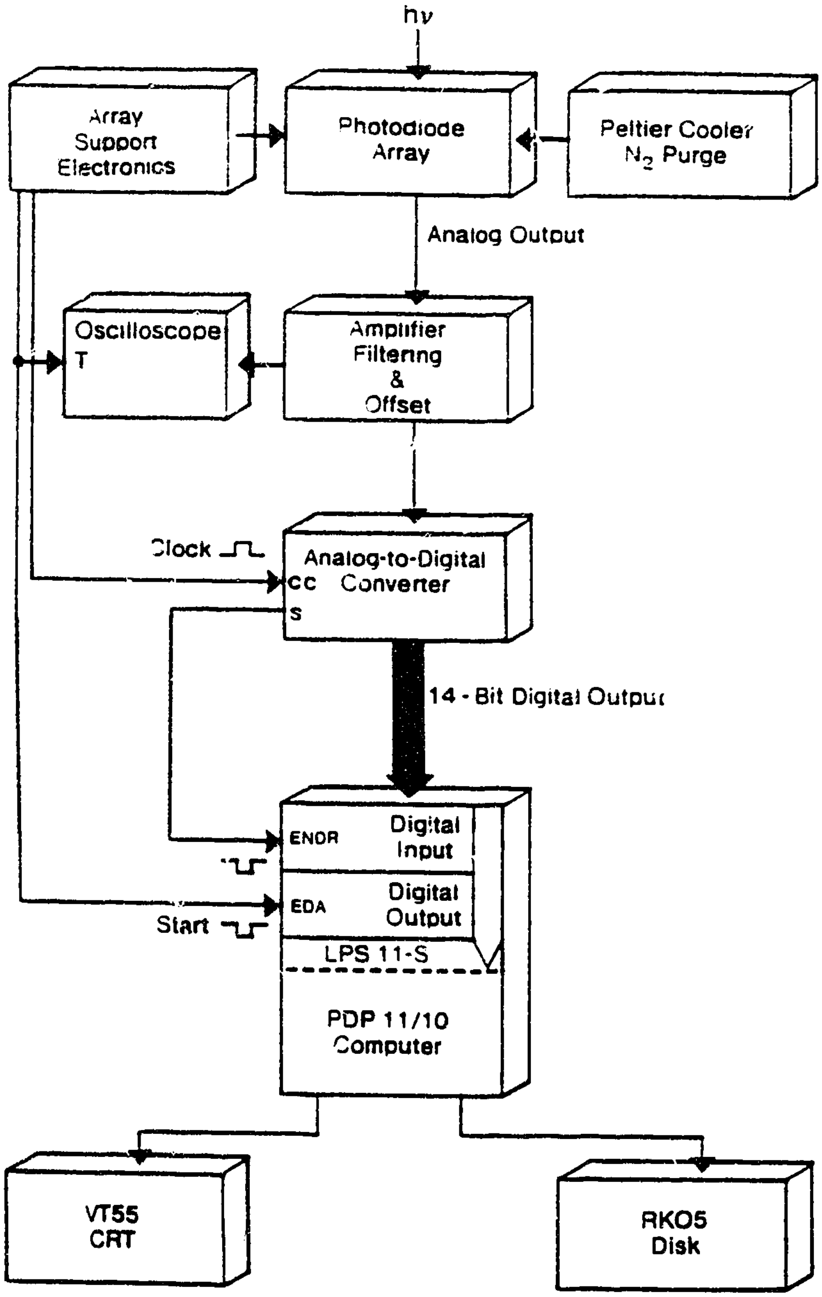
hν
Array Support Electronics
Photodiode Array
Peltier Cooler N_2 Purge
Analog Output
Oscilloscope
T
Amplifier Filtering & Offset
Clock
Analog-to-Digital Converter
CC
S
14 - Bit Digital Output
ENDR
Digital Input
EDA
Digital Output
Start
LPS 11-S
PDP 11/10 Computer
VT55 CRT
RK05 Disk

Figure 13. Computerized data acquisition system.

control the DSID described in the last section of this chapter. A completely integrated system for the ICP analysis of discrete samples was therefore realized (Figure 3).

The spectrometer portion of this system will be described in the next section. Descriptions of the computer and the spectrometer interfacing hardware will come next, followed by a discussion of the hardware used to interface the DSID to the computer.

Software was written to receive, process, and store the information acquired by the spectrometer and to properly synchronize DSID operation.

B. Photodiode Array-Photomultiplier Tube (PDA-PMT) Combination Spectrometer

1. Optics

The optical layout of the PDA-PMT spectrometer designed by Salin and Horlick (173) is given in Figure 14. A hole cut in the side of a Heath 0.34 m grating-based monochromator (Table IV.1) accommodated an additional folding mirror. When swung into the monochromator, this mirror deflected dispersed light (solid line, Figure 14) onto the face of a linear silicon photodiode array detector. With this mirror

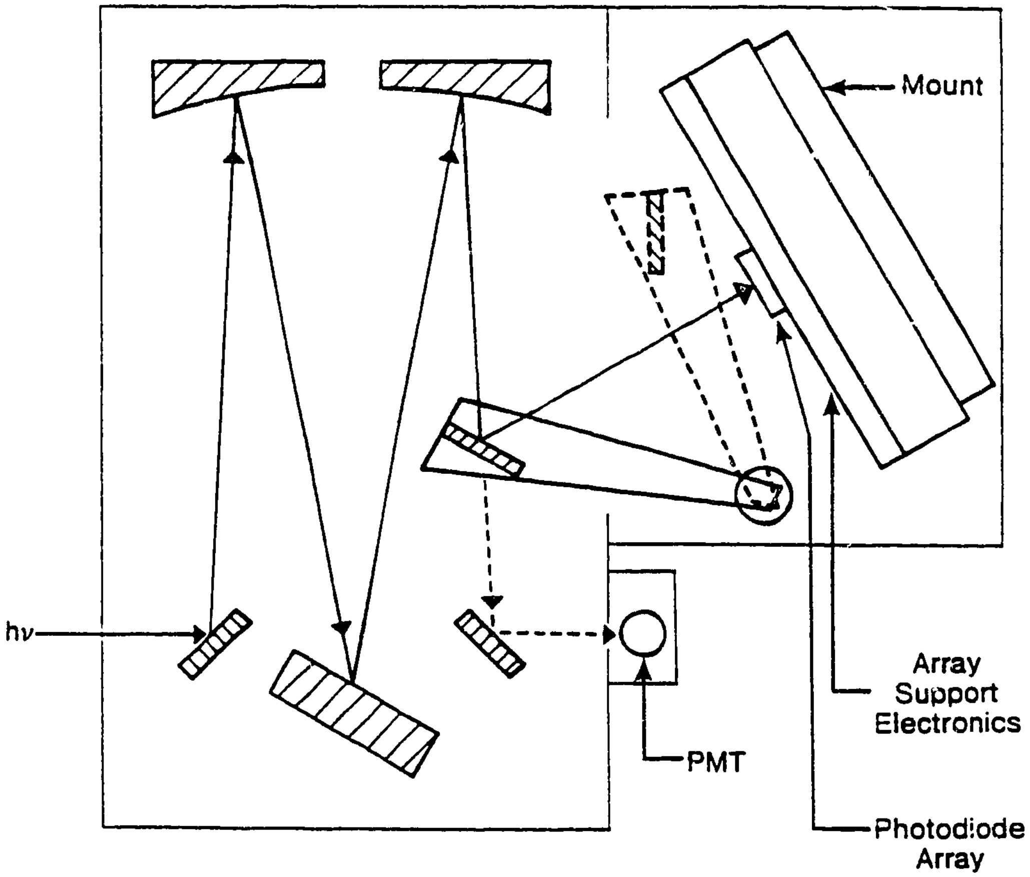
Mount
hν
Array
Support
Electronics
PMT
Photodiode
Array

Figure 14. PDA-PMT spectrometer.

TABLE IV.1

PDA-PMT SPECTROMETER SPECIFICATIONS

Monochromator

Parameter	Specification
Model	Heath EU-700, GCA/McPherson Instruments, Acton, Mass.
Mount	Single-pass Czerny-Turner with entrance and exit beams on common axis
Focal length	0.35 m
Gratings	Schoeffel/McPherson Instruments, Acton, Mass., 1,200 lines/mm (2,500 Å blaze) and 2,400 lines/mm (holographic, 5,000 Å blaze)
Wavelength range	1,900-10,000 Å
Reciprocal dispersion	20 Å/mm (1,180 lines/mm grating) and 10 Å/mm (2,400 lines/mm grating)
Slit width	5-2,000 µm
Slit height	12 mm
Slew/scan control	Heath EU-700-51

Continued...

TABLE IV.1 (Continued)

Photodiode Array (PDA)

Parameter	Specification
Model	RL 1024S, EG&G Reticon, 345 Patrero Ave., Sunnyvale, CA. 94086
Size	1,024 2.5 mm high elements on 25 x 10^{-3} mm centers
Spectral response range	2,500-10,000 Å
Spectral response peak	7,500 Å

PDA Peltier Coolers

Specification	Parameter
Model	CPL4-71-06L, Melcor, 990 Spruce St., Trenton, N.J., 08638
Temperature	-15°C
Purge	N_2, 0.5 l/min
Power supply	LMEO-14, Lambda Electronics Corp., Melville L.I., N.J.

Continued...

TABLE IV.1 (Continued)

PDA Support Electronics

Parameter	Specification
Model	RC-10245A, Reticon
Readout frequency	12.8 kHz
Integration time	Switchable from 80 ms to 5.5 min
Power supply	EU 801-11 Heath, Mississauga, Ontario

Photomultiplier Tube (PMT)

Parameter	Specification
Model	1P28, RCA, Lancaster, PA, 17604
Spectral response range	2,000-6,600 Å
Spectral response peak	3,500 Å
Mount	PR-1402 RF, Products for Research, Inc., Danvers, Mass., 01923
Power supply	244 high voltage supply, Keithley Instruments, Inc., Cleveland, Ohio

Spectrometer Output Electronics

Parameter	Specification
Picoammeter	414S, Keithley
Current amplifier	427, Keithley
Chart recorder	555, Linear Instruments Corp., 17282 Eastman Ave,Irvine, CA 92714

positioned outside the monochromator, the dispersed light would follow its normal path (dashed line, Figure 14) to the exit slit. In this fashion, the spectrometer could be used in either a single or multichannel mode.

In the single-channel mode, a PMT (Table IV.1) mounted just outside the monochromator's exit slit monitored a single wavelength of radiation. Although limited to single channel detection in this configuration, the PMT offered the important advantages of high sensitivity and wide dynamic range. These characteristics were important for determining analytical detection limits and working ranges.

In the multichannel mode, a wavelength region was monitored by the linear silicon photodiode array. As the name implies, this device consists of a linear array of individual silicon diode sensor elements. The particular array used in this work (Reticon RL 1024S, Table IV.1) had 1024 diodes on 25×10^{-3} mm centers, each diode being 2.5 mm high. Sensor element areas were therefore 6.25×10^{-2} mm each and the total array length was 25.6 mm or 1 inch. The array was mounted in a 22 lead dual-in-line integrated circuit package. The array length and the monochromator's dispersion at its focal plane determined how large a wavelength region was actually viewed by the array.

With a 1,180 lines/mm grating mounted in the monochromator, the reciprocal dispersion was about 20 Å/mm so the array viewed a wavelength region 512 Å long. The monochromator was modified to accept a newer 2,400 lines/mm grating by drilling two holes in its grating mount. These holes accepted the guide pins on the newer grating. Since the monochromator's reciprocal dispersion was halved with the higher resolution grating, the array viewed 256 Å in this case.

The actual wavelength region monitored by the array and the individual wavelength detected by the PMT were readily selected by a slew/scan control unit (Table IV.1) attached to the monochromator. As noted in Table IV.1, the wavelength range accessible with the monochromator was from 1,900 to 10,000 Å. Both the array and PMT had spectral response ranges within this coverage but had peak sensitivities in the red and UV regions, respectively (Table IV.1). Most of the work reported in following chapters was carried out in the 2,000-3,000 Å region.

2. Detector Support Electronics and Array Cooling

Output signals from the PMT were monitored with either a picoammeter or chart recorder. A current amplifier was used to generate a usable signal voltage for the chart recorder (Table IV.1). The PMT and amplifier had rise times (10%-90%) of ≤ 1.6 ns and ≥ 15 ms, respectively. The chart recorder had a full scale pen deflection time of 0.36 s. These fast response times, together with the PMT's sensitivity, made this detection system suitable for the recording of low intensity transient signals.

Although the photodiode array could also be used to acquire transient signals, the acquisition mechanism differed from the PMT. Whereas the PMT gave essentially instantaneous output, the array integrated signal intensity. More complex support electronics were required to control signal integration time and read out the integrated signal values from each diode of the array. A readout board available commercially from Reticon (RC-1024S evaluation board, Table IV.1) was used with the array.

A complete discussion of the Reticon linear photodiode arrays, their readout electronics and applications to spectroscopy can be found in two 1976 papers by Horlick (174,175) and references therein. More recent applications of these detectors to ICP spectroscopy are described in additional papers by Horlick and coworkers (176,177,178,179,180,181).

In short, the individual diodes of the array operate in the charge storage mode and therefore have an intrinsic capacitance. They are brought to their initial charged state by the application of a reverse bias of 5 V. Two mechanisms act to deplete this initial charge: photon- and thermally-induced electron hole-pair production. The amount of charge required to return a particular diode to its initial reverse bias state is therefore a measure of both light intensity and dark current integrated over the period between full charging.

Since the diodes are read out sequentially, this integration period can be no shorter than the readout time for 1,024 diodes. This readout time is in turn governed by the RC-1042S readout board's master clock frequency. The clock is fed to a free-running 4-bit counter. This counter therefore cycles through a full count of 16. With each increment of 4, the counter addresses an on-board read-only memory (ROM) to generate appropriately phased signals for array initialization and readout. Among these ROM signals are diode sampling pulses which control the sequential readout of individual diodes. The frequency of these pulses is one fourth that of the master clock. With each full count of 16, the counter sends a signal to additional cascaded 4-bit counters. These additional counters are switch-settable divide-by-N counters and their final output is used to initiate array readout. They therefore control array integration time and increment at one fourth the rate at which the ROM is addressed.

The Reticon RC-1024SA readout (evaluation) board (Table IV.1) comes equipped with 3 integration counters. The maximum integration count is normally therefore 4,096 with all twelve switches closed (4 switches for each counter for a total of 2^{12} counts). In light of the above discussion, this corresponds to 16,384 (2^{14}) sampling pulses or 65,536 (2^{16}) master clock cycles. With the master clock set at, say 45 kHz, the maximum available integration time would then be 1.4 seconds.

In order to achieve longer integration times without further reducing the master clock rate (and hence reducing array performance), Horlick (174) added two additional 4-bit counters and associated switches to the integrating cascade of his Reticon RC400 readout board. The total integrating count was therefore brought up to 1,048,576 (2^{20}) or 23 s. Since room temperature dark current would contribute significantly to total signal at integration times greater than about 500 ms, Horlick (174) used a Peltier cooler to bring the array temperature down to about -15°C. He noted a 2-fold reduction in dark current for each 11°C drop in temperature. Frost was kept off the array window by purging moisture from the array housing with dry nitrogen gas.

A similar addition of integrating counters and cooling was made by Salin and Horlick (173) to the array used in this work (Table IV.1). The master clock was adjusted to 51.2 kHz and 12 external integration switches provided ready selection of integration times from 0.08 s to 5.46 min (delay counts of 2^8 to 2^{20}). The sampling pulses were used to form an output clock signal of 12.8 kHz. Two Peltier modules mounted on either side of the array effected cooling by means of a copper bus bar in contact with the rear surface of the array's integrated circuit package.

Three important outputs were available from the array portion of the PDA-PMT spectrometer: the analog signal corresponding to light intensity integrated by each of the 1,024 diodes, a clock formed from diode sampling pulses and a start pulse corresponding to the terminal count of the integration counters. The manner in which these outputs were interfaced to a DEC PDP 11/10 computer will be discussed in the next section.

C. Minicomputer Systems and Interfacing

1. Introduction

Two DEC PDP 11/10 minicomputer systems (Table IV.2) were used in this work; one for data acquisition and storage and the other for data processing. The larger 32k word memory computer supported a sophisticated graphics processor and associated software and was used for data processing. Both computers were equipped with dual 1.25 M word disk drives. Acquired spectra could be viewed on the 16k word computer's video terminal before and after storage on disk. A built in printer/plotter on this terminal could be used for hardcopy. Better print out and plotting were obtained with the larger computer's associated Decwriter or Zeta Plotter, respectively.

A Laboratory Peripheral System (LPS) was used to receive data from the PDA-PMT spectrometer and to control the DSID. These functions will be described in the following sections.

TABLE IV.2

MINICOMPUTER SYSTEM SPECIFICATIONS

All components from Digital Equipment Corporation (DEC), Maynard, Mass. unless otherwise noted.

Minicomputers

Parameter	Specification
Model	DEC PDP 11/10
Memory	16 and 32 k word
Storage	Decpack RKO5, 2.5 k byte
Operating system	RT11SJ-V02C

Terminals

Parameter	Specification
16 k Word system	VT-55-FA Decscope, full keyboard and CRT, printer/plotter
32 k Word system	VR17L CRT with VT11 Graphic Display Processor; Decwriter II; 130 PO7 Zeta Plotter, Zeta Research, Inc., 1043 Stuart St., Lafayette, CA.

Continued...

TABLE IV.2 CONTINUED

Laboratory Peripheral System (LPS 11-S)

Parameter	Specification
Analog input	LPSAD-12 12-Bit ADC with 8-channel multiplexing
Digital input/output	LPSDR 16-Bit digital I/O and two programmable relays
Clock	LPSKW Programmable clock and two Schmitt triggers

2. Laboratory Peripheral System (LPS) and Analog-to-Digital Conversion of the PDA Output

The functional subunits of the LPS are given in Table IV.2. The LPSDR digital I/O was used to receive data from the photodiode array spectrometer (Figure 14). The PDA signal was first amplified (Table IV.3) and offset from its normal 0 to +3V range to fill the ±5V input range of a 14-bit analog-to-digital converter (ADC, Table IV.3). The amplifier's output was visualized with an oscilloscope (Table IV.3) triggered on the array's start pulse. The clock output from the array was routed to the convert command (cc) input of the ADC. Digital output from the ADC was then interfaced to the LPSDR as shown in Figure 15.

Three 7404 hex inverters (Figure 15) were used to convert the ADC's +5 V true output logic to the LPSDR's 0 V true logic. The LPSDR digital input pin assignments for the ADC's 14-bit output are given in Figure 15. The 16-bit input register associated with the LPSDR was set in the Word Transfer Mode meaning that input data was unlatched and had to be held on the input lines long enough to be read. Since the ADC held data on the output lines between convert commands (78 ms period) and few software program steps were needed for a read cycle, no problems were encountered with

TABLE IV.3

PDA ANALOG SIGNAL PROCESSING ELECTRONICS

Amplifier

Parameter	Specification
Supplier	Tektronix, Inc., P.O. Box 500, Beaverton, Oregon 97077
Model	AM502 Differential amplifier
Power supply	TM506 Power Module

Oscilloscope

Parameter	Specification
Supplier	Tektronix
Model	SC502 15 MHZ Oscilloscope
Power supply	TM506 Power Module

ADC

Parameter	Specification
Supplier	Analog Devices, P.O. Box 280, Norwood, Mass. 02062
Model	ADC 1131J 14-Bit high speed (12µs) analog-to-digital converter
Power supply	HPPT 015-001 Triple output power supply, Hammond Manufacturing, Buffalo, N.Y.

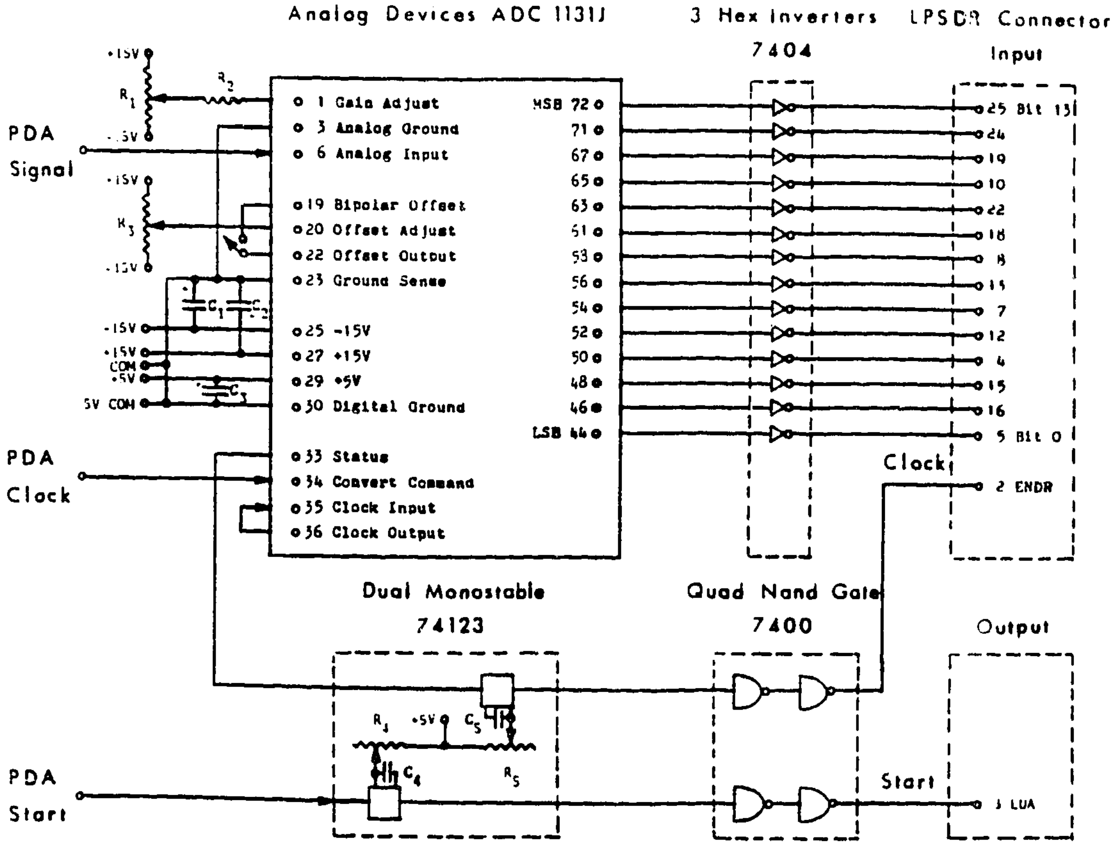
Analog Devices ADC 1131J
3 Hex Inverters
7404
LPSDR Connector
Input
+15V
R1
R2
-15V
PDA
Signal
+15V
R3
-15V
C1
C2
-15V
+15V
COM
+5V
C3
5V COM
PDA
Clock
1 Gain Adjust
3 Analog Ground
6 Analog Input
19 Bipolar Offset
20 Offset Adjust
22 Offset Output
23 Ground Sense
25 -15V
27 +15V
29 +5V
30 Digital Ground
33 Status
34 Convert Command
35 Clock Input
36 Clock Output
MSB 72
71
67
65
63
61
53
56
54
52
50
48
46
LSB 44
25 Bit 15
24
19
10
22
18
8
11
7
12
4
15
16
5 Bit 0
Clock
2 ENDR
Dual Monostable
74123
Quad Nand Gate
7400
Output
R4
+5V
C5
C4
R5
PDA
Start
Start
3 LUA

Figure 15. PDA signal processing electronics; $R_1=R_3=100k\Omega$, $R_2=30k\Omega$, $R_4=R_5=1M\Omega$; $C_1=C_2=C_3=15\mu F$, 25V, $C_4=C_5=0.001\mu F$.

the unlatched data transfer mode.

On completion of data conversion, the ADC's status line (Figure 15) went low. This high-to-low transition was transformed to a 1 ms negative-going pulse with a monostable. The pulse was suitable, after pull-up by two NAND gates, for transmission to the External New Data Ready (ENDR) pin of the LPSDR's input connector (Figures 13 and 15). A pulse on the ENDR line set a flag in the status register associated with the LPSDR which in turn notified the acquisition program of data ready to be read in. This ENDR line can therefore be thought of as a data input clock.

As shown in Figures 13 and 15, the array's output start signal was similarly converted to a 1 ms negative-going pulse. This pulse was then transmitted to the External Data Accept (EDA) pin of the LPSDR's output connector which in turn set another flag in the status register. This flag notified the acquisition software of a new cycle of array output.

3. DSID Control

As discussed in section D of the previous chapter, two 3-way solenoid valves wired in parallel were used to switch argon between purge and snuffer lines and simultaneously insert or retract a sample assembly on a head of argon. These valves were brought under software control via one of the two programmable relays available on the LPSDR (Table IV.2). These relays were not designed for inductive loads and high voltage spikes made direct switching of external 115 VAC solenoid lines unreliable. An LPSDR relay was therefore used to switch the logic input of an external optically-isolated relay (Teccor Electronics, #T3523). This type of relay was capable of switching 115 VAC at high currents (about 2 A) with no voltage spiking and little off-state current leakage. It utilized TTL input signals (+5 VDC) for direct computer interfacing. An external SPDT (center off) switch provided a choice between manual or computer control of the solenoid valves by routing 5 VDC either directly to the optical relay or first through the LPSDR mechanical relay.

Sample carousel rotation was controlled via the remaining LPSDR relay and an additional optically-isolated relay. Choice between manual or software control was again provided by an external SPDT switch. Software setting or clearing of flag bits in the LPSDR status register caused closing or opening, respectively, of the mechanical relays.

CHAPTER V

AUTOMATED SAMPLE PREPARATION WITH THE DSID

A. Introduction

When liquids or powdered organic solids such as orchard leaves were directly inserted into an ICP with the DSID described in Chapter III, a sudden vigorous evolution of vapor would destablize and often extinguish the plasma discharge. In the case of liquid samples, this problem was avoided by drying before insertion.

At first, drying of liquid samples was accomplished by an extension of the procedure used by Salin and Horlick (124). A carousel of samples was dried by injecting each sample into the ICP source load coil followed by the application of about 50 W of forward power for about one minute. After all samples were dried in this manner, the plasma was ignited and the samples sequentially reinserted for analysis. This approach was effective but time-consuming.

In an effort to control the sudden evolution of gases from powdered organic samples, boiler caps were placed on the graphite dc arc electrode sample cups. However, the irreproducible nature of rapid decomposition of these solid samples continued to degrade analytical precision. It became clear that most powdered samples of this type would require at least partial ashing prior to insertion if analytical precision was to be improved.

Although RF inductive heating could be employed for the drying of small volumes (several μl) of liquids, it could not be used for the ashing of powders. Application of RF power high enough to promote ashing gave reflected power levels which could not have been tolerated for more than a few seconds without damaging the ICP source. Some other method of sample ashing was needed.

As one important impetus for the development of the direct insertion method was the possibility of avoiding tedious sample workup, procedures for simple and rapid sample preparation were desired.

In addition, since one of the attractive features of the direct sample insertion technique was a minimum of sample handling, it was preferable to execute any preparation in the sample cup used for final atomization. This would help keep sample contamination and loss to a minimum.

The incorporation of a preparation process amenable to automation and capable of handling all sample types for direct insertion ICP analysis with satisfactory precision and accuracy was the ideal goal. A survey of the literature puts this rather ambitious goal in perspective.

B. A Survey of Methods of Sample Drying and Decomposition for Use With the DSID

Dahlquist and Knoll (182) evaluated wet digestion with an $HNO_3/HClO_4$ mixture, dry ashing in a muffle furnace, and DTPA (diethylenetriaminepentaacetic acid) extraction for the pretreatment of animal and botanical tissue, soil and human serum samples. The author's DTPA extraction procedure was preferred over dry ashing for biological samples due to losses associated with the latter technique. However, the digestion procedure wasn't free of problems. The concentrations of alkali element and ammonium salts limited the amount of dry biological sample weight used to 1.0 g per 50 ml of final solution. The resulting dilution ratios for trace elements made their determination unreliable if not impossible. The elements Cd, Co, Cr, Ni, Pb, and V were at or near their quantitative determination limits (defined as five times the detection limit) after the $HNO_3/HClO_4$ digestion procedure. Cadmium was not quantitatively determinable in NBS SRM orchard leaves. The same was true for lead in NBS SRM bovine liver. Some form of separation and preconcentration would be required before determining these two elements.

DeBoer and Maessen (183) encountered the same problems with these two elements in a more recent study. Lead could not be determined in NBS SRM bovine liver after $HNO_3/HClO_4$ digestion in a microwave oven or after digestion with HNO_3 in a Teflon-lined steel bomb. Neither Pb or Cd could be determined after solubilization of the liver with TMAH (teramethylammonium hydroxide). In addition to these decomposition procedures, the authors examined direct extraction with dilute HNO_3, digestion with an H_2SO_4/H_2O_2 mixture, electronic low temperature ashing, and muffle furnace ashing. The authors assessed all the procedures in terms of the suitability of the final sample solution for ICP analysis in terms of accuracy and precision of the final determination and the occurrence of matrix effects. They also extended their assessments to less readily quantifiable criteria associated with sample preparation. These criteria included usable sample sizes and dilution factors, risk of contamination and the laboriousness, time requirements, and safety of the procedures (important factors in terms of automation). The elements Mn, Zn, Cu, Fe, Cd, and Pb were simultaneously determined by ICP spectrometry after each pretreatment.

The two "direct" procedures, extraction with dilute HNO_3 and solubilization with TMAH, were deemed simple and safe with the latter procedure being well suited to processing large batches of samples. However, the largest degree of contamination from reagents was associated with the TMAH method. In addition, TMAH reference solutions were unstable so the use of standard additions was required. The elements Cu and Fe were not fully extracted with dilute HNO_3. Extraction with HNO_3 and muffle furnace ashing required by far the most time (24 hours).

Among the acid digestion procedures, the H_2SO_4/H_2SO_4 digestion required the most operator attention. The authors referred to the restriction of this method to samples with low calcium contents because of the danger of coprecipitation of trace metals with $CaSO_4$. Variations in H_2SO_4 content among the digested samples made individual acid corrections a requirement. Contamination arising from the H_2O_2 was noted.

Large dilution after digestion with HNO_3/$HClO_4$ was necessary to prevent clogging of the ICP's nebulizer (the authors suggested using a high solids nebulizer to avoid this problem). This digestion was simple and fast. It was safe as long as beakers of water were placed along with samples in the microwave oven to lessen the rate of HNO_3 evaporation.

The authors suggested that electronic power regulation would be a more efficient method of controlling evaporation rate.

The HNO_3 bomb digestion was also safe as long as overloading and overheating were avoided. Very careful manipulation of small sample volumes was required.

The bomb digestion and all of the remaining wet extraction and digestion procedures provided acceptable limits of precision and accuracy. Of all the decomposition procedures, the TMAH and $HNO_3/HClO_4$ digestions required the least operator attention. Satisfactory precision and accuracy was won from the two dry ashing procedures only with the expenditure of much time. Systematic errors were avoided in muffle furnace ashing by utilizing a carefully selected temperature-time scheme and crucible material. The samples were heated in clear quartz at the rate of 50°C per hour to a final temperature of 520°C. Even with these precautions small retention losses of Cu and Fe were noted.

The minimum electronic ashing time for 1 g of sample was twelve hours. Preliminary investigations indicated that up to five days would be required for botanical samples. Electronic ashing provided excellent accuracy for all elements investigated but gave poor precision for lead.

The electronic and muffle furnace ashing and H_2SO_4/H_2O_2 digestion procedures gave the lowest dilution factors (5 ml/g sample) of all the pretreatments examined.

DeBoer and Maessen (183) concluded that the most important factor governing the precision of digest analysis results was the ratio of the analyte's concentration to its ICP detection limit. Although all procedures examined were in general suitable for ICP analysis, certain digestion procedures excluded the determination of elements present below the ng/g level in the original sample. These elements would have to be preconcentrated before their determination. This would further complicate the analysis as compatible digestion and preconcentration schemes would have to be developed.

A few recent isolated studies in which pretreatment of more intractable samples is considered are available. Of note is a paper by Botto (184) describing the use of an automatic Claisse (Claisse Fluxer, Claisse Scientific Corp., Inc., Quebec.) fusion device for coal ash analysis and a paper by Caruso, Fricke and coauthors (185) describing a rapid pressure dissolution procedure for agricultural crop analysis.

The De Boer and Maessen (183) and Dahlquist and Knoll (182) comparison studies focused on the decomposition of a few biological samples. That the problems associated with sample pretreatment for ICP analysis are rapidly become more complex as a greater variety of sample types are considered is reflected in the absence of additional thorough comparison studies.

The impact of this lack of progress in sample pretreatment is reflected on by Vigler, et al. (186) in a short review entitled "Sample Preparation Techniques for AA and ICP Spectroscopy." They state that although the "...demand for more precision, lower detection limits and greater throughput of samples..." has led to a greater use of atomic absorption and ICP emission spectrometric finishes, this in turn appears to have created a problem as the diversity of samples submitted for analysis requires that a number of different pretreatment schemes be available at all times. As the authors note, they were required to provide the "...analysis of anything from an air filter sample to analysis of titanium ore for zirconium content."

It is no wonder that the authors concluded their article with the following statement:

> We and many other groups are continuing efforts to find faster, safer and more sensitive methods for dissolving samples. Furthermore, with the increasing attention to laboratory automation, it

> is even more desirable to achieve a "universal" method of sample preparation, so that one set of calibration standards may be used for as many samples as possible (186).

As pointed out in Chapter I, however, it is just this "increasing attention to laboratory automation" in response to both escalating sample loads and sample variety which is initiating a trend away from sample dissolution and toward direct solid sample presentation requiring little, if any, preparation.

What is disappointing, if not surprising, however, is the relative scarcity of research directed toward the development of an automated "universal" solid sample drying and decomposition procedure. As mentioned in Chapter I, automation has generally been implemented at the data processing end of analysis and automatic sample preparation has been confined mostly to clear solutions. As de Galan, et al. (26) point out in an overview of automation in atomic spectrometric analysis: "The sample still forms the most difficult object for automation. This goes for the hardware of sample treatment and for the software to account for the sample's influence on the analysis."

Perhaps sample preparation in conjunction with direct sample insertion into the ICP could offer significant advantages over the methods just discussed. It is then of interest [illegible] r examine sample drying and decomposition methods in [illegible] e that they might be modified for use with the DSID.

1. Sample Drying

Two of the most commonly employed methods for the dehydration of both geological and biological solid samples before trace analysis are oven-drying and freeze-drying (lyophilization). These techniques are also used to concentrate liquid samples before analysis. In terms of ease of automation and efficiency, however, neither of these methods were attractive for use with the DSID. Automation of lyophilization would have been difficult. Sample transfer into compartments requiring seals and careful pressure control in order to avoid sample loss were considered disadvantages. In addition, any sample transfers would pose the threat of contamination.

The same arguments applied in the case of two other common drying methods: vacuum drying at room temperature and dehydration in a desiccator over compounds such as phosphorous pentoxide.

Depending on the particular sample matrix and the properties of the analyte, these methods (especially oven drying) could introduce additional errors due to analyte loss. For example, the National Bureau of Standards (NBS) advised in their certificates of analysis for the three biological standards used in this work (SRM 1571 orchard leaves, SRM 1570 spinach, and SRM 1573 tomato leaves): if samples of the standards were oven-dried, the temperature was to be maintained at 85°C for the specified time. Drying at higher temperatures would have reportedly resulted in large losses of volatiles. Freeze-drying was the only other recommended dehydration procedure for these samples.

A recent series of papers by Iyengar and co-workers (187,188,189) detail the problems of trace element loss from solid biological samples subjected to various drying procedures. Tables II and IV of the second paper (188) summarize the literature data on element loss from biological samples during freeze- and oven-drying, respectively.

The problems of analyte losses during drying are not confined to biological samples. For example, as W.M. Johnson and J.A. Maxwell advise in their book "Rock and Mineral Analysis" (190), the drying of stream sediment samples should be carried out at low (105°C) temperature and if trace elements such as mercury are to be determined, oven drying must not be used.

In the certificates of analyses for the three geological samples used in the present work (SRM 1632 coal, SRM 1635 subbituminous coal, and SRM 1633 coal fly ash), the NBS advised that oven drying be avoided.

The above examples illustrate the fact that care must be exercised even in the dehydration stage of sample pretreatment. Close attention must be paid to the relative volatilities of the elements to be determined as they exist in the specific sample matrix. It is important to note that an element added to a particular sample before drying may not behave in the same fashion as its natural counterpart. Care must be taken to insure that a "spike" element exists in a form which is natural for a particular matrix. Otherwise, unsuspected analyte loss might occur during sample drying.

The introductory considerations suggested that some form of open system in which sample material need not be dehydrated in a sealed compartment would be more readily automated. However, as the studies referenced above indicate, drying at elevated temperatures in an open atmosphere might result in analyte loss. An ideal system would deliver only enough energy to drive off water vapor from sample material residing in an open cup. The sample cup and contents could then be rapidly transferred to the next pretreatment stage (eg. ashing) and finally directly enter the plasma discharge. The hazard of contamination due to sample transfers would therefore be eliminated.

Such an ideal system might incorporate microwave radiation for dehydration. A microwave frequency of 2450 MHz (the frequency used in commercial microwave ovens) would presumable excite only water molecules leaving the remaining sample constituents unchanged.

Microwaves have been employed for industrial process control of inorganic chemical moisture content with significant reductions in drying times relative to thermal oven treatment (191). Microwave drying has also successfully reduced the time involved in moisture content determinations of organic material such as soil (192). A 1980 report (193) suggested the use of microwave drying as an efficient pretreatment step in elemental analysis.

Reductions in drying times from about 8 hours to 15 minutes for 10 g portions of bovine liver, lucerne leaves, and carp subjected to microwave drying were reported by T.-S. Koh (193). No significant effect on trace element concentrations was noted. Even selenium was completely retained in microwave-treated samples of NBS bovine liver and orchard leaves.

Although the above results are encouraging, microwave drying in its current form has a major disadvantage. This is the fact that samples need to be placed in a sealed compartment. If this method were to be successfully coupled with direct insertion, the microwave beam would have to be directed into a sample cup in an open system. Aside from questions of safety, such apparatus would probably be difficult to engineer.

2. Sample Decomposition

The problems pertaining to sample dehydration discussed to this point are more serious in the case of sample decomposition. The more vigorous conditions required for decomposition make automation more difficult and generally increase the chances of significant analyte loss and sample contamination.

Thorough reviews of decomposition procedures for inorganic (194) and organic (195,196) samples have appeared recently. A very complete text by R. Bock (197) concerning decomposition techniques in analytical chemistry was published in 1979. The introductory chapter contains an excellent discussion of sources of error in the various decomposition techniques. Decomposition techniques and possible sources of error in organic elemental analysis are discussed in a text by Ma and Rittner (198). In addition, prevention of contamination and loss during manipulation and analysis of microscale samples is covered in a text by Ma and Horak (199).

Of particular interest in terms of developing automated sample pretreatment for use with the DSID is a brief review of methods for speeding-up and automating decomposition presented in the introduction of Bock's (197) text. The brevity of this section of his introduction reflects the lack of progress in this area to 1979. Only five references are given concerning automation.

This material will now be up-dated with a view to finding an automatic technique suitable for use with the DSID. For the purpose of this discussion sample decomposition procedures will be divided into two main categories: thermal and chemical reagent-based.

a. Thermal Decomposition

The most straightforward approach to thermal sample decomposition simply involves dry ashing in an open crucible placed in a furnace with ambient air as the oxidizing agent. Furnace temperatures from 500 to 600°C are common and the technique is useful for example in preparing coal samples for dc arc emission analysis. The method is time-consuming, however. For instance Bollo-Kamara (200) reported that dry-ashing small (about 1 gram) coal samples for dc arc elemental analysis required an average of five to six hours. In addition, two hour interval stirring during ashing, reheating to constant weight after ashing, and a final grinding and overnight oven drying at 120°C were required before analysis.

Aside from being time-consuming, dry-ashing is complicated by potential problems of element loss. As was the case with dehydration, an awareness of matrix-specific losses is necessary to successfully apply dry-ashing. The first thorough investigation of element loss from organic samples during dry-ashing was reported by Gorsuch (201) in 1959. Gorsuch (164) also went on to examine more closely losses due to volatile chloride formation during dry ashing.

Gorsuch's 1959 and 1962 (201, 164) papers are the first thorough studies concerning trace metal recovery after sample pretreatment and are often referenced. The first significant extension of Gorsuch's work was reported in 1969 by Strohal, et al. (202). In contrast to earlier work, Strohal and coworkers utilized natural incorporation of radiotracers in their studies of biological tissue-specific losses. The complexity of tissue-specific dry ashing losses is further exemplified in more recent papers by van Raaphorst, et al. (203) and Rowan, et al. (204).

The paucity of automated dry ashing procedures is to be expected in light of the above examples. Losses of the elements of concern from specific matrices must be investigated before a reliable dry ashing procedure can be developed. Procedures must be modified in a time-consuming process for each matrix. If these preliminary investigations could somehow be automated, perhaps a more general automatic dry ashing method could be developed.

b. Chemical Reagent-Based Decomposition

For the purposes of this discussion, chemical reagent-based decomposition will be divided into four main types: open-flask digestion, reflux digestion, bomb digestion, and fusion. This particular organization will facilitate the discussion in terms of automation.

There are some general problems with all four types of decomposition which must be seriously considered along with any proposals for automation. Many of these problems were encountered with the thermal decompositions reviewed previously. In particular, interaction of the sample with its container via reaction, adsorption, or diffusion can lead to analyte loss (negative error). Losses caused by volatilization or expulsion of spray, foam, or dust can also occur.

Contamination (blank values, positive error) is a ubiquitous problem with chemical reagent-based decomposition. Reagents and solvents, often used in large quantities, are the most likely source of contaminants. Desorption from the sample container during the decomposition is another serious possibility. In addition, contamination from particles in the atmosphere should be considered, especially in ultratrace work.

Problems of contamination and loss become more critical as the severity of decomposition conditions increases (for instance, reaction with the crucible can occur during fusion) and as sample size decreases. As Ma (199) points out, after obtaining a representative sample, "...the next serious problem is the prevention of contamination during micro-scale manipulation and analysis." These factors further complicate efforts to automate reagent-based decomposition.

i. Open Flask Digestion

Wet digestion in an open container can be an effective and simple alternative to digestion in one of the more complex variations of reflux equipment. However, the risk of loss by volatilization or contamination by reagents must be understood. An early radioisotope study by Pijck, et al. (205) illustrated the risks involved in open digestion without refluxing. Of the fourteen elements investigated, four (Sb, As, Au, Fe, and Hg) could not be fully recovered from biological material without the use of a condenser.

If, in a certain analysis, loss by volatilization and contamination by reagents are not critical problems, a conical (Kjeldahl) flask or beaker covered with a watch glass may be used to advantage. Gorsuch (201) suggested conical flasks as a second choice after the Bethge apparatus for use in wet digestions. The long necks of conical flasks will both promote some refluxing and catch most foam. Care must be exercised in heating, however, to prevent bumping and the sudden ejection of material from the flask.

The beaker/watch glass combination provides more surface area for digestion with less reagent but requires more operator attention. As Siemer and Brinkley (206) point out, spattering and drying of sample on the watch glass is a constant problem. These authors suggest as an alternative the use of an Erlenmeyer flask fitted with a simple reflux cap originally designed by Smith (207). This cap prevents spattering losses and permits the addition of reagents during decomposition.

According to Gorsuch (201), dry ashing was as popular among laboratories in 1959 as wet digestion for the decomposition of organic matter prior to trace metal determination. By 1982, in contrast, wet digestion in an open container was the method of choice for this type of analysis (196). An emphasis on liquid sample presentation to new sources like the ICP was probably the main reason for the historic shift in the intervening years back to wet digestion. Obviously, wet digestion converts the sample directly to liquid form whereas an extra step would have to follow dry ashing. If the operator manipulations associated with open container wet digestion could somehow be eliminated, the technique would certainly become even more popular.

A gain in the popularity of wet digestion may occur as two developments reported by Knapp (208) and Koirtyohann, et al. (209) in 1975 become more widely recognized. Knapp (208) designed a heating block with an array of digestion vessel wells. Long-necked quartz tubes could be inserted in the wells to any depth desired. Digestion rate was controlled with a combination of insertion well depth, residence time at a particular depth, and heating block temperature. Batch operation was possible giving an output of about ten samples per hour. This apparatus was later incorporated into a mercury cold vapor analysis by Knapp, Tolg, and coworkers (210). Reliable determinations of mercury at the 5 ng level in several organic and inorganic matrices was achieved.

Koirtyohann, et al. (209) extended the idea of sample dehydration in a microwave oven (191) to digestion. An NBS SRM bovine liver or orchard leaves sample (90.5 g or less) contained in an Erlenmeyer flask along with an $HNO_3/HClO_4$ acid mixture was completely digested in about three minutes. Samples were also readily digested in batches; twelve 0.5 g samples required only fifteen minutes.

Significantly, no frothing or bumping occurred during decomposition in the microwave oven. In addition, there were no explosions during a six month period of use. Acid fumes were evacuated from the oven into a trap containing a base such as solid $CaCO_3$. Therefore, no special perchloric acid hoods were necessary. An additional trap placed in the oven's air intake reduced the risk of external contamination. Although no loss study was undertaken, flame AA results for Zn and Cd in the SRMs agreed well with the NBS values. Similar agreement for As, Cr, Se, and Ni in the orchard leaves and As, Se, and Co in the bovine liver was found using neutron activation analysis (NAA).

Efficient alternatives for the open-container wet digestion of some samples have certainly been provided by Knapp (208) and Koirtyohann, et al. (209). It is unlikely, however, that these alternatives, or any form of wet digestion at atmospheric pressure, would be as effective in the digestion of more resistant materials such as silicate minerals.

ii. Reflux Digestion

The major drawback of reflux digestions is the extended time required. For example, Gardner (211) found that it was necessary to let coal samples stand overnight in acid to reduce frothing during the subsequent Bethge reflux and distillation. The total analysis time for coal was therefore as long as 24 hours.

Some progress in speeding up reflux digestion has recently been reported by Bajo and coworkers (212). Using an HNO_3/H_2SO_4 mixture in a specially-constructed reflux apparatus, clear digests were obtained from resistant organic materials in relatively short times. For instance, average-size samples (0.2-1 g) of charcoal, polypropylene, and even graphite and lard were completely digested in less than three hours.

A novel oxygen combustion-reflux digestion apparatus initially designed by Tolg and Morsches (213) in 1966 and recently commercialized by Tolg and coworkers (214) also significantly reduces total digestion time, the risk of contamination, and the number of operator manipulations. The apparatus is based on the efficient Schoniger (215) oxygen flask decomposition for trace analysis. In 1981 Tolg and coauthors (214) applied a commercial version ("Trace-O-Mat") of the original combustion reflux apparatus in a study of trace element recovery. Element recoveries from seven NBS biological SRMs were excellent. Complete digestion required only one hour for a sample of 1 g or less. However, batch operation was not possible.

Analyte loss during reflux wet digestion was first considered in a thorough fashion by Gorsuch (201) in 1959. His radiochemical tracer technique wasn't suitable for the study of contamination so this subject was treated only in a qualitative sense. Gorsuch carried out his wet digestions in a modified Bethge apparatus. This choice not only permitted control of oxidation rate but minimized the risk of contamination. Relative to digestion in an open flask, smaller volumes of reagents are required for refluxing in the Bethge apparatus. The risk of contamination from reagents is therefore also minimized.

iii. Bomb Digestion

One of the traditional approaches to the decomposition of intractable materials like silicates is wet digestion at elevated pressure; commonly referred to as bomb digestion. Bomb digestion is also preferred with determinations of the volatile semimetals and nonmetals in organic samples (198). In fact, bomb digestion developed from historical procedures such as the Carius method for halogens (216) in which organic samples were decomposed with acid in sealed glass tubes.

More modern developments such as tubes with ground seals and gaskets and steel vessels (bombs) with screw caps increased the method's convenience. In the case of steel bombs, this convenience was initially offset by the problem of high blanks. The development of platinum and Teflon linings and seals improved this situation (197), but in the case of Teflon, useful seal lifetime was short (217). Eventually, alternative seal designs which eliminated this latter problem were proposed (217,218). A radioisotope study conducted by Van Eenbergen and Bruninx (219) demonstrated the reliability of modern Teflon-lined bomb design. Of the twenty two elements investigated, small losses were observed only for Mo, Ge, and Ru. Precipitation on the Teflon lining was the likely explanation for this loss. Their data, together with previously published data for ten additional elements (219), indicates that loss is essentially eliminated in modern bomb digestions.

It is interesting to note that although bomb digestion offers the significant advantage of freedom from losses, little effort has been devoted to the development of an automated system. Only isolated improvements such as the reduction of reaction time by agitation (197) or the development of better seals (217,218) and digestion reagent systems (217) have occurred. The long-standing problem of explosion risk has no doubt impeded progress, but it is still surprising that so little has been done.

iv. Fusion

Fusion [illegible] alternative technique for the decomposition of refractory materials such as geological samples. In this technique a sample is brought into contact with a high concentration of molten salt (flux) such as sodium carbonate in a crucible at high temperature (up to about 1000°C). Once the decomposition reaction is complete, the fused mass is usually allowed to cool in the crucible. Subsequent dissolution is necessary for most final determinations, but the solid mass ("button") can be used directly for x-ray fluorescence (XRF) analysis (220).

The main drawbacks of fusion are loss due to volatilization, contamination due to reaction with the fusion crucible, and the addition of high concentrations of cations to the sample (216). High salt concentrations can cause errors in the final determination such as light scattering and molecular absorption in ETA-AA and ionization interference in flame-AA. The use of other fluxes may necessitate time-consuming and error-prone schemes for the separation or suppression of interfering cations (217). In addition to all of these drawbacks, losses to the fusion crucible due to reduction and alloying can also occur (217). A lengthy discussion by Bock (197) illustrates the magnitude and complexity of this final problem.

Even in the face of these multiple problems, some progress has been made toward automating the fusion process. A special tube furnace designed by Govindaraju (221) could fuse two 650 mg powdered rock samples every 1.5 minutes.

Less complex fusion devices are available commercially from, for example, Angstrom (Puff Automatic Fusion Device, Angstrom, Inc., Chicago, Illinois) and Claisse Scientific (Claisse Fluxer, Claisse Scientific Corp., Inc., Quebec, Quebec). These devices are essentially combinations of

Fisher burners with mechanisms for agitation of platinum crucibles. Of the two devices, the Claisse unit is more advanced as it can automatically dissolve the hot melt by pouring it into a beaker of acid and then agitating the beaker.

The main theme which emerges from the forgoing review of general pretreatment procedures is that no single approach adequate for all sample types has yet been devised. The small amount of progress in automating pretreatment has been restricted to specialized procedures. A truly "universal" automated sample pretreatment is still in the future.

C. The Role of the DSID

The problem regarding dilution ratios pointed out by Dahlquist and Knoll (182) was reflected on by one of the original developers and main proponents of ICP spectroscopy, V. A. Fassel, at an international Atomic Energy Agency symposium in 1978 (222).

He suggested that in addition to overcoming "recently recognized 'problems'" such as nebulization-transport effects,

> drastic reductions in the limits of detection which can be achieved with most present ICP-AES systems, and increased application of ICP-AES for multielement determinations on small volume samples are also anticipated as advanced sample introduction techniques come into wider use (222).

Yet no single "advanced sample introduction technique" has found general acceptance for the introduction of small volume samples to date. The DSID described in Chapter III was proposed as a new and potentially very useful alternative for the introduction of small volume samples into the ICP.

The solid sample pretreatments reviewed in this chapter put the DSID in even better light. The dilution ratio problem associated with some of the wet digestions could be overcome with the DSID. A small volume liquid sample would be delivered in its entirety into the plasma. The inefficiency associated with nebulizer introduction systems would therefore be avoided and a higher effective concentration of analyte would reach the plasma. The more rapid wet digestion methods such as $HNO_3/HClO_4$ digestion in a microwave oven could then enjoy wider application.

Better yet, chemical reagent-based decomposition might be entirely bypassed in favor of decomposition executed in the DSID itself. The problem of dilution would therefore be avoided and contamination would be reduced.

It was necessary to look beyond the normal techniques discussed to this point in order to find sample drying and decomposition methods suitable for use with the DSID. Two successful techniques, CO_2 laser- and sub-plasma-sample preparation, could be thought of as special modifications of sample pyrolysis.

D. CO_2 Laser Sample Preparation

1. Introduction

The essential difference between dry ashing and pyrolysis is that no oxidant is employed in the latter technique. The variation of pyrolysis most closely resembling dry ashing is called thermogravimetric analysis (TGA). In this approach, only temperature and weight loss parameters are recorded-pyrolysis products are not identified. The petrochemical industry utilizes TGA heavily and automatic commercial instruments such as the Perkin-Elmer TGS-I are available (223).

The petrochemical industry also widely employs a version of pyrolysis in which the fragments formed during pyrolysis during the "cracking" of large organic molecules are separated and identified. Characteristic primary and secondary fragments help identify the parent molecules. For example, high polymers (plastics) are quickly identified by pyrolysis techniques.

Pyrolysis energy supply devices include furnaces, capacitive discharge- or induction-heated filaments, and lasers. The laser offers some important advantages relative to the other pyrolysis devices.

As Guran, et al. (224) pointed out in 1970, pyrolysis techniques utilizing hot wires, heated tubes and cups or heated chambers may suffer from lack of reproducibility caused not only by variations in sample temperature, but by large temperature gradients in the pyrolysis chamber, catalysis of decomposition by hot metal surfaces, and tar formation.

Most current laser pyrolysis devices are based on ruby lasers (694.3 nm emission) with pulsed outputs ranging in duration from about 100 µs to 100 ms with energies of a few joules per pulse. Under these conditions, laser pyrolysis of organic compounds gives predominantly low molecular weight fragments like C_2H_2, CH_4, CO, and CO_2. Higher molecular weight fragments can be obtained by defocussing the ruby laser beam or switching to a lower energy CO_2 laser. For example, Sharky, et al. (225) found that an unfocused beam from a low power (10 W) CO_2 laser worked well for coal sample pyrolysis. Reproducibility is best with thin film samples and most samples must either be placed on an absorbing substrate or mixed with an absorbing substance (197). Powdered nickel is preferred over graphite or charcoal as an absorbing additive since it does not affect pyrolysis fragment distributions (226).

The above examples illustrate some of the potential of laser pyrolysis. The great advantage here is the fact that a controlled amount of energy can be rapidly and specifically deposited into a given sample.

This same important advantage should apply to sample drying and ashing. With respect to the thermal decomposition techniques examined here, a new drying and/or ashing technique based on a laser would appear to have great promise in terms of automation. An open system could be constructed in which sample-carrying cups would be essentially independent of the pretreatment energy source. The appropriate amount of laser energy could be directed into an individual sample at the right moment in an overall analytical sequence.

As far as sample drying is concerned, no seals would have to be made and broken and sample material would remain in the same open cup for the following ashing step. This is in contrast to the previously discussed lyophilization and vacuum desiccation techniques. Sample loss would therefore be eliminated.

Furthermore, since energy would be delivered directly into the sample at a controlled rate along a directed beam and across a narrow wavelength band, the sample cup material and atmosphere above the sample would remain at a lower temperature. In contrast to the dry ashing techniques mentioned previously, some advantage might therefore be gained in terms of analyte loss due to volatilization and reaction with the sample cup material.

2. Laser Development

A continuous-wave carbon dioxide gas laser previously constructed in our laboratory (227) was employed in initial sample ashing experiments (Figure 16a and Table V.1). This longitudinal gas discharge laser emitted infrared radiation at 10.6 micrometers with an estimated (by IR scintillation

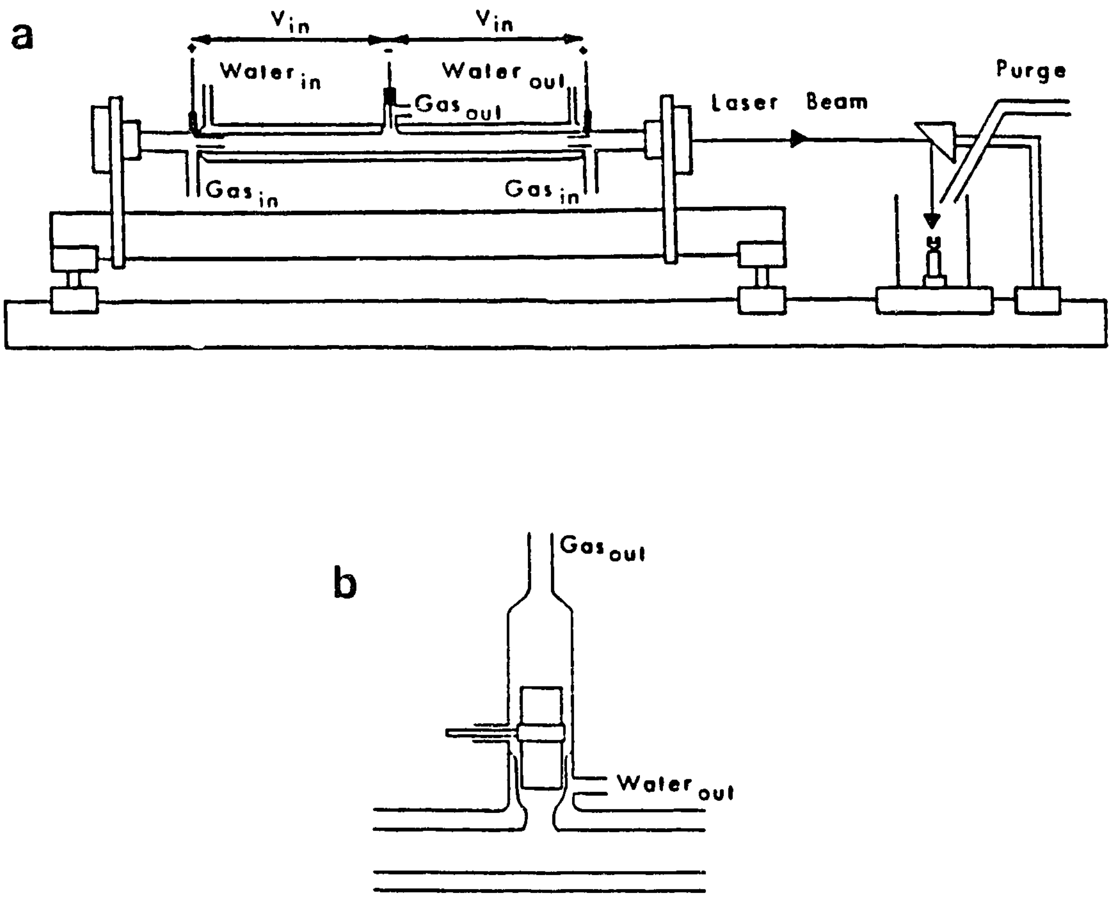
a
V in
V in
+
-
+
Water in
Water out
Gas out
Gas in
Gas in
Laser Beam
Purge
b
Gas out
Water out

Figure 16. (a) CO_2 laser asher, (b) anode modification.

TABLE V.1

LASER SPECIFICATIONS

Based on Apollo Lasers (6357 Arizona Circle, L.A.
California, 90045) Model 580 CO_2 laser

General Dimensions

Parameter	Specification
Overall length	130 cm
Discharge tube length	99 cm
Outside tube diameter	3.8 cm
Discharge tube diameter	1.5 cm

Optics From Apollo Lasers

Parameter	Specification
Output reflector	#656-074 ZnSe
Rear reflector	#656-086 100% Au plated Ge

Running Conditions

Parameter	Specification
Lasing gas	5% CO_2, 15% N_2, bal. He at 50 mbar pressure
Applied potential	10.5 kV (at about 60mA) across each half of the discharge tube
Purge gas	about 10 l min^{-1} Ar or O_2

plates) power of 50 W. Higher output power could not be maintained for more than a few seconds without overheating and degradation of the laser tube's center (common) pin electrode (anode). The application of more than about 7 kV across the laser tube also overheated and destroyed the power supply's ballast resistors (Figure 17).

Experiments indicated that greater output power was required for the rapid ashing of certain sample types. The laser was upgraded for this reason. The discharge tube was modified to accommodate replacement of the center pin with a larger cylindrical stainless steel electrode (Figure 16b). The water jacket surrounded the lower end of the new electrode for efficient cooling.

This improvement, together with the installation of a fan for ballast resistor cooling, permitted continuous laser operation at maximum applied potential (10.5 kV per side at 50 mbar). It was then possible to generate an output power of approximately 80 W. This was sufficient for rapid ashing of organic samples.

Both the laser and an asbestos sample holder were mounted on an optical rail bed. A front-surfaced mirror mounted on the rail bed deflected the laser's 7 mm diameter output beam down onto samples. A standard 1/4 inch diameter graphite sample cup occupied about 84% of the unfocussed

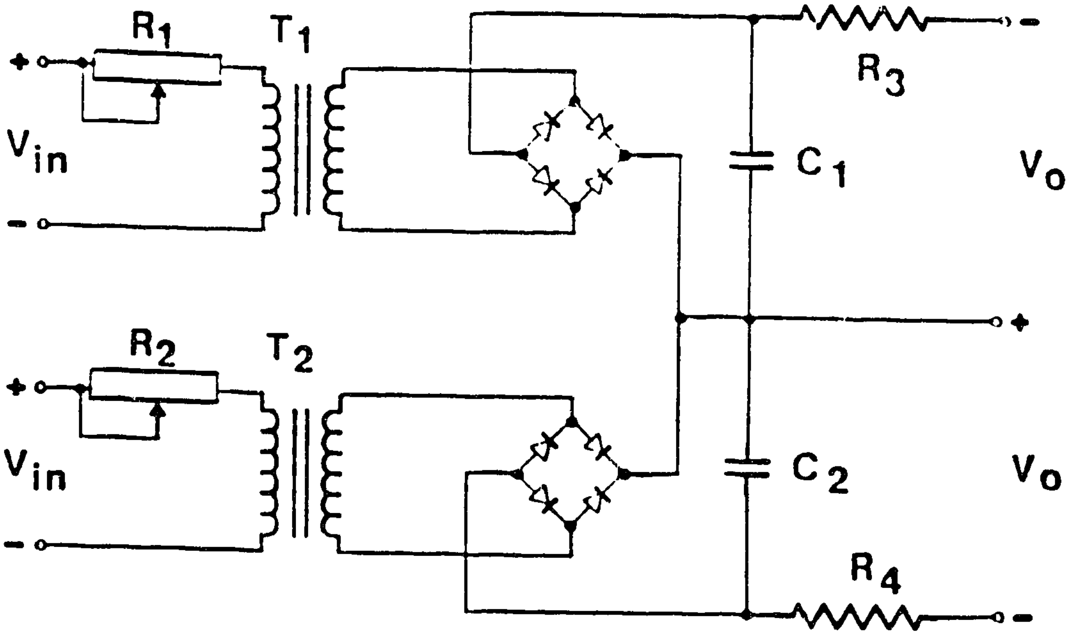
R1
T1
+
Vin
-
R2
T2
+
Vin
-
R3
C1
Vout
-
+
C2
Vout
R4
-

Figure 17. CO_2 laser power supply circuit diagram; $R_1=R_2=0\text{-}115V$ reostat; $R_3=R_4=100k\Omega$, 200W ballast resistor; $T_1=T_2=15kVAC$, 60mA neon sign transformer; $C_1=C_2=1.6\mu F$, 25kV; $V_{in}=115VAC$, 60Hz; $V_{out}=10.5$ kVDC @ 50 mbar laser discharge tube gas pressure.

beam's cross-sectional area. During inert atmosphere ashing experiments, the sample holder was placed in a one-liter glass beaker purged with argon (Figure 16a).

Laser output power was controlled by adjustment of the discharge tube's voltage, gas pressure, and output and rear reflector alignment. Laboratory rheostats (Figure 17) were used to vary the voltages applied across the two sections of the discharge tube. Flow of gas into the laser was controlled with a needle valve and pressure was monitored with a vacuum gauge (Figure 18 and Table V.2). A thermal conductivity gauge was used to check the integrity of the laser tube and vacuum pump.

The laser's output power was monitored by directing the beam onto an asbestos block and observing the intensity of visible emission. After optimizing tube voltage and gas pressure, the output and rear reflectors were aligned to give the highest intensity and smallest diameter spot on the asbestos.

Because of the relatively high cost of premixed gas, gas mixing capability was added to the laser (Figure 18). By [illegible] adjustment of three rotameters, the correct ratio of N_2, He, and CO_2 gases could be delivered by a three-way valve into a mixing tube attached to the laser gas supply. Laser output powers obtained with gases supplied in this fashion

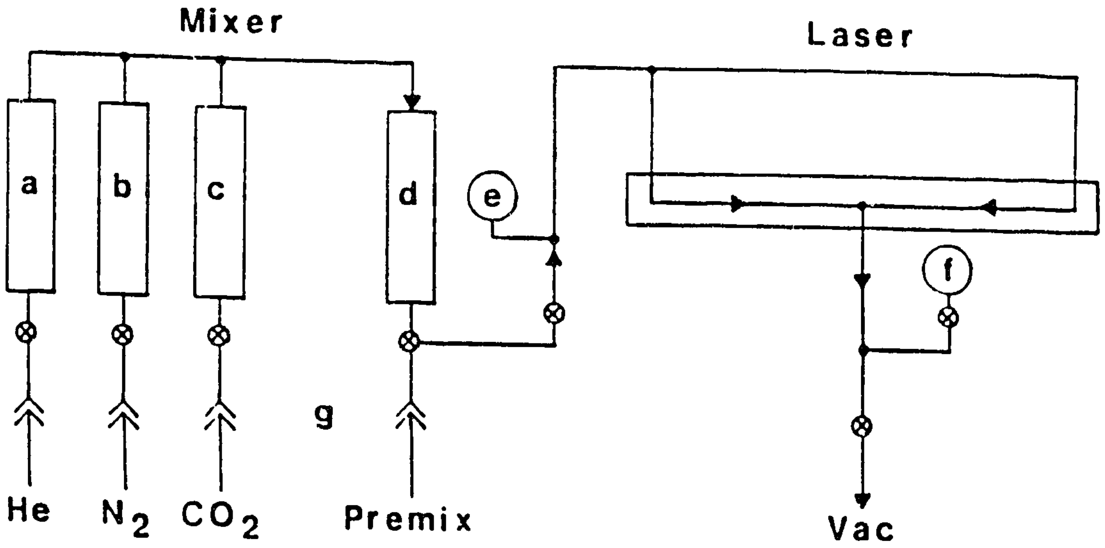
Mixer
Laser
a
b
c
d
e
f
g
He
N_2
CO_2
Premix
Vac

Figure 18. Laser gas supply and vacuum system. (See Table V.2 for component identification).

TABLE V.2

LASER GAS SUPPLY CIRCUIT SPECIFICATIONS

Mixer Rotameters

Supplied by Matheson Gas Products, E. Rutherford, N.J.

Component	Figure Label
150 mm Tube Cubes and panel mount flowmeter units:	
#605 tube (He)	(a)
#603 tube (N_2)	(b)
#601 tube (CO_2)	(c)

Mixer Mixing Tube

Home-built

Component	Figure Label
Wire gauze baffling	(d)

Mixer Bulkhead Unions

Supplied by Crawford Fitting (Canada), Niagara Falls, Ont.

Component	Figure Label
Swagelok 1/4" fractional tube to 1/8" male NPT	(g)

Laser Gauges

Component	Figure Label
Input line (Edwards)	(e)
Output line (Varian)	(f)

and from a single premixed cylinder were equivalent.

E. Positioner for Sub-Plasma Sample Preparation

1. Introduction

If samples could be located at various positions under the inductively coupled plasma discharge, drying and ashing rates could be controlled simply by varying sample position. The discharge itself would provide the radiation required for sample preparation. No additional external source of energy would be necessary. This technique would constitute a new form of automatic sample preparation by pyrolysis/photolysis.

Organic compounds have been degraded with ultraviolet light from mercury or xenon arc lamps. In a typical photolysis apparatus the sample and arc lamp are placed at opposite foci of an ellipsoidal mirror. As in laser pyrolysis, decomposition times depend on source and sample parameters and can range from a few seconds to several hours. Increased absorption of radiation can be affected by adding a mercury-iron (II) compound to the sample. If iodine or bromine is added as a sensitizer, even completely fluorinated compounds (such as Teflon) can be quantitatively decomposed by irradiation with a xenon lamp (228). Fragments from organic compounds including peptides, hydrocarbons, insecticides, and plastics have been analyzed following photolysis (197).

A derivative of photolysis called flash-photolysis has been used for rapid sample pyrolysis (197). An inorganic compound

is subjected to a short, intense burst of light from, for example, a high power xenon arc lamp. As in the case of laser pyrolysis, energy is rapidly deposited into the sample and (relative to filament pyrolyzers) simpler fragmentation patterns result.

Electrical sample decomposition utilizing radio-frequency excitation of oxygen is also of interest in terms of the new sub-plasma pretreatment.

In 1962 Gleit and Holland (229) of Tracerlab announced a new method for the decomposition of organic substances at low temperatures. These authors were dissatisfied with conventional approaches such as furnace dry ashing for the same reasons as discussed previously in this chapter.

Gleit and Holland's (229) alternative "...employ(ed) a high frequency electromagnetic field to produce a stream of reactive oxygen, which decompos(ed) the organic substances." Previous inductively coupled decomposition techniques employed either metal powder mixed with the sample (the Curie point method) or a metal sample container for heating directly in an RF field. Like the earlier systems, theirs was closed in order to minimize atmospheric contamination and volatile element loss. The important difference was the placement of sample downstream from the induction coil. General heating of the sample was then minimized as "highly excited states of oxygen" selectively reacted with the organic samples (no mechanism was proposed). Sample temperatures of less than 100°C reduced element volatilization and diffusion losses.

For example, a desiccated sample of whole human blood (1.0 ml original volume) gave completely acid-soluble ash after a 1.5 hour treatment. Oxygen flowed through a 150 W, 13.56 MHz RF discharge and then over the blood sample at a pressure and rate of 400 µm Hg and 4 ml/min, respectively. Radiotracer experiments revealed that thirteen elements, including arsenic and lead were completely recovered from the blood samples. A 92% recovery was reported for mercury. In contrast, a twenty-four hour muffle furnace ashing at 400°C gave 23% and less than 1% recoveries of As and Hg, respectively.

Gleit and Holland's "electrically excited oxygen low temperature decomposition" apparatus also produced completely acid-soluble ash from muscle, fat, feces, ion exchange resin, cellulose and PVC filter paper, activated charcoal, and even a 40 g rat.

Tracerlab offered a commercial version of Gleit and Holland's (229) original apparatus which soon found an important application in the coal industry. Using a Tracerlab LTA 500A low temperature asher, Gluskoter (230) obtained in about 90 hours a light gray ash from a bituminous coal sample (about 1.5 g, dried and ground to 840 μm) placed 5 cm downstream from the 13.56 MHz oxygen discharge. This ash contained residues of calcite ($CaCO_3$), pyrite (FeS_2), kaolinite ($(OH)_8Si_4Al_4O_{10}$), and other clay minerals in contrast to the calcium oxide, ferric oxide, and dehydrated clay minerals found in the usual red ash resulting from high temperature ashing.

Although "electronic low temperature ashing (LTA)" was an important improvement over traditional muffle furnace ashing in providing unaltered mineral matter residue, long ashing times remained a significant drawback. This specific problem was addressed by Williams (231) in 1982.

Williams (231) refers to the recommendation of an electronic LTA manufacturer to use tetrafluoromethane (CF_4, Freon 14) for the acceleration of ashing rate. He attributed the increased ashing rate to the greater sample penetrating power of the fluorine atom (due to its smaller diameter).

Williams (231) reasoned that Teflon sample dishes placed in an LTA might provide high concentrations of atomic fluorine where they were needed most-close to the sample. Significant reductions in ashing times for various samples were noted when Teflon dishes were employed. For example, 3.5 g of dried boysenberries in syrup were reduced to less than 0.2 g of ash in four hours using Teflon dishes. When aluminum dishes were used, the same extent of ashing required eleven hours.

It is interesting to recall at this point that Kirkbright used the formation of volatile fluorides to advantage in his graphite rod-ICP work (172,122). Reflection on Williams' (231) results suggests a modification of Kirkbright's procedure (172) applicable to the present study. Why not use Teflon sample cups with the DSID?

As Williams (231) proposed, high concentrations of atomic fluorine would be generated in close proximity to the sample. This might provide for more complete volatilization of refractory elements than was realized by Kirkbright (122). (Recall that he generated atomic fluorine from gaseous freon (172)). Switching from graphite to Teflon sample cups would also restrict possible carbide formation to any carbonaceous material in, or generated from, the sample itself.

Even though the environment encountered by a Teflon cup held beneath an atmospheric pressure ICP discharge will be different than the low pressure environment experienced by a Teflon cup in an "electronic LTA," it is likely that Teflon cups will be a useful adjunct to the proposed sub-plasma preparation of certain samples. Teflon cups were machined for use with the DSID (see Chapter III) in order to test these ideas. Experimental results are given in Chapter VI.

2. Positioner Development

The technique proposed for ashing samples directly under the running plasma discharge has advantages over both electronic low temperature ashing and muffle furnace ashing in terms of analyte loss. As sample temperature was increased by positioning the sample closer to the discharge, volatilized elements could be detected by their subsequent atomic emission. Therefore, appropriate ashing conditions could be selected rapidly. Rapid monitoring of losses and adjustment of parameters is not possible with the other ashing methods (or any of the pretreatments for that matter). Any losses occurring during sample dehydration could be monitored and responded to in the same fashion.

Manual insertion experiments revealed that a temperature gradient existing under a running plasma could be effectively utilized for controlled sample drying and ashing.

In the DSID system described in Chapter III, however, samples were pneumatically transported from the carousel tray directly into the plasma. There was no provision for stopping a sample assembly at intermediate positions. It was not possible to precisely locate a sample transport assembly at any point beneath its stop with lower insertion gas flow rates. In addition, variation in sample weights would have necessitated a constant readjustment of insertion gas flow. The installation of a complicated feedback system to overcome the problems would have vitiated the straightforward pneumatic approach.

The compact and functional positioner depicted in Figure 19 was therefore devised to mechanically locate samples under the plasma. The insertion gas again served only to deliver sample assemblies to, and support them against, a stop. The stop was inside the positioner, however, and was vertically translatable with an accuracy of about 0.5 mm. As a result, samples could be moved in a controlled fashion from about 25 mm below the plasma to the center of the RF coil. This enabled the automatic programming of samples through dry, ash, and atomization stages. This "in situ" sample

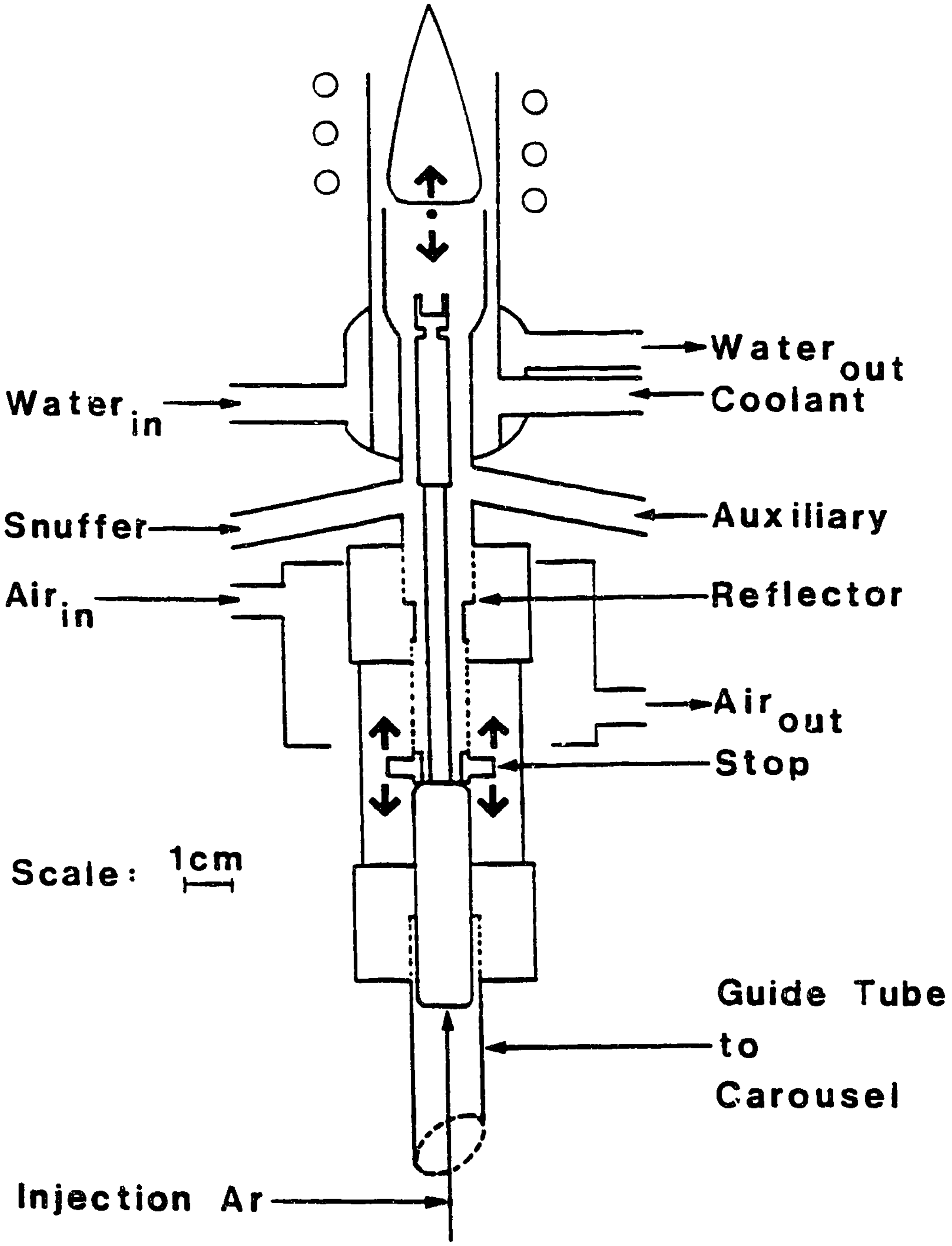
Water out
Coolant
Water in
Snuffer
Auxiliary
Air in
Reflector
Air out
Stop
Scale: 1cm
Guide Tube to Carousel
Injection Ar

Figure 19. Sub-plasma sample positioner and water-cooled torch.

pretreatment greatly increased the efficiency of the DSID.

a. Cooling

The sample positioner was fabricated entirely from plastic to help preclude formation of filamentous discharges between it and the plasma. Although filaments were successfully avoided in this fashion, Ar/O_2 and Ar/H_2 mixed gas plasmas elevated temperatures within the ICP source housing to a point where expansion of plastic components became a problem.

Expansion caused jamming of the movable stop and thus loss of control over the sample pretreatment and atomization sequence. This was partially remedied by air cooling from a jacket suspended around the upper end of the positioner (Figure 19). Unfortunately, jamming would still occasionally occur when the stop was near its upper limit of travel.

It was noted that the torch guide tube conducted sufficient heat to the positioner during mixed-gas plasma operation to cause expansion and jamming of the stop. Since the ICP torch was mounted in the positioner, this expansion also caused the torch to become loose. Stable centering of the torch in the RF load coil was necessary for both the prevention of arcing and the maintenance of optical integrity.

Torch stability and positioner function was improved after installation of a water cooling jacket in the lower end of the torch (Figure 19). Although a water jacket which extended completely to the positioner gave the best results, it made centering of the inner concentric tube difficult during torch construction. This alignment is very important in sustaining a symmetrically stable plasma discharge. A compromise in water jacket design was therefore accepted.

A discoloring and expansion of plastic inside the positioner just below the torch was observed after several hours of argon/oxygen mixed gas plasma operation. This led to a recurrence of stop malfunction even though the positioner was being cooled. Ultraviolet radiation directed from the plasma by the torch was the probable cause. The insertion of a reflective metal collar at the base of the torch (Figure 19) eliminated this problem and no further difficulties in positioner operation were encountered.

b. Mechanical Detail

Details of positioner construction are given in Figure 20 and Table V.3. Although fabrication of the entire positioner from the more heat resistant plastic Vespel would probably have eliminated the need for cooling, its cost was prohibitive. Only the stop was machined from Vespel; inexpensive Delrin plastic was chosen for the remaining components.

The stop was shaped much like a vertebra; the hollow center allowing passage of a transport assembly's stem and sample cup, its lower edge retaining the assembly's pneumatic plug, and its two outer arms acting as mechanical linkages to the positioner drive.

The stop arms extended out through a slotted tube (stop guides, Figure 20) to a threaded collar which in turn fit inside a threaded barrel. Rotation of this barrel between two fixed retainers therefore caused vertical translation of the stop. The stop guides were made slightly shorter than the sample plugs in order to maintain an insertion gas seal.

The sample positioner was geared via a small steel chain to a motor mounted inside the RF coil housing. Any vibrations transmitted to the positioner by this drive mechanism had to be damped since the positioner also

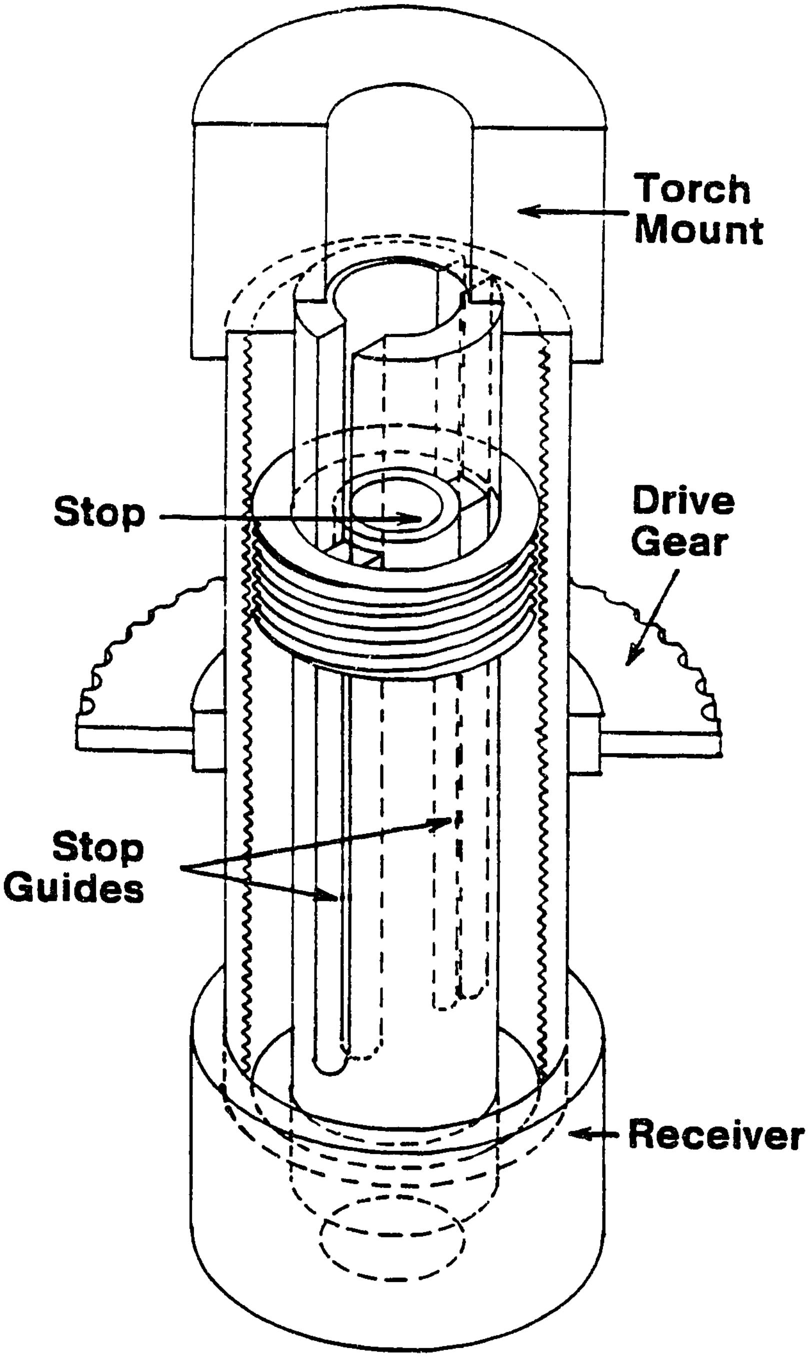
Torch Mount
Stop
Drive Gear
Stop Guides
Receiver

Figure 20. Positioner mechanical detail.

TABLE V.3

SAMPLE POSITIONER SPECIFICATIONS

All parts machined from Delrin (Dupont) plastic except as noted.

Outer Barrel

Parameter	Specification
O.D.	32 mm
I.D.	24.7 mm
Length	48.1 mm
Drive gear	53.7 mm o.d., Bakelite, 44 teeth

Stop Collar

Parameter	Specification
O.D.	25.5 mm
I.D.	20 mm
Height	7.1 mm
Width	2.8 mm
Thread pitch	
Collar-to-stop attachment	2.6 mm wide x 1.9 mm deep recess drilled in each side of collar. 1.5 mm wide holes continued from recesses to the inner surface of collar for screws to hold the stop.

Continued...

TABLE V.3 (Continued)

Stop

Parameter	Specification
Material	Vespel (Dupont) plastic
O.D.	10.4 mm
I.D.	9.1 mm
Stop-to-collar attachment	4.8 mm long x 2.7 mm wide x 4 mm high arms tapped in ends to receive collar screws.

Stop Guide Tube

Parameter	Specification
O.D.	20 mm
I.D.	0.6 mm
Length	58.9 mm
Stop guide slots	3.1 mm wide extending 51.7 mm down from top of tube.
Receiver attachment	Two 2.8 mm wide tapped holes drilled in bottom of tube.
Torch mount fastening	Two 2.8 mm wide tapped holes 2.4 mm down from top of tube and 90° from each slot. This fastening also prevented collapse of slots.

Continued...

TABLE V.3 (Continued)

Torch Mount Outer Barrel Retainer

Parameter	Specification
O.D.	35 mm
I.D.	32 mm for 3.4 mm as retainer for outer barrel then 20 mm for 4.2 mm as seat for stop guide tube and finally 13.5 mm remaining distance to top surface as mount for torch guide tube.
Length	21 mm
Mount-to-stop guide tube seat attachment	Two 2.8 mm tapped holes entering opposite sides of stop guide tube seat from mount's outer surface.

Receiver Outer Barrel Retainer

Parameter	Specification
Construction	Similar to torch mount but stop guide tube seat 6.4 mm deep with holes for fastening drilled through to bottom surface.

functioned as a torch mount. The manufacturer's original torch mount was removed and replaced by the sturdy positioner clamp shown in Figure 21a. This clamp effectively eliminated any unwanted vibrations.

For flexibility during experimentation, either a sample transport assembly guide tube or a demountable aerosol tube (Figure 21b) could be plugged into the positioner's receiver. This meant that either solution nebulization or direct insertion experiments could be conveniently set up without disturbing the ICP torch or sample positioner. A nebulizer and spray chamber were mounted below the ICP source and could be swung in above the sample carousel and connected to the demountable aerosol tube via a ball joint.

c. Computer Control

The same type of optically-isolated relays as were discussed in Chapter IV were used to interface the sample positioner drive motor to the LPS unit. A schematic of the control signal generation circuit and drive mechanism is given in Figure 22. The drive motor was mounted at the inside rear of the ICP torch box so that its output shaft faced up. A positioner drive gear and lead screw were attached to this shaft. A tracking nut with a protruding pin

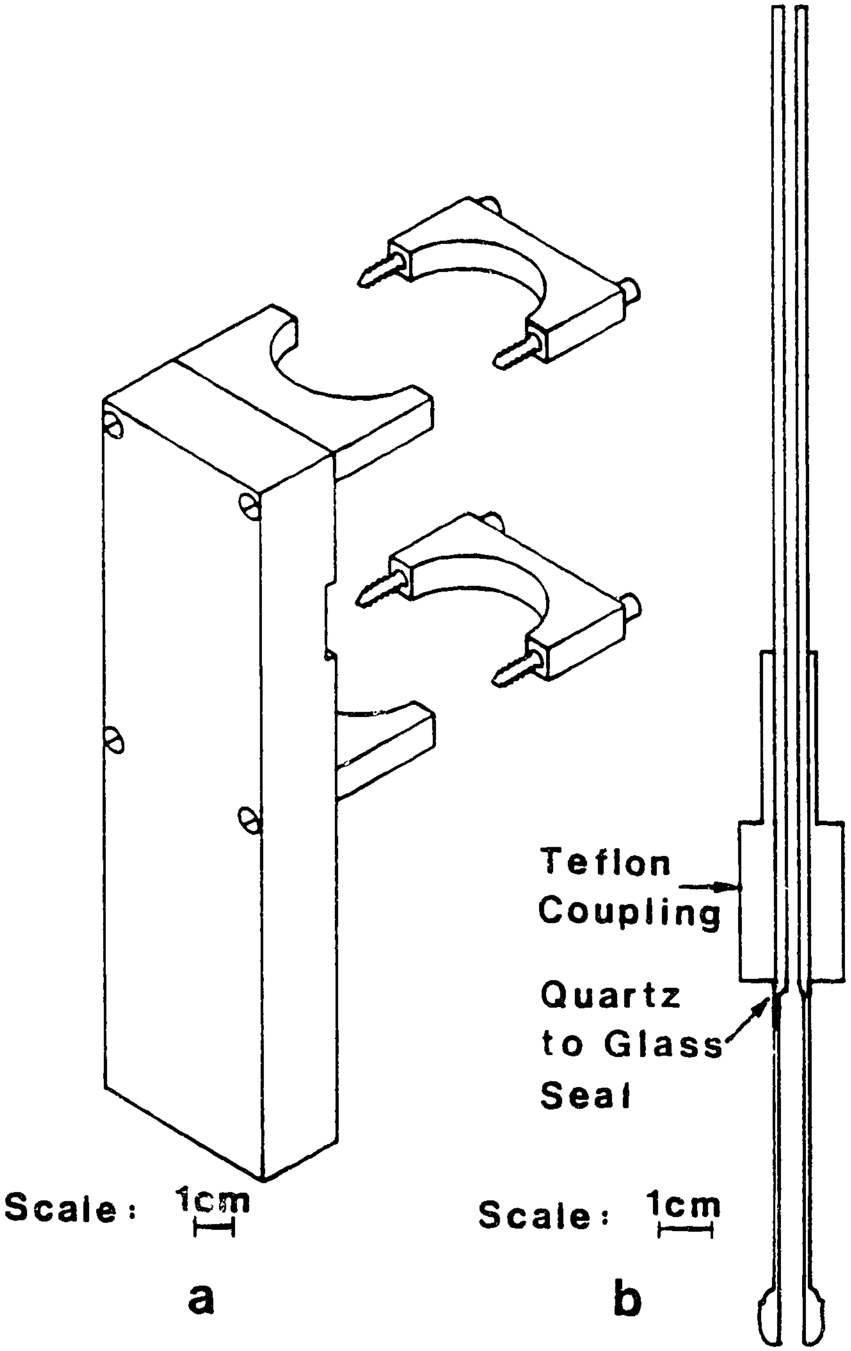
Teflon Coupling
Quartz to Glass Seal
Scale: 1cm
a
Scale: 1cm
b

Figure 21. (a) Positioner clamp, (b) demountable aerosol tube.

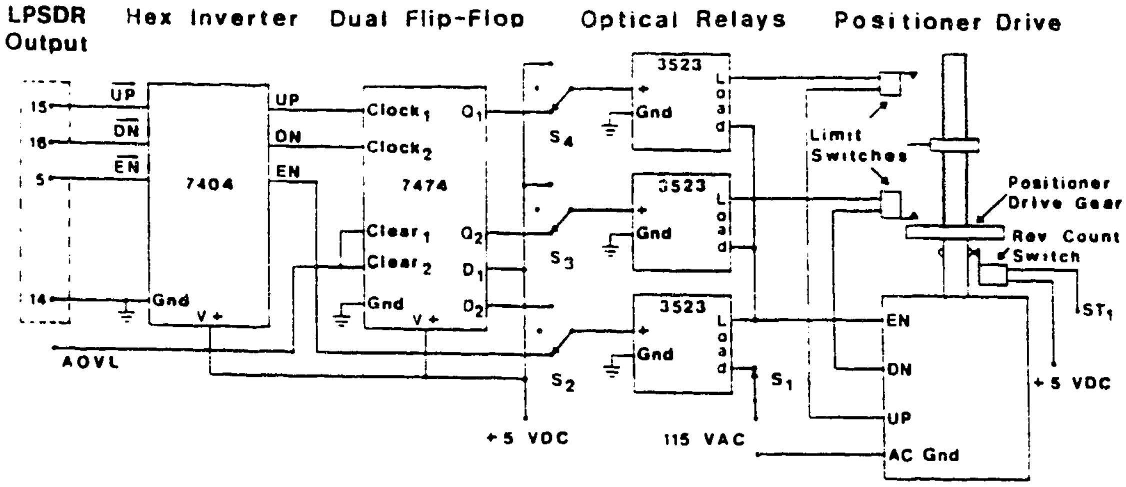
LPSDR Output
Hex Inverter
Dual Flip-Flop
Optical Relays
Positioner Drive
15
16
5
14
$\overline{UP}$
$\overline{DN}$
$\overline{EN}$
7404
Gnd
V+
AOVL
UP
DN
EN
Clock$_1$
Clock$_2$
Clear$_1$
Clear$_2$
Gnd
V+
7474
Q_1
Q_2
D_1
D_2
S_4
S_3
S_2
S_1
+5 VDC
3523
+
Gnd
Load
115 VAC
Limit Switches
Positioner Drive Gear
Rev Count Switch
ST_1
EN
DN
UP
AC Gnd
+5 VDC

Figure 22. Sample positioner control signal generation circuit and drive mechanism.

was installed on the lead screw. The pin passed through a vertical slot guide (not shown in Figure 22) which prevented rotation of the tracking nut. This pin opened microswitches (in series with UP and DN lines) at the upper and lower ends of the lead screw to prevent jamming of the positioner.

The drive motor had a main and two opposing secondary coils for clockwise and counterclockwise rotation. By leaving the main coil energized while switching off either of the secondaries, a breaking action resulted and runover was effectively eliminated. Three input signals were therefore required to control the motor: primary coil and clockwise and counterclockwise secondary coil energize (EN, UP, and DN, respectively, Figure 22).

These input signals were generated under software control by loading a 3-bit binary number into the output register of the LPSDR digital I/O unit (Table IV.2). Register bit 0 corresponded to the control signal EN, bit 1 to DN, and bit 2 to UP. Since the motor's primary coil remained energized during positioner operation, the EN signal was routed directly to the corresponding optical relay (Figure 22). The UP and DN signals were first inverted (7404 hex inverter) and then fed to the clock inputs of a 7474 dual D-type edge-triggered flip flop (Figure 22). Since the two flip flop data lines were tied high, an edge transition at a clock input would cause the Q output to go and remain high. These Q outputs were then fed to two additional optically-isolated relays for switching of the motor's secondary coils. Manual control of positioner operation was provided by SPDT (center off) override switches (S_2 - S_4, Figure 22).

The amount of vertical sample displacement provided by the positioner was also software controlled. Two opposed lobes on the positioner motor's drive shaft closed a microswitch twice per shaft revolution (Figure 22). The resulting 5 VDC pulses were then fed to the Schmitt trigger 1 (ST_1, Figure 22) input of the LPSKW programmable clock (Table IV.2). The status register associated with the LPSKW clock was programmed so that each firing of the Schmitt trigger would cause the clock to increment from a preset value until overflow occurred. Each revolution of the drive shaft caused the counter to increment by 2 and vertically displaced the sample cup by 0.5 mm. Preset values could thus be calculated and loaded into the counter for any desired amount of sample displacement.

When the LPSKW counter overflowed, a flag was set in the clock status register. In the drying, ashing, or cooling stages of sample pretreatment, positioner displacement could be terminated by polling this overflow flag and then clearing a 7474 flip flop holding an UP or DN relay closed (Figure

22). Software polling of this flag during sample insertion was not possible, however, as data was being read in from the PDA at that time. In addition, the counter overflow pulse normally available at the front panel of the LPS was disabled when the Schmitt trigger was utilized for counter base frequency.

The carry bit from the last 4-bit binary up/down counter (DEC IC 74193) of the LPSKW clock was therefore hardwired to the clear inputs of the positioner controller. This carry bit line was designated as D3-2 AOVL from E6 on the LPSKW board (drawing D-CS-M7016-0-1 in the LPS directory). The AOVL line is identified in Figure 22.

CHAPTER VI

DIRECT LIQUID INTRODUCTION WITH THE DSID

A. Introduction

Continuous flow and discrete systems for sample introduction and preparation were contrasted in terms of their potential for automation in Chapter I. Nebulization, normally a continuous flow sample introduction technique, has been the preferred method of liquid introduction for ICP spectroscopy, but its limitations are well known. If only liquids could be introduced into the ICP with 100% efficiency, especially if the analyst has only a few microliters of hard-won sample!

The answer to this problem lies in moving away from traditional continuous flow liquid introduction and toward some new form of discrete sample introduction. An historical perspective of discrete sample introduction into flames and plasmas was given in Chapter II and it was concluded from this overview that the automatic direct sample insertion device or DSID described in Chapter III was the best way to automatically deliver small liquid samples into the ICP.

However, three other notable avenues to more efficient liquid introduction into ICPs have been pursued by other workers: discrete nebulization, direct nebulization, and volatile analyte generation. These approaches will now be briefly examined. Table VI.1 provides a summary of these historical advances.

1. Discrete Nebulization

An alternative approach to decreasing the volume of sample required for nebulization is simply to introduce small individual pulses of aerosol into the source. This technique, called discrete nebulization, was reviewed by Cresser in 1981 (232).

The technique dates back to 1955 with a publication by Solomon and Caton (233) on the flame emission microdetermination of sodium and potassium. They aspirated 0.5 ml aqueous solutions into an oxyacetylene flame attached to a modified Beckman DU spectrophotometer. Transient emission signal recordings were used to construct calibration plots. The aspiration of air between samples caused baseline shifts in the recordings but did not affect performance. A useable baseline was established by aspirating deionized water. The precision and accuracy of their measurements compared favorably with results obtained with continuous nebulization.

TABLE VI.1

ADVANCES IN CONTINUOUS FLOW LIQUID INTRODUCTION FOR FLAMES AND PLASMAS

Technique	Source	Matrix/ sample size (sample/hr)	Element	%RSD/ Level (D.L.)	Yr./ Ref.
discrete nebulization	ICP	oil-xylene, blood/25uL	Al, Cr, Cu	ppm	'72/ 235
discrete nebulization	ICP	diluted or digested blood and serum/5uL	Fe, Ti, U, Zn	<3(Y as int. std.)/ ppm	'81/ 236
discrete nebulization	N_2O_2/ C_2H_2 flame	aqueous/ 40uL	Zr	1.7/ppm	'82/ 238
rapid flow analysis	ICP	serum electrolyte 10uL (240)	Ca, Fe, Mg, Na	<5	'82/ 239
hydride generation	ICP	NBS biological SRMs	As, Bi, Ge, Sb, Se, Sn	< ppb	'82/ 253
volatile chelate generation	ICP	NBS bovine liver, human serum	Fe, Zn	Quant. recover	'81/ 254
mercury cold vapor	MIP	aqueous/2mL	Hg	pg	'81/ 257
GC	MIP	sea, tap, pond water & urine	F		'82/ 266

However, when discrete nebulization was applied to ICP spectroscopy, the aspiration of air between samples caused destabilization of the source. Broekaert and Leis (44) found that flushing the nebulizer sampling funnel with argon between samples or using a peristaltic pump between the funnel and the nebulizer was necessary to avoid destabilization of an argon ICP running at less than 2 kW. In a later paper, Broekaert, Leis, and Laqua (234) reported that increasing ICP power above 2 kW obviated the need for these precautions and sample volumes as small as 20 µl could be nebulized reproducibly from a simple funnel.

It is interesting to note that in the first report on discrete nebulization-ICP spectroscopy, Greenfield and Smith (235) didn't encounter problems of destabilization by air. However, they did employ a 5.5 kW argon plasma. Their system consisted of a micropipet connected via capillary tubing to a nebulizer. The nebulizer was attached to a heated desolvation chamber which was followed by the high power ICP. They obtained quantitative results for ppm levels of Al, Cr, and Cu in 25 µl oil/xylene samples and demonstrated the technique for ppm levels of metals in µl volume blood samples.

Recent applications of the discrete nebulization technique are essentially minor variations on this theme.

For example, Uchida's group (236) used a capillary tube connected to a standard cross-flow nebulizer to aspirate drops of solution of less than 100 µl volume from small holes in a teflon rod into an ICP source. Entrainment of air was minimal as the capillary tube was quickly transferred from blank to sample solution and back to blank solution.

The elements Fe, Ti, U, and Zn at ppm levels in 5 µl sample volumes gave relative standard deviations of less than 3% when yttrium was used as an internal standard. However, precisions for Al and Na were much worse. Recoveries of several elements from 50 µl samples of diluted or digested blood and serum were in good agreement with values obtained by continuous nebulization.

Kojima and Iida (237) have developed an automatically triggered integrator useful for studying the effects of injection volume and sample flow rate on the temporal behavior of signals generated by discrete nebulization. The integrator was triggered by sample electrical conductance sensed between the platinum nebulizer needle and a platinum electrode in the sampling funnel.

Using this system in conjunction with flame atomic absorption and emission spectrometry, these authors found that signal peak height increased with increasing sample volume up to about 100 µl. For most of the elements studied, a minimum sample volume of 50 µl was required to give a linear calibration and RSDs below 5%. Aspiration of air between samples was not a problem with the nitrous oxide-acetylene flame used in the experiments.

Any problems of source destabilization caused by the aspiration of air are eliminated in an alternative discrete nebulization technique that utilizes the injection of sample into a continuously flowing carrier stream.

For example, Ito and coworkers (238) developed a discrete nebulization system for ICP spectroscopy based on the syringe injection of a sample into one arm of a T-connector. The plug of sample was delivered to the nebulizer in a carrier stream flowing through the other arm of the T-connector. An RSD of 1.7% for 40 µl of 1 ppm zirconium was achieved with this sample introduction system.

Alexander and coinvestigators (239) developed a similar injection technique for ICP spectroscopy called Rapid Flow Analysis (RFA). Again, samples were injected into a T-connector, but the carrier stream was delivered by a 10-roller peristaltic pump to a modified Babington nebulizer. Three rollers of the pump were always in contact with the delivery tubing to reduce pulsing. Using this system the authors achieved an injection rate of 240 10 µl samples per hour with RSDs below 5% for multielement solutions. Similar results were obtained for Na, Ca, Mg, and Fe in serum electrolyte samples.

2. Alternatives to Nebulization

Another possible approach to increasing the efficiency of liquid sample introduction into atomic emission sources is to eliminate the spray chamber section of the nebulizer entirely and inject the sample aerosol directly into the source. This is affected by total consumption burners in flame spectroscopy, however, desolvation and vaporization efficiencies can be poor and the burners are noisy (240).

Greenfield (32) reports that a U.K. patent exists on a direct injector for ICP spectroscopy but gives no details. Horlick (241) reports that preliminary experiments with direct liquid injection into an ICP indicate a possible no-win situation. Analyte ion line/neutral atom line intensity ratios are decreased, suggesting a degradation of excitation efficiency with increased solvent (H_2O) input.

Hydride Generation

Alternative techniques are being developed which can preconcentrate certain analytes and at the same time altogether eliminate the need for nebulizers and spray chambers. The best known of these techniques is hydride generation. Volatile hydrides of some of the group IV, V, and VI elements are formed by reaction with the reducing agent sodium borohydride and the volatile hydrides are then swept into the atomic source by a carrier gas (242).

The first example of hydride generation as a sample introduction method for ICP spectroscopy was reported by Kirkbright and coworkers (243). Further refinement of this continuous generation system led to decreases of about an order of magnitude in detection limits as compared to conventional nebulization (244). Very significant (three to four orders of magnitude) improvements in detection limits have more recently been achieved with a discrete hydride generation/condensation system. Hahn's group (245) achieved sub-part-per-billion detection limits for As, Bi, Ge, Sb, Se, and Sn by first preconcentrating the hydrides of these elements in a liquid argon cold trap. The trap was then warmed and the hydrides were transported to an ICP source in a stream of argon gas. The authors reported good recoveries of all elements but selenium and tin from several NBS biological reference materials.

b. Volatile Chelates

Another interesting approach to forming volatile analyte species which may have more general utility than the hydride method is being pursued by Black and Browner (246). They have successfully analyzed some transition metals with ICP spectroscopy by sweeping volatile fluorinated ß-diketonates of the metals into the emission source. For example, direct reaction of trifluoroacetylacetone with NBS bovine liver in a sealed flask followed by purging of the reaction vapor into an ICP gave quantitative recoveries of iron and zinc. Excellent recoveries of the same elements from human blood serum were also reported. Advantages of this method of sample introduction include the avoidance of time-consuming and contamination-prone pretreatments, increased selectivity and sensitivity by volatilization of analyte away from its matrix, and elimination of the usual problems associated with standard nebulization. Although the method is presently limited to some of the transition metals, synthesis of specially tailored ligands may extend its utility. One significant drawback to the method, however, is the need to calibrate real samples by standard additions.

c. Mercury Cold Vapor Techniques

Mercury is an atypical case with respect to volatile analyte formation techniques since it (in reduced form) has a vapor pressure great enough to permit its direct transfer in a carrier gas to the analysis cell. Ideally then, there is no need for hydride or chelate formation and mercury can be reduced in a straightforward manner with Sn(II). This is the basis of the so-called mercury cold vapor technique (247). If mercury is present at the parts-per-trillion level (pg/ml) as in seawater, however, preconcentration with gold is required (248).

Contamination or loss associated with this preconcentration technique can be avoided in a variation of the mercury cold vapor technique reported by Tanabe and associates (249). These authors achieved a detection limit of 8 pg of mercury in a 2 ml solution by venting analyte vapor to an atmospheric pressure helium microwave induced plasma (MIP).

d. Volatile Compounds and Gases

Aside from the metallic elements, compounds which are gases at room temperature (halogens, etc.) or which can be volatilized at moderate temperatures (low molecular weight organics) are also candidates for straightforward introduction into an atomic source such as an ICP.

For example, Windsor and Denton (250) have eluted hydrocarbons and halogenated compounds with carbon numbers ranging from four to nine from a gas chromatograph into an ICP for empirical formula determination. Molecular formulas for the hydrocarbons were also calculated with the aid of chromatographic retention indices. The authors stated that the molecular formulas for compounds containing oxygen or nitrogen could not be calculated as usable emission lines for these elements had not been observed between 1,900 Å and 6,600 Å in the ICP. The authors had previously (251) achieved sub-microgram detection limits for organic compounds containing C, H, S, P, I, B, and Si using ICP emission lines in this region.

Near-infrared emission from oxygen (252) and nitrogen (253) have subsequently been utilized by Fry and coworkers for quantitative analysis of organic compounds eluted from a gas chromatograph. They have also used a gas sampling loop interfaced to an ICP to achieve sub-microgram detection limits for the halogens F (254), Br, and Cl (255).

Similar detection limits for the non-metals N (256), C, H, Cl, Br, I, and S (257) and, more recently, F (258) have been achieved by Tanabe and coworkers with a convenient GC-atmospheric pressure helium MIP combination. In the latter study, fluoride was determined in sea, tap, and pond water and in urine with the sensitivity and accuracy of a fluoride ion selective electrode (F-ISE). Unlike the F-ISE, however, this system could determine total fluorine and was free from magnesium and lanthanum ion interferences.

B. Liquid Analysis with the DSID

The ICP source described in Chapter III was used for all experiments. Running conditions were as given in Table III.1 unless otherwise noted. The plasma coolant gas percentages referred to in the following sections were calculated based on soap bubble flow meter calibrations of the ICP's flowmeters (see Chapter III.B.2) Measurements were taken with the combination Photodiode Array-Photomultiplier Tube (PDA-PMT) spectrometer described in Chapter IV. The plasma was imaged onto the PDA-PMT's entrance slit in a two-to-one ratio with a 10 cm focal length quartz lens. The spectrometer's general operating conditions were those given in Table IV.1. More specific spectrometer conditions will be noted along with the spectra that follow. Computer programs were written in order to acquire and process data from the PDA-PMT. Some of the programs also controlled the Direct Sample Insertion Device (DSID). Single element and multielement solutions were made up fresh from 1000 ppm stock solutions before each day's experiments. The stock solutions were prepared according to information given by Ward (259). Initially, 10 µl volume micro syringes (Kusano) were used to transfer liquid sample aliquots to the DSID sample cups. It was soon found that micropipets (Eppendorf) gave more precise transfer and were much easier to use. A 10-100 µl variable digital micropipet (Eppendorf) was then purchased and used for the majority of experiments.

1. Graphite Sample Cups in an Argon Plasma

In the first experiments with liquid samples, boiler caps were placed on the dc arc graphite electrode sample cups (see Chapter III.B.3). The cups were rapidly inserted into an argon plasma without preliminary evaporation of solvent. The cups were inserted into the plasma to a height which placed the tip of the boiler cap adjacent to the top of the second turn down from the top of the load coil.

An example spectrum obtained from 10 µl of 1000 ppm Zn solution (equivalent to 10 µg zinc) is given in Figure 23. The data was integrated over a period of 32 s and the fixed pattern background was subtracted from the data. The PDA-PMT spectrometer's entrance slit was 25 µm wide and the plasma was run at 1.5 kW of forward power.

The plasma was destabilized and often extinguished by the sudden ejection of water vapor using this approach. This in turn resulted in poor analysis precision. For example, relative standard deviations (RSDs) for six replicates of 10 µg of zinc ranged from 18.2% (Zn II 202 nm) to 32.6% (Zn I 214 nm).

Improvement in precision was obtained by desolvating liquid samples before insertion. Samples were sequentially desolvated by injection into the load coil (plasma extinguished) with a forward power of 50 W applied for 75 s.

Relative standard deviations for a group of six samples of the same zinc solution now ranged from 9.5% (Zn I 214 nm) to 12.3% (Zn II 202 nm). Taking the ratios of the Zn II 202 nm and Zn II 206 nm lines gave an RSD of 4%.

A multielement stock solution containing the elements cadmium, zinc, manganese, indium, and nickel was prepared

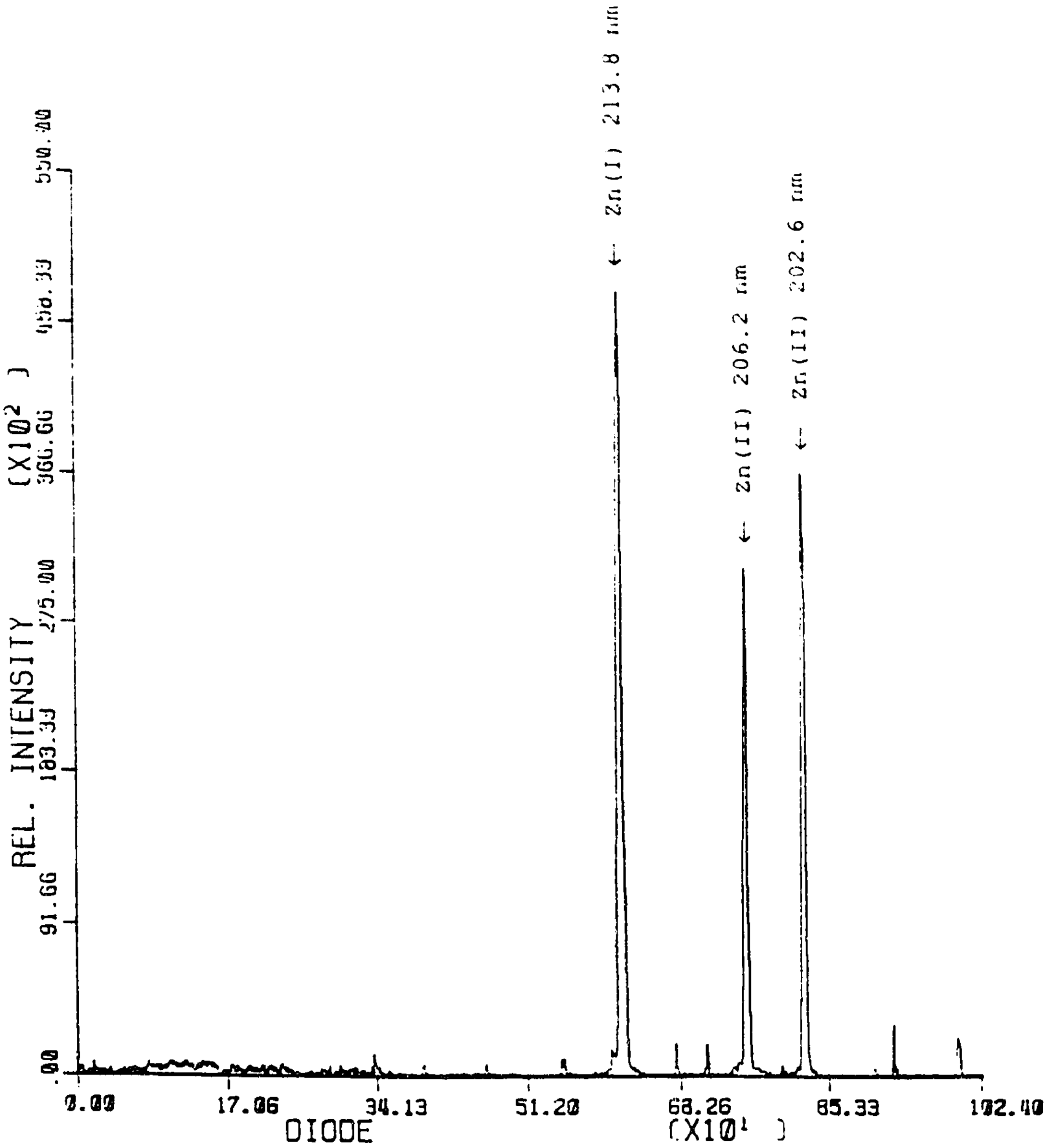

Figure 23. Spectrum from 10 µl 1000 ppm zinc solution (10 µg Zn) in graphite cup.

for use in further experiments. These particular elements not only reflected a good range of volatilities (they are arranged here in the order of decreasing volatility in the dc arc [illegible] also represented some of the more important elements that might be determined in biological/environmental samples. Most of these elements were present in the NBS SRMs ([illegible] and 1635 coal, 1633 coal fly ash, 1570 spinach, 1571 orchard leaves, and 1573 tomato leaves) available in our laboratory. Their individual concentrations after dilution of the stock solution were chosen to give good signal strengths at moderate (0.32 s) PDA spectrometer integration times. It was found that a 10 µl aliquot of the multielement stock solution diluted to give 20 ppm of cadmium, manganese, and zinc, 200 ppm of nickel, and 500 ppm of indium gave a 0.32 s spectrum with all analyte peaks on scale with good intensities.

The analyte emission lines were chosen as a trade-off between sensitivity (according to (261)) and the desire that they ideally all fit into the spectral window acquired by the PDA spectrometer. Fortunately, all the elements in the multielement solution had their most sensitive lines in a spectral range from about 200 to 260 nm - a range nicely covered by the PDA spectrometer.

The sample size to be used for further experiments was chosen after a study of sample size vs. analysis precision. Aliquots of the multielement solution were desolvated as described above and then injected into a 1.5 kW argon plasma. Fifty 0.32 s spectra were averaged and then fixed-pattern background was subtracted. The PDA-PMT spectrometer slit width was 90 µm. As Table VI.2 reveals, a 10 µl sample aliquot gave the lowest percent relative standard deviation so this size was used in further studies.

The degradation of precision with increasing sample size is likely due to the repeated addition and drying of small volumes (10 µl) to achieve greater total volume. This procedure was dictated by the small sample cup used here (15 µl volume).

The relationship between the number of spectrum points (individual photodiode array diodes) used to calculate analyte intensity and the precision of intensity values was also examined. The samples were desolvated 10 µl aliquots of a 50 ppm cadmium and zinc mixture and thirty-two wavelength scans of 0.32 s each were obtained with a PDA-PMT slit width of 25 µm from a 1.5 kW argon plasma.

In a range of one (peak value only) to eleven (total peak area) points, the summation of five points gave the best percent relative standard deviation (0.8%) for the ratio of

TABLE VI.2

SAMPLE SIZE VS. PRECISION

Sample Size, µl	%RSD, Cd I 228.8 nm
10	3.1
30	19.8
60	20.1
90	29.3

Zn II 202 nm to Cd II 214 nm emission intensity. Therefore, five points were taken across spectral peaks to calculate intensities in further studies.

The data from three replicate samples were used in the precision studies reported thus far and in the remaining studies. The choice of three replicates was the result of a trade-off between more representative average analyte intensity values and the efficiency of the direct sample insertion system.

The experimental results to this point indicated that the data acquisition and processing stages of the experiment were functioning properly. Any further reductions in relative standard deviations would have to be won by improving the actual sample vaporization process.

2. Graphite Sample Cups in an Argon-Oxygen Mixed Gas Plasma

It was hoped that by mixing oxygen with the argon coolant gas supply that a plasma environment could be created which would promote the more rapid, complete, and precise volatilization of analyte from graphite sample cups. The Stallwood jet (262) had been successfully applied in traditional dc arc work for just these reasons.

The gas mixing and control systems for these experiments are described in Chapters III and IV. Modifications to the ICP source box were required so that the internal plumbing could withstand the higher temperatures developed around the argon-oxygen plasma. The plasma torch was also modified to withstand higher temperatures. These modifications are described in Chapter III. Computer software was developed for temporal studies of analyte emission. The multi-element solution containing Mn, Zn, Cd, Ni, and In was utilized in the temporal studies.

The oxygen content of the plasma coolant supply could be varied from zero to six percent and still permit the insertion of a sample cup. If more than six percent oxygen was used at a forward plasma power of 1.5 kW, the plasma became too small to permit insertion of the sample cup. Lowering forward power below 1.5 kW resulted in a plasma so small that it contacted only the tip of the sample cup's boiler cap.

A sample cup could be inserted into a ten percent oxygen plasma if a forward power setting of 2.5 kW was used. Under these conditions a graphite sample cup and its cap were completely consumed in about one minute. These higher power and oxygen levels were not used in later experiments, however, because the plasma torch and torchbox plumbing couldn't withstand the correspondingly higher temperatures.

The relative enhancement of analyte (200 ng of Mn, Cd, and Zn, 2 μg of Ni, and 5 μg of In) emission intensities with the addition of one percent oxygen is depicted in Figure 24a and b. The data was integrated over a period of 60 s and both fixed pattern and spectral background were subtracted from the data. The PDA-PMT spectrometer's entrance slit was 30 μm wide and the plasma was run at 2 kW of forward power. The large carbon peak at 248 nm left residual background after subtraction. This residual has been stripped out for clarity. A background spectrum obtained with an empty graphite sample cup inserted in an argon-oxygen plasma is given in Figure 25a (conditions were as in Figure 24 except for a six percent oxygen level). In the spectral region of interest (208 to 264 nm) the carbon neutral atom emission at 247.8 nm predominates. Figure 25b shows the result of combined spectral and fixed-pattern background subtraction. The main analyte emission lines are identified in Figure 26 (conditions were as in Figure 24).

The emission behavior of the same elements over time in the spectral region extending from 211 nm to 266 nm is illustrated in the pseudo-3-D plot of Figures 27 (conditions were as for Figure 24 except that background was not

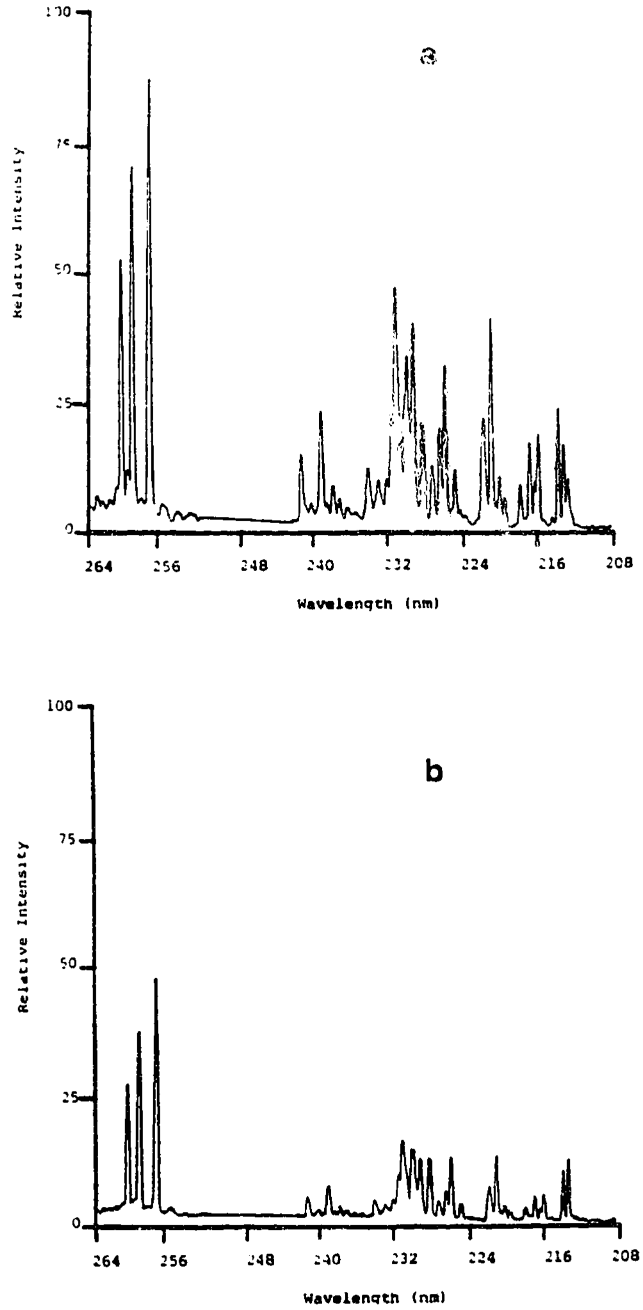

Figure 24. Multielement spectra from graphite sample cup in plasma with 1% O_2 (a), and without O_2 (b).

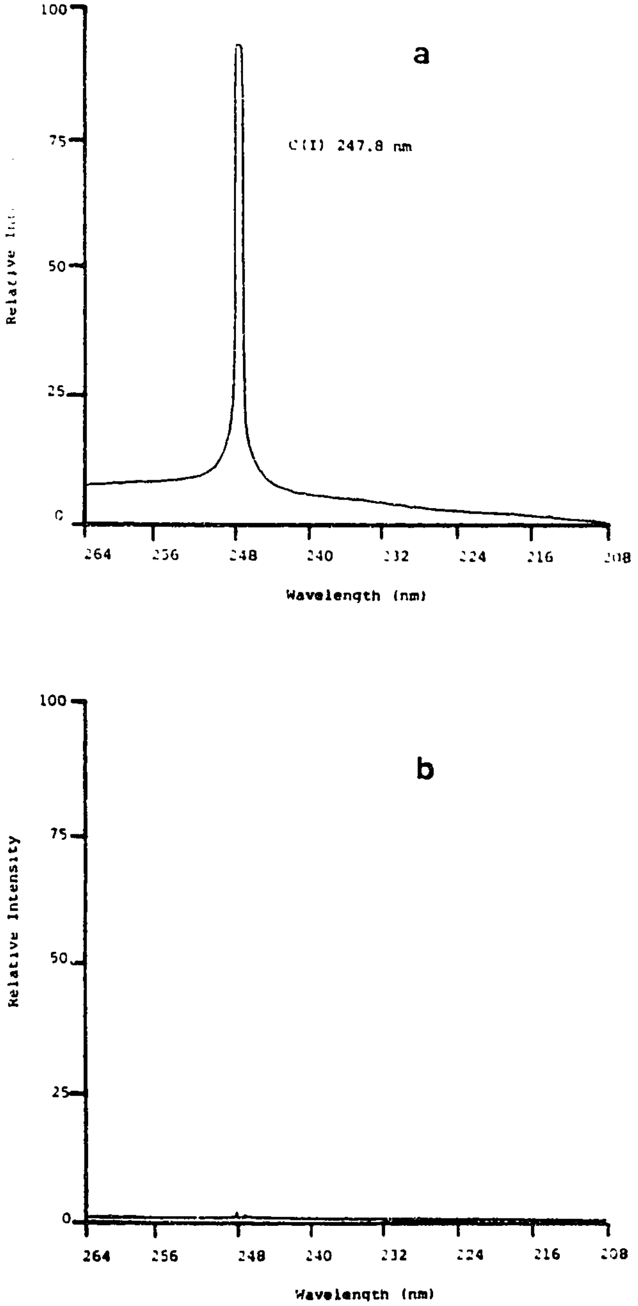

Figure 25. Background emission from graphite sample cup in an Ar-6% O_2 plasma (a), and residual after spectral and fixed-pattern background subtraction (b).

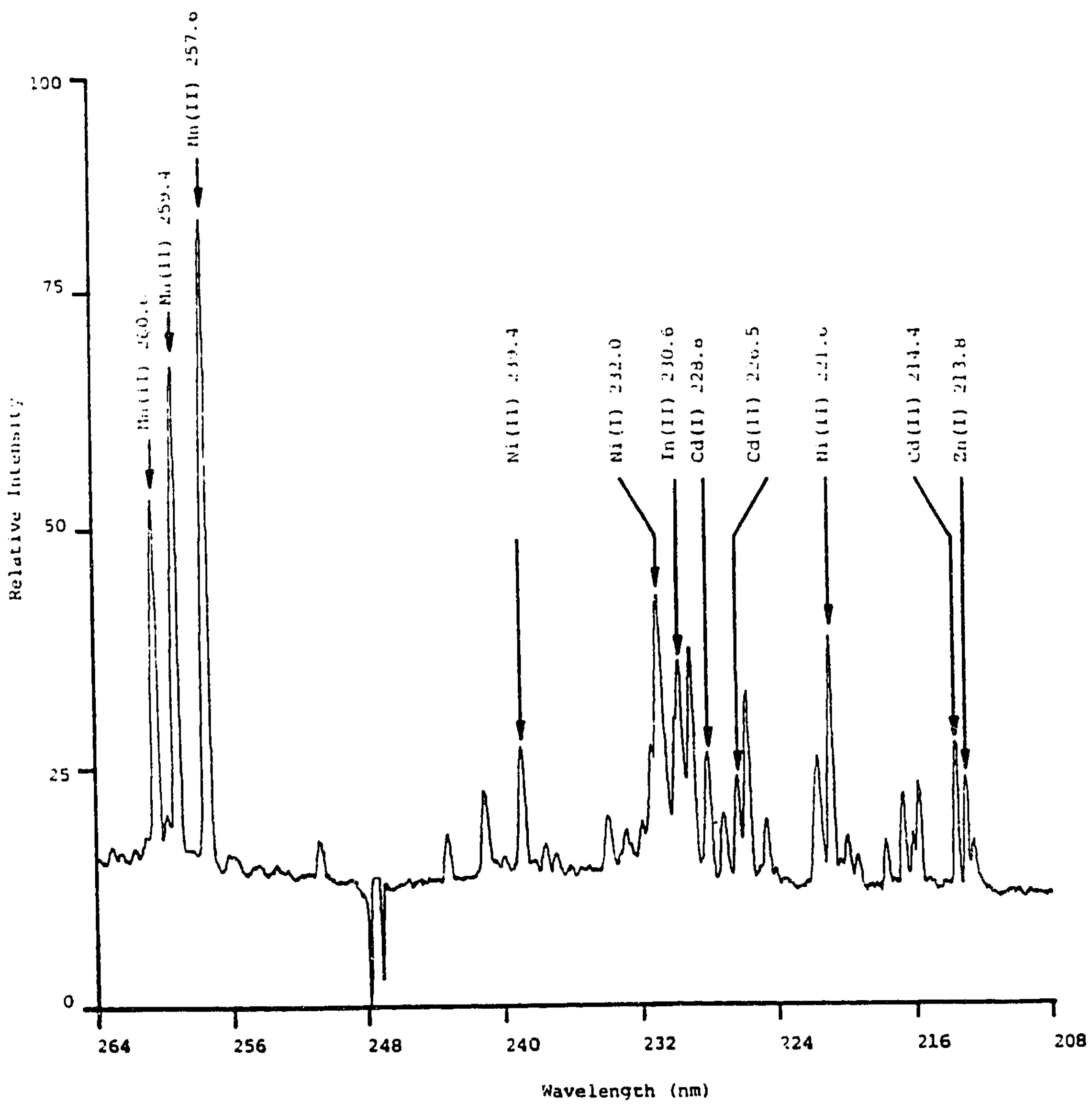

Figure 26. Multielement spectrum from graphite cup in an Ar-1% O_2 plasma.

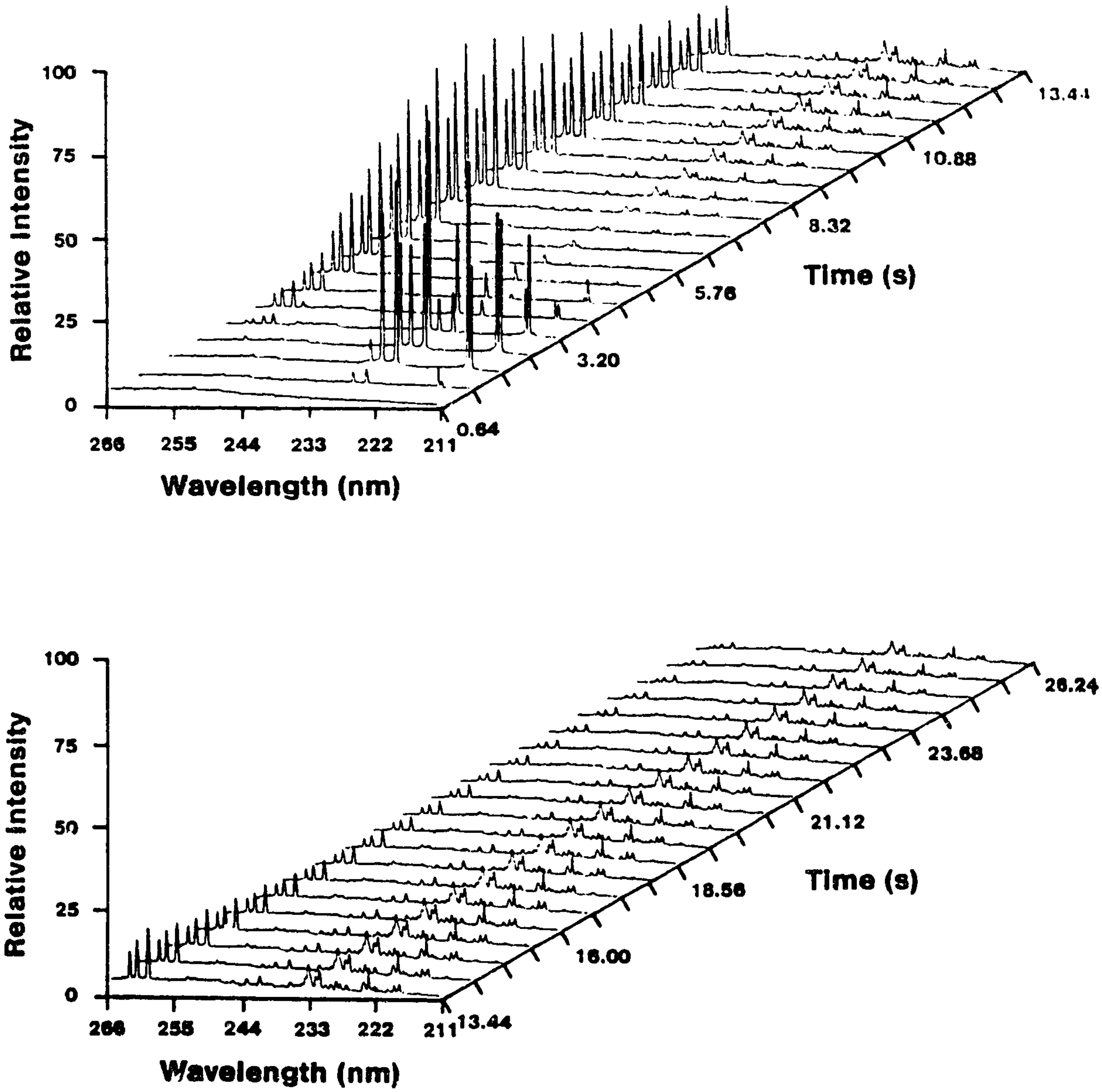

Figure 27. Temporal behavior for Mn, Cd, Zn, Ni, and In in a graphite cup in an Ar-0.5% O_2 plasma.

subtracted and the oxygen level was 0.5%). Temporal data of this type was acquired for desolvated solutions inserted into mixed-gas plasmas with coolant gas oxygen compositions ranging from zero to six percent.

A computer program was written that permitted the selection of an individual emission line in a spectrum drawn from a time study group. Two dimensional intensity-vs.-time profiles were then automatically generated for the individual emission line. Time profiles for the selected line at various argon-oxygen coolant gas compositions were then overlaid for comparison. Individual time profiles could also be integrated for precision comparison.

Individual temporal profiles at various argon-oxygen coolant compositions for the elements In, Cd, Zn, Mn, and Ni are given in Figures 28 through 30 (experimental parameters were as in Figure 27). These elements fall into three groups according to their temporal behaviors. The elements In, Cd, and Zn display very similar time behavior. Their emission signals rise rapidly to relatively high peak intensities and then quickly return to the baseline within a few seconds. Nickel, on the other hand, displays a protracted time behavior with relatively low peak intensity. Significant nickel emission intensity remains 30 s after insertion of the graphite sample cup into the plasma. The element manganese

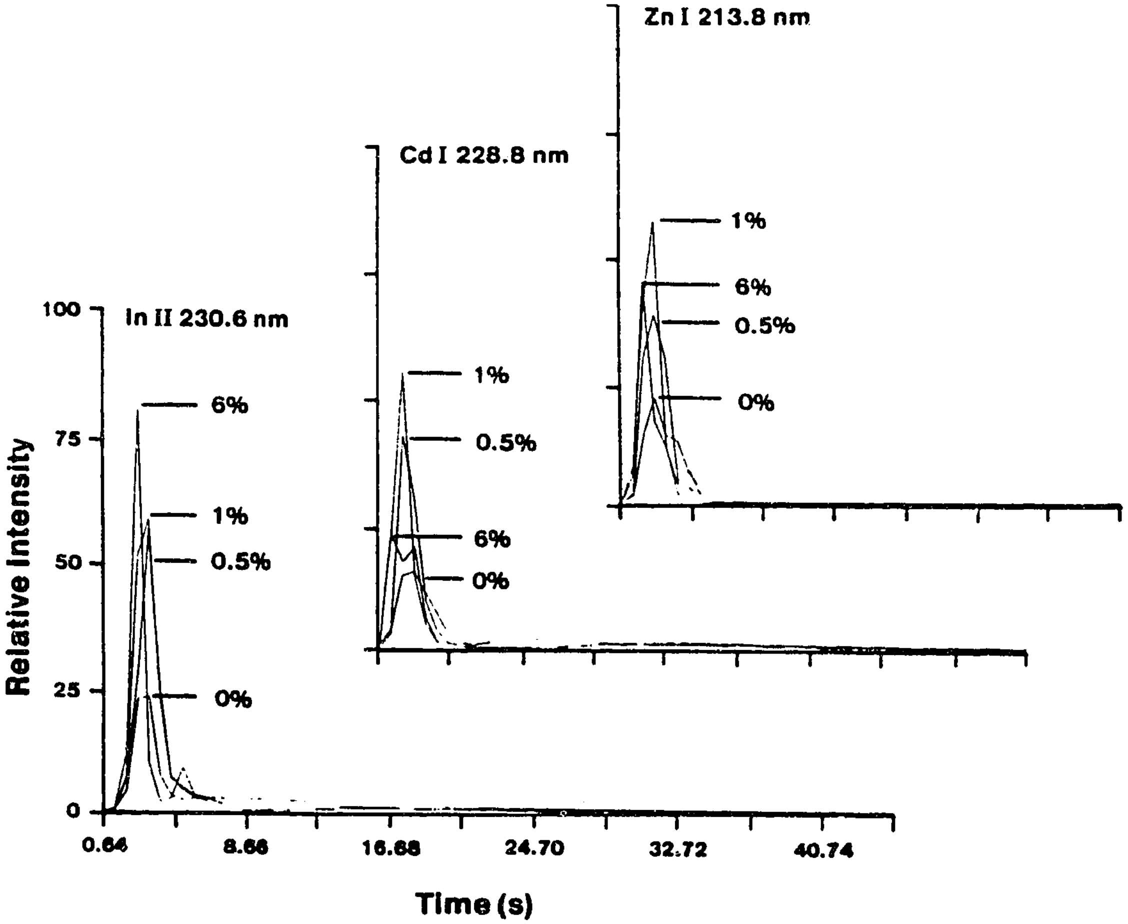

Figure 28. Temporal profiles for In II 230.6 nm, Cd I 228.8 nm, and Zn I 213.8 nm emission with graphite sample cup in Ar and Ar/O_2 mixed gas plasmas (% indicates level of O_2 added to Ar coolant).

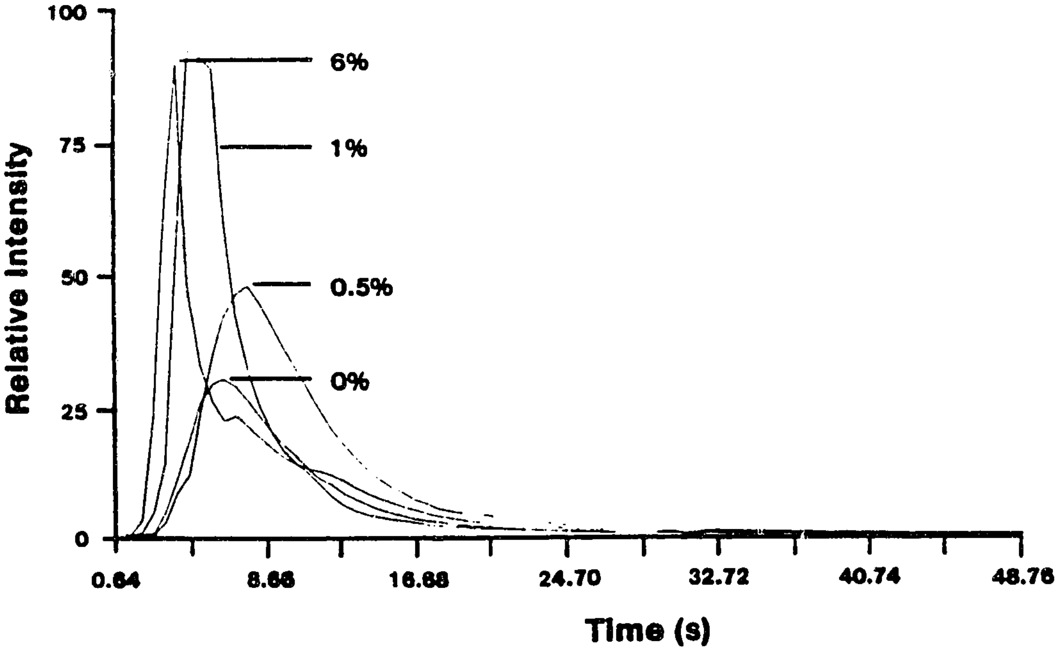

Figure 29. Temporal profiles for Mn II 257.6 nm emission with graphite sample cup in Ar and Ar/O_2 mixed gas plasmas (% indicates level of O_2 added to Ar coolant).

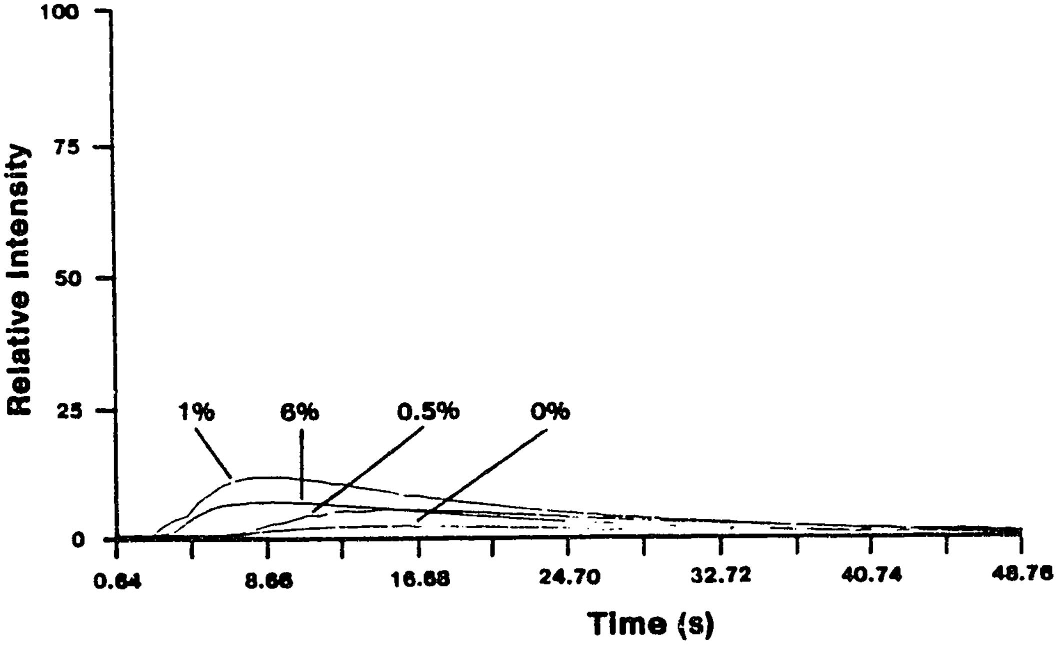

Figure 30. Temporal profiles for Ni II 221.6 nm emission with graphite sample cup in Ar and Ar/O_2 mixed gas plasmas (% indicates level of O_2 added to Ar coolant).

gives emission intensity profiles of intermediate character. Intensity values rise rapidly as in the In, Cd, Zn group, but they decline toward the baseline at a slower rate as in the case of nickel.

Some rationale for the particular grouping of these temporal profiles is suggested by the melting and boiling points of the individual elements. Nickel would be expected to volatilize at the slowest rate as it has both the highest melting point (1453°C) and highest boiling point (2732°C).

The element manganese would be expected to volatilize at an intermediate rate since it has boiling and melting points of intermediate magnitudes (1244°C and 1962°C, respectively).

Of the elements studied, Zn, Cd, and In have the lowest melting points (419.58°C, 320.9°C and 156.61°C, respectively) and Zn and Cd have the lowest boiling points (907°C and 765°C, respectively). Indium, however, has a relatively high boiling point (2080°C). The elements zinc and cadmium would therefore be expected to volatilize at the highest rates.

The relationship between time behavior and melting and boiling points doesn't provide a complete explanation in the case of indium, but based just on this element's boiling point, one would expect it to behave more like manganese which has a boiling point of similar magnitude.

Peak emission intensities for all the elements but indium followed the same trend in behavior relating to percent oxygen composition. Peak intensity climbed from a minimum of zero percent oxygen in the plasma coolant gas to a maximum intensity with one percent oxygen. Peak intensity then declined when the oxygen composition was increased to six percent in all cases but indium. The peak emission intensity for indium increased further with six percent oxygen.

Another general trend in the temporal behavior of emission intensities is evident in Figures 28 to 30. The maximum emission intensity for all elements but nickel is reached sooner with six percent oxygen added to the coolant. Intensity maxima occur at about the same time for six percent and one percent oxygen in the case of nickel. Intensity values also return to baseline levels most rapidly with 6% O_2.

It can therefore be concluded that, in general, the maximum concentration of oxygen in the coolant gas provides the most rapid analyte volatilization whereas an argon-1% oxygen composition gives the highest peak emission intensities. It was then of interest to discover which gas compositions resulted in the best intensity measurement precision.

The precision of analyte volatilization was estimated from integrated analyte emission intensity values. Software was written to permit the selection of an individual emission line in any spectrum within a time series of spectra. Once the peak of an emission line was identified, any number of points on either side of the peak value could be selected for inclusion in a summation. Off-line values could also be selected for subtraction. This group of points representing the emission line was then automatically summed with corresponding points throughout any group of spectra selected from a given time series.

Integration of the same emission line in alternate time series (temporal profiles) was then conducted. Finally, relative standard deviations (RSDs) were calculated from the totals.

Relative standard deviations calculated in this manner indicated that no improvement in precision was obtained for the elements Zn, Cd, and Ni as the percentage of oxygen in the plasma coolant gas was increased. In fact, precision deteriorated in all cases but manganese where only slight improvement was noted. Relative standard deviation data for three exemplary replicates is given in Table VI.3.

As a check on the operation of the direct insertion system to this point, an intensity calibration was run for

TABLE VI.3

PERCENT OXYGEN VS. PRECISION

Desolvated 10 µl solutions of 20 ppm Mn, Cd, Zn; 200 ppm Ni.

RELATIVE INTENSITY %RSD

	Line(nm)			
$\%O_2$	Zn(I)213.8	Cd(I)228.8	Ni(II)221.6	Mn(II)257.6
0	9.6	10.5	23.7	11.4
1	19.4	19.3	19.4	9.6
6	20.4	37.4	50.0	8.5

RELATIVE INTENSITY/Cd(I) RELATIVE INTENSITY % RSD

	Line(nm)		
$\%O_2$	Zn(I)213.8	Ni(II)221.6	Mn(II)257.6
0	1.3	24	1.1
1	1.3	5.0	11.9
6	15.6	11.7	34.3

zinc concentrations equivalent to an absolute mass range of 100 ng to 2000 ng zinc. As per the findings discussed in section B.1 above, three 10 µl aliquot replicates of each zinc solution were used and five spectral points were summed across each sample's zinc emission line (Zn I 213.8 nm). The samples were inserted (after drying) into a 2 kW argon-1% oxygen plasma and the PDA-PMT spectrometer slit width was 30 µm. The resulting log-log calibration of five averaged zinc masses against their averaged relative emission intensities had a slope of 0.62, an intensity axis intercept of 1.9, and a correlation coefficient of 0.96.

3. The Effect of Internal Standards and Sample Cup Age on Precision

At this point it was decided to try and improve precision by utilizing an internal standard. In addition to the elements listed in Table VI.3, the element tellurium was tried as an internal standard at a concentration of 1000 ppm. This element was chosen because it was known to exhibit temporal behavior similar to that of the elements cadmium and zinc in the dc arc (260). In addition, the NBS SRMs utilized in the solid sample studies described in Chapter VII did not contain tellurium.

Among these elements, cadmium gave the best improvement in precision. Unfortunately, tellurium gave no improvement. The improvements in precision obtained by taking the ratio of integrated emission line intensities and the integrated intensity of Cd I 228.8 nm emission are given in Table VI.3.

At this point in the direct insertion studies, the sub-plasma sample preparation device (positioner) described in Chapter V.E was ready for use and sample solutions were dried with it instead of by inductive heating in the ICP's load coils. In an initial check of the performance of the positioner, a 10 µl aliquot of a 480 ppm manganese solution was observed to dry completely within forty seconds in a position 1.5 cm under a 1.5 kW argon-oxygen plasma. No manganese emission was observed (the triplet at about 257 nm was watched) during the drying process.

The sample positioner was then used to study the relationship between sample cup age (number of uses) and analysis precision. The percent relative standard deviation of the cadmium II 214.4 line intensity was observed to significantly worsen with sample cup usage. An RSD of 2.9% was obtained for 15 µl of 50 ppm cadmium in a fresh sample cup using a 1.5 kW argon-one percent oxygen plasma and a 50 µm PDA-PMT slit width. By the third use of the same cup the

RSD had increased to 7.1%, and by the fifth use it had reached 20.2%.

4. Alternate Sample Cup and Plasma Coolant Gas Compositions

Although the deterioration of analysis precision with repeated use of the graphite sample cups could be avoided by using fresh cups in each analysis, it might not always be convenient to employ cadmium as an internal standard as a means to increase precision with the fresh cups. Therefore, alternate sample cup materials and plasma coolant gas compositions were investigated in an attempt to improve the precision of analyte volatilization.

Graphite sample cups were treated with boric acid and titanium dioxide in an effort to form boron or titanium carbide (263) on the cup's inner surface. It was hoped that carbide formation would reduce the porosity of the graphite surface and thus enhance analyte volatilization.

The boric acid treatment was carried out by first filling a graphite cup with a 5000 ppm boric acid solution and then drying it under a running plasma. The precision of cadmium analysis wasn't improved when the boron-treated graphite sample cup was used in an argon-one percent oxygen coolant plasma (it was about 5% RSD for treated and untreated graphite cups). In addition, precision degraded rapidly with use of a boron-treated sample cup. By the fifth use, precision for cadmium emission intensity measurements had dropped to about 20% RSD.

A thirteen second spectrum of a boron-treated graphite cup in a 1.5 kW plasma over the 250 nm wavelength region (with fixed-pattern background subtraction) is shown in Figure 31. This spectrum reveals a strong boron emission and the progressive volatilization of boron from the graphite would account for the deterioration in precision.

In an alternative approach, the boron-treated sample cups were used in an argon-1% nitrogen plasma. It was hoped that a less oxidizing plasma environment might improve analysis precision by extending the life of any surface carbide, but no improvements were observed under these conditions.

Treatment with titanium was carried out by first half filling a fresh sample cup with titanium dioxide and then inserting the cup into an argon-nitrogen plasma until the oxide was reduced to metal. The cup was then removed from the plasma and cooled and any metal residue discarded. Cadmium samples consisting of 15 µl of 50 ppm cadmium solution were then added to the cups. After drying, the samples were inserted into the argon-nitrogen plasma for

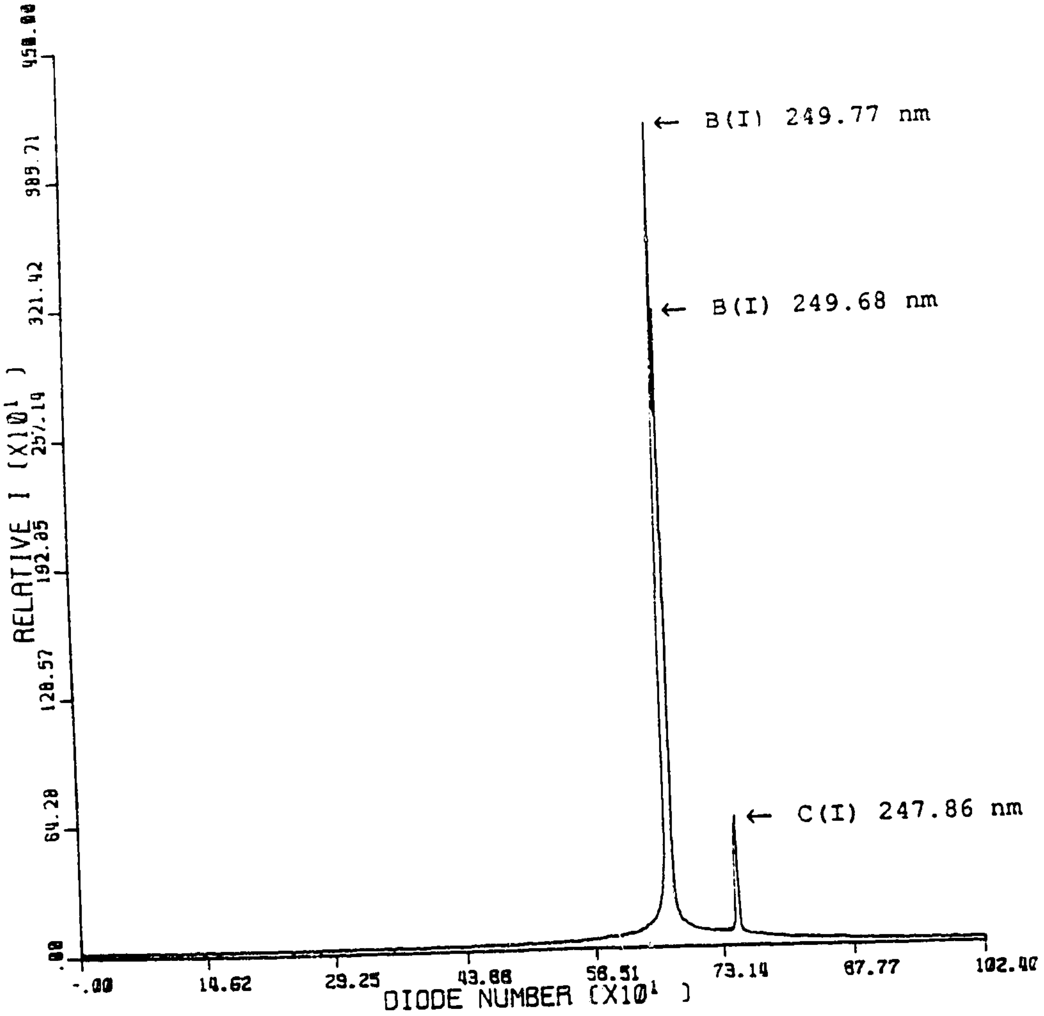

Figure 31. Boron emission from a boron-treated graphite sample cup.

analysis. Unfortunately, the precision of cadmium intensity measurements was severely degraded relative to the precision achieved with untreated cups.

In light of these results, it was suspected that sufficient carbide was not forming on the sample cup's inner surface. In an attempt to provide a less porous surface than graphite, a boron nitride sample cup was machined to the same dimensions as a standard 3/8 inch graphite dc arc electrode.

When inserted in a 1 kW argon plasma, an intense green plume was observed above and surrounding the plasma during the first minute. This green emission became faint and a black film began to form on the upper half of the sample cup during the second minute. Although the sample cup appeared to be in good condition after three minutes in the plasma, a significant weight loss of 13.7 mg was recorded. In addition, the black film was readily dislodged from the sample cup after cooling. The dislodged residue was likely to cause jamming of the pneumatic insertion system. For these reasons boron nitride was abandoned as a cup material

5. Metal Sample Cups in an Argon-Hydrogen Mixed Gas Plasma

As treatment of graphite sample cups with carbide-forming compounds failed to improve analysis precision and as the alternative boron nitride sample cup was rapidly degraded in the plasma, the use of metal sample cups in an argon-hydrogen plasma was now considered. It was reasoned that the analyte would still volatilize from a less porous surface than graphite, but it would also experience a reducing environment. This reducing environment might promote the rapid conversion of analyte cations to lower melting and boiling metallic forms.

Metal furnaces ("micro-tubes") and argon-hydrogen atmospheres have been investigated for use in electrothermal atomic absorption spectroscopy in order to overcome the same problem of poor analysis precision, especially with carbide-forming elements. Suzuki and Ohta and colleagues (264,265) have investigated electrothermal atomization from molybdenum microtubes in argon-hydrogen atmospheres and found, for example, that strontium's absorption signal is compressed and strengthened at an optimal mixture of 300 ml/min argon and 200 ml/min hydrogen. These authors list (265) among the advantages of metal micro tube atomization: relatively low input power, higher heating rate, smaller thermal gradient, no carbide formation, long life, and lower background emission. They have observed that poorer results are obtained when oxide is seen on the microtube and conclude that the hydrogen is preventing oxide film formation.

Similar advantages have been observed by Suzuki and Ohta (266) and by Sychra and coworkers (267) with tungsten microtubes in argon-hydrogen atmospheres.

In the hope that some of these same advantages might apply to the use of metal sample cups in the ICP, cups were machined from the very high melting and boiling elements molybdenum, tantalum, and tungsten (melting and boiling points 2622°C & 4825°C, 2996°C & 5429°C, 3410°C & 5900°C, respectively). Descriptions of the metal sample cups are given in Chapter III. The emission intensity temporal behaviors of the elements Zn, Cd, In, Mn, and Ni were studied with each type of metal cup in an argon-one percent hydrogen coolant plasma. The computer programs developed for studying temporal behaviors in the argon-oxygen mixed gas plasmas were utilized.

A one percent level of hydrogen in the coolant gas gave a plasma similar in appearance to that obtained with one percent oxygen in the coolant. Both plasmas were slightly smaller and much brighter than a one hundred percent argon plasma. The argon-hydrogen plasma appeared to be more robust in terms of sample insertion. Sample cups were more readily inserted into the smaller plasmas obtained with hydrogen levels above one percent than with the corresponding oxygen levels. A one percent level of hydrogen in the coolant gas was chosen for further study as higher levels were considered to pose a safety hazard.

At the time the investigations of metal cups began, the experiments with solid sample introduction described in Chapter VI had proceeded to a point where a higher resolution grating was necessary. The 1200 lines/mm grating in the PDA-PMT spectrometer was replaced with a new 2400 lines/mm grating. Example spectra obtained using each grating are given in Figures 32 and 33 for comparison. A 15 µl aliquot of a solution containing 50 ppm cadmium and 25 ppm zinc was used to obtain these spectra. The data was integrated for nineteen seconds, the PDA-PMT spectrometer's entrance slit was set at 30 µm, and the plasma was run with 1.5 kW of forward power. The higher resolution grating was used in all remaining experiments.

Temporal profiles for the elements Mn, Zn, Cd, In, and Ni volatilizing from graphite, Mo, Ta, and W cups are given in Figures 34 through 38. A 15 µl volume of a multi-element solution containing 20 ppm Mn, Zn, and Cd, 200 ppm Ni and Cr, and 500 ppm In was pipetted into the various cups. The experimental parameters were an argon-1% hydrogen coolant gas, 1.5 kW of forward power and a 25 µm PDA-PMT spectrometer slit width. Thirty wavelength scans of 1.28 s integration period each were collected.

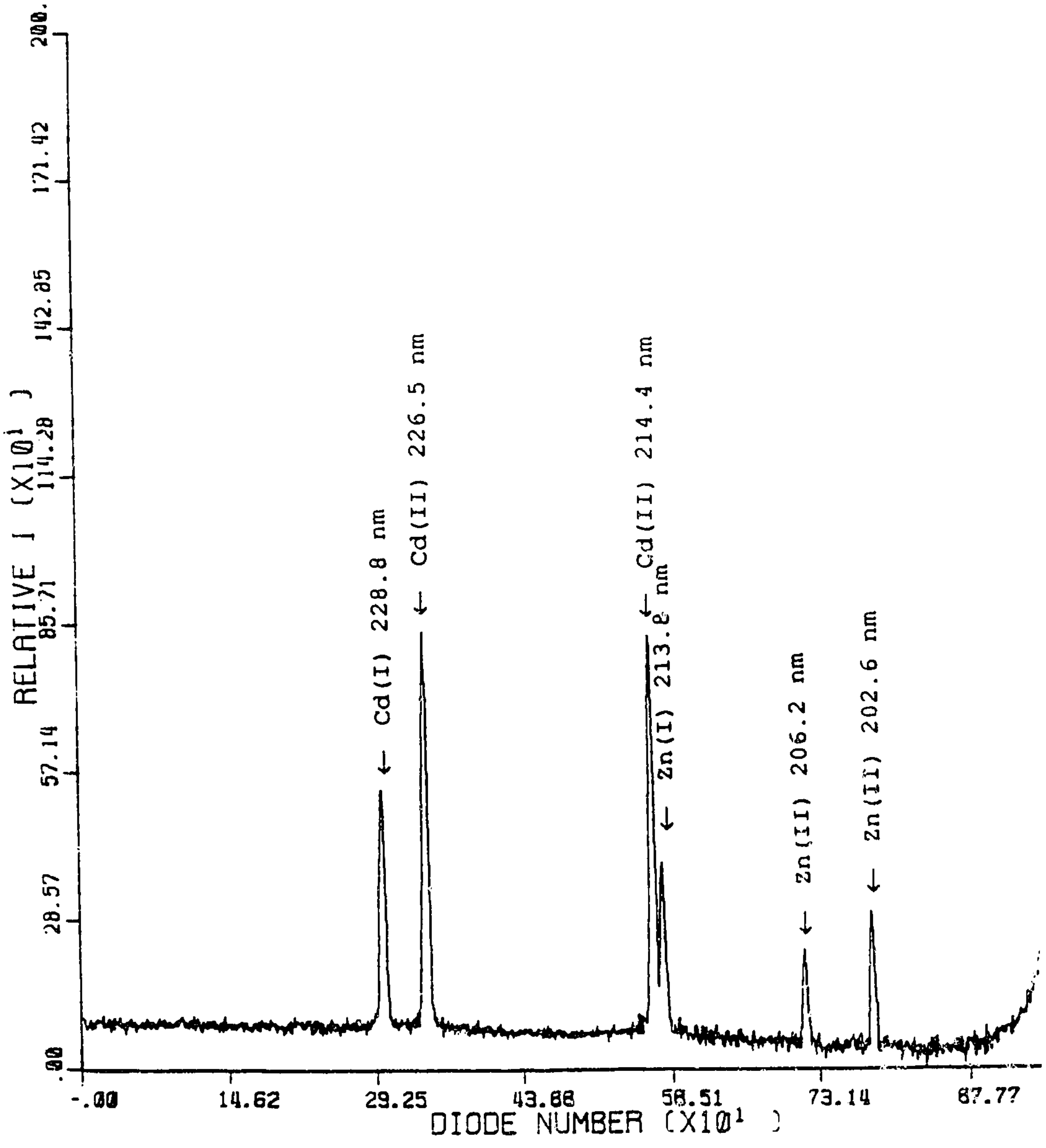

Figure 32. Cadmium and zinc spectrum obtained with a 1200 lines/mm grating. Graphite cup in an Ar-1% O_2 plasma.

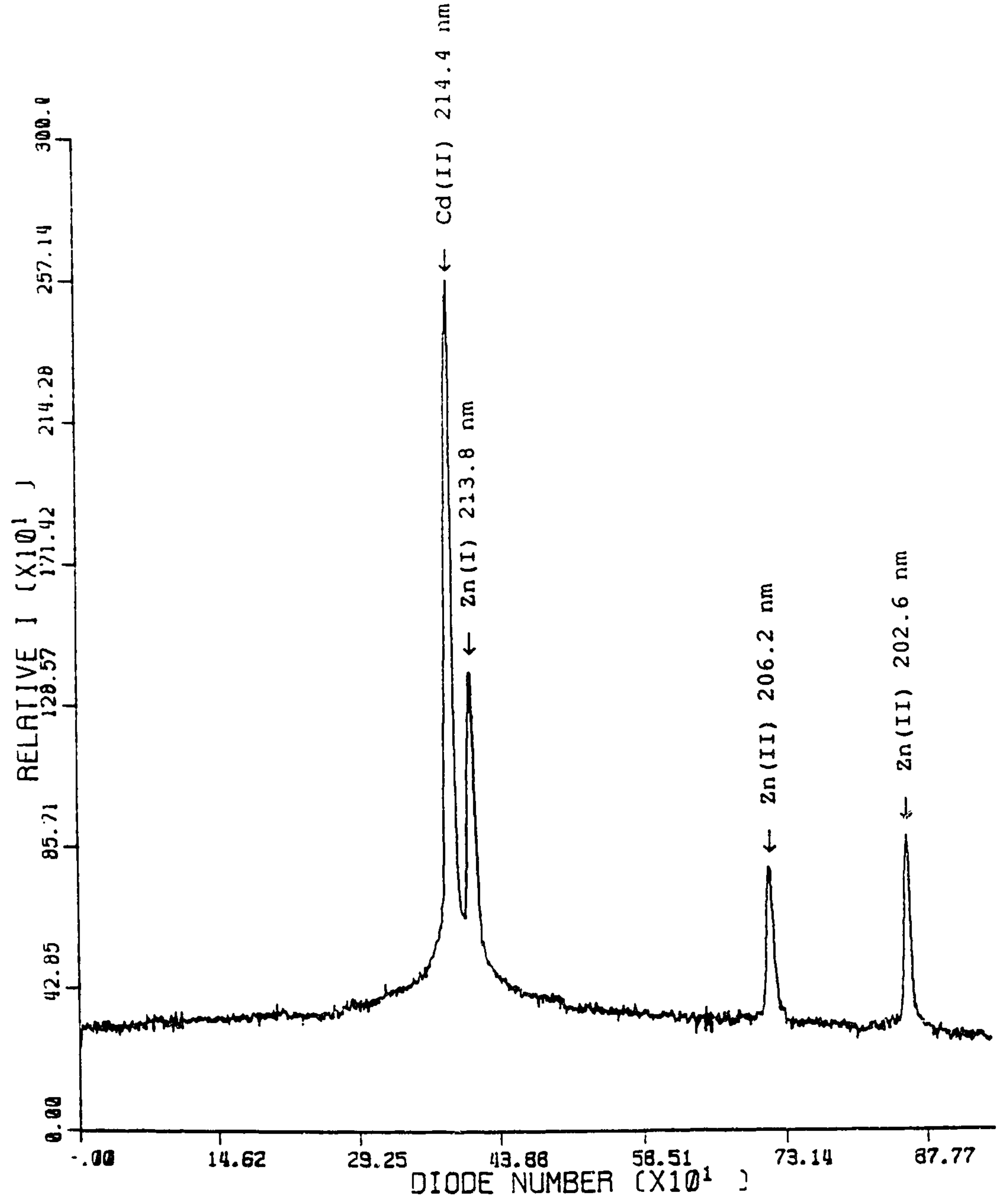

Figure 33. Cadmium and zinc spectrum obtained with a 2400 lines/mm grating. Graphite cup in an Ar-1% O_2 plasma.

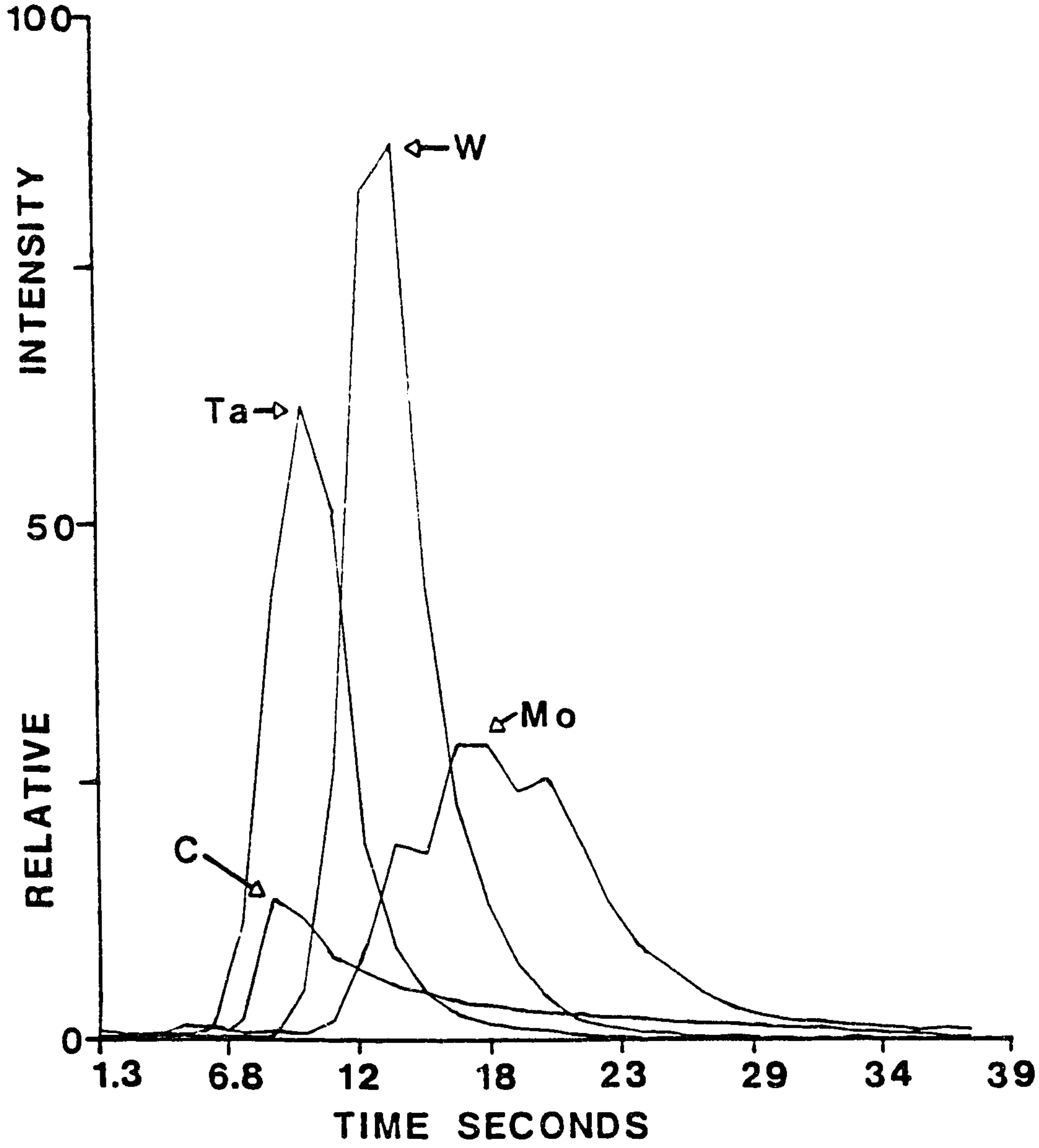

Figure 34. Temporal profiles for Mn II 257 nm emission intensity with graphite (C), Mo, Ta, and W sample cups.

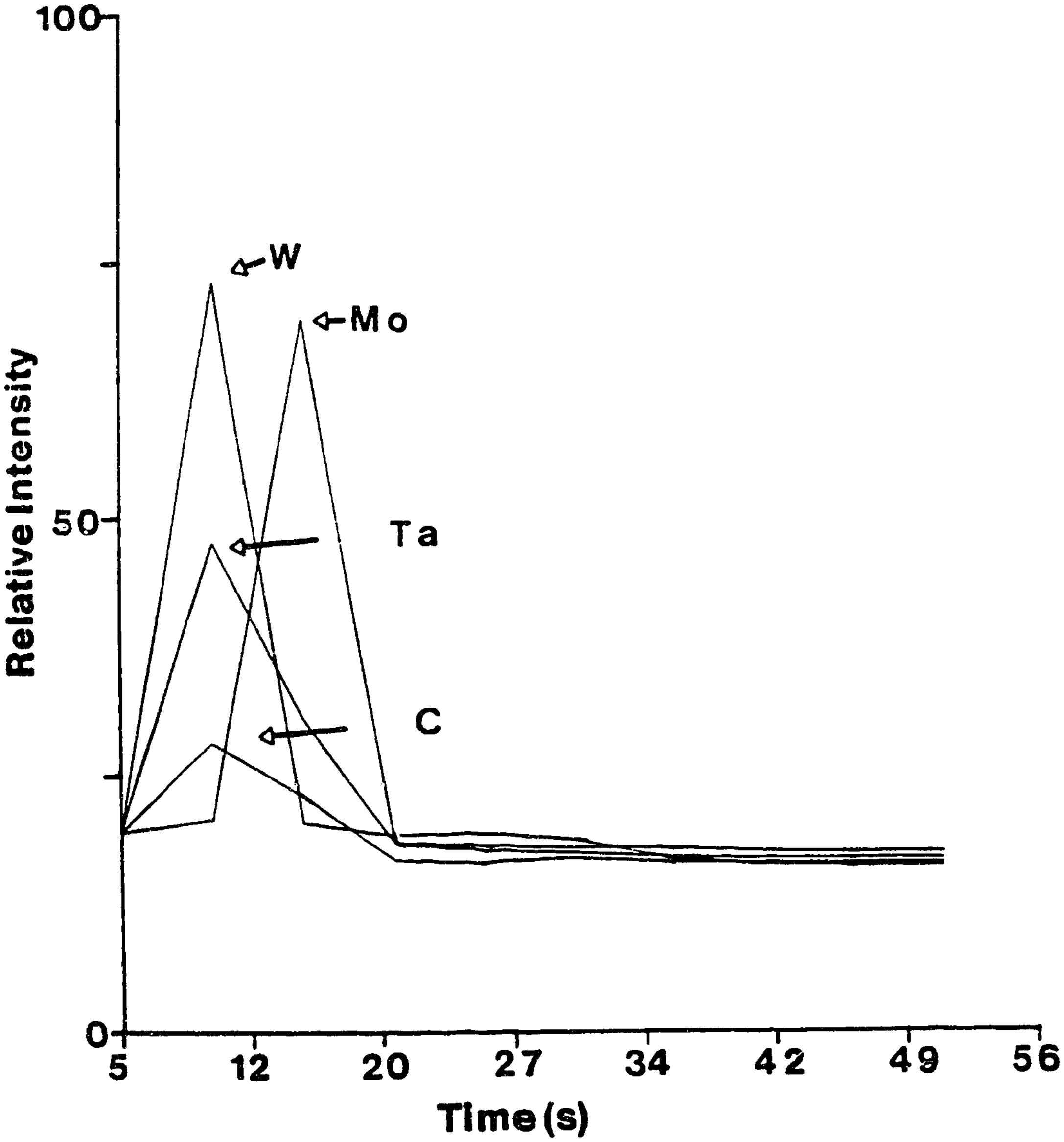

Figure 35. Temporal profiles for Zn I 213.8 nm emission intensity with graphite (C), Mo, Ta, and W sample cups.

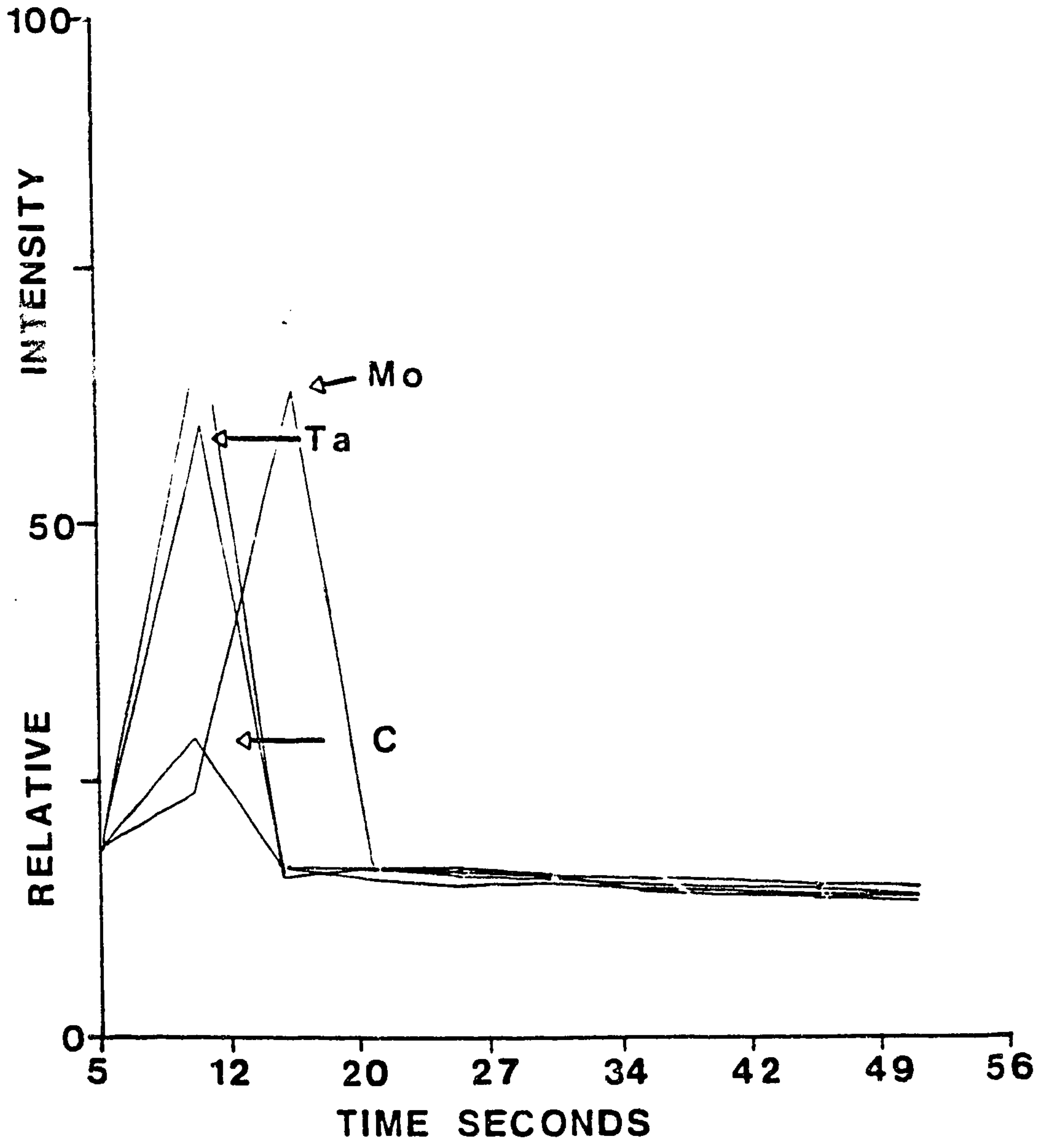

Figure 36. Temporal pr .les for Cd II 214 nm emission intensity with graphite (C), Mo, Ta, and W sample cups.

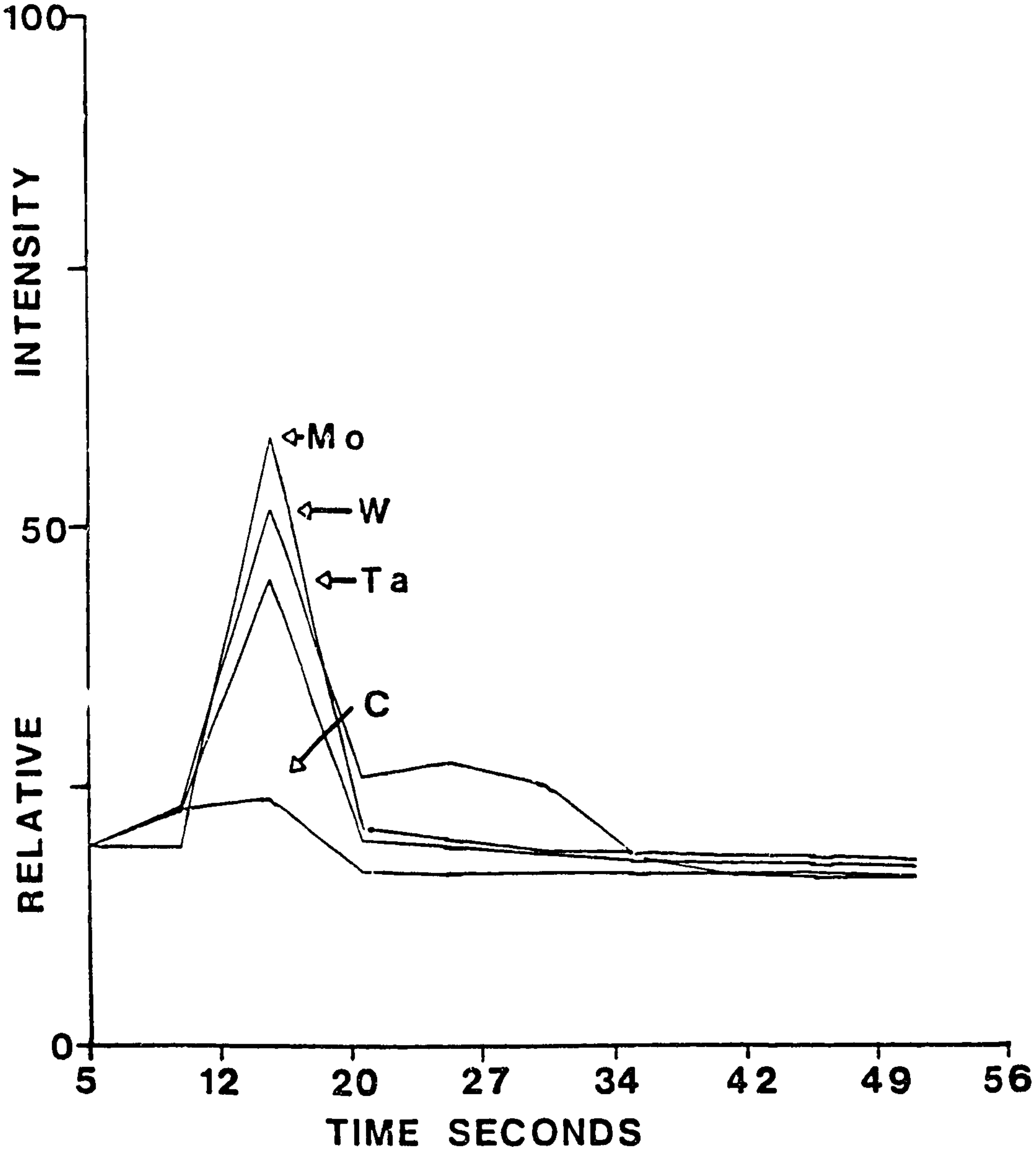

Figure 37. Temporal profiles for In II 230.6 nm emission intensity with graphite (C), Mo, Ta, and W sample cups.

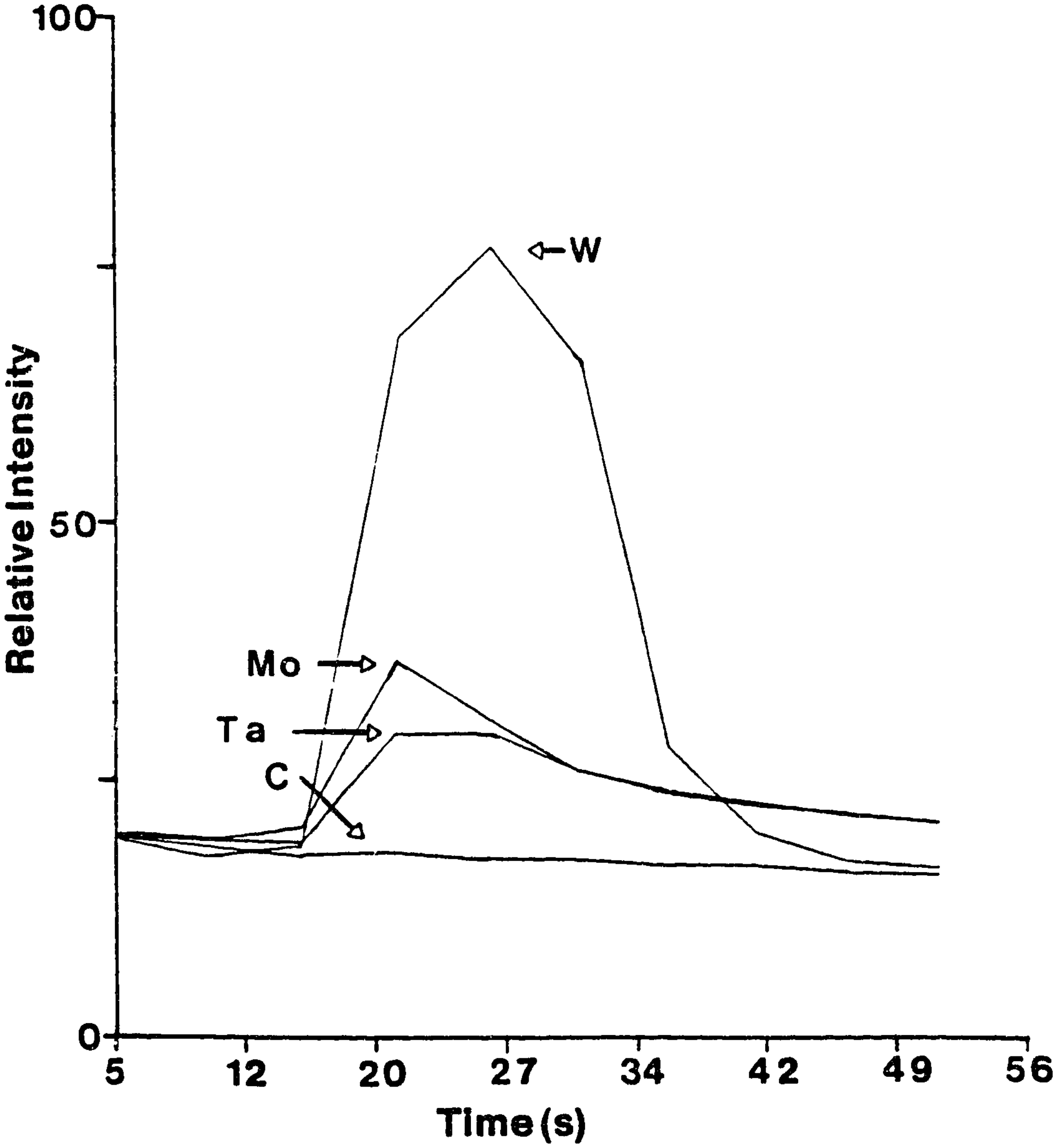

Figure 38. Temporal profiles for Ni II 221.6 nm emission intensity with graphite (C), Mo, Ta, and W sample cups.

All of the metal cups gave greater analyte peak emission intensities than graphite cups. The profiles for Zn and Cd were nearly identical, with the greatest emission intensities and most rapid volatilization obtained with the tungsten cup. The tungsten cup provided the greatest intensity in the case of manganese emission, but volatilization of this element was most rapid from the tantalum cup. The indium profiles were unique in that peak emission intensity occurred from all cups at virtually the same point in time. Peak indium intensity was greatest with the molybdenum cup.

The most striking time behaviors were obtained for nickel emission. Although all metal cups provided greater peak emission intensity than the graphite cup, the tungsten cup provided a large increase in both peak intensity and area. In Figure 39 the temporal emission intensity profile of nickel is compared with temporal profiles for the elements Zn, Cd, and In (Mn was left out for clarity) using the tungsten cup (experimental conditions were as in Figures 34 to 38). Although the peak emission intensity for nickel occurred later than for the other elements, the intensity fell to baseline in less than a minute. This was a significant improvement over the behavior previously obtained with a graphite cup in an argon-oxygen mixed-gas plasma.

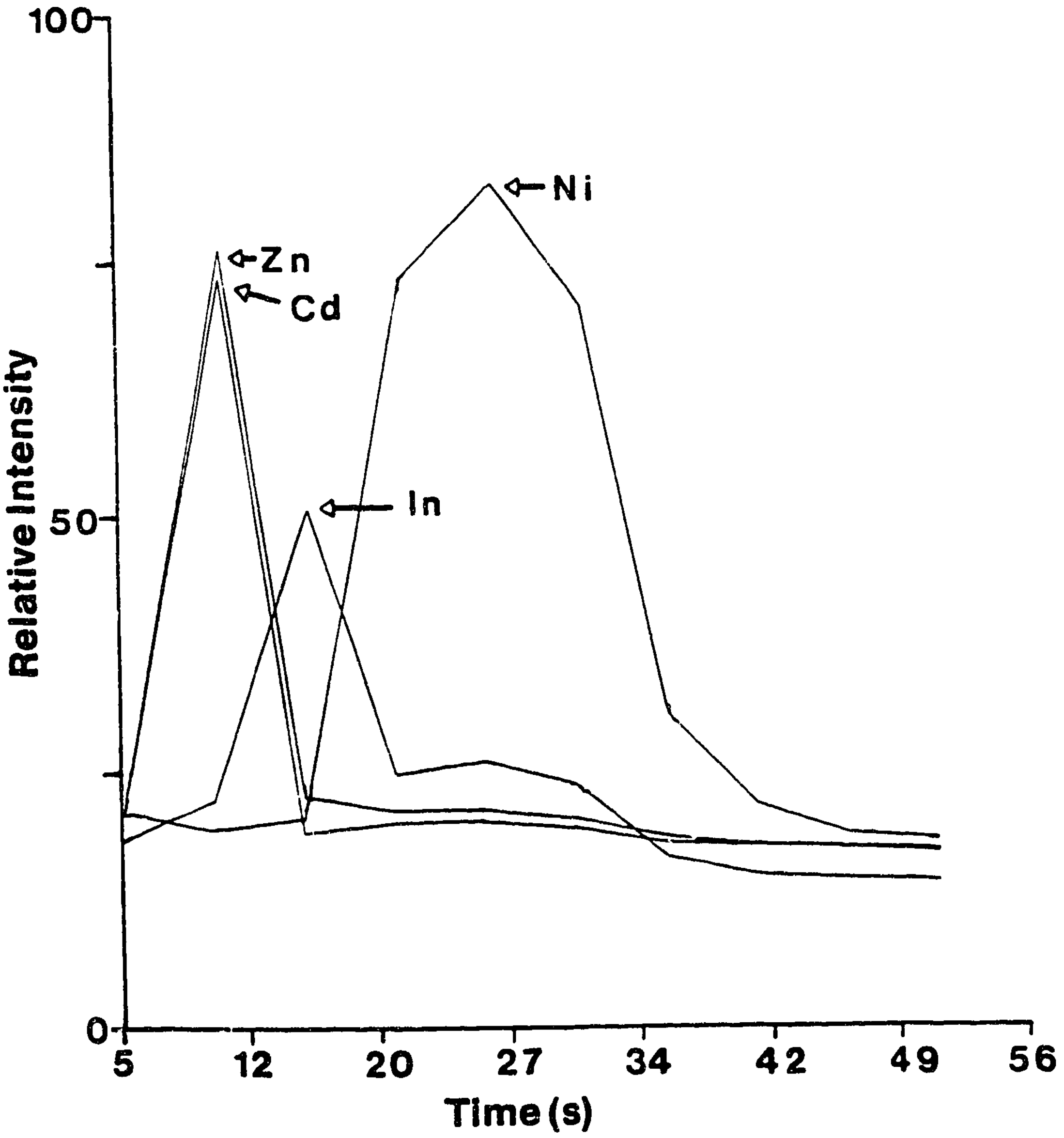

Figure 39. Relative temporal emission profiles of Zn, Cd, In, and Ni with W sample cups.

Precision data was obtained for each of the elements determined with the argon-one percent hydrogen plasma and metal cups as it was for the same group of elements determined with various argon-oxygen plasmas and graphite cups. The data is summarized and compared with previous data in Table VI.4. Tungsten sample cups in an argon-1% hydrogen plasma gave the best precisions for cadmium and nickel. The best precision was obtained for zinc using a molybdenum cup. A tantalum cup gave the best precisions for manganese and indium.

Based on these encouraging results, it was decided to test the detection limit and concentration working range capabilities of tungsten sample cups. The PDA-PMT spectrometer was used in the single-channel mode (see Chapter II for details) and emission intensity data was manually taken from strip chart recordings. The detection limits were calculated using the 2σ criterion, ie.: D.L.=2(peak-to-peak strip chart baseline noise/5) for an absolute sample weight of 10 ng. The 10 ng sample weight was obtained by pipetting a 10 μl aliquot of 1 ppm Zn, Cd, Pb, or Ni solution into a tungsten sample cup. The detection limit results are given in Table VI.5 and a working curve for nickel is shown in Figure 40.

TABLE VI.4

ALIEN GAS AND CUP MATERIAL VS. PRECISION

		% RSD		LINE (nm)		
CUP	COOLANT	Zn	Cd	Ni	Mn	In
		214	228	222	258	231
GRAPHITE	Ar	9.6	10	24	11	
	Ar / 1% O_2	19	19	19	10	
	Ar / 6% O_2	20	37	50	9.0	
GRAPHITE	Ar / 1% H_2	6.6	4.5	18	15	4.1
Mo		.83	3.3	10	5.8	5.0
Ta		9.2	11	40	.15	.90
W		1.8	2.6	4.5	2.5	.97
		300	300	3000	300	7500
				WT ng		

TABLE VI.5

DETECTION LIMITS WITH METAL CUPS

Element LINE (nm)	**Detection Limit (pg)**
Zn I 213.8	18
Cd II 214.4	21
Pb II 220.4	440
Ni II 221.6	900

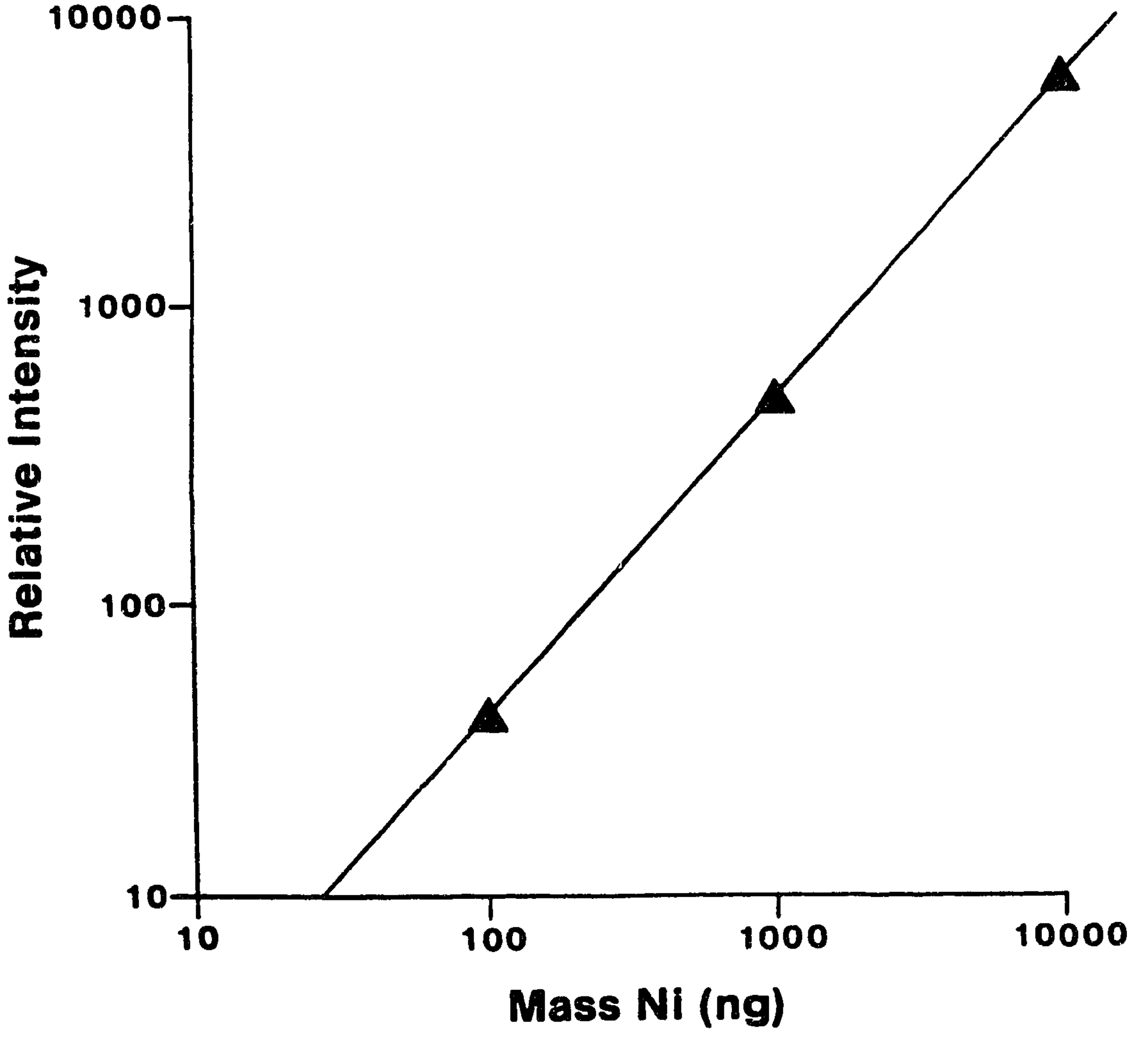

Figure 40. Working curve for nickel with tungsten sample cups.

An example strip chart recording of the emission signal from 1 ng of zinc in a tungsten cup in an argon-1% hydrogen plasma is presented in Figure 41. For this particular experiment the spectrometer slit was set to 50 µm, the amplifier gain was 10^8, and 800 volts was applied to the photomultiplier tube.

There are several interesting features present in this temporal profile. First of all, a significant decline in the baseline was noted to commence upon insertion of the sample cup into the plasma. A drop in baseline intensity upon cup insertion would correspond to an initial loss of plasma energy to cup heating. The maximum cup temperature is probably reached when the baseline intensity has stabilized at a lower average value. This baseline was noted to quickly return to its original average value upon retraction of the sample cup from the plasma.

Secondly, since the entire zinc emission temporal profile occurred during this drop in the baseline intensity and therefore at a temperature lower than the cup's maximum temperature, further improvements in analytical figures of merit might be possible if the rate of sample cup heating could somehow be accelerated. Decreasing the sample cup's mass might provide the answer.

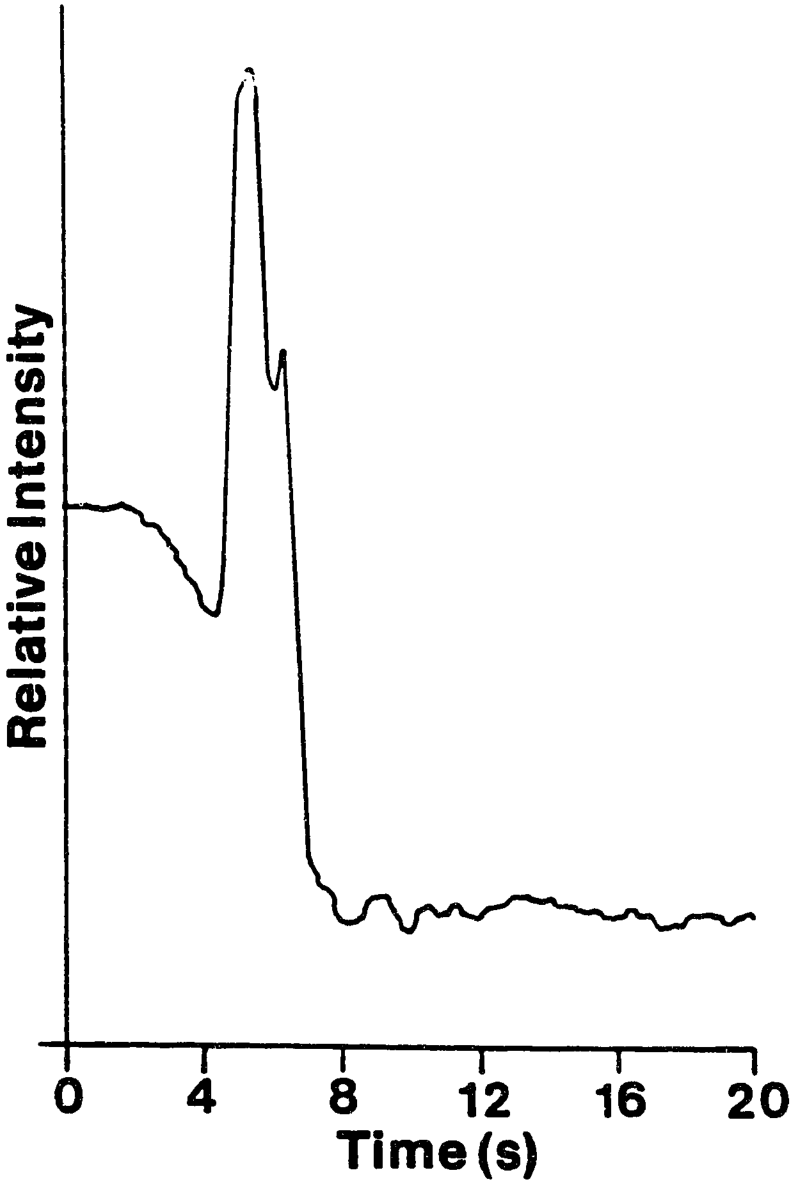

Figure 41. Temporal emission profile for 1 ng of Zn with tungsten sample cup in Ar-1% H_2 plasma.

Finally, a shoulder present on the zinc profile suggests the possibility of two competing mechanisms of analyte vaporization. Perhaps an increase in sample cup heating rate would eliminate the shoulder on zinc's temporal profile.

At this point it appears that the best analytical figures of merit can be achieved by selecting the optimal sample cup material and plasma conditions for individual analytes. These selections can be guided by an examination of the temporal emission profiles of individual analytes.

However, the intriguing possibility exists that one set of "universal" conditions for a wide range of analytes might be achieved once the relationships between sample cup heating rate, sample cup mass, and analyte vaporization mechanism are fully understood. There is great potential for further experimentation.

CHAPTER VII

DIRECT SOLIDS INTRODUCTION WITH THE DSID

A. Introduction

The problems encountered in flame and plasma spectroscopy with the preparation and introduction of "difficult" samples were outlined in Chapter I. The various methods available to convert the more intractable samples into clean liquids were compared in terms of their potential for automation in Chapter V.

As was the case for the introduction of small liquid samples, the answer to the problem of delivering viscous liquids, suspensions, and solids into the ICP will be found by utilizing a new form of discrete sample introduction. The automatic DSID described in Chapter III provides a new and efficient means to both prepare (as described in Chapter V) and deliver the more difficult sample types into the ICP.

The historical perspective of sample introduction into flames and plasmas given in Chapter II dealt only with discrete samples, but some investigators have also modified the traditional concentric or cross-flow nebulizer with its accompanying spray chamber in an attempt to introduce the more difficult samples. These variations of the continuous flow sample introduction theme will be examined for comparison purposes. A summary of these historical advances is given in Table VII.1

1. Nebulization of "Difficult" Samples

The standard concentric or cross-flow nebulizers are prone to clogging by high salt solutions and their uptake rate is influenced by solution viscosity. This latter problem can be overcome by force-feeding the nebulizer with a peristaltic pump (268). Two solutions to the first problem have been developed.

a. Traditional Nebulizers

A pair of accessories designed at Applied Research Laboratories (Dearborn, Michigan) permit nebulization of solutions with up to 10% dissolved organic components or 20% to 30% dissolved inorganic components into an ICP (269). The first accessory is a bubbler which saturates nebulizer carrier argon gas with water vapor to help prevent evaporation of salt solutions at the nebulizer tip. The second is an injector which automatically delivers a plug of water into the carrier argon line between samples. This

TABLE VII.1

ADVANCES IN CONTINUOUS FLOW SOLID INTRODUCTION FOR FLAMES AND PLASMAS

Technique	Source	Matrix/ sample size (sample/hr)	Element	%RSD/ Level (D.L.)	Yr./ Ref.
slurry atomization	flame	tomato, blood	Ca, Cu, Fe, Zn		'77/ 271
slurry atomization	flame	fresh beef liver and steak (12)	Cu, Mn, Zn		'81/ 272
slurry atomization	ICP	high salt solutions			'78/ 273
spark discharge	air/ acetylene flame	iron rod	Cr, Mn	0.2-2pph	'51/ 277
dc arc aerosol generator	capillary arc plasma	low alloy, stainless and tool steels	Cr, Cu, Mn, Mo, Si	0.02-25 pph	'71/ 278
		low alloy & stainless	Ni		
		low alloy steels	Al, C, P, S		
dc arc aerosol generator	N_2O_2/ acetylene flame	steel	Cr, Mn, Ni		'71/ 279

Continued...

TABLE VII.1 (Continued)

Technique	Source	Matrix/ sample size (sample/hr)	Element	%RSD/ Level (D.L.)	Yr./ Ref.
spark aerosol generator	air/C_2H_2 flame	Al alloys	Cu	(0.1pph)	'76/ 280
	ICP	Al alloys	Cu	(0.3ppt)	
		Al alloys	Mg	(0.2ppt)	
			Zn	(15ppt)	
		brass	Fe	0.025-0.23pph	
spark	ICP	powdered rock/1g	Cu	30/2ppm 15/45ppm	'78/ 282
direct slurry introduction	H_2/ or C_2H_2/O_2 flame	ground soil suspended in glycerol	Al	15-20	'62/ 283
			Fe	12	
			K, Na	1	
			Mn, Sr	5	
			Rb	10	
direct powder introduction (swirl cup)	natural gas/O_2 flame	powdered quartz	Ba, Ca, K	(1mg)	'68/ 284
			Na, Li	(0.1mg)	
direct powder introduction (swirl cup)		powdered quartz	Al, Ca, Fe, Mg, Ti	Qual. photo-plate/ 10ppm	'70/ 291
direct powder introduction (fluidized bed)	ICP	magnesium oxide (66 µm)/3.5g	Be	6.5/10ppm (0.1ppm)	'71/ 292
			B	10/10ppm (2.5ppm)	

washes out any material which may collect in the nebulizer tip during the analysis.

b. Babington Nebulizers

The second answer to the nebulization of "difficult samples" problem was developed in the early 1970s by a former NASA engineer, R.S. Babington (270). He hit on the idea of letting the solution to be nebulized flow *over* the nebulizer orifice instead of through it. Gas was injected into a glass sphere and emerged from a slot in the sphere to directly atomize into 1 to 50 μm diameter drops a liquid film on the sphere's surface. Therefore, any liquid which could be poured over the sphere and wet its surface could be atomized.

Fuel and lubricating oils, paint, and even slurries of soups and teas were successfully nebulized by Babington. He also developed shrouds and impact beads for his nebulizer to eliminate large droplets. In this fashion, fogs with constituent particle diameters of less than 10 μm were produced and proved valuable in applications such as medical inhalation therapy.

Recognizing the potential of Babington's system to handle samples which would normally clog standard nebulizers, Fry and Denton (271) applied the new nebulization principle to atomic spectroscopy in 1977. Using a miniaturized version of the Babington nebulizer, they aspirated samples with up to 50% suspended solids and with particle sizes up to 1 mm into a flame atomic absorption spectrometer. Slurries and suspensions of raw samples including tomato sauce and whole blood were successfully analyzed for Zn, Cu, Fe, Ca, and other elements.

In a more recent extension of this work, Mohamed and Fry (272) determined Cu, Zn, and Mn in fresh beef liver and steak by flame AAS. Normally, tissue samples of this type could not be handled even by a Babington nebulizer as the larger particles would settle out in the spray chamber and therefore bias the analysis. The authors employed a high speed homogenizer to reduce tissue sample to micron size range particle slurries before pumping into a modified Babington nebulizer. The authors obtained analytical results from raw samples within five minutes, with their so called "slurry atomization" procedure.

A modified Babington nebulizer operating at an argon flow rate suitable for interfacing to an ICP (1 l/min vs about 10 l/min for Fry and Denton's flame nebulizer) was designed by Suddendorf and Boyer in 1978 (273). The precisions and detection limits for the determinations of elements in high salt solutions compared favorably with results obtained with crossflow nebulizer systems.

c. Disadvantages of Nebulization

A problem not adequately handled even by Babington nebulizers which can arise in slurry nebulization is the nonrepresentative transport of particles into the emission source. As mentioned above in relation to animal tissue samples, dense particles with compositions differing from light particles may settle out before reaching the source. As elucidated by Eisentraut and coworkers (274), this problem is particularly severe in the nebulization of lubricating oils containing suspended wear metals. Large fractions of the metallic particles collect on the nebulizer spray chamber walls and end up going down the drain instead of into the source. Although dissolution of the particles with hydrofluoric acid prior to nebulization can overcome this problem (275), the point of slurry atomization is of course to avoid such pretreatments. As Eisentraut has stated: "The need still exists, however, for a totally efficient system that is free from torturous paths and other impediments which restrict the quantitative analysis of samples containing suspended metal particles" (246).

2. Direct Solids Nebulization

One approach to a more efficient system for the introduction of sprays, mists, or aerosols* containing solid particles avoids the nebulizer and spray chamber altogether. Like the direct liquid injection method mentioned previously, particle dispersions are introduced directly into the atomic source. A variety of means have been employed to generate and deliver the particle dispersion.

a. Conducting Samples

i. Arc and Spark Discharges

One of the earliest reports of direct solids nebulization was given by Hemsalech and Dewatterville in 1907

---

*Sprays, mists, and aerosols can be defined as being comprised of particles with diameters greater than 25 µm, betwe[illegible] and 10 µm, and below 10 µm, respectively (270). Generally, if the particles are originally dispersed in some supporting medium, the term slurry nebulization is used. If not, the term direct solids nebulization applies.

(276). They constructed a device for the direct introduction of metal particulates into a flame. The electrodes of a spark discharge enclosed in a chamber were constituted from the metal of interest. A spectrum of the sparked metal could be obtained after routing the sputtered particles through four meters of tubing to a burner.

Monvoisin and Mavrodineanu (277) improved on this early design by incorporating the spark discharge directly in the base of a specially designed air/acetylene burner. By using rods of iron alloy as spark electrodes they could deliver 10-35 µm particles directly into the base of the flame via the air supply. Quantitative results were reported for manganese and chromium in the alloy but concentration ranges spanned only 0.2% to 0.5% and 0.4% to 2%, respectively. Matrix iron lines were chosen for internal standardization and detection was by photoplate.

Two decades after Monvosin and Mavrodineanu's work, Jones, Dahlquist, and Hoyt (278) at Applied Research Laboratories developed an improved metal sampler capable of producing particles with diameters in the µm range. Their "aerosol generator" consisted of a cylindrical silver anode mounted inside a flat boron nitride insulator. The insulator sealed against the metal sample which in turn acted as the cathode of an dc arc struck between it and the silver anode.

Material removed by the arc flowed on an argon carrier gas stream through the center of the anode and "...into any desired excitation device." In this case, the authors routed metal aerosols into their "capillary arc plasma" and successfully determined Cu, Mo, Cr, Mn, and Si in low alloy, stainless, and tool steels, nickel in low alloy and stainless steels, and C, S, P, and Al in low alloy steels by emission spectroscopy. Concentrations ranged down to about 0.02% for aluminum and the non-metals and up to about 25% for nickel and chromium.

In this same year (1971), Winge, Fassel, and Kniseley (279) routed aerosol from a similar generator (supplied by ARL) into an air/acetylene flame and determined Mn, Cr, and Ni in steel by atomic emission. Since the aerosol generator and source could be separated by eight feet of tubing without degrading performance, the authors suggested the technique might have potential for remote sampling applications.

In 1976, Human et al. (280) reported on the development of a metal aerosol generator like the one just described but based on a spark discharge. The metal sample again acted as cathode and a thorium-treated tungsten rod functioned as the anode. The spark chamber was connected to a nitrous oxide or air/acetylene burner for atomic absorption measurements, and to a hydrogen-oxygen-argon burner for atomic fluorescence analysis, or to an ICP for emission analysis. The detection limit for copper in aluminum alloys was 0.1% by air/acetylene flame atomic absorption or fluorescence and 0.0003% by ICP emission. ICP emission gave detection limits of 0.0002% and 0.015% for magnesium and zinc, respectively, in these alloys. Iron determined in brass with ICP excitation gave a linear calibration from about 0.025% to 0.23%. The authors suggested that non-conducting samples might be analyzed in a similar fashion by mixing them with a powdered metal such as copper.

ii. Toward Separate Optimization of Sampling and Excitation

The various aerosol generators described above were developed in an effort to avoid some of the limitations of traditional metals analysis. In particular, Monvoisin and Mavrodineanu (277) wanted to avoid tedious sample dissolution and Human et al. (280) were interested in eliminating the extensive grinding required for other powder-feed devices. The ARL people (278) and Fassel et al. (279) were particularly concerned with avoiding some of the limitations of traditional arc and spark emission spectrographic analysis of metals. Fassel and coworkers (279) pointed out that the conventional point-to-plane, rod electrode, and similar discharge techniques "...suffered from one or more of the problems of poor sensitivity, poor precision, and selective sampling of the sample surface by the electrical discharge. Also, *the electrical discharge parameters which gave the best excitation conditions often did not provide optimum conditions for sampling of the metal*" (italics added). The rationale for development of the aerosol generator was therefore, in the words of Jones et al. (278), "Separation of the vaporization or sampling step from the excitation step (to) provide the possibility of arranging the excitation discharge so as to minimize various effects such as self-absorption and matrix effects, and separately to optimize the sampling step."

Applications of this concept of separate vaporization or sampling and excitation are becoming more common. Before giving further illustrations, however, some relevant terms should be clarified. Vaporization refers to the transformation of dry solid sample (eg. salt particles) to the vapor phase with the input of energy. If sufficient energy is available, the molecular species present in the vapor phase will equilibrate with ionic species and neutral atoms. This latter transformation is referred to as atomization. If an atomic absorption or fluorescence experiment is being conducted, optimization of this production of neutral atoms would be desired. Further energy input to promote neutral atoms to various excited states would be necessary for an atomic emission experiment. This final step is referred to as excitation.

Unfortunately, the divisions between these various steps aren't so clear-cut in real analytical systems. For example, the metal samplers outlined above produce not only metal vapor but fine particles (by sputtering or nebulization) during the sampling step. The spectroscopic source would therefore be responsible for some vaporization as well as atomization and excitation. It is also possible that a separate sampling device such as a graphite furnace would produce free atoms as well as molecular vapor and that both would be delivered to the spectroscopic source.

For the sake of convenience, the more general terms separate sampling and excitation will be used. Sampling may therefore involve any or all of the nebulization (sputtering), vaporization, and atomization processes.

Separate optimization of sampling and excitation is possible with a commercial instrument available from Jarrell-Ash. Their model 975 ICP Atom-Comp spectrometer can be outfitted with a Separate Sampling and Excitation Analysis System (SSEAS) capable of routing metal aerosol directly into an ICP discharge for emission analysis. Marks et al. (281)

have used this system for the direct analysis of nickel-base super alloys. Since these alloys often contain Ta, W, and Nb, hydrofluoric acid digestion is required but can result in the loss of boron and silicon as volatile fluorides. The spark-to-ICP method therefore avoids digestion and in addition obviates the need for alloy standards, the expense of which is difficult to justify in an industrial research and development setting.

b. Non-Conducting Samples

i. Spark Discharges

A spark discharge has also been employed as an aid in introducing powdered non-conducting samples into an ICP. Scott (282) used a spark discharge between graphite electrodes to elutriate particles from one gram samples of -200 mesh powdered rock samples placed below the spark. The particles were swept into an ICP by argon carrier gas. Intensity values for copper in the rock samples had 30% variation at the 2 ppm level and 15% variation at the 45 ppm level.

b. Direct Powder and Slurry Introduction

Ground non-conducting samples have also been sprayed directly into atomic sources without the aid of a spark. In 1962, Gilbert (283) sprayed ground soil sample suspended in glycerol into a large bore Beckman hydrogen- or acetylene-oxygen atomizer burner. Emission wavelength scans gave reproducibilities on the order of one percent for soil components like sodium and potassium, five percent for manganese and strontium, twelve percent for iron, fifteen to twenty percent for aluminum, and ten percent for rubidium. Gilbert stated that further efforts were necessary to improve the results for difficult elements like aluminum, to extend the method to trace elements, and to investigate the effects of particle size distributions, interferences, standards, choice of slurry medium and the solubility of elements in the support media.

Some further progress along these lines was initiated by Woods (284) in 1968. Recognizing that quantitative results could only be obtained by exciting all the sample after reliable powder introduction, she designed a swirl cup natural gas-oxygen total consumption burner. However, problems with oxidant pressure regulation and control of powder density, dryness, particle size, quantity, and sticking degraded detection limits. Minimum detectable quantities in powdered quartz matrix were 1 mg for $BaCl_2$, CaF_2, and KCl and 0.1 mg for NaCl and LiF.

A different approach to powder spraying was taken by Caudert and Vergnaud (285) in 1970. These authors diluted the powdered catalysts palladium-on-carbon, alumina and molecular sieve with 100-fold of calcium carbonate and delivered the mixtures from a hopper into the base of an air/acetylene flame with a spiral conveyor. Atomic absorption analysis gave reduced sensitivities compared to liquid nebulization and matrix matching was required.

It has also been difficult to obtain quantitative results with direct nebulization of powders into the ICP source. Fassel (286) has remarked that although such methods "...have been used successfully for the analysis of several types of powdered samples, particle size and density discrimination effects and aggregation of fine particles may limit the scope of application of this approach."

In 1961, Reed (287) described an inductively coupled plasma torch with a central gravity powder feed used for growing crystals and in 1962 (288) he suggested using such a torch for spectroscopic analysis of solids. In 1964 Greenfield et al. (289) made some preliminary qualitative spectroscopic observations of powdered solids and slurries injected into a modified Reed torch.

Hoare and Mostyn (290) delivered lithium salt and alumina powders into an ICP with a "powder injector assembly." This assembly consisted of a vibrating cup into which argon was injected and then routed up through a capillary tube into the ICP torch. The powdered sample in the cup was therefore carried on the argon stream into the plasma discharge. As can be imagined, "...a low injection velocity and small particle size are essential for the powder injection system." In fact, the authors observed that "...large particles can be seen to pass through the plasma virtually unchanged."

Although this "Swirl Cup" injection method provided useful qualitative results, quantitation was hampered by the fact that samples and standards needed to be closely matrix-matched.

A similar ICP powder injector was employed by Pforr and Aribot (291), but their results were limited to a qualitative photographic plate analysis of Ca, Mg, Ti, Fe, and Al at about 10 ppm levels in powdered quartz.

A fluidized bed chamber was investigated by Dagnall et al. (292) as an alternative to the swirl cup for injection of powders into the ICP. In this arrangement the sample was placed on a sintered glass disk at the bottom of a pyrex tube. Argon injected from beneath the disk formed a fluidized bed of powder and carried a cloud of particles upward into the plasma. The authors obtained detection limits of 0.1 ppm for beryllium and 2.5 ppm for boron in samples comprised of 66 μm diameter particles of magnesium oxide. Relative standard deviations for 10 ppm levels of the beryllium and boron in 3.5 g samples of the MgO were 6.5% and 10%, respectively.

Although Greenfield had a hand in a large share of the research just cited, he stated in a 1976 review of plasma spectroscopy that "First-hand experience of the problems leads to the impression that the partial success so far gained has been obtained on carefully selected matrices, and that a general, practical solution to the several problems of injecting powders into plasmas and performing quantitative analysis, has yet to be found" (32). That the same situation exists today is reflected in Fassel's use of the second half of this quote to summarize the status of direct powder analysis in 1982 (286).

An interesting development which has potential for reducing dependence on matrix matching in the direct analysis of powders has been reported by Fuller and Thompson (293). They have demonstrated that matrix matching is less important for rock samples if the rock is ground to particles of 4 μm or less diameter and suspended in acrylic copolymer gels. Electrothermal atomization-AAS analysis of samples of 100 ml of gel containing up to one gram of suspended rock powder gave a calibration graph for copper with a slope identical to that generated from aqueous standards. Electrothermal atomization-AAS results for copper at 20 ppm to 300 ppm levels compared well with dissolution-flame-AAS data. The authors suggested that such gel suspensions might be sprayed directly into a flame. Fuller et al. have written a review of slurry atomization (294).

Although Fuller's approach has promise, the problem of sample grinding remains. It would be preferable to avoid this step altogether. This problem, together with the others discussed above in reference to direct powder and slurry nebulization and normal and discrete nebulization of solutions, therefore suggests that continuous flow sample introduction into atomic sources is not the best approach when it is desirable to handle a wide variety of sample types.

B. Oil and Solid Analysis with the DSID

All NBS plant and geological SRMs were dried before weighing according to the directions in the certificates of reference accompanying the standards. Single element and multielement solutions were made up fresh from 1000 ppm stock solutions before each day's experiments. The stock solutions were prepared with the same procedures used in Chapter VI.

The ICP running conditions were as given in Table III.1 unless otherwise noted. The plasma was imaged onto the PDA-PMT's entrance slit in a two-to-one ratio with a 10 cm focal length quartz lens. The spectrometer's general operating conditions were those given in Table IV.1. More specific spectrometer conditions will be noted along with the spectra that follow. Computer programs were written in order to acquire and process data from the PDA-PMT.

1. Preparation and Insertion of Oil Standards

Spectrametrics, Inc. (Andover, MA), was interested in testing the DSID's ability to analyze wear metals in lubricating fluid and therefore provided to us the following standards containing five different iron powder sizes in oil:

<5 µm (A), 5-10 µm (B), 10-20 µm (C), 20-30 µm, and about 80 µm (E). All standards corresponded to 100 ppm of iron.

The company informed us that analysis with a conventional nebulizer-ICP combination failed beginning with sample C. They felt that this was probably due to iron particles settling out before reaching the plasma. Since all iron particle size ranges were important in wear metals analysis and since an alternative oil sample digestion procedure was considered too hazardous, the company was very interested in our direct insertion technique.

a. Laser Ashing

The Spectrametrics oil standards were ashed with the CO_2 laser asher (see Chapter V.D) running at about half power. If the ashing was carried out in air, dense smoke was produced and it was feared that analyte loss might result. Ashing was therefore carried out under an argon atmosphere for the first minute and then for an additional minute in air. No residue was observed in the graphite sample cup after 15 µl aliquots of oil were subjected to this treatment.

b. Oil Analysis by Direct Insertion into the ICP

The 1.5 kW argon-one percent oxygen plasma that was found to be very useful in the analysis of aqueous solutions was used to analyze the Spectrametrics oil samples. Initial experimental conditions were set using 10 µl aliquots of 1000 ppm aqueous iron standard. The average of fifty wavelength scans with the PDA-PMT spectrometer integration period set at 0.64 s was used to monitor iron 238 nm and 259 nm line emission intensity.

Under these conditions, analysis precision for 30 µl of laser desolvated 100 ppm iron solution was 4.1% RSD (three replicates, iron 259 nm line), but the corresponding precision for 30 µl of Spectrametrics standard D was 18%. The precision was degraded to 31% when the oil aliquot was reduced to 10 µl.

As the precision of analysis of standard D didn't improve when the experimental parameters of percent oxygen in the plasma coolant gas, plasma forward power, and number of replicate samples were increased, it was suspected that the poor analysis precision was arising from the sampling step of the analysis. On the suggestion of Dr. B. Kratchovil (Department of Chemistry, University of Alberta), calculations were performed in order to approximate how many iron particles would be expected in each 5 µl increment of the Spectrametrics oil standard D.

It was assumed that the Spectrametrics oil had the same density as vegetable oil, 7.86 g cm^{-1} or 7.86 Kg m^{-3}. If an average standard D particle had a radius of 12.5 * 10^{-6} m then its corresponding volume would be 8.2 * 10^{-15} m^3 and its mass would be 6.4 * 10^{-2} µg. It was further assumed that 1 ml was equal to 1 g of bulk solution so that a 5 µl aliquot of the oil would have a mass of 5 * 10^{-3} g. Knowing that the equivalent iron concentration in the oil was 100 ppm, each 5 µl aliquot of oil would then contain 5 * 10^{-1} µg or **7.8 particles of iron**.

Actual counts of iron particles in aliquots of sample D were performed under a microscope for comparison purposes. The standard was first shaken for thirty minutes with a Spex mixer and then 10 µl aliquots were quickly pipetted onto microscope slides. Iron particles were differentiated from dust, etc. with a magnet held under the microscope slide. The average iron particle count obtained from ten microscope slides was 14.7 with an RSD of 19.4%.

This average count of 25 µm diameter particles was very close to the 15.6 particles calculated for a 10 µl volume of oil. The relative standard deviation of this count emphasizes the fact that the poor precision of the direct insertion ICP analysis is due in large part to poor sampling.

2. Preparation and Insertion of Plant Standards

a. Laser Ashing

For an initial check of the CO_2 laser asher's performance with biological tissue, about 10 mg of dried NBS SRM orchard leaves was pressed into standard 3/8 inch graphite cups for ashing. When the ashing was carried out in air, the sample ignited within a few seconds. The samples were thereafter purged with argon to prevent ignition. Running the laser at about half power and exposing the sample to the laser beam for two minutes in an argon atmosphere followed by one minute of exposure in air appeared to be the best conditions for ashing of the NBS plant standards. With these conditions, plant standards were ashed to a white powder.

b. Sub-Plasma Ashing

Utilizing the temperature gradient inside the torch under the running plasma eliminated the need for the inductive drying of samples before the plasma was ignited and analysis begun. Treatment of samples in this way might also be more economical than CO_2 laser preparation.

An initial check of the sub-plasma asher's (see Chapter V.E) performance was carried out with enough dried NBS SRM orchard leaves packed to fill standard 1/4 inch graphite cups. When these cups were inserted to within about 0.5 cm of a 1.5 kW argon-oxygen plasma, the plant standard was ashed within about one minute. However, unlike the completely white ash resulting from CO_2 laser treatment, this ash contained some blackened solid.

In contrast to the laser ashing procedure, analyte loss could be tracked during the sub-plasma ashing process by looking for analyte emission from the plasma. This fact was used to advantage in quickly determining the best sample ashing position beneath the plasma. No zinc or manganese emission was observed when the orchard leaves were ashed 0.5 cm under the plasma.

c. Analysis by Direct Insertion into the ICP

As in the case of the oil sample analyses, the plant samples were inserted into an argon-one percent oxygen plasma. A comparison of the temporal behavior of zinc II

206.2 nm and cadmium II 226.5 nm elemental emission from laser-ashed and unashed 12 mg samples of NBS SRM 1571 orchard leaves revealed that analyte emission began much sooner from the ashed standard. As Figure 42 shows, not only did the analyte emission begin quickly, it was also significantly more intense for the laser-treated standard. Both the zinc and cadmium emission intensity peaked and then returned to baseline within about three seconds.

The precision of zinc determination in 12 mg samples of laser-ashed orchard leave standards was checked next and found to be 3.1 %RSD using the zinc II 206.2 nm emission line. The plasma was run at 2 kW of forward power and the PDA-PMT spectrometer slit width was 30 μm. Spectral data was collected for sixty seconds and fixed-pattern background was subtracted.

With the exception of laser-ashing, the same conditions were next employed in the determination of zinc in 24 mg samples of the orchard leaves and our remaining NBS standard plant materials 1570 spinach and 1573 tomato leaves. The sub-plasma positioner was used this time to ash the samples.

The positioner was programmed to dry the samples in two stages for 120 s 2 cm below the plasma and then for 15 s 1 cm below the plasma. Ashing was then carried out for 1 s within 0.5 cm of the plasma. No analyte emission was detected from

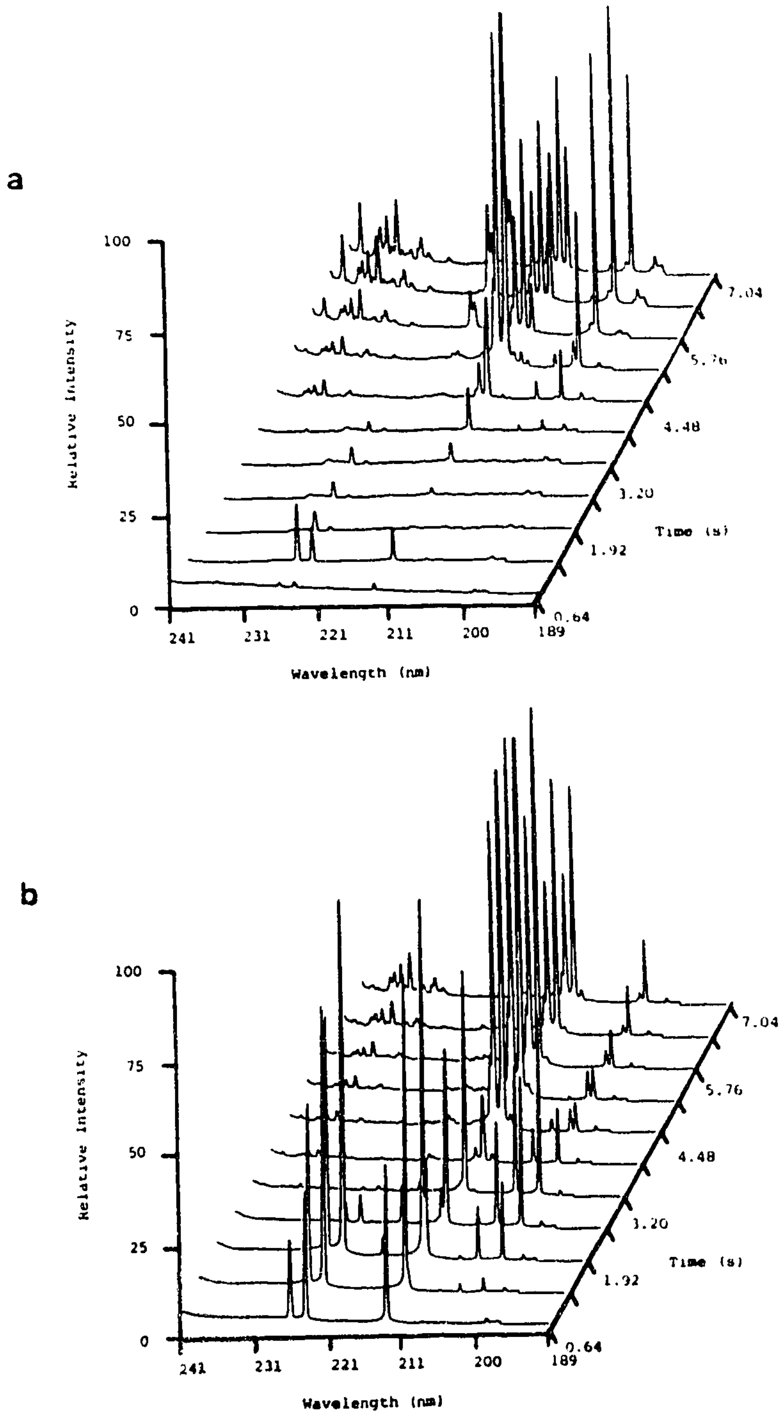

Figure 42. Temporal behavior of elemental emission from unashed (a), and laser-ashed (b) NBS SRM 1571 orchard leaves.

the samples during this pretreatment. The results of these determinations are presented in Figure 43.

3. Preparation and Insertion of Geological Standards

Geological SRMs 1635 subbituminous coal, 1632 coal, and 1633 coal fly ash were analyzed for zinc using the same experimental conditions as those just described. Sample sizes (about 30 to 40 mg) were chosen to keep the absolute mass of zinc in each in about the same range as the biological standards. The results of these determinations are presented in Figure 44.

The same conditions were then employed to determine zinc in all the biological and geological standards in sequence. Figure 45 shows the results of this sequential analysis.

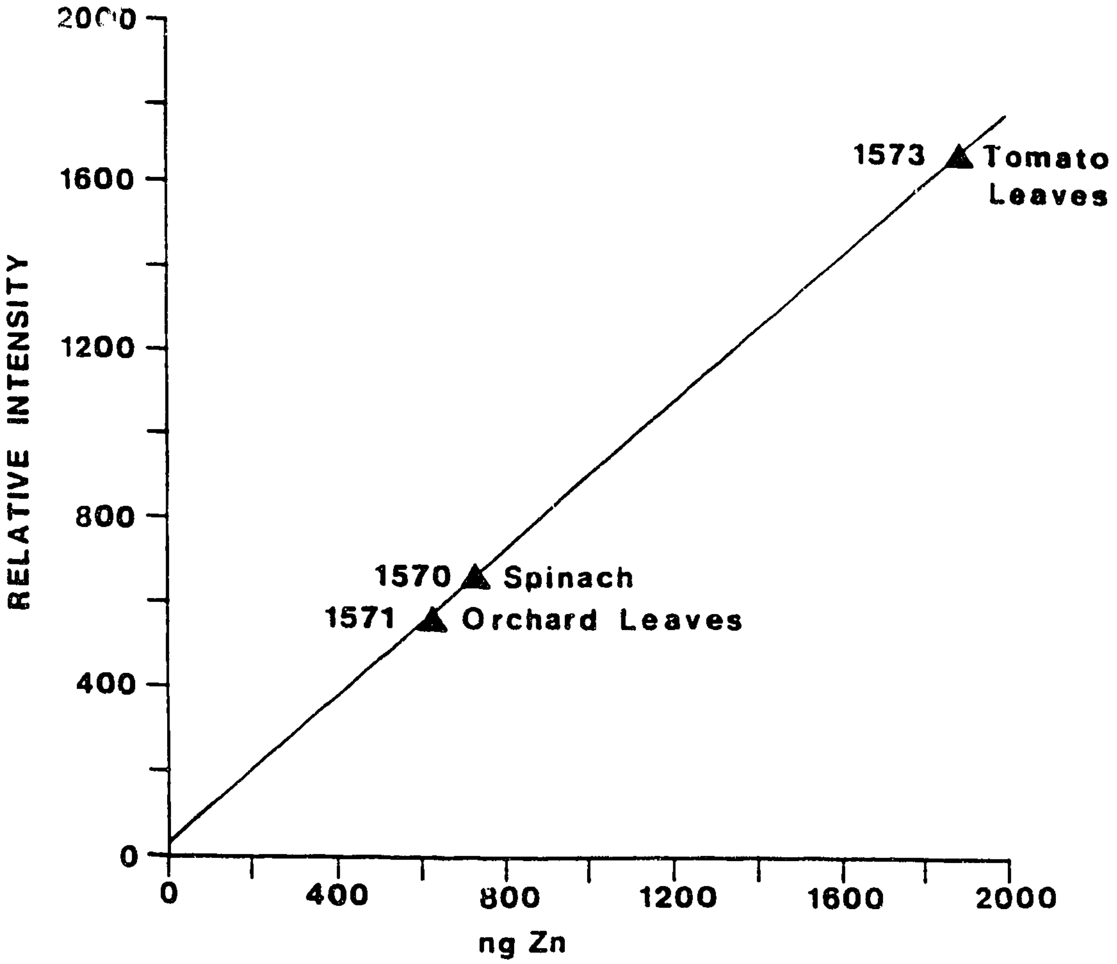

Figure 43. Calibration plot for zinc in biological SRMs

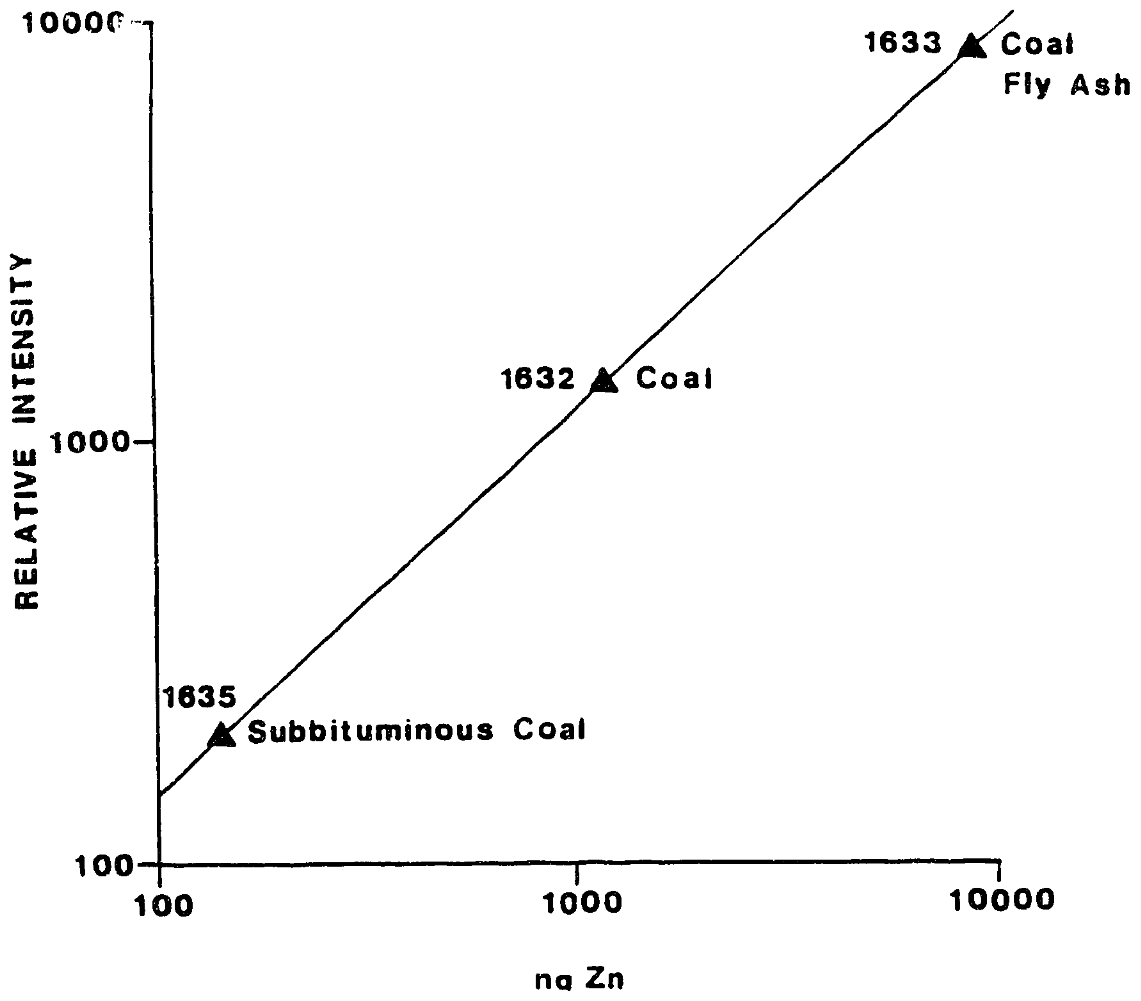

Figure 44. Calibration plot for zinc in geological SRMs.

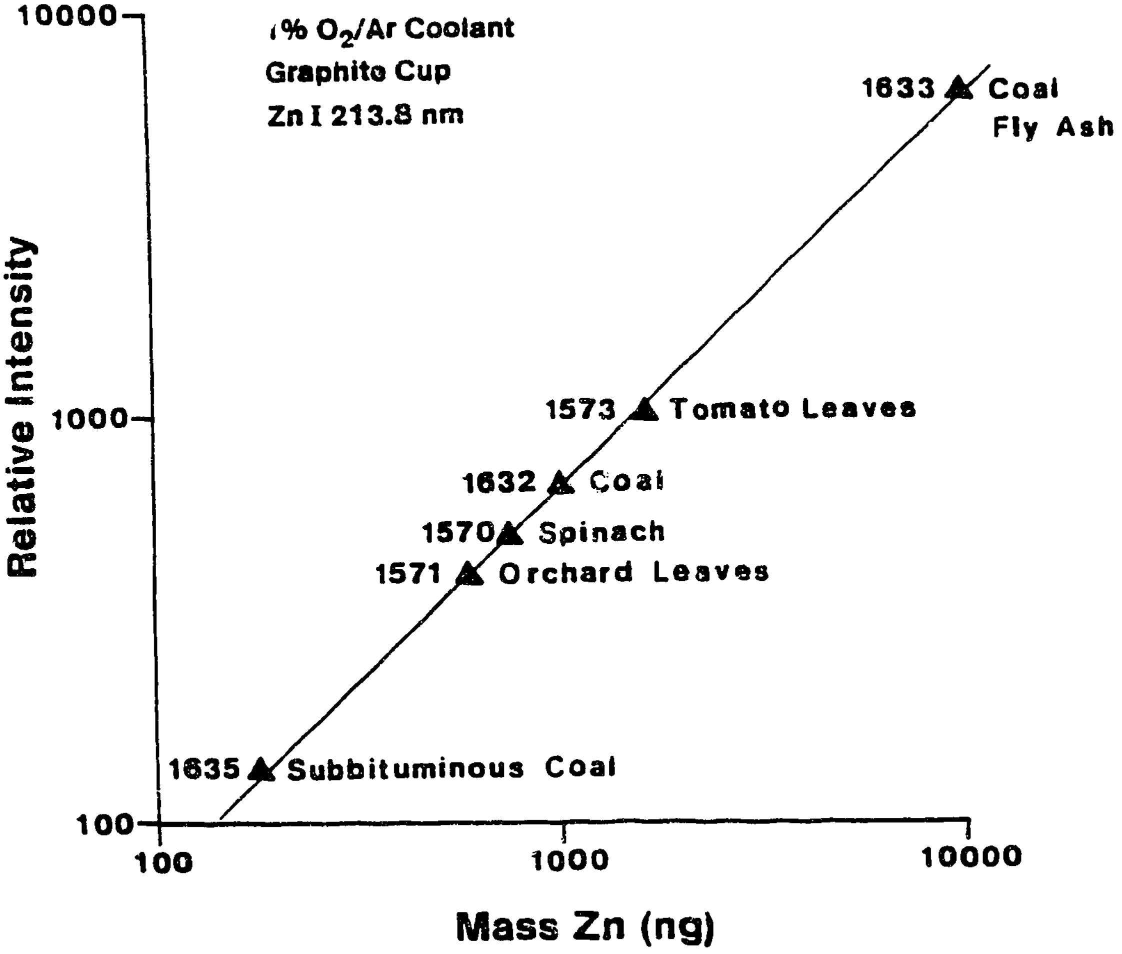

Figure 45. Calibration plot for zinc in biological and geological SRMs.

CHAPTER VIII

SUMMARY

The DSID described in this work expands and improves the analytical capability of the ICP. The main limitation of the traditional nebulizer/spray chamber-based systems, inefficient sample introduction, has been overcome.

Simultaneous multielemental analysis of microliter volume liquid and milligram mass solid samples is now possible. Also, a reduction in sample preparation complexity results from both an inherent 100% efficient sample delivery into the plasma discharge and from the ability to pretreat samples underneath the discharge. A decrease or elimination of sample contamination also results from this simplification.

Finally, a flexible and modular DSID design brings the goal of total system automation closer to reality.

As V. Karanassios and G. Horlick point out in their recent review entitled "Direct sample insertion devices for inductively coupled plasma spectrometry," (295) there are some limitations to be aware of. For instance, since the DSID uses small samples, homogeneity may be a problem and one should be aware of possible sampling error.

In addition, since it is difficult to separate sample vaporization and excitation processes, individual optimization of these processes isn't possible and matrix effects may therefore become important. However, the combination of simplified instrumentation and the judicious application of the extensive electrothermal vaporization and dc arc experience may overcome this limitation.

Probably the main stumbling block to the successful application of this experience is the poor understanding of the important experimental parameters in direct sample insertion work. And this lack of understanding stems from the historic lack of good dedicated hardware and software for this type of work.

V. Karanassios and G. Horlick have developed a computer-controlled direct sample insertion device (296) based on the system described in this work in an effort to overcome this problem.

The 24-sample capacity carousel of the original pneumatic/mechanical system was used to hold sample probes consisting of graphite or metal cups or metal loops.

The original photodiode array/PMT spectrometer was replaced with a new direct reader measurement system that could rapidly digitize complete transient signals simultaneously from four channels. New software was developed that handled automation, control, fault diagnosis, data acquisition, and peak-type signal processing.

Since direct sample insertion device type, probe geometry, composition, insertion sequence, speed and final insertion position inside the plasma, forward power, plasma gas composition, sample matrix, and analyte volatility all affect analyte temporal behavior, an easy-to-use computerized system was necessary to facilitate parameter investigation. And since analyte emission peak widths ranged from several seconds to few hundred milliseconds, a data acquisition system with a variable acquisition rate, multichannel capabilities, and a wide bandwidth was necessary.

An IBM PC outfitted with a 27.5 kHz data acquisition board provided for a wide data acquisition bandwidth. Front-ending the data acquisition board with a sample-and-hold amplifier, a programmable gain amplifier, and an analog multiplexer provided the variable data acquisition rate and multichannel capabilities. Any four channels of a direct reading polychromator could be read simultaneously. Software transportability was assured by implementing code in easy to use BASIC. This software offered peak integration, smoothing, and background subtraction with video interaction.

Analyte temporal behaviors were readily examined on the computer screen and, for example, it became apparent that the spectral overlap of the copper 213.51 nm line on the zinc 213.856 line could be avoided by temporal separation. The direct spectral overlap of the nickel 213.858 nm line could be avoided in a similar fashion.

Using this efficient computer system, V. Karanassios, G. Horlick, and M. Abdullah went on to more extensively characterize the pneumatic/mechanical DSID (297). Analyte emission temporal behaviors were studied in terms of sample probe geometry, composition, insertion speed and position, and forward plasma power.

A long undercut graphite electrode turned out to be the best sample probe geometry because it resulted in an intense signal with a short appearance time. The authors also concluded that a fast sample insertion to the top of the plasma load coil and a relatively high plasma power (1.75 to 2.00 kW) should be used for the best analytical performance.

The temporal emission signals for the elements Ag, Cd, Cu, Mg, Mn, Si, Sn, and Zn all returned to baseline in less than 35 s, but Co, Cr, Fe, and Ni signals still had significant intensity even after 60 s. Of the refractory elements studied, Sr, Ca, and Al exhibited only low intensity signals and Zr and Ti gave no emission signals.

In Chapter VI of the current work, it was discovered that the refractory behavior of nickel could be overcome by using metal cups (particularly tungsten) in a hydrogen/argon mixed gas plasma. Presumably, any refractory oxide formed in the sample cup was reduced to the more volatile metal. This approach to dealing with refractory metals needs further investigation.

V. Karanassios, M. Abdullah, and G. Horlick (298) employed their newly-developed data acquisition system and the pneumatic/mechanical DSID to study another promising method of dealing with refractory samples: *in situ* (directly in the sample cup) chemical modification. The addition of an excess of a halide-containing reagent causes preferential formation of a high-volatility halide of the analyte.

This method provided a simple alternative to other approaches including high powered plasmas and mixed gases, special electrode geometries, metal cups, chemical modification by addition of halocarbons to the plasma gas, or pyrolytically- or carbide-coated or metal-lined sample cups.

The authors studied the vaporization characteristics of the refractory and carbide-forming elements Al, B, Ca, Sr, and Zr in the presence of KCl, KF, NaCl, and NaF. A 10 µl aliquot of modifier was added to a dried solution residue (the cup was dried in aluminum holder in a hot plate), the residue was again dried, and then inserted into the plasma.

They found that a 10 µl spike of 0.25 M NaF worked best, giving quantitative determinations of the above elements.

It was also found that cups that contained carbide-forming elements could be reused after an insertion with 10 µl of 0.25 M NaF, followed by insertion with 20 µl concentrated HCl, followed finally by a dry run.

Computer-acquired temporal emission profiles suggested to the authors that analyte oxo-anion salts decomposed to form the corresponding oxides during the sample dry/ash cycle. A further increase in cup temperature caused either reduction of the oxide to the corresponding metal or carbide formation.

A forward plasma power setting of 1.25 kW resulted in a sample cup temperature of only about 1800°C. Therefore, refractory oxides and carbides of Al, Ca, Sr, and Zr won't volatilize as all have boiling points near or above this temperature.

A double peak observed for strontium might be explained by its initial reduction to the metal with corresponding volatilization at about 10 s to give a sharp emission peak and then formation of refractory SrC_2 to give a later broad peak.

No emission peaks were seen for calcium or zirconium, and further study was needed to explain the prolonged time behavior of aluminum.

With NaF modification, an especially good improvement for zirconium, which is difficult to determine by dc arc, was achieved. Whereas no signal was observed for Ti, Zr, and B without modification, detection limits of 0.8, 0.4, and 10 ng respectively, were achieved with NaF modification. Little change in detection limits was observed for the non-carbide forming elements cobalt and iron and little change in the temporal profiles of the volatile elements Ag, Cd, and Zn was noted. Linear working curves spanning over three orders of magnitude were obtained for aluminum and calcium and a working curve covering over two orders of magnitude was plotted for zirconium.

The direct determination of boron in powdered $CaSO_4$ was also possible. The authors noted that recently developed ICP methods for boron involved lengthy sample preparation so an efficient DSID method employing in-cup chemical modification was tried as an alternative. Both standard additions and synthetic standards (consisting of a mixture of H_3BO_3 and $CaSO_4$) were used for 2 mg samples. The addition of 10 µl of 0.5 M NaF was used for chemical modification and a linear

(1 to 1000 ppm) working curve for boron was achieved with both standardization techniques.

It is apparent from this recent work that chemical modification is important for the successful general implementation of DSID techniques.

Although the pneumatic/mechanical DSID described in this thesis achieved the initial goals it was designed to accomplish-improved precision over manual insertion and automatic sequential sample handling and pretreatment-and as such it was central to the characterization and chemical modification studies outlined above, its two main weaknesses became apparent over time. It's vertical positioning accuracy of about plus or minus 0.5 mm was inferior to what could be obtained with computer-controlled stepper motor-driven positioning and its pneumatic/mechanical control was more cumbersome than purely mechanical control. However, it should be noted that rapid sequential pneumatic sample delivery might still be superior in some situations (for example, when a long distance between the plasma unit and sample loading area is required).

An alternative "second" generation automated direct sample insertion system for inductively coupled plasma-atomic emission spectrometry reported by Shao and Horlick (155,see

Chapter II) has been further refined by W.T. Chan and G. Horlick (299).

This system combines stepper motor driven sample positioning with the multichannel high-speed electronics for data acquisition described above (emission data can be simultaneously acquired from six channels of a direct-reading polychromator) and a robot arm for automatic exchange of graphite sample cups. In addition, a glass shutter is used to seal the bottom of the ICP torch when a sample is not inserted. This provides an alternative to the "snuffer" line or helium central gas that had previously been used to minimize filament formation and reduce reflected power when a sample cup was inserted in the plasma.

This DSID replaces the standard nebulizer/spray chamber of a commercial ARL 34000 ICP system. The original integrators on the PMTs of the ARL's direct reader were too slow for transient signal acquisition and were also replaced with the faster electronics.

Samples are dried 35 mm below the load coil (blc) for 30-60 s, ashed 16-24 mm blc for various periods of time, and then fully inserted into the plasma in less than two seconds (from the bottom of the torch). By step counting, the insertion position is known to better than 0.1 mm.

Detection limits (3σ of background) are in the picogram range for volatile elements like zinc and cadmium (10 µl solutions). Detection limits for Zn, Cd, Cu, Pb, and Fe are 1.2, 4.5, 14, 21, 30 pg, respectively.

This system has also been employed to study the effects of dry and ash cycles on analyte temporal behavior by W.T. Chan and G. Horlick (300).

The lead emission temporal profiles from dried $Pb(NO_3)_2$ samples contain double peaks. These two peaks may be due to $Pb(NO_3)_2$ decomposing to $PbO_{(s)}$ at 925 K which, in the absence of reducing agent, sublimes to $PbO_{(g)}$ or, in the presence of carbon, the oxide is reduced to $Pb_{(l)}$ which either vaporizes as $Pb_{(g)}$ at about 1000 K or is reduced to $Pb_{(g)}$ directly.

Lead emission temporal signals from dried $PbCl_2$ are more complicated with three peaks, the first of which is probably due to sublimation of $PbCl_2$ and since the chloride is hydrolyzed to the oxide, the second and third peaks are similar to those given by the nitrate.

The temporal profiles for *ex situ* vs. *in situ* drying are simpler, possibly because a thin film of sample forms during the longer external drying times and therefore the main volatilization process involves sample contact with the graphite cup's reducing surface.

The strong dependence of the nickel emission profile on ashing cycle can be rationalized by examining the following reaction: $3NiO_{(s)} + 4C_{(s)} \dashrightarrow Ni_3C_{(s)} + 3CO_{(g)}$. This reaction has a free energy of 260 kJ mol^{-1} at 298 K and a free energy of -19 $kJmol^{-1}$ at 800 K. Therefore, at a temperature of about 1000 K, nickel carbide forms from the oxide in a graphite sample cup.

Apparently, the best sample treatment must be determined empirically, although a knowledge of sample cup temperature in the plasma would certainly expedite the process.

W.T. Chan and G. Horlick (301) have made recent progress in understanding the thermal properties of the direct sample insertion cup and even though maximum cup temperatures of from 1600°C to 4000°C have been reported in the literature, a temperature of only about 2000°C is to be expected. It turns out that metal boiling point is only an indication of possible maximum cup temperature since a substantial metal vapor pressure can exist below the metal's boiling point. It is better to use an "appearance temperature" as in ETV-AAS. Also, it is best not to use the boiling points of carbides since lower-boiling oxides may be the actual species formed in the sample cup. In the end, it's best to use a direct measurement of cup temperature (as with an optical pyrometer).

Based on their model of radiative and conductive heat losses from the sample cup, about 112 W (60.5 W of emissive power plus 51.7 W of heat conduction) of power is input to the sample cup. Therefore, minimization of conductive heat loss will improve the rate of cup temperature rise and minimization of radiative heat loss will maximize the final cup temperature. These ideas can be used as basis for future cup design.

Since the sample cup temperature rise rate depends on the thermal conductivity and conductive area of the sample cup, the heat capacity and the emitting area of the cup, and on the emissivity of the cup material, a cup material can be chosen and fabricated based on these parameters.

Low emissivity materials like silicon carbide and aluminum oxide might seem like good choices, but they are difficult to machine so the use of a graphite cup with a thin stem is superior.

It might also seem reasonable to use a tantalum or tungsten metal cup for a faster temperature rise, but the heat capacity of a metal cup is actually about two times greater than a graphite cup simply because of its greater mass. The emissivity of unoxidized tantalum or tungsten cup is about one quarter that of graphite at 1500°C, but an oxide forms with prolonged use. Once again, a graphite cup is preferred because it will have a faster temperature rise.

An understanding of the important direct sample insertion experimental parameters has led to a better optimization of the technique and an overall enhancement of ICP atomic emission spectroscopy. It now appears that even greater gains can be made in ICP-mass spectrometry (ICP-MS).

V. Karanassios and G. Horlick (302) have constructed a computer-controlled, stepper-motor driven, horizontal direct sample insertion device for inductively coupled plasma-mass spectrometry that can be attached to a commercial ICP-MS. The insertion system was designed with automation (robotic sample changing) in mind.

Like the original ICP atomic emission systems, standard ICP/MS instruments use nebulizers for sample introduction. Therefore, the same advantages that the DSID brought to ICP spectroscopy, namely, the direct introduction of microliter liquids and milligram powders/solids with little sample pretreatment, should also be possible for ICP/MS.

However, important additional advantages for MS work are possible. First of all, solvent interferences from matrix polyatomics and matrix and analyte oxides can be reduced or eliminated. And secondly, since sample processing can occur during insertion, some non-spectroscopic interferences can also be eliminated.

The authors modified a Fassel-type torch by widening the central tube from a 1.5 mm diameter to a 7 mm diameter, removing the central tube's tip, and installing a mechanical shutter at the torch's base.

Long undercut graphite sample cups ("4021 L") were machined from SPEX HPND+4021 electrodes, and molybdenum and tantalum cups were machined from rods and placed on long undercut graphite electrodes. The authors also fashioned a tungsten wire sample probe 8 cm long by 1 mm diameter which carried two loops, 5 mm in diameter each.

Solution volumes of 10 microliters were applied to these probes and dried in aluminum holder on a hot plate (the wire loops were dried with an IR lamp). The final sample insertion was rapid-the final 22 mm of travel was covered in 0.2 s. Aligning the top of the sample cup with the top of the load coil was previously found to be the best position for transient signals in DSI-ICP-AES work and it was also used here. The filament seen upon sample retraction in earlier DSID systems was not seen here. The authors suggested that this might be due to the "center-tap ground" (grounding of the middle turn of the load coil) used in their commercial Elan ICP-MS system. The extra plasma stability relative to earlier systems may have also been due to this feature.

The new sample insertion system improved the mean time between samples relative to typical nebulizer-based systems.

Even though the ICP/MS was a sequential analysis system, temporal analysis and multielement capability was achieved through an understanding of the experimental parameters and the application of new software. The authors concluded that the number of data points acquired per second depended on the number of elements/masses scanned in given dwell time. There was necessarily a trade-off between data acquisition rate and the number of peaks acquired.

Temporal analysis revealed that the central gas flow rate had little effect on peak height or shape. Higher plasma power gave sharper, higher intensity peaks. The central gas (nebulizer) flow rate is apparently not as important here as it is in traditional ICP instruments.

The background spectral characteristics of this system were studied further by V. Karanassios and G. Horlick (303). The authors found that the background spectra for a "dry" plasma (no sample or solvent) and for graphite, Mo, Ta, and W direct insertion probes are simpler than nebulized aqueous solution background spectra.

These results are mostly due to the elimination of water (which gives rise to oxygen- and hydrogen-containing species) and the fact that the direct insertion probes themselves don't add complex species to the background.

The authors also found that bringing the ICP torch closer to MS sampling cone or using an extended torch reduced air entrainment and further simplified "dry" plasma spectra. Further spectral simplification would probably only be achieved by eliminating trace water from the argon gas supply.

Background scans of a graphite probe inserted into the plasma looked the same as spectra for a "dry" plasma, but $^{36}Ar^+$ and $^{38}Ar^+$ peaks were of lower intensity because of a reduction of plasma energy due to an inductive coupling with the graphite probe.

Background scans of Mo, Ta, and W probes were essentially the same as for the "dry" plasma in the 1 to 80 amu mass range. At higher masses molybdenum peaks and tin and tantalum peaks from metal impurities were seen for the molybdenum cup. Only two high mass peaks were seen for the tantalum cup-one of which was an oxide or mono-isotopic gold impurity. Zirconium and cesium high mass impurity peaks and tungsten isotopes were seen for the tungsten wire loop probe.

The authors concluded that interference-free determinations were possible with the direct sample insertion-based ICP-MS system that weren't possible using a nebulizer-based system. It was also suggested that perhaps the DSI-ICP-MS technique could be used for the direct qualitative and semi-quantitative analysis of solid metals.

The same authors have recently taken a closer look at spectral interferences and matrix effects in DSI-ICP-MS (304).

The DSI technique can reduce or eliminate the two main problems in ICP-MS: spectral interferences from analyte and matrix based molecular ions (mainly oxides) and non-spectroscopic matrix effects caused by an excess of an element causing a suppression of a lighter element's signal.

Oxide signal levels can be reduced to about 0.1% of full scale by the elimination of water and differential volatilization can eliminate the suppressive matrix effect of uranium on zinc. The chemical modification of a sample with NaF is a key factor in the latter case.

An aliquot of 10 µl of 0.25 M NaF was injected into the sample cup and dried on aluminum hot plate. In the case of barium, peak height observation revealed that less than 1% of barium was released on the first sample insertion. The remaining barium was released on the second insertion and the barium oxide to barium ratio was only 0.1% (which was much better than the approximate 4% level seen in nebulizer sample introduction). Cerium and vanadium could also be released from the sample cup by chemical modification with NaF.

The element uranium is also a good carbide former and so it can be separated from highly volatile zinc in the time domain. Again the carbide-forming element was released by NaF addition.

We have seen that application of properly designed direct sample insertion devices has benefited both ICP-atomic emission spectroscopy and ICP-mass spectrometry.
V Karanassios and Horlick have suggested in a recent review (295) that the next generation of direct sample insertion systems should incorporate a combination of fast stepper motor driven insertion, high plasma power, mixed plasma gases, and sample matrix modification. The use of laser ablation-perhaps inside the plasma-might also be of benefit. This new generation of systems should be able to handle difficult samples like high temperature ceramics, catalytic materials, and solid metal samples. A higher level of automation/robotics will also be required.

An intermediate level of automation was central to the success made to this point. Further gains will require the integration of an even higher level of automation.

V. Karanassios and G. Horlick suggest (13) that a higher level of automation will be achieved by making the computers attached to analytical instrumentation more "instrument-like" instead of the old approach of making individual analytical instruments more "computer-like." In other words, an "instrument metaphor," like Apple Computer's "desk-top" metaphor (based on Xerox's Smalltalk) used in the Macintosh line of personal computers, should be implemented in the analytical laboratory.

These authors have developed a "distributed intelligence" approach to computerization of a spectrometer-one computer for data acquisition and one for interaction with the user. The "instrument metaphor" is implemented on the latter computer with a new "human processor interface" or HPI.

The old hardware dials, meters, and other controls are now mapped onto the computer's screen by the HPI. Instrument operation now becomes intuitive-a concept that has been very successful in Apple Macintoshes. A commercial implementation of this unique concept can now be found in National Instrument's "LabView."

A distributed intelligence approach to advanced automation also helps slow instrument obsolescence. Spectrometer design remains relatively constant over time, but new personal computers or PCs are appearing almost every day. The HPI can be transported to a new PC when necessary without having to redesign the data acquisition electronics.

The authors chose to use an IBM PC for data acquisition and an Apple Macintosh for the HPI. Perhaps now one type of PC, the Apple Macintosh, could be used for both jobs since powerful data acquisition cards (available for the "Mac" from, for example, National Instruments) can be plugged into the card slots found in the Mac II line of PCs.

The authors' system exhibits artificial intelligence characteristics as it incorporates both "self-learning" expressed in the flagging of a new user with appropriate warnings based on the automatic analysis of past instrument user averages, and an atomic spectroscopy data base that is graphically accessible.

Perhaps it would now be useful to consider a further extension of the "desk-top" metaphor. We can imagine a logical progression from "desk-top" to "instrument" to "laboratory" metaphor. At the "laboratory" metaphor level, a scientist would interact with a completely automated analytical laboratory environment via a new generation "HPI." This new HPI might take the form of a three-dimensional "virtual reality." It's not difficult to imagine the user of such a system going beyond the daily routine of analytical determinations and initiating a set of completely automatic laboratory experiments.

BIBLIOGRAPHY

1 M.I. Abdullah and J.P. Riley in "Automation in Analytical Chemistry", European Technicon Symposium, Paris, 1966, Mediad Inc., N.Y., 1967.

2 B.K. Afghan, P.D. Goulden, and J.F. Ryan, Water Research, 6, 1475 (1972).

3 J.H.U. Brown and J.F. Dickson III, Science, 166, 334 (1969).

4 W. Worthy, R. Dagani, S. Stinson, and J. Krieger, Chemical & Engineering News, 21 (March 24, 1986).

5 U. von Buchstab, Canadian Research, 15, 33 (1982).

6 R.W. Arndt and R.D. Werder in "Topics in Automatic Chemical Analysis 1:, J.K. Foreman and P.B. Stockwell, Eds., John Wiley & Sons, N.Y., 1979.

7 D. Dingeldein, Canadian Research, 15, 4 (1982).

8 Research & Development, 29, 40 (1987).

9 S. Polcyn, Omni, 5, 35 (1983).

10 P.B. Stockwell and J.K. Foreman in "Topics in Automatic Chemical Analysis 1", J.K. Foreman and P.B. Stockwell, Eds., John Wiley & Sons, N.Y., 1979.

11 G. Horlick, Phil. Trans. R. Soc. Lond. A, 305, 681 (1982).

12 Science/Technology Concentrates, Chemical & Engineering News, 26 (November 25, 1985).

13 V. Karanassios and G. Horlick, Appl. Spectrosc., 41 360 (1987).

14 M.A. Vaughn and G. Horlick, Appl. Spectrosc., 41, 523 (1987).

15 R.E. Dessy, J. Chem. Inf. Comput. Sci., 25, 282 (1985).

16 E. Hayden, Research & Development, 29, 61 (1987).

17 R. Dagani, Chemical & Engineering News, 7 (August 12, 1985).

18 D. '. Burns and D.L. Rome, Research & Development, 70 (April 1986).

19 J.Krieger, W. Worthy, R. Dagani, and S. Stinson, Chemical & Engineering News, 65, 24 (March 23, 1987).

20 A.P. Thakoor, A. Moopenn, J. Lambe, and S.K. Khanna, Appl. Opt., 26, 5085 (1987).

21 G. Horlick, Anal. Chem., 54, 276R (1982).

22 L.M. Holmes, Laser Focus, 23, 24 (1987).

23 V. Berry, American Laboratory, 19, 126 (1987).

24 T.L. Isenhour, J. Chem. Inf. Comput. Sci., 25, 292 (1985).

25 G. [illegible]rlick, Chemistry in Canada, 21 (May 1983).

26 [illegible] deGalan, G.R. Kornblum, and M.T.C. de Loos-Vollebregt "Recent Advances in Analytical Spectroscopy", K. Fuwa, Ed., Pergamon Press, N.Y., 1982.

27 [illegible]thny, Anal. Chem., 53, 15A (1981).

28 R.F. Browner and A.W. Boorn, Anal. Chem., 56, 786A (1984).

29 R.F. Browner and A.W. Boorn, Anal. Chem., 56, 875A (1984).

30 L.T. Skeggs, Anal. Chem., 38, 31A (1966).

31 G.T. Bender, "Principles of Chemical Instrumentation," W.B. Saunders Co., Philadelphia, 1987, Chapter 25: "Automation in Clinical Chemistry."

32 S. Greenfield, H.McD. McGeachin, and P.B. Smith, Talanta, 23, 1 (1976).

33 R.F. Browner, Pittsburgh Conference, Atlantic City, N.J., 1983, paper No. 548 (abstract).

34 C.D. West and D.N. Hume, Anal. Chem., 36, 412 (1964).

35 D.R. Luffer and E.D. Salin, Anal. Chem., 58, 654 (1986).

36 K.W. Olson, W.J. Haas, and V.A. Fassel, Anal. Chem., 49, 632 (1977).

37 J.A. Koropchak and D.H. Winn, Anal. Chem., 58, 2558 (1986).

38 L.S. Dale and S.J. Buchanan, J.A.A.S., 1, 59 (1986).

39 L.R. Layman and F.E. Lichte, Anal. Chem., 54, 638 (1982).

40 R.H. Wendt and V.A. Fassel, Anal. Chem., 37, 920 (1965).

41 R.F. Browner, A.W. Boorn, and D.D. Smith, Anal. Chem., 54, 1411 (1982).

42 J. Farino and R.F. Browner, Pittsburgh Conference, Atlantic City, N.J., 1983, paper No. 455 (abstract).

43 W. Sunderland, R.S. Hodge, W.G. Boyle, and E. Fisher, Appl. Spectrosc., 26, 559 (1972).

44 J.A.C. Broekaert and F. Leis, Anal. Chim. Acta, 109, 73 (1979).

45 D.L. Krottinger, M.S. McCracken, and H.V. Malmstadt, American Laboratory, 9, 51 (1977).

46 B.W. Renoe, K.R. O'Keefe, and H.V. Malmstadt, Anal. Chem., 48, 661 (1976).

47 L.R. Layman, J.G. Crock, and F.E. Lichte, Anal. Chem., 53, 747 (1981).

48 M.E. Ruddel and S.W. McClean, Anal. Chem., 53, 1946 (1981).

49 G.L. Moore, A.E. Watson, and P. Humphries-Cuff, Spectrochim. Acta, 37B, 835 (1982).

50 J.R. Garbarino and H.E. Taylor, Anal. Chim. Acta, 134, 153 (1982).

51 R. Balciunas, F.J. Holler, P.K. Notz, E.R. Johnson, L.D. Rothman, and S.R. Crouch, Anal. Chem., 53, 1484 (1981).

52 C.B. Ranger, American Laboratory, 14, 56 (1982).

53 B.D. Mindel and B. Karlberg, Laboratory Practice, 30, 719 (1981).

54 J. Ruzicka, Fresenius Z. Anal. Chem., 329, 653 (1988).

55 G.R. Beecher and K.K. Stewart, Clin. Nutr., 1, 411 (1975).

56 J. Ruzicka and E.H. Hansen, Anal. Chim. Acta, 78, 145 1975).

57 C.B Ranger, Anal. Chem., 53, 20A (1981).

58 S. Greenfield, Spectrochim. Acta, 38B, 93 (1983).

59 D.E. Davy and G.J.H. Metz, J. Anal. Atom. Spectrom., 3, 375 (1988).

60 J.M. Martin and P.J. Ihrig, Appl. Spectrosc., 41, 986 (1987).

61 O. Astrom, Anal. Chem., 54, 190 (1982).

62 G.S. Pyen and R.F. Browner, Appl. Spectrosc., 42, 508 (1988).

63 M.S. Black, M.B. Thomas, and R.F. Browner, Anal. Chem., 53, 2224 (1981).

64 P.A.M. Ripson and L. deGalan, Spectrochim., Acta, 36B, 71 (1981).

65 A. Faske, K.R. Snable, A.W. Boorn, and R.F. Browner, Pittsburgh Conference, Atlantic City, N.J., 1983, paper No. 147 (abstract).

66 J.R. Dean, L. Ebdon, H.M. Crews, and R.C. Massey, J. Anal. Atom. Spectrom., 3, 349 (1988).

67 D.M. Fraley, ICP Information Newletter, 4, 557 (1979).

68 D.M. Fraley, D. Yates, and S.E. Manahan, Anal. Chem., 51, 2225 (1979).

69 C.H. Gast, J.C. Kraak, H. Poppe, and F.J.M.J. Maessen, ICP Information Newsletter, 4, 553 (1979).

70 D.M. Fraley, D.A. Yates, S.E. Manahan, D. Stallings, and J. Petty, Appl. Spectrosc., 35, 525 (1981).

71 D.R. Heine, M.B. Denton, and T.D. Schlabach, Anal. Chem., 54, 81 (1982).

72 W.D. Spall, J.G. Lynn, J.L. Andersen, J.G. Valdez, and L.R. Gurley, Anal. Chem., 58, 1340 (1986).

73 I.S. Krull, D. Bushee, R.N. Savage, R.G. Schleicher, and S.B. Smith Jr., Anal. Lett., 15, 267 (1982).

74 Zs. Horvath and R.M. Barnes, Anal. Chem., 58, 1352 (1986).

75 J.J. Thompson and R.S. Houk, Anal. Chem., 58, 2541 (1986).

76 H. Berndt and W. Slavin, At. Absorpt. Newsl. 17, 109 (1978).

77 W.R. Wolf and K.K. Stewart, Anal. Chem., 51, 1201 (1979).

78 J.F. van Staden, Fresenius Z. Anal. Chem., 312, 438 (1982).

79 F.C.A. Killer in "Automation in Analytical Chemistry," Technicon Symposium, N.Y., 1966, Mediad Inc., N.Y., 1967.

80 S. Barabas in "Automation in Analytical Chemistry," Technicon Symposium, N.Y., 1966, Mediad Inc., N.Y., 1967.

81 D. Leyden and W. Wegscheider, Anal. Chem., 53, 1059A (1981).

82 H.V. Malmstadt, D.L. Krottinger, and M.S. McCracken in "Topics in Automatic Chemical Analysis 1," J.K. Foreman and P.B. Stockwell, Eds., John Wiley & Sons. N.Y., 1979.

83 S.R. Gambino, Anal. Chem., 43, 20A (1971).

84 H.V. Malmstadt, E.A. Cordos, and C.J. Delaney, Anal. Chem., 44, 26A (1972).

85 N.G. Anderson, Amer. J. Clin. Pathol., 53, 778 (1970).

86 R.L. Coleman, W.D. Shults, M.T. Kelly, and J.A. Dean, American Laboratory, 3, 26 (1971).

87 N.G. Anderson, Anal. Biochem., 23, 207 (1968).

88 N.G. Anderson, Science, 166, 317 (1969).

89 O. Suovaneimi and J. Jarnefelt, American Laboratory, 14, 106 (June 1982).

90 T.H. Crouch, Scientific Computing & Automation, 2, 26 (January/February 1986).

91 B. Howard, G. Levy, V. Berry, and G. Ouchi, American Laboratory, 19, 144 (1987).

92 G.J. Schmidt and M.W. Dong, American Laboratory, 19, 62 (February 1987).

93 B.J. McGrattan and D.J. Macero, American Laboratory, 16 (September 1984).

94 J.G. Liscouski, J. Chem. Inf. Comput. Sci., 25, 288 (1985).

95 E. Garfield, Current Contents, 26, 3 (July 14, 1986).

96 J.P. Bell, R.A. Simpson, and A.G. Mayer, American Laboratory, 19, 106 (May 1987).

97 Webster's II New Riverside University Dictionary, Riverside Publishing Co., Houghton Mifflin Co., Boston, 1984.

98 K.Capek in "Of Men and Machines," A.O. Lewis, Jr., Ed., E.P. Dutton & Co., Inc., N.Y., 1963.

99 R. Dessy, Anal. Chem., 55, 1100A (1983).

100 R. Dessy, Anal. Chem., 55, 1232A (1983).

101 Research & Development, 29, 33 (May 1987).

102 Research & Development, 29, 58 (May 1987).

103 B.E. Kropscott, L.B. Coyne, R.R. Dunlap, and P.W. Languardt, American Laboratory, 19, 70 (June 1987).

104 W.R. Iversen, Electronics, 152 (September 4, 1986).

105 V. Berry and J. Hahn, American Laboratory, 20, 88 (July 1988).

106 J.P. Coates, Spectroscopy, 1, 14 (1986).

107 G.D. Owens and R.J. Eckstein, Anal. Chem., 54, 2347 (1982).

108 J. Brosemer and J. Liscouski, American Laboratory, 18, 80 (September 1986).

109 A.N. Papas, M.Y. Alpert, S.M. Marchese, J.W. Fitzgerald, and M.F. Delaney, Anal. Chem., 57, 1408 (1985).

110 R.J. Eckstein, G.D. Owens, M.A. Baim, and D. A. Hudson, Anal. Chem., 58, 2316 (1986).

111 L.E. Wolfram, Research & Development, 28, 74 (July 1986).

112 M. Dulitzky, American Laboratory, 18, 104 (June 1986).

113 D.P. Binkley, American Laboratory, 18, 68 (February 1986).

114 W.A. Schlieper, T.L. Isenhour, and J.C. Marshall, Anal. Chem., 60, 1142 (1988).

115 J.C. Wass and N.J.C. Packham, LCGC, 6, 420 (1988).

116 H.G. Fouda and R.P. Schneider, American Laboratory, 20, 116 (May 1988).

117 T.L. Chester, D.P. Innis, and G.D. Owens, Anal. Chem., 57, 2243 (1985).

118 J. Haggin, Chemical & Engineering News, 65, 63 (April 20, 1987).

119 R.M. Barnes, Spectroscopy, 1, 24 (1986).

120 D. Sommer and K. Ohls, Fresenius Z. Anal. Chem., 304, 97 (1980).

121 G.F. Kirkbright and S.J. Walton, Analyst, 107, 276 1982).

122 G.F. Kirkbright and Z. Li-Xing, Analyst, 107, 617 (1982).

123 Z. Li-Xing, G.F. Kirkbright, M.J. Cope, and J.M. Watson, Appl. Spectrosc., 37, 250 (1983).

124 E.D. Salin and G. Horlick, Anal. Chem., 51, 2089 (1979).

125 R.M. Barnes, "Emission Spectroscopy," Dowden, Hutchinson and Ross, Inc., Stroudsburg, Penn., 1976, Chapter 1: "The Early Years."

126 F. Szabadvary, "History of Analytical Chemistry," Pergamon Press, N.Y., 1966, Chapter 11: "Optical Methods."

127 J.A. Ramsay, J. Exptl. Biol., 27, 407 (1950).

128 J.A. Ramsay, R.H.J. Brown, and S.W.H.W. Falloon, J. Exptl. Biol., 30, 1 (1953).

129 P.A. Bott, Analyt., Biochem., 1, 17 (1960).

130 P.A. Oberg, H.R. Ulfendahl, and B.G. Wallin, Analyt., Biochem., 18, 543 (1967).

131 G.M. Katz, Analyt., Biochem., 26, 381 (1968).

132 B.V. L'vov and G.V. Plyushch, Zh. Prikl. Spektrosk., 10, 903 (1969).

133 H.L. Kahn, G.E. Peterson, and J.E. Schallis, At. Absorpt. Newsl., 7, 35 (1968).

134 H.T. Delves, Analyst, 95, 431 (1970).

135 H.L. Kahn and J.S. Sebestyen, At. Absorpt. Newsl., 9, 33 (1970).

136 F.J. Fernandez and H.L. Kahn, At. Absorpt. Newsl., 10, 1 (1971).

137 J.D. Kerber and F.J. Fernandez, At. Absorpt. Newsl., 10, 78 (1971).

138 D. Clark, R.M. Dagnall, and T.S. West, Anal. Chim. Acta, 58, 339 (1972).

139 E.D. Olsen and P.I. Jatlow, Clin. Chem., 18, 1312 (1972).

140 E.D. Prudnikov, Zh. Prikl. Spektrosk., 17, 352 (1972).

141 M.M. Joselow and J.D. Bogden, At. Absorpt. Newsl., 11, 127 (1972).

142 R.D. Ediger and R.L. Coleman, At. Absorpt. Newsl., 12, 3 (1973).

143 K.M. Aldous, D.G. Mitchell, and F.J. Ryan, Anal. Chem., 45, 1990 (1973).

144 F.J. Fernandez, At. Absorpt. Newsl., 12, 70 (1973).

145 J.K. Grime and T.J. Vickers, Anal. Chem., 46, 1810 (1974).

146 D.G. Mitchell, A.F. Ward, and M. Kahl, Anal. Chim. Acta, 76, 456 (1975).

147 M. Kahl, D.G. Mitchell, G.I. Kaufman, and K.M. Aldous, Anal. Chim. Acta, 87, 215 (1976).

148 D.G. Pachuta and L.J. Cline Love, Anal. Chem., 52, 438 (1980).

149 D.G. Pachuta and L.J. Cline Love, Anal. Chem., 52, 444 (1980).

150 K.W. Jackson, L. Ebdon, D.C. Webb, and A.G. Cox, Anal. Chim. Acta, 128, 67 (1981).

151 H. Ramage, Nature, 126, 279 (1930).

152 W.A. Roach, Nature, 144, 1047 (1939).

153 A.A. Venghiattis, At. Absorpt. Newsl., 6, 19 (1967).

154 K. Govindaraju, G. Mevelle, and C. Chouard, Chemical Geology, 8, 131 (1971).

155 Y. Shao and G. Horlick, Appl. Spectrosc., 40, 386 (1986).

156 N.W. Barnett, M.J. Cope, G.F. Kirkbright, and A.A.H. Taobi, Spectrochim. Acta, 39B, 343 (1984).

157 H. Haraguchi, M. Abdullah, T. Hasegawa, M. Kurosawa, and K. Fuwa, Bulletin of the Chemical Society of Japan, 57, 1839 (1984).

158 M. Abdulla, K. Fuwa, and H. Haraguchi, Spectrochim. Acta, 39B, 1129 (1984).

159 M Abdulla and H. Haraguchi, Anal. Chem., 57, 2059 (1985).

160 A.G. Page, S.V. Godbole, K.H. Madraswala, M.J. Kulkarni, V.S. Mallapurkar, and B.D. Joshi, Spectrochim. Acta, 39B, 551 (1984).

161 A. Lorber and Z. Goldbart, Analyst, 110, 155 (1985).

162 C.W. McLeod, P.A. Clarke, and D.J. Mowthorpe, Spectrochim. Acta, 41B, 63 (1986).

163 M. Reisch, H. Nickel, and M. Mazurkiewicz, Spectrochim. Acta., 44B, 307 (1989).

164 T.T. Gorsuch, Analyst, 87, 112 (1962).

165 C.V. Monasterios, A.M. Jones, and E.D. Salin, Anal. Chem., 58, 780 (1986).

166 I.B. Brenner, A. Lorber, and Z. Goldbart, Spectrochim. Acta., 42B, 219 (1987).

167 M.M. Habib and E.D. Salin, Anal. Chem., 56, 1186 (1984).

168 E.D. Salin and R.L.A. Sing, Anal. Chem., 56, 2596 (1984).

169 M.M. Habib and E.D. Salin, Anal. Chem., 57, 2055 (1985).

170 D.W. Boomer, M. Powel, R.L.A. Sing, and E.D. Salin, Anal. Chem., 58, 975 (1986).

171 R.L.A. Sing and E.D. Salin, Anal. Chem., 61, 163 (1989).

172 G.F. Kirkbright and R.D. Snook, Anal. Chem., 51, 1938 (1979).

173 E.D. Salin and G. Horlick, unpublished work.

174 G. Horlick, Appl. Spectrosc., 30, 113 (1976).

175 G. Horlick, Anal. Chem., 48, 784A (1976).

176 T.E. Edmonds and G. Horlick, Appl. Spectrosc., 31, 536 (1977).

177 K.R. Betty and G. Horlick, Appl. Spectrosc., 32,31 (1978).

178 G. Horlick and M.W. Blades, Appl. Spectrosc., 34, 229 (1980).

179 M.W. Blades and G. Horlick, Appl. Spectrosc., 34, 696 (1980).

180 M.W. Blades and G. Horlick, Spectrochim. Acta, 36B, 861 (1981).

181 M.W. Blades and G. Horlick, Spectrochim. Acta, 36B, 881 (1981).

182 R.L. Dahlquist and J.W. Knoll, Appl. Spectrosc., 32, 1 (1978).

183 J.L.M. DeBoer and F.J.M.J. Maessen, Spectrochim. Acta, 38B, 739 (1983).

184 R.I. Botto in: "Developments in Atomic Plasma Spectrochemical Analysis," R.M. Barnes, Ed., Heyden, London, 1981.

185 R.W. Kuennen, K.A. Wolnik, F.L. Fricke, and J.A. Caruso, Anal. Chem., 54, 2146 (1982).

186 M.S. Vigler, A.W. Varnes, and H.A. Strecker, American Laboratory, 12, 31 (1980).

187 G.V. Iyengar, K. Kasperek and and L.E. Feinendegen, Sci. Total Environ., 10, 1 (1978).

188 G.V. Iyengar, K. Kasperek, and L.E. Feinendegen, Analyst, 105, 794 (1980).

189 G.V. Iyengar, K. Kasperek, and L.E. Feinendegen, Anal. Chim. Acta. 138, 355 (1982).

190 W. Johnson and J.A. Maxwell, "Rock and Mineral Analysis," 2nd Ed., John Wiley, N.Y., 1981, p. 68.

191 J.A. Hesek and R.C. Wilson, Anal. Chem., 46, 1160 (1974).

192 P.V. Lade and H. Nejadi-Babadaijin: "Soil Specimen Preparation for Laboratory Testing," American Society for Testing and Materials, Philadelphia, 1976.

193 T.-S. Koh, Anal. Chem., 52, 1978 (1980).

194 D.C. Bogen in: "Treatise on Analytical Chemistry," P.J. Elving, E. Grushka and I.M. Kolthoff, Eds., Part 1, "Theory and Practice," 2nd Ed., Vol. 5, John Wiley and Sons, N.Y., 1982.

195 E.C. Dunlop and C.R. Ginnard in: "Treatise on Analytical Chemistry," P.J. Elving, E. Grushka and I.M. Kolthoff, Eds., Part 1, "Theory and Practice," 2nd Ed., Vol. 5, John Wiley and Sons, N.Y., 1982.

196 T.S. Ma, C.Y. Wang, and M. Gutterson, Anal. Chem., 54, 87R (1982).

197 R. Bock, "A Handbook of Decomposition Methods in Analytical Chemistry," International Textbook Co., London, 1979.

198 T.S. Ma and R.C. Rittner, "Modern Organic Elemental Analysis," Dekker, N.Y., 1979.

199 T.S. Ma and V. Horak, "Microscale Manipulations in Chemistry," John Wiley and Sons, N.Y., 1976.

200 Bollo-Kamara, M.Sc. Thesis, The University of Alberta, 1979.

201 T.T. Gorsuch, Analyst, 84, 135 (1959).

202 P. Strohal, S. Lulic, and O. Jelisavcic, Analyst, 94, 678 (1969).

203 J.G. van Raaphorst, A.W. van Weers, and H.M. Haremaker, Freisenius Anal. Chem., 293, 401 (1978).

204 C.A. Rowan, O.T. Zajicek, and E.J. Calabrese, Anal. Chem., 54, 149 (1982).

205 J. Pijck, J. Gillis, and J. Haste, Intern. J. Appl. Radiation Isotopes, 10, 149 (1961).

206 D.D. Siemer and H.G. Brinkley, Anal. Chem., 53, 750 (1981).

207 G.F. Smith, Anal. Chim. Acta, 8, 397 (1953).

208 G. Knapp, Fresenius Z. Anal. Chem., 274, 271 (1975).

209 Abu-Samra, J.S. Morris, and S.R. Koirtyohann, Anal. Chem., 47, 1475 (1975).

210 G. Kaiser, D. Gotz, G. Tolg, G. Knapp, B. Maichin, and H. Spitzy, Fresenius Z. Anal. Chem., 291, 278 (1978).

211 D. Gardner, Anal. Chim. Acta, 93, 291 (1977).

212 S. Bajo, U. Suter, and B. Aeschliman, Anal. Chim. Acta, 149, 321 (1983).

213 B. Morsches and G. Tolg, Fresenius Z. Anal. Chem., 219, 61 (1966).

214 G. Knapp, S.E. Raptis, G. Kaiser, G. Tolg, P. Schramel, and B. Schreiber, Fresenius Z. Anal. Chem, 308, 97 (1981).

215 W. Schoniger, Mikrochim. Acta, 123 (1955).

216 I.M. Kolthoff, E.B. Sandell, E.J. Meehan, and S. Bruckenstein, "Quantitative Chemical Analysis," 4th Ed., Macmillan, N.Y., 1969.

217 B. Bernas, Anal. Chem., 40, 1682 (1968).

218 R. Uhrberg, Anal. Chem., 54, 1906 (1982).

219 A. Van Eenbergen and E. Bruninx, Anal. Chim. Acta, 98, 405 (1978).

220 S. Turmel, R. LeHouillier, and F. Claisse, Can. J. Spect., 23, 125 (1978).

221 K. Govindaraju, Analysis, 3, 116 (1975).

222 V.A. Fassel and W.J. Haas Jr., "Determination of Trace Materials by Inductively Coupled Plasma-Atomic Emmission Spectrometry," International Symposium on Nuclear Activation Techniques in the Life Sciences, International Atomic Energy Agency, Vienna, May 22-26, 1978.

223 L.F. Albright and B.L. Crynes, Eds., "Industrial and Laboratory Pyrolyses," Amer. Chem. Soc., Wash. D.C., 1976.

224 B.T. Guran, R. J. O'Brien, and D.H. Anderson, Anal. Chem., 42, 115 (1970)

225 A.G. Sharkey Jr., J.L. Shultz, and R.A. Friedel, Nature, 202, 988 (1964).

226 N.E. Vanderborgh in: "Analytical Pyrolysis," C.E.R. Jones and C.A. Cramers, Eds., Elsevier, N.Y., 1977.

227 J. Carr and G. Horlick, unpublished work.

228 M.D. Vitalina and V.A. Klimova, Journal of Analytical Chemistry of the U.S.S.R., 33, 1127 (1978).

229 C.E. Gleit and W.D. Holland, Anal. Chem., 34, 1454 (1962).

230 H.J. Gluskoter, Fuel, 44, 285 (1965).

231 E.V. Williams, Analyst, 107, 1006 (1982).

232 M.S. Cresser, Prog. Anal. At. Spectrosc., 4, 219 (1981).

233 A.K. Solomon and D.C. Caton, Anal. Chem., 27, 1849 (1955).

234 J.A.C. Broekaert, F. Leis, and K. Lagua, Fresenius Z. Anal. Chem., 301, 105 (1980).

235 S. Greenfield and P. B. Smith, Anal., Chim. Acta, 59, 341 (1972).

236 H. Uchida, Y. Nojiri, H. Haraguchi, and K. Fuwa, Anal. Chim. Acta, 123, 57 (1981).

237 I. Kojima and C. Iida, Analyst, 107, 1000(1982).

238 T. Ito, E. Nakagawa, H. Kawaguchi, and A. Mizuike, Mikrochimica Acta, I, 423 (1982).

239 P. W. Alexander, R.J. Finlayson, L.E. Smythe, and A. Thalib, Analyst, 107, 1335 (1982).

240 G.D. Christian in "Instrumental Analysis," H.H. Bauer, G.D. Christian, and J.E. O'Reilly, Eds., Allyn & Bacon, Boston, 1978.

241 G. Horlick, unpublished data.

242 R.G. Godden and D.R. Thomerson, Analyst, 105, 1137 (1980).

243 M. Thompson, B. Pahlavenpour, S.J. Watson, and G.F. Kirkbright, Analyst, 103, 568 (1978).

244 K.A. Wolnik, F.L. Fricke, M.H. Hahn, and J.A. Caruso, Anal. Chem., 53, 1030 (1981).

245 M.H. Hahn, K.A. Wolnik, F.L. Fricke, and J.A. Caruso, Anal. Chem., 54, 1048 (1982).

246 M.S. Black and R.F. Browner, Anal. Chem., 53, 249 (1981).

247 W.R. Hatch and W.L. Ott, Anal. Chem., 40, 2085 (1968).

248 S.H. Omang, Anal. Chim. Acta, 53, 451 (1971).

249 K. Tanabe, K. Chiba, H. Haraguchi, and K. Fuwa, Anal. Chem., 53, 1450 (1981).

250 D.L. Windsor and M.B. Denton, Anal. Chem., 51, 1116 (1979).

251 D.L. Windsor and M.B. Denton, Appl. Spectrosc., 32, 366 (1978).

252 R.M. Brown, Jr. and R.C. Fry, Anal. Chem., 53, 532 (1981).

253 R.M. Brown, Jr., S.J. Northway, and R.C. Fry, Anal. Chem., 53, 934 (1981).

254 R.C. Fry, S.J. Northway, R.M. Brown, and S.K. Hughes, Anal. Chem., 52, 1716 (1980).

255 S.K. Hughes and R.C. Fry, Anal. Chem., 53, 1111 (1981).

256 K. Tanabe, K. Matsumoto, H. Haraguchi, and K. Fuwa, Anal. Chem., 52, 2361 (1980).

257 K. Tanabe, H. Haraguchi, and K. Fuwa, Spectrochim, Acta, 36B, 633 (1981).

258 K. Chiba, K. Yoshida, K. Tanabe, M. Ozaki, H. Haraguchi, J.D. Winefordner, and K. Fuwa, Anal. Chem., 54, 761 (1982).

259 A.F. Ward, Technical Aid Note #4, Jarrell-Ash Division, Fisher Scientific Company, Waltham, MA.

260 A.N. Zaidel, "Tables of Spectral Lines," IFI/Plenum, N.Y., 1970.

261 M.L. Parsons, A. Forster, and D. Anderson, "An Atlas of Spectral Interferences in ICP Spectroscopy," Plenum Press, N.Y., 1980.

262 B.J. Stallwood, J. Opt. Soc. Am., 44, 171 (1954).

263 L.K. Storms, "The Refractory Carbides," Academic Press, N.Y., 1967.

264 M. Suzuki and K. Ohta, Talanta, 28, 177 (1981).

265 M. Suzuki, K. Ohta, T. Yamakita, and T. Katsuno, Spectrochim. Acta, 36B, 679 (1981).

266 M. Suzuki and K. Ohta, Anal. Chem., 57, 26 (1985).

267 P. Puschel, Z. Formanek, R. Halavac, D. Kolihova, and V. Sychra, Anal. Chim. Acta, 127, 109 (1981).

268 P.W.J.M. Boumans and F.J. deBoer, Spectrochim. Acta, 32B, 365 (1977).

269 C.D. Carr and J.E. Borst in "Applications of Plasma Emission Spectrochemistry," R.M. Barnes, Ed., Heyden, Phil., 1979.

270 S. Dresner, Popular Science, 202, 102 (May 1973).

271 R.C. Fry and M.B. Denton, Anal. Chem., 49, 1413 (1977).

272 N. Mohamed and R.C. Fry, Anal. Chem., 53, 450 (1981).

273 R.F. Suddendorf and K.W. Boyer, Anal. Chem., 50, 1769 (1978).

274 L.S. Saba, W.E. Rhine, and K.J. Eisentraut, Anal. Chem., 53, 1099 (1981).

275 J.R. Brown, L.S. Saba, W.E. Rhine, and K.J. Eisentraut, Anal. Chem., 52, 2365 (1980).

276 G.A. Hemsalech and M.C. DeWatteville, Compt. Rend., 144, 1338 (1907).

277 J. Monvoisin and R. Mavrodineanu, Spectrochim. Acta, 4, 396 (1951).

278 J.L. Jones, R.L. Dahlquist, and R.E. Hoyt, Appl. Spectrosc., 25, 628 (1971).

279 R.K. Winge, V.A. Fassel, and R.N. Kniseley, Appl. Spectrosc., 25, 636 (1971).

280 H.G.C. Human, R.H. Scott, A.R. Oakes, and C.D. West, Analyst, 101, 265 (1976).

281 J.Y. Marks, D.E. Fornwalt, and R.E. Yungk, Spectrochim. Acta, 38B, 107 (1983).

282 R.H. Scott, Spectrochim. Acta, 33B, 123 (1978).

283 P.T. Gilbert, Jr., Anal. Chem., 34, 1025 (1962).

284 J.S. Woods, Appl. Spectrosc., 22, 799 (1968).

285 M.A. Coudert and J.M. Vergnaud, Anal. Chem., 42, 1303 (1970).

286 V.A. Fassel in "Recent Advances in Analytical Spectroscopy," K. Fuwa, Ed., Pergamon Press, N.Y., 1982.

287 T.B. Reed, J. Appl. Phys., 32, 2534 (1961).

288 T.B. Reed, International Science and Technology, 42 (June 1962).

289 S. Greenfield, I.L. Jones, and C.T. Berry, Analyst, 89, 713 (1964).

290 H.C. Hoare and R.A. Mostyn, Anal. Chem., 39, 1153 (1967).

291 G. Pforr and O. Aribot, Freizenius' Z. Anal. Chem., 10, 78 (1970).

292 R.M. Dagnall, D.J. Smith, T.S. West, and S. Greenfield, Anal. Chim. Acta, 54, 397 (1971).

293 C.W. Fuller and I. Thompson, Analyst, 102, 141 (1977).

294 C.W. Fuller, R.C. Hutton, and B. Preston, Analyst, 106, 913 (1981).

295 V. Karanassios and G. Horlick, Spectrochim. Acta Rev., 13, 89 (1990).

296 V. Karanassios and G. Horlick, Spectrochim. Acta., 45B, 85 (1990).

297 V. Karanassios, G. Horlick and M. Abdullah, Spectrochim. Acta., 45B, 105 (1990).

298 V. Karanassios, M. Abdullah and G. Horlick, Spectrochim. Acta., 45B, 119 (1990).

299 W.T. Chan and G. Horlick, Applied Spectroscopy, 44, 380 (1990).

300 W.T. Chan and G. Horlick, Applied Spectroscopy, 44, 525 (1990).

301 W.T. Chan and G. Horlick, Spectrochim. Acta. B, submitted.

302 V. Karanassios and G. Horlick, Spectrochim. Acta., 44B, 1345 (1989).

303 V. Karanassios and G. Horlick, Spectrochim. Acta., 44B, 1361 (1989).

304 V. Karanassios and G. Horlick, Spectrochim. Acta., 44B, 1387 (1989).